Glutamate-gated chloride channels in the parasitic nematode Haemonchus contortus

Delany, Natalie Samantha

Award date:
1998

Awarding institution:
University of Bath

Glutamate–Gated Chloride Channels in the Parasitic Nematode, *Haemonchus contortus*

Submitted by Natalie Samantha Delany
for the degree of PhD
at the University of Bath
1998

Copyright

Natalie S. Delany

ProQuest LLC
789 East Eisenhower Parkway
P.O. Box 1346
Ann Arbor, MI 48106-1346

Abstract

Two full-length cDNAs encoding putative glutamate receptor subunits denoted HG4 and HG5 have been isolated from the parasitic nematode *Haemonchus contortus*. The translated sequence for HG4 shared an 80.25% identity with the glutamate gated chloride channel beta subunit, GluClβ, isolated from the free-living nematode *Caenorhabditis elegans*. This suggested that the HG4 receptor subunit was the parasitic orthologue of GluClβ. Similarly, the translated sequence derived for HG5 was 56 % identical to the *C. elegans* inhibitory glutamate receptor subunit GluClα1. This suggested that HG5 might be α-like in nature.

Co-expression of GluClα1and -β in *Xenopus* oocytes forms avermectin sensitive receptors. It was postulated that HG4 was a component of an equivalent complex in *H. contortus*. The translated sequence of HG4 from an avermectin-resistant population of nematodes was found to be identical to the consensus sequence derived from a susceptible population. This confirmed that the switch from avermectin susceptible to resistant phenotypes did not result from a genetic mutation coded by the mRNA. Amplification of the 5' end of HG5, encoding the predicted ligand-binding domain, from a resistant-population revealed that there was no difference in the sequence to that from susceptible worms.

HG4 expression was mapped in adult *H. contortus* using immunocytochemical techniques. Labelling was restricted to the commissures with a fainter staining observed in ventral and dorsal cords. Expression spanned from the mid-region of the pharynx to the mid-body region. These findings suggested that glutamate transmission occurs via HG4 associated receptors between the AVE interneurone and connecting motor neurones. Commissures within this region form branches that connect to the sublateral cords. Communication between these cords and surrounding muscle play a role in regulating the head movement of the worm. It was therefore predicted that exposure of *H. contortus* to avermectin result in the paralysis of somatic muscles in the anterior portion of the worm.

Acknowledgements

The work described was carried out at the School of Biology and Biochemistry at Bath University under the supervision of Dr. Adrian Wolstenholme and was funded by the BBSRC, I therefore give thanks to all the above for their support.

I would like to give special thanks to Dr Adrian Wolstenholme who has been an inspiration throughout this work. His advice and guidance have been invaluable. I would also like to thank Dr David Laughton for his continual advice that "it will be alright". I am also grateful to Dr Adrian Rogers who introduced me to a number of the techniques used for generating antibodies.

I give my heartfelt thanks to my parents, for their help, understanding and unfailing assistance throughout my time at Bath.

Especial thanks to Louisa Yoeh whose friendship I greatly valued. Thanks must also be given to Dr Tom Skinner and Suchitera Jaggannathan for their friendly encouragement and enthusiasm.

Finally, thanks must be given to Dr Munn (Babraham Institute, Cambridge) and Dr Gerald Coles (Department of Clinical Veterinary Science, University of Bristol, Langford, Bristol) for their donations of tissue samples.

List of Contents

List of Figures

List of Tables

Abbreviations

avr	avermectin
bp	base pairs
BSA	Bovine Serum Allbumin
DEPC	diethyl pyrocarbonate
DNA	Deoxyribonucleic acid
dNTP	Deoxyribonucleoside triphosphate
DTT	Dithiothreitol
EDTA	Ethylenediaminetetracetic acid
ELISA	Enzyme linked immunosorbant assay
FITC	Fluorescein isothiocyanate
GABA	γ-Aminobutyric acid
GFP	Green fluorescent protein
GluClR	Glutamate gated chloride channel receptor
GSAP	Gene specific antisense primer
GSSP	Gene specific sense primer
IPTG	Isopropylthio-β-D-galactoside
kbp	kilobase pairs
LB	Luria Bertani
mRNA	messenger ribonucleic acid
nAChR	nicotinic Acetylcholine receptor
NADPH	nicotinamide adenine dinucleotide phosphate, reduced
nts	nucleotides
OAc	Acetate anion
PAGE	Polyacrylamide gel electrophoresis
PBS	Phosphate buffered saline
PCR	Polymerase Chain Reaction
PEG	Polyethylene glycol
Pwo	*Pyrococcus wosei*
RACE	Rapid Amplification of cDNA ends
RNA	Ribonucleic acid
RNase	Ribonuclease
SDS	Sodium Dodecyl Sulphate
Taq	*Thermus aquaticus*
TBPS	t-Butylbicyclophosphosphorothionate
TEMED	N, N, N', N'-tetramethylethylenediamine
TGIC	Transmitter gated ion channel
TM	Transmembrane domain
TMB	3, 3', 5, 5'-tetrmethylbenzidine
TRITC	Tetramethylrhodamine B Isothiocyanate
unc	uncoordinated

X-Gal	5-bromo-4-chloro-3-indoyl-β-D-galactopyranoside

1 Introduction

This chapter provides an overview of parasitic nematodes, detailing the devastating affects incurred upon infection and hence the need to limit further spread. Nematodes causing disease specific to humans or livestock are described, with particular reference made to *Haemonchus contortus,* one of the most common worms infecting both sheep and goats on a global scale. Methods for controlling infection by this nematode are considered, with chemotherapy being the most popular approach taken by farmers. As with all anthelmintics so far administered to nematode infected livestock, *H. contortus* has developed drug resistant populations. Consequently there is concern that this particular measure will become inefficient in the future, with nematode populations becoming harder to control. Some of the most popular drugs used by farmers are discussed including details of known targets, mechanisms of action and the genetic changes, which produce resistance in certain nematode populations. To date nematode studies have concentrated on two species of nematode, *Caenorhabditis elegans* and *Ascaris suum.* Their popularity for genetic studies is discussed, including reasons for preferential use over nematodes such as *H. contortus.* Studies on these model systems corroborate findings that the majority of drug targets are localised within the nervous system of the nematode. A complete reconstruction of the *C. elegans* nervous system has been accomplished, the architecture of which is summarised in order to identify which neurones are targeted by which drugs. Target sites associated with neurones include a superfamily of ligand-gated ion channels of which both inhibitory and excitatory receptors are members. These are discussed to clarify the mechanisms of anthelmintic action and why drug resistance is triggered. This thesis details an attempt to isolate the avermectin target from the parasitic nematode *H. contortus.* Characterisation of this target has been combined with existing knowledge of model systems to develop an understanding of the drug mechanism in actual parasites.

1.1 Nematode Classification

Nematodes, also known as round worms or helminths, have cylindrical non-segmented bodies that possess bilateral symmetry. They are composed of two concentric tubes, the mesoderm (body wall) and the endoderm (gut), which are separated by a fluid-filled cavity known as the pseudocoelum as displayed in figure 1 (Wood, 1988). It has been estimated that four out of five animals on this planet are helminths (Platt, 1994). Free-living nematodes may feed entirely on micro-organisms present in decaying matter, or suck juices from plants. Other species have developed successful methods with which to parasitise animals. Most parasitic nematodes are dioecious, having male and female organs in separate individuals with fertilisation of eggs occurring in the female. Life cycles are highly conserved with the worm undergoing four moults, passing through four larval stages (L1-L4) before reaching maturity, at which stage females are generally larger than males (Wood, 1988).

In 1987, Adamson revised the classification of nematodes dividing them into two broad

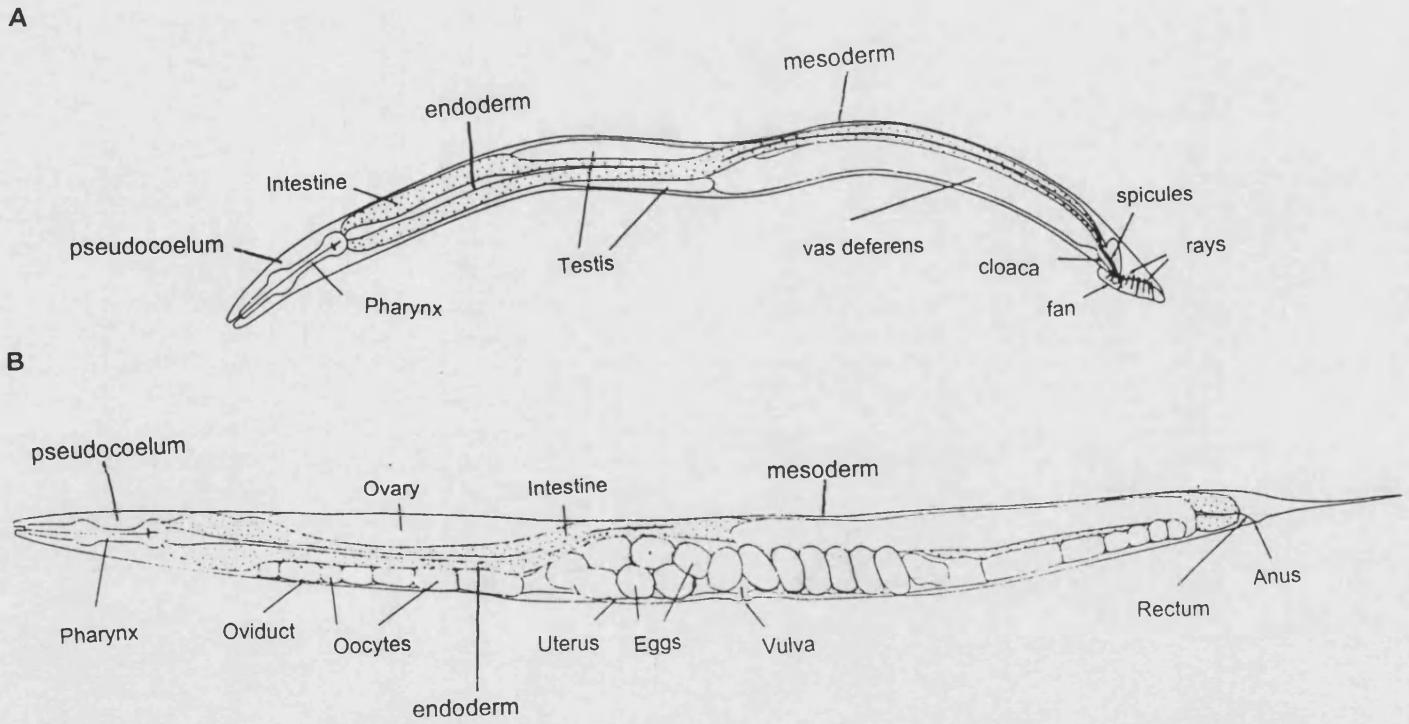

Figure 1, Anatomy of *Caenorhabditis elegans*. a) male and b) hermaphrodite. The major anatomical features are highlighted with reference made to the mesoderm (body wall), endoderm (gut) and the pseudocoelum (fluid filled cavity).

subclasses; subclass I (Adenophorea) and subclass II (Secernentea), depending on whether caudal sense glands (phasmids) were present. The Adenophorea lack phasmids and were of the order Enoplida. Nematodes of this order fell into one of two superfamilies: Trichuroidea or Dioctophymatoidea. The subclass Secernentea possessed phasmids and were classified in one of five orders- Order 1: Rhabditida, Order 2: Ascaridida, Order 3: Oxyurida, Order 4: Strongylida and Order 5: Spirurida. Strongylida were classified further into 4 superfamilies: Ancylostomatoidea (hookworms), Strongyloidea, Trichostrongyloidea, and Metastrongyloidea. The Spirurida were also classified into 6 different superfamilies: Filarioidea (filarial worms), Dracunculoidea, Gnathostomatoidea, Thelazoidea, Habronematoidea and Physaopteroidea. A summary of this classification is illustrated in Figure 2 with examples of some of the worms that fit into the various families listed.

1.2 Parasitic Infection

The majority of nematodes are free-living microbivores, however many species have adopted a parasitic lifestyle and can be found in host organs, tissues and cells. Colonisation of parasites within these structures can have severe effects, which may lead to death if not treated. In the following section examples of both human and livestock parasites are described. The cause of parasitic transmission, severity of host symptoms and the identification of high-risk host populations are included.

1.2.1 Human parasitic nematodes

In humans, both the whip worm *Trichuris trichiura* and the pin worm *Enterobius vermicularis* inhabit the gastro-intestinal tract, where they attach onto the gut wall and consume the hosts blood via the epithelial lining. Each of these species is distributed globally with the former most prevalent in humid tropical countries and the latter in temperate climates, infecting mainly children (Whitfield, 1993).

Parasites such as *Ascaris lumbricoides* and the hookworm *Necator americanus* journey through various organs whilst undergoing development, their ultimate destination being the alimentary canal. A female *N. americanus* can grow to 1.3 cm long whilst female *A. lumbricoides* can measure up to 35 cm in length (Jeffery & Leach, 1972). Both species are found globally, the latter prevalent in the Far East and tropical Africa and the former in the tropics and subtropics such as the Southeast states of the USA (Whitfield, 1993). *Ascaris* eggs, present in water or contaminated foodstuffs, are swallowed by the human host and pass into the duodenum where they hatch into L2 larvae. These burrow into the mucosa and migrate to the liver. From this point they can enter the lymphatic system or the veins which carry them to the heart. From here they journey to the lungs where they moult twice, ascending the trachea where they re-enter the digestive tract upon being swallowed.

Similarly, the hookworm follows the same route, but only does so if the L3 larvae penetrate the skin thus gaining access to the veins. If on the other hand the host ingests L3 larvae,

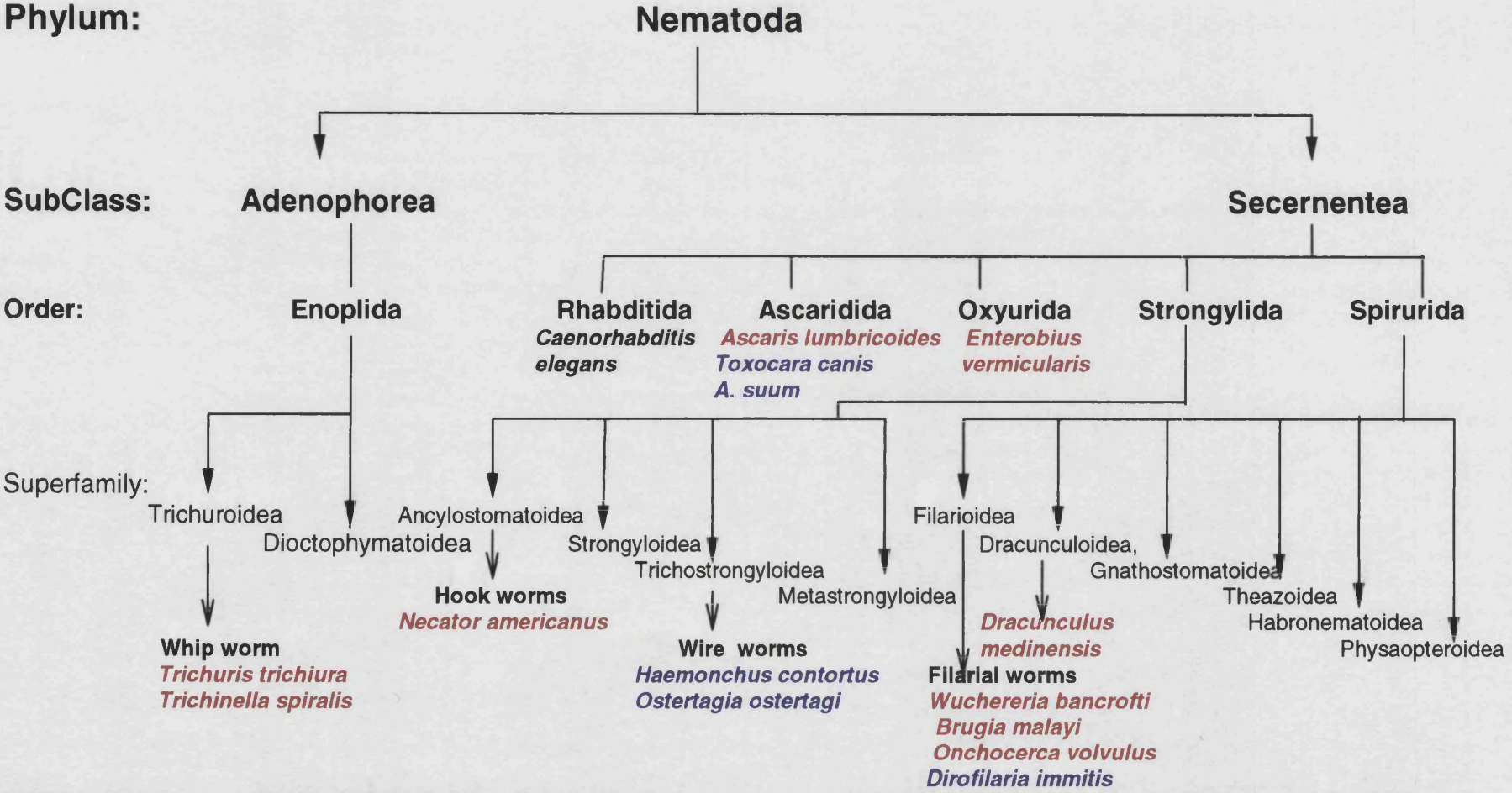

Figure 2, An Outline of the classification of the Phylum Nematoda: includes examples of free-living worms, **human parasites** and **domesticated livestock/animal parasites**

they travel directly to the gut where they develop to adulthood. The adults may also perforate the lining of the jejunum or duodenum inducing peritonitis.

Dracunculus medinensis, also known as the guinea worm, is the largest of the human parasitic nematodes, growing to lengths of up to one meter (Whitfield, 1993). They are ingested through drinking water contaminated with water-borne animals called cyclops containing L3 larvae. These penetrate the gut and develop into adults over a 12-week period at which stage they mate and then move through the body causing tremendous pain until they reach the ankle. Eight to ten months after the original infection the mature female, carrying about a million L1 larvae, induces a blister on the hosts skin. Worms emerge from these sites causing patients to suffer extreme pain accompanied by fever, nausea and vomiting. In the following months the patient can remain ill due to an increased susceptibility to super-infections. A global campaign was initiated in 1980 by the World Health Organisation (Reviewed by WHO, 1997) to eradicate dracunculsis as no drug or vaccine existed to treat the disease. Steps were made to prevent the completion of the parasites life cycle by the systematic filtering of all drinking water, disinfecting stagnant water holes and installation of water pumps. A press release by the WHO (1995) reported that guinea worm disease remained prevalent in India and Yemen, as well as in 16 countries in Africa south of the Sahara. It was estimated that 130 million people were at risk of infection, of which 99% lived in Africa.

A disease known as lymphatic filariasis is caused by infection of filarial nematodes such as *Wuchereria bancrofti* and *Brugia malayi* (Whitefield, 1993). Both adult worms and microfilaria (L1 larvae) settle within the lymphatic vessels of the human host, where they develop over a 15 month period. Microfilariae are able to invade the blood stream, where they may remain as immature forms for up to 2 years. Transmission to other humans is achieved by the involvement of an intermediate host, the mosquito of genera *Aedes*, *Mansonia*, *Culex* or *Anopheles*. Microfilariae present in the blood meal of a mosquito invade the flight muscles via the hemocoel, moulting twice to give infective L3's. These migrate to the proboscis where they are released into another human host when the mosquito takes another feed. L3 larvae then travel to the lymphatic system during which time they moult twice to give adults. Adult worms grow to several centimetres in length damaging lymphatic ducts. They are also extremely resilient, surviving attack by the host immune system by expressing epicuticular enzymes (glutathione peroxidase, catalase and superoxide dismutase) to disarm the oxygen radical attack of activated immune effector cells (Cookson *et al.,* 1993, Ou *et al.*, 1995, Tang *et al.*, 1994). A condition, called elephantiasis, develops after infection causing body parts such as the legs, arms, scrotum, vulva or breasts to become grossly swollen and covered with sores. Other symptoms of infection include acute fevers, inflammation of the lymphatic system and pulmonary eosinophilia. In 1996 more than 120 million people world-wide were estimated to be infected of which 106 million were infected with *W. bancrofti* and 12.5 million people with *B. malayi* and the closely related *B. timori* (WHO, 1996).

The disease Onchocerciasis is caused by the infection of the filarial worm, *Onchocerca volvulus* and is most prevalent between the West African savanna and forest areas. Here nematodes are transmitted by the Simulium genus of black fly which breed in fast flowing freshwaters (reviewed by Whitfield, 1993). Unsheathed L3 larvae, released from the blackfly, penetrate human skin and mature to adults, growing up to 50 cm in length, in the subcutaneous tissue (Jeffery & Leech, 1975). Unlike *W. bancrofti* and *B. malayi,* microfilariae from *O. volvulus* do not travel around the blood system but rather localise under the skin where they cause the majority of side affects associated with the disease. Initial light infections induce itchy rashes, contrasting with subsequent long heavy infections leading to patchy pigmentation changes of the skin. Chronic infection also causes the skin to thicken, becoming coarse in texture whilst losing its elasticity. Elephantiasis of the genitals and river blindness are two symptoms commonly observed in infected individuals, the latter developing when microfilariae move through the skin to the eye impairing vision.

The whipworm *Trichinella spiralis*, a parasitic nematode that invades cells in the human host, causes the disease called trichinosis. The worm is globally distributed, in a range of carnivorous and omnivorous mammals, with larvae being transmitted when uncooked infected flesh is eaten. Adult parasites reside in the small intestine where they burrow into epithelial cells causing damage to the lining of the gut wall. However, the majority of harm is attributed to the larvae migrating to voluntary muscles forming cysts within muscle cells. Symptoms of heavy infections include vomiting, diarrhoea, high fever and muscular pain, with severe cases causing cardiac and central nervous system damage (Whitfield, 1993)

1.2.2 Livestock parasitic nematodes

Nematodes of veterinary importance include the gastro-intestinal parasites *Haemonchus contortus* infecting sheep & goats and *Ostertagia ostertagi* found in cattle (Grønvold *et al.*, 1993). With both species of nematodes, L3-larvae are ingested whilst the ruminant is grazing and migrate to the stomach where they undergo two moults, transforming them into adults. Blood feeding starts when the adults attach onto the gut lining, using teeth present in the buccal cavity. Sheep infected with *H. contortus* can carry several thousand worms, each consuming 15 μl of blood per day (reviewed by Smyth, 1994). This action inevitably drains the sheep of blood. With *O. ostertagi* carrying out the same process in cattle, similar symptoms are induced.

The ascarid *Ascaris suum,* parasitises pigs, undergoing a similar life cycle and migrational path as that described for the human parasite, *A. lumbricoides*. Migrating *A. suum* larvae cause allergic reactions and respiratory problems such as bronchitis. High levels of worms can encourage migration out of the gut into the bile duct, pancreatic duct, oesophagus, mouth and sometimes the liver (Whitfield, 1993).

Other nematodes found in domesticated animals include the filarial parasite *Onchocerca*

gutturosa present in the connective tissue of cattle. Adult *Ascaridia galli* inhabits the small intestine of chicken, and the strongylida *Dictyocaulus viviparus* resides in the lungs of cattle.

1.3 *H. contortus*

H. contortus is one of the most common nematodes to parasitise sheep and goats in Britain. An increased understanding of the genetic make-up of this parasite is required to optimise methods for controlling its transmission. Difficulties encountered in previous studies of the nematode are discussed. Two alternative helminths, *Caenorhabditis elegans and Ascaris suum* have however been successfully studied and are also reviewed. Findings for these systems are currently used to predict processes occurring in *H. contortus.*

1.3.1 Appearance and Life Cycle

The wireworm *Haemonchus contortus* is a highly pathogenic sheep parasite. It is also known as the barbers pole worm as the female has a characteristic red strip spiralling along its body (Figure 3a). This is due to the white ovaries twisting around the red intestine. Adult *H. contortus* reside in the true stomach or abomasum of sheep, cattle, goats and other small ruminants. Adult worms are dioecious, whereby both male and females worms are needed to reproduce. Adult males are 10-20 mm in length with a diameter of 0.4 mm whilst females are 18-30 mm in length with a 0.55 mm diameter (Jeffery & Leech, 1972). It is estimated that the females *H. contortus* can lay 20,000 eggs per day, each egg being approximately 66.5-79 x 43.3-46.6 μm in size (Blaxter & Bird, 1987 and Anderson, 1992). These pass out of the sheep with the faeces and hatch to release first stage L1-larvae. These free-living L1 microbivores are 340-350 μm in length having a valve termed the oesophageal bulb and a slender, sharply pointed tail. L1-larvae commence eating an hour after hatching and grow to a length of 400-450 μm over a period of 14-17 hours. At this stage they become lethargic and moult to give second stage L2-larvae, possessing prominent lateral alae, ridges which stretch the length of the cuticle. These resume feeding for a further 40 hours, at which point they undergo lethargy and a moult, but unlike the previous moults the cuticle is not shed. The resultant infective L3-larvae are therefore enclosed in two cuticles, the outermost of which is called the sheath. The ensheathed larvae are 754-756 μm in length still possessing lateral alae, yet the tail differs being less attenuated and conical in shape at the tip. L3-larvae climb up blades of grass and wait to be eaten by grazing sheep. Once ingested, ecdysis is triggered whereby larvae exsheath whilst en route to the abomasum, upon arrival they burrow into gastric pits between the villi and commence feeding. As the larvae reach a length of 655-840 μm they experience a third lethargic period followed by a moult giving way to L4-larvae. The L4-larva has a buccal cavity containing teeth allowing it to hook onto the mucosal layer accessing the host's blood. After seven days of blood feeding activities, sexes can be clearly differentiated, males being 2.7-3.0 mm in length and females 3.7-4.0 mm.

Following a further 12 days including a final 24 hours of lethargy, a fourth moult is initiated, liberating adults. This cycle is depicted in Figure 3b.

Figure 3a. A female adult *Haemonchus contortus*, photograph provided by Dr E. Munn.

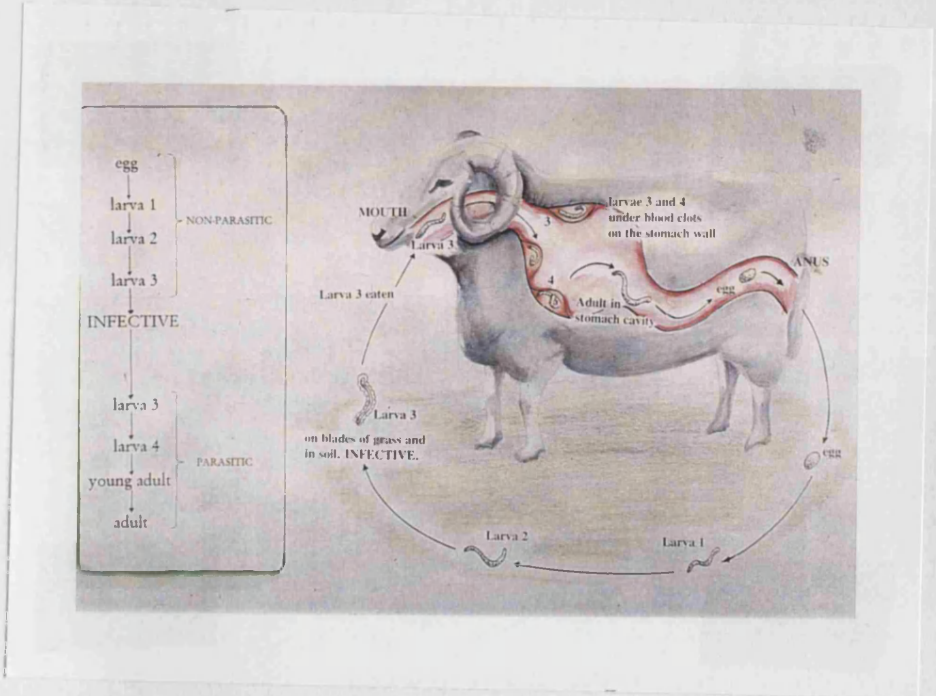

Figure 3b. The Life cycle of *H. contortus*. Drawn by Dr D. Cope

1.3.2 Model Nematodes

H. contortus is difficult to study since no *in vivo* culturing technique has been developed to incorporate the nutrients and environmental cues experienced within the sheep gut (Stringfellow, 1986). The size of the worm also presents a problem when attempting electrophysiological studies. Use of two other closely related nematodes, *Caenorhabditis elegans* and *Ascaris suum,* as model systems have circumvented many of the problems posed by the experimental use of *H. contortus.* These systems and their uses are described next.

1.3.2.1 *Caenorhabditis elegans*

Caenorhabditis elegans, reviewed by Wood (1988), is an ideal experimental model system for studying nematodes. It is a small free-living soil nematode, an adult being 1.5 mm in length, feeding primarily on bacteria. Nematodes can therefore be easily maintained in the laboratory by growing on *Escherichia coli* coated agar plates at 20 °C. It is also possible to cultivate large numbers of worms by mass culture in liquid media (Lewis & Fleming, 1995). This species has two sexes, hermaphrodites and males, the former produce both oocytes and sperm allowing them to reproduce by self-fertilisation, also known as selfing. Hermaphrodite/male crossing can produce over 1000 progeny compared to the 300 eggs laid during selfing. Under optimal conditions a *C. elegans* life-cycle typically spans over three days from fertilisation to adulthood, during which time it undergoes 4 successive moults. Adults are then able to live for a further 17 days, hermaphrodites living slightly longer than males. This short life-cycle is therefore well suited to the ease of cultivation within a laboratory.

The transparency of the body is also advantageous as it allows features such as cell numbers and their positions to be observed during the worm's development. *C. elegans* anatomy is also simple and the consistency of structures observed between individuals remains constant. With the aid of electron microscopy, the complete nematode anatomy has been reconstructed with adult hermaphrodites having a total of 959 somatic nuclei and adult males having 1031 (Sulston *et al.*, 1983). Information on locations and characteristics of these somatic cells and cell lineage has been established. Details of the latter include timing, locations and ancestral relationships of all the cell divisions during development. A technique called laser microsurgery has proved a useful tool, whereby cells undergo laser ablation within the living organism allowing the resulting phenotype to be examined (McIntire *et al.*, 1993b).

The simplicity of the nematode is also a valuable factor, having an estimated genome size of 100 x 10^6 base pairs, organised into six chromosomes (Hodgkin *et al.*, 1995). Hermaphrodites have 2 sex-linked X-chromosomes whilst males possess a single X-chromosome, remaining chromosomes are autosomal in nature. The genome is $1/30^{th}$ the size of the human genome and 20 times the size of the *Escherichia coli* genome. It is 36 %

GC rich with coding sequences having a high GC content and non-coding regions possessing a high AT content (Sulston & Brenner, 1974). The complete genomic sequence will be available by the end of 1998 (Hodgkin *et al.*, 1995). Detailed genetic mapping is also in progress and can be accessed by the *C. elegans* database, AceDB (Hodgkin *et al.*, 1995). This involves the cloning and analysis of mutationally defined genes such as a group of uncoordinated worms, defined as the *unc* mutants. This has led to the production of a physical map of the entire genome, which is nearing completion. One limitation with the *C. elegans* model is that electrophysiology, although possible (Raizen & Avery, 1994), is not easy due to the small size of the neurones, muscle cells and pharynx. The pig parasite *Ascaris suum* is a more suitable nematode for such studies, possessing large cells that are more amenable to the electrode attachment required for electrophysiological recordings (Martin, 1993).

1.3.2.2 *Ascaris suum*

Ascaris suum is a large parasitic nematode, 30 cm in length, ultimately residing in the pig's intestine. Worms can be collected from abattoirs and then preserved in a warm saline solution for about five days (Martin *et al.*, 1996). The large size of its muscles and nerve cells makes it an attractive system to study the electrophysiological action of exposure to a variety of chemicals including neurotransmitters and anthelmintics. This technique has yielded information on the nervous system of *A. suum,* which corresponds closely with data collected on *C. elegans.*

1.4 Controlling infection

H. contortus pathogenicity is attributed to its blood feeding activities. Feeding initiates haemorrhaging of the abomasum wall. Blood plasma and proteins are lost in addition to the haemoglobin and iron from red blood cells. A loss of these components can cause anaemia and hypoalbuminaemin (Crompton & Joyner, 1980). Consequently, production of milk, wool and meat becomes reduced, and in severe cases the sheep can die. A variety of methods can be used and prevent *H. contortus* transmission. It should be noted that these measures are also used to control a range of other nematode infections. It is currently believed that a combination of these control measures may prove more successful than the use of single methods (Strong & Wall, 1990).

The most popular method chosen by farmers however is chemotherapy. In the short term, this method has proven most effective however incorrect usage is rendering it less efficient. This will therefore become a problem in the long run as more anthelmintic resistant nematode populations evolve. The most commonly used drugs including the avermectins are described, with details of modes of action. Avermectins are the most recent class of anthelmintics to be discovered and are the most potent drugs on the market. Even though avermectins possess activity against a broad spectrum of nematodes there are however a number of species that remain resilient to the drug and are referred to below.

1.4.1 Physical control

Nematode infection of livestock can be effectively reduced through management activities (Strong & Wall, 1990). Pasture resting counteracts the possibility of transmission by rotating livestock to clean pastures and by alternating grazing between various species. Allowing animals to graze in larger fields to lower livestock density also reduces infection. A cramped condition where grass is scarce encourages animals to feed closer to faeces elevating the risk of infection. Dung removal is also recommended, involving either sweeping or vacuuming infected dung from the fields. It is also advantageous to expose young animals to minor larval infection thus stimulating some degree of immunity to the parasite for later life.

1.4.2 Biological control

An alternative approach to controlling parasitic spread of nematodes by ruminants is to kill the helminths whilst they are undergoing the free-living stages of their life cycle. Searches for parasitic predators have resulted in the discovery of a family of nematophagous fungi. This family can be split into three categories; the nematode trapping fungi, such as *Arthrobotrys oligospora* and *Duddingtonia flagrans*, endoparasitic fungi of which *Harposporium anguillae* is a member and fungal parasites such as *Verticillium chlamydosporium* (Waller, 1993 & Grønvold *et al.*, 1993).

The nematode trapping fungus *A. oligospora* grows saprophytically, developing vegetative mycelium, which in the presence of nematodes grow trapping organs. Moreover, induction is most effective when highly motile larvae are present, resulting in the formation of constricting (active) or non-constricting (passive) rings, sticky hyphae, adhesive networks or knobs (Nansen *et al.*, 1988). Fungi in this class may also secrete chemo-attractants and/or chemotoxic substances to nematodes. For example, following an hour of entrapment by *A. oligospora,* the nematode cuticle is penetrated by the fungus, which then secretes a nematotoxin that either kills or paralyses the trapped helminth (Balan *et al.,* 1974). This is followed by the formation of an infectious bulb within the nematode from which trophic hyphae grow out causing internal destruction.

In contrast, endoparasitic fungi possess trapping nets anchoring the nematode near spore containing fungal structures called conidia. Upon entrapment, released spores are consumed by the nematode, lodging in the muscle tissue of the oesophagus and developing into an infectious thallus that absorbs the body contents. (Grønvold *et al.*, 1993)

A reduction in levels of larvae was observed when nematode trapping fungi such as *D. flagrans* were added directly onto the dung infected with *O. ostertagi* and *Dictyocaulus viviparus* (Grønvold *et al.*, 1993). A disadvantage of this approach is that it is highly dependent on climatic conditions. An alternative to covering dung with large quantities of fungi is to feed nematode infected cattle with endoparasitic fungi. Calves infected with *O. ostertagi* were fed with the fungus *D. flagrans* and the levels of eggs in the faecal deposits

were then monitored to ascertain the level of the fungus through the digestive tract. The fungus appeared to survive its journey through the animal as cow pats after treatment contained reduced levels of larvae. There is the possibility that alternative predators such as bacteria, protozoa or viruses may offer a means of biological control (Waller, 1992).

1.4.3 Vaccines

A naturally occurring immune response occurs when ruminants are infected with gastro-intestinal nematodes thus providing a degree of protection. This was demonstrated when ferrets were successively infected with third-stage larvae of the canine heartworm *Dirofilaria immitis* (Blair & Campbell, 1981). The anthelmintic drug, avermectin, was administered two months post-infection of 30 larvae thus flushing the nematodes out of the ferrets. Three months following this, the ferrets were re-exposed to an equal number of larvae followed by termination after a further two months using avermectin. Three months following the second administration of drug ferrets were challenged with 30 larvae. The 4 ferrets surviving this treatment were necropsied after 6 months. Two were free of infection whilst the other two were each infected with a single worm.

Vaccination is a way of elevating levels of immunity to antigens following infection producing a response higher than that obtained naturally. This approach to control is a relatively new field of research with some vaccines presently undergoing clinical trials. In 1987, a vaccine enriched with a concealed antigen called contortin, a protein associated with the luminal surface of the intestinal epithelium of *H. contortus,* was tested (Munn *et al.*, 1987). In this case, it is only when the worm feeds on the host's blood that the antigen is recognised by antibodies and other effector components present in the meal. Sheep administered with this vaccine displayed a significant reduction in worm burden and egg counts.

More recently, it has been demonstrated that a natural immune response was associated with the humoral recognition of excretory-secretory (ES) products from *H. contortus* of molecular weights ranging from 10 to greater than 100 KDa. Infected Texel sheep raised significantly high levels of IgG to two low molecular weight antigens of 15 and 24 kDa in size (Schallig *et al.*, 1994). These two proteins were partially purified by gel filtration using total adult ES products to monitor their ability to induce protective immunity against *H. contortus* in sheep (Schallig & Leeuwen, 1997). Five sheep were challenged with 20,000 *H. contortus* L3-larvae 5 weeks post-vaccination of the 15/24 kDa ES immunogen. After ten weeks post-primary vaccination, one of the sheep had not developed protection against the parasite, however for the remaining four sheep, a mean reduction of faecal egg counts by 99.9% was observed as well as a 97.6 % mean reduction in abomasal worm burden. Discrepancies in degrees of protection may be genetically linked, causing variation in the ability of individuals to respond to parasites.

1.4.4 Chemotherapeutics

Chemical control is the most successful short-term treatment employed by farmers. There are over 200 chemical compounds currently available to farmers to treat livestock parasites (Strong & Wall, 1990).

Highly toxic chemicals based on arsenic, mercury, tar and petroleum were some of the original treatments administered to animals experiencing parasitic infestations. However, these compounds more often than not poisoned livestock. A second class of compounds called the organochlorines, such as DDT, where developed aiming to reduce toxicity to hosts. Unfortunately, DDT's unforeseen persistence, spreading up the food chain led to the ban on its use in many countries.

Since the 1940's the rate of discovery of novel drugs has been approximately one every 5 years, with potency towards the parasite increasing with each new discovery (McKellar & Benchaoui, 1996). Consequently, doses to hosts tend to be reduced by half with each succeeding novel compound. Gutteridge has reviewed these novel anthelmintic drugs in 1993; details of these are described below with corresponding structures presented in figure 4.

Anthelmintics available to control gastro-intestinal nematode infestations include the organophosphates Haloxon (for horses), Dichlorvos (for pigs) and Naphthalophos (for sheep). Each of these drugs acts as a potent inhibitor of acetylcholine esterases present at synapses in the nematode's nervous system. This enzyme breaks acetylcholine down into acetic acid and choline, the former of which is taken up presynaptically. Degradation by esterases is very efficient, inactivating the neurotransmitter. Inhibition of this break down would thus prolong exposure of acetylcholine at synaptic junctions leading to longer depolarisation times causing muscle paralysis.

Another drug that targets the helminth's nervous system is piperazine and is often used to treat infected small animals. The compound selectively opens GABA gated chloride channels present at neuromuscular junctions; hyperpolarisation produced by an influx of chloride ions into muscle cells leads to flaccid paralysis. It has subsequently been found that piperazine binds reversibly to the channel, simply immobilising the worm rather than killing it. Immobilisation enabled the natural expulsion of the nematodes by bowel movement.

Benzimidazoles were discovered in 1964 to have a broad-spectrum activity against gastro-intestinal parasites. This class of compounds has limited solubility leading to poor absorption when ingested thus making them ideal candidates for treatment of intestinal helminth infections. The mode of action of these drugs involves an interaction with the cytoskeletal protein, tubulin, inhibiting its polymerisation into microtubules by binding to the nucleotide GTP–binding site (Kwa *et al.*, 1995). Benzimidazole selectively binds to helminth tubulins since the rate of dissociation of the drug to mammalian tubulin is much higher than for its

Benzimidazole

Levamisole

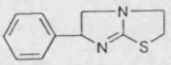

Clonstachydiol

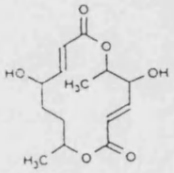

Morantel

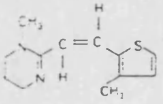

Dichlorvos

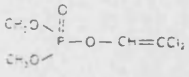

Naphthalophos

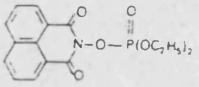

Dioxapyrrolomycin

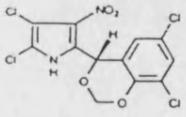

Paraherquamide

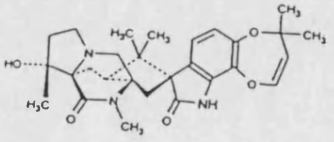

Haloxon

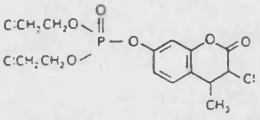

PF1022A

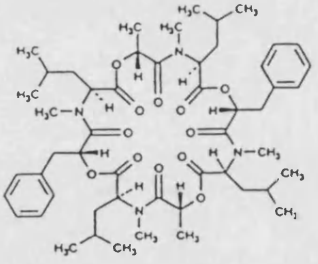

Ivermectin

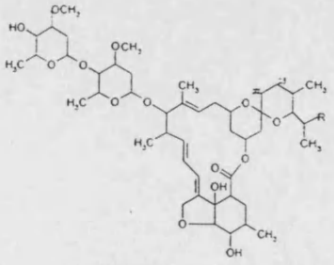

Piperazine

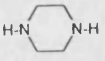

Figure 4, Anthelmintic drugs used to control parasitic nematode infection.

parasitic counterpart (Lacey & Gill, 1994).

Levamisole, morantel and pyrantel were also introduced in the 1960s and target nicotinic acetylcholine receptors located in the helminth nervous system (Lewis *et al.*, 1980). This group of drugs act as agonists, mimicking the effect of acetylcholine at the excitatory receptor, opening the channel for cation influx depolarising cells (Coles *et al.*, 1975). Continued depolarisation leads to muscular paralysis thus preventing movement by the nematode.

In 1981, a new class of compounds known as the avermectins was introduced as a novel anthelmintic treatment. Avermectins are macrocyclic lactones produced by the filamentous bacterium *Streptomyces avermitilis* (Burg *et al.*, 1979). The synthetic derivative of the natural occurring avermectin 1B is called ivermectin. This possesses a single bond rather than a double bond between carbon 22 and 23 (Sutherland & Campbell, 1990). The potency of ivermectin is 25 fold higher than contemporary products, thus requiring nanomolar doses for administration to infected livestock (McKeller & Benchaoui, 1996). Avermectins target inhibitory ion channels present in the nervous system of the worm inducing an irreversible influx of Cl^- ions through inhibitory glutamate-gated receptors resulting in paralysis. This was confirmed by injecting mRNA isolated from the free-living nematode *Caenorhabditis elegans* into *Xenopus* oocytes. Pharmacological studies on these revealed the activation and potentiation of glutamate gated chloride currents by avermectin and a series of analogues (Arena *et al.*, 1995).

Ivermectin was initially used to treat livestock and by 1986, it had captured 16 % of the world-wide anti-parasitic sales. Approximately 800 million cattle had been treated with ivermectin by the year 1990 and awareness that the drug could be used in the control of insects and human parasites was developing. The human filarial disease, onchocerciasis, has since been successfully treated with ivermectin (Plaisier *et al.*, 1995).

In *Haemonchus contortus,* avermectin affects three different structures: the gut lining, the pharynx, and somatic muscle (Geary *et al.*, 1993). At concentrations greater than approximately 10^{-8} M, ivermectin reduces the motility of the worm. The observed drug induced paralysis was confined to the mid-body region of the parasite, contrasting with the head and tail regions where normal motility action was maintained. This observation was believed to be a result of the drug binding to GABA receptors which are known to bind avermectin at μM concentrations (Holden-Dye *et al.*, 1988 and Martin & Pennington, 1989). At avermectin concentrations of 10^{-10} M, a reduction in ingestion by *H. contortus* was visualised by detection of FITC-labelled *Escherichia coli.* It was also discovered that the drug paralysed the pharynx when present at concentrations greater then 10^{-10} M, preventing the influx of nutrients into the digestive tract (Geary *et al.*, 1993).

Temporary paralysis of the pharynx has been induced by immersion of first stage *C. elegans*

larvae into 0.15 5 1-phenoxyl-2-propanol. The subsequent addition of ivermectin triggered coiling and prolonged immobilisation of the larvae at final concentrations of 50 mg/ml (Smith & Campbell, 1996). These findings indicate that avermectin uptake is not solely dependent on the ingestion by pharyngeal pumping.

From these findings it was evident that avermectin inhibits pharyngeal pumping more potently than motility, however it is not yet known whether the drug kills the worm by terminating its feeding abilities thus leading to arrested development and starvation. Death by starvation is likely to occur over a period of time, as adult parasites possess ample supplies of glycogen and would therefore not, as is the case, cause a rapid expulsion of worms out of the host. It has been suggested that avermectin may kill worms by preventing pharyngeal related functions, such as the regulation of internal pressure through which it maintains its rigid body shape (Laughton *et al.*, 1997a & Wolstenholme, 1997). It is also possible that the levels of drug administered to the host are sufficient to promote paralysis of the somatic muscle causing a rapid reduction in motility as is the case seen with piperazine (Del Castillo *et al.*, 1964).

Electrophysiological recordings on the model system, *Ascaris suum*, support the findings that avermectin paralyses worms without causing hypercontraction or flaccid paralysis. In particular, avermectin B1a appears to block transmission between the interneurones along the nerve cords and excitatory motor neurones (Kass *et al.*, 1980). The drug has little or no effect on excitatory neuromuscular transmission however it is able to inhibit transmission between inhibitory motor neurones and muscles. Blockage of interneurone stimulation of excitatory motor neurones by 5 μg/ml of avermectin B1a was reversed by subsequent addition of 10 μg/ml picrotoxin. This compound however, has no effect on avermectin blocked inhibitory motor neuronal synapses. Both picrotoxin and ivermectin inhibit the positive allosteric modulator (^{35}S)-TPBS binding to locust GABA receptors at nM concentrations (Bermudez *et al.*, 1991). This suggests that the blocking effect of avermectin may act near the picrotoxin-binding site. Avermectin effects were mimicked by two GABAergic agonists, muscimol and piperazine, inferring the drug contributes to a GABAergic mechanism (Kass *et al.*, 1984). These results suggest the presence of 2 distinct sites of action in *A. suum.*

Contrasting with the efficacy of avermectin on *H. contortus*, control of other nematode species is not so straightforward. Ivermectin given as a single dose acts as an effective microfilariacide for *Onchocerca volvulus.* However, adult filariae appear to remain unscathed by single doses of drug (Awadzi *et al.*, 1986). Following administration, embryos within the female continue to develop into microfilariae. The drug prevents expulsion of these, causing an accumulation of large numbers of microfilariae in the uterus. These gradually degrade *in utero* and resorb back into the female (Albiez *et al.*, 1988). After exposure to the drug, the adult worm slowly resumed production and release of microfilariae. It has been suggested

that the mass of decomposing tissue may block the passage to the uterus, preventing sperm to reach the seminal receptacles. This would deter any likelihood of fertilisation hindering the adult's ability to reproduce (Duke *et al.*, 1990).

Repeated dosage to infected patients with ivermectin gives no statistically significant differences to those observed in control patients. However a general trend of increased levels of moribund and dead females was observed in ivermectin treated patients. The average number of males per nodule, and hence the ratio of male to female worms, was reduced in ivermectin treated groups (Duke *et al.*, 1991a,b). The lack of efficacy of ivermectin in adults of the related filarial nematode, *O. ochengi*, was found not to be a result of failure to penetrate host nodules (Cross *et al.*, 1997). This was established by monitoring the distribution of subcutaneously injected ivermectin in infected cattle using high-pressure liquid chromatography.

The heartworm, *Dirofilaria immitis,* is a filarial nematode that parasitises ferrets and dogs. Avermectins action towards this nematode is similar to that observed for *O. volvulus* in that it causes the rapid removal of microfilariae from the blood (Blair & Campbell, 1979). Further studies have shown that maturation of nematode larvae can be prevented in dogs if ivermectin is administered 31 to 60 days after infection. If however, the drug is given 90 days following infection, maturation into adults occurs in 3 out of 5 dogs (Blair & Campbell, 1980).

Filarial nematodes are not the only class of helminths that respond in different ways to ivermectin. Variation in sensitivity to this drug also exists for members of the Ancylostomatoidea superfamily of hookworms. *Ancylostoma ceylanicun* and *Necator americanus* both infect hamsters. The latter is insensitive to ivermectin whilst the former is 300 times more sensitive in relation (Rajasekeriah *et al.*, 1989; Behnke *et al.*, 1993). *In vitro* comparison of these two hookworms demonstrated that the difference in drug sensitivity was neither attributed to the host-parasite relationship or variation in drug uptake via the cuticle (Richards *et al.*, 1995). This suggests variation in drug target site and therefore characterisation of the target from each of the described models may reveal the molecular action of the drug.

Prospective anthelmintics include paraherquamide, PF1022A, dioxapyrrolomycin and clonstachydiol. Paraherquamide is isolated from the fungus *Penicillum charlesii* and has successfully treated experimental infections of *Haemonchus contortus* in sheep (Blanchflower *et al.*, 1991). Its mode of action is believed to be different to benzimidazole and avermectin targets since nematode isolates, resistant to the latter two drugs, are eradicated by paraherquamide (Shoop *et al.*, 1990). The fungal compound, PF1022A paralyses worms by stimulating inhibitory GABA receptors on muscles while simultaneously inhibiting the cholinergic mechanism synergistically (Terada, 1992). The drug was first discovered in a screening using chickens infected with *Ascaridia galli* (Sasaki *et al.*, 1992).

The compound was also shown to be effective against *H. contortus* infection in cattle. Binding assays on *Ascaris suum* somatic muscle preparations revealed binding to $GABA_A$ type receptors with affinity, K_i of 7.41+/- 8.5 nM, 10 fold higher than piperazine, having a K_i of 856+/- 69.7 nM (Chen *et al.*, 1996). Effective control of *H. contortus* in *in vitro* experiments using Dioxapyrrolomycin, a metabolite from *Streptomyces* species, has been successful however the mode of action has yet to be identified (Conder *et al.*, 1992). A similar achievement was demonstrated with the use of a fungal metabolite, clonstachydiol isolated from *Clonostachys cylindrospora* (Grabley *et al.,* 1993).

1.5 Resistance

As previously discussed, chemotherapy is the most frequently used method of control to treat the main groups of nematode infected farm animals, sheep, goats, cattle, pigs and horses. However, this type of therapy is becoming increasingly ineffective since drug resistance has developed throughout the nematode population (Conder & Campbell, 1995). The most affected areas where nematodes are resistant to broad-spectrum drugs are South Africa, Australia and South America. The absence of drugs to combat multi-resistant populations has forced many farmers in South Africa to stop rearing sheep. Surveys carried out in countries such as Uruguay, Argentina, Paraguay, and Brazil reveal a prevalence of nematode resistant populations of 40-90% for benzimidazole, 22-84% for levamisole and up to 73 % for ivermectin (Geerts *et al.*, 1997). In comparison, resistance in Europe has not yet reached equivalent levels of severity. In this section the reasons for spread of resistance are discussed, as well as the molecular mechanisms responsible for this change in phenotype. Hopefully understanding these effects will help to minimise the spread of anthelmintic resistance across nematode populations as well as limiting the occurrence of further resistant traits.

Conder and Campbell (1995) have reviewed a number of factors contributing to the ability of nematodes to survive drug therapy. Under dosing encourages resistance and is frequently carried out by farmers who underestimate the animals weight. Farmers also tend to treat their livestock with reduced doses in order to cut costs. Sub-therapeutic doses allow survival of marginally resistant heterozygous individuals, which are then able to contribute resistant genes to subsequent generations. An error commonly made is for farmers to allow infected sheep and goats to graze together. Farmers often treat their goats with the same amount of drug as they would to their sheep; this under-dosing in goats will therefore encourage resistant populations that can then spread to sheep sharing the same pastureland. Some drugs, with the exception of avermectins, do not possess persistent activity in animals, allowing rapid re-infection after treatment. This can lead to frequent dosing and resistance. Another error that farmers tend to make is the frequent administration of a single drug until it no longer works (Reinemeyer *et al.*, 1992). A more successful result is observed when the animal is exposed to a variety of drug classes. Computer models predict that resistance can

be inhibited when two drugs are used simultaneously, while annual rotation is less effective (Barnes *et al.*, 1995).

Climatic conditions play a role in the development of resistant populations. A good example of this was found on a Greek island where sheep and goats became heavily infected with resistant worms (Coles *et al.*, 1995). The animals on this island suffered from an extended drought, preventing the survival of the majority of helminths outside the host. However, the worms that did survive became extremely resilient displaying a resistance to anthelmintics. In this particular case a resistant population was present after two drug doses had been administered. In more humid tropics 10 to 15 treatments per year have been necessary to prevent re-infection of *H. contortus* in sheep (Geerts *et al.*, 1997).

So far, each class of chemicals used to combat nematode infection has resulted in the development of resistant populations of nematodes (Conder & Campbell, 1995). Resistance towards a drug is believed to be a consequence of either decreased drug uptake, an increase in drug metabolism, or an alteration at the drug-receptor site. Studies to date suggest that it is the latter event which is the key factor contributing to resistance rather than the former two suggestions. Mechanisms for resistance towards the three broad-spectrum drugs, benzimidazole, levamisole and avermectin are under examination as a means of improving control.

1.5.1 Benzimidazole

A survey was completed in 1992 to determine the presence of benzimidazole resistant parasitic nematodes on sheep and goat farms around England (Hong & Coles, 1996). Out of the tested sheep farms in the south-west, 44 % had sheep that were infected with resistant worms compared to 15 % in the north east. Similarly 65 % of the non-dairy goat farms tested in England and Wales each had benzimidazole resistant populations. Close inspection of the nematodes confirmed that the main species found in sheep was *Ostertagia circumcincta* and *Haemonchus contortus* in goats.

Resistance developed towards benzimidazole is associated with a point mutation of Phe200 to Tyr200 in the β-tubulin isotype 1 gene near the GTP-binding domain II in *C. elegans* (Driscoll *et al.*, 1989). A similar point mutation is observed in the β-tubulin isotype 1 gene of several species of fungi whereby Gln198 is mutated to a Lys or Gly when comparing resistant and susceptible populations (Wheeler *et al.*, 1995) providing further proof that this alteration is a causative mutation. The *tub-1* gene coding for β-tubulin isotype 1 was isolated from *H. contortus* genomic DNA and transformed into *C. elegans* by injection (Kwa *et al.*, 1995). This model nematode had previously undergone gamma irradiation so that its own β–tubulin locus *ben-1* had been deleted. Expression of the *tub-1* gene restored benzimidazoles mode of action, however injection of a mutated *tub-1* gene carrying a tyrosine at position 200 instead of a phenylalanine prevented the disruption of microtubules in the presence of the drug

conferring resistance.

1.5.2 Levamisole

Levamisole resistance has been observed in the trichostrongylid nematodes, *Ostertagia circumcinta* and *Trichostrongylus colubriformis.* In Australia, resistance of these nematodes to levamisole is present on up to 90% of sheep raising properties. This level of resistance is similar in other countries, however it is lower in Europe where levamisole resistance in *H. contortus* is rare (Overend *et al.*, 1994 & Waller *et al.*, 1995). Ligand binding studies suggest that levamisole binds to two populations of acetylcholine receptor in *H. contortus.* Two different binding sites have been detected, one of high affinity with a K_d of $2.9x10^{-9}$ M and B_{max} of $4x10^{-9}$ mol/mg of protein and the other of lower affinity of K_d 2-10 μM (Sangster, 1996 & Sangster *et al.*, 1991). The affinity of the first population of levamisole receptors remained the same in susceptible and resistant isolates, however the K_d and B_{max} of the lower affinity receptors increased. This suggested that levamisole resistance in *H. contortus* resulted from increased levels of low affinity levamisole receptors. Interestingly, in *C. elegans,* mutations in the *unc-50 gene*, which does not encode a receptor subunit causes a decrease in levamisole binding. It has been suggested that this protein plays a role in receptor gene transcription or receptor assembly (Lewis *et al.*, 1987).

Comparison of a levamisole receptor subunit denoted *Hca1* from levamisole-susceptible and -resistant *H. contortus* revealed levels of 98.5-100% homology at the amino acid level upon examination of 4-5 individual clones taken from each of the two populations (Hoekstra *et al.*, 1997). From these results it was concluded that any polymorphisms that were detected in the clones were not consistent and were thus not associated with levamisole resistance.

1.5.3 Avermectin

The mechanism for resistance towards avermectins is still unknown. The most common resistance developed in *C. elegans* isolates allows worms to survive exposure to low levels of drug (Novak & Vanek, 1992). Comparison of resistant and susceptible populations revealed a series of recessive mutations that map to more than 20 loci. Two genes, *avr-1* and *avr-5,* are allelic to the previously known loci *che-3* and *osm-3* respectively, each displaying phenotypes defective in dye-filling (Perkins *et al.*, 1986 & Stravich *et al.*, 1995). This term reflects the ability of chemosensory receptors, known as the amphids and phasmids, to take up a dye. The ability to visualise pores on the surface of the nematode by filling with dye has been utilised as a marker to identify nematodes that possess amphids and phasmids with those that don't thus facilitating the classification of different species. Wild-type *C. elegans* have both amphids and phasmids, however the *che-3* and *osm-3* animals lack the ability to take up dye though their chemosensory receptors. Cloning of the *avr-1* gene identified a cytoplasmic dynein protein, believed to play a role in the amphidial neuronal transport process. It has been postulated that *C. elegans* takes up the drug via the amphids, allowing it to reach its target (Blaxter & Bird, 1997). In contrast, avermectin resistant nematodes are

thought to prevent avermectin uptake as a result of defective proteins present at the amphids.

It is also possible that resistance has developed as a result of an alteration at the drug-receptor site. As already mentioned, avermectin binds irreversibly to glutamate-gated chloride channels in avermectin susceptible-worms (Arena *et al.,* 1992). Resistance therefore may result from a mutation in the DNA coding for the receptor thus blocking avermectin binding. This would in effect prevent the irreversible opening of the channel to chloride ions. Studies using ivermectin-susceptible and -resistant isolates of *H. contortus* L3 larvae reveal high affinity ivermectin binding sites with a K_d of 0.13 nM and a B_{max} of 0.4 pmol/mg for both isolates (Rohrer *et al.*, 1994). In this particular case, both isolates possess the same avermectin binding properties, suggesting that a modification at the target site is not involved in the development of resistance. There is some debate as to whether these results represent a true model for resistance, as nematodes were laboratory derived rather than field isolates.

Contrasting with the latter findings the avr-15 gene was found to confer ivermectin sensitivity on *C. elegans.* Dent and co-workers (1997) discovered that this gene encoded two alternatively spliced channel subunits, GluClα2-A and –B, both of which being components of the glutamate gated chloride channel. Comparison of the two spliced products, from avermectin-susceptible and –resistant worm pools, revealed a guanine to alanine transition at the third position of the W271 codon of GluClα2A, thus creating an opal stop codon. A Northern blot confirmed that levels of both transcripts were reduced for both GluClα2-A and -B at least two fold and four fold respectively. This was accounted for by the ability of *C.elegans* to degrade mRNAs containing nonsense mutations such as the opal stop codon in resistant worms at position 271.

1.6 Nematode anatomy

The majority of anthemintics used so far target the nematode's nervous system. It is however also apparent that nematodes are becoming resistant to the majority of these drugs. This will inevitably cause a problem for farmers in the future. One approach to overcome this is to study the worm's nervous system in hope of determining the underlying principles for the development of resistance. This approach may also yield novel targets for mechanism based screening programmes. Locomotion and feeding by nematodes is mediated by the nervous system. In this section the neural anatomy of *C. elegans* is described so that an understanding of how anthelmintics interact with specific neurones can be obtained. A similar connectivity network is seen in *A. suum.* This neuronal map is therefore believed to be a good model for other nematodes including *H. contortus.*

1.6.1 Locomotion

Nematodes achieve locomotion by alternate contraction and relaxation of dorsal and ventral

muscles dictated by the nervous system. This gives rise to a sinusoidal wave propagation along the length of their bodies (Wharton, 1986). Forward motion is achieved by waves of contraction initiated at the anterior of the worm passing down to the posterior. Likewise, backward movement is accomplished by wave propagation in a posterior to anterior direction. A consequence of this specific movement is that the worm is forced to lie on its side. The efficiency with which nematodes move improves with the amount of friction they experience with their environment. The presence of longitudinal lateral ridges (alae) of cuticle spanning the length of their bodies helps increase the level of friction. The head region of the nematode has a greater degree of freedom moving in both a lateral and dorso-ventral direction. This is a direct result of innervating lateral muscles as well as dorsal and ventral muscles in the head, permitting the worm to detect environmental cues.

1.6.2 Nervous system

The most characterised nematode nervous system is that of the free-living worm, *Caenorhabditis elegans*, reconstructed from electron micrographs of 50 nm thick serial sections (White *et al.*, 1986). The hermaphrodite nervous system is composed of 302 neurones, of which at least 12 are sexually specialised involving egg laying. In contrast, males have 381 neurones, 87 of which are sexual, most of which are present in the tail innervating the copulatory bursa. The following descriptions have been summarised from the work of White *et al.* (1986) unless otherwise stated.

1.6.2.1 Sensory cells

Nematodes monitor environmental cues using a combination of sensory organs or sensilla receptive to chemicals, pressure, touch and temperature. Each sensillium is composed of a socket cell, a glial-like cell known as a sheath cell and one or more nerve endings. Papillae, receptive to chemical stimuli, have an internal channel, which is formed by the sheath and socket cells, and opens up through the cuticle to the outside. Nerve endings reach out onto the surface of the channel allowing exposure to the external environment. Mechanosensory organs are different in that they do not have a channel that opens up to the exterior. Rather, their nerve endings penetrate the sheath cell instead of being exposed on the cuticular lining.

Specialised sensilla are abundant in the head of the nematode and are most concentrated around the mouth or buccal cavity. At the entrance of the buccal cavity there are 6 cephalic lips, a finger-like projection or bristle stems from each of these forming a circle of inner labial papillae. Surrounding the inner circle is an outer circle of a further 6 papillae and exterior to this, is a cephalic circlet of 4 papillae. The 6 inner labial sensilla are chemosensory organs, whilst the outer circle of papillae and the cephalic circlet are mechanoreceptors. Each papilla contains one or more nerve endings, which are supplied by sub-dorsal, lateral or sub-ventral cords extending from the papillary ganglia. These ganglia link directly to the anterior side of the nerve ring. Amphids are the main chemoreceptive organs in the nematode and are located one in each lateral quadrant, in line with the cephalic circlet. A total of 8 sensory

neurones have dendritic nerve endings that come into direct contact with the external environment via the open channel, and a further 4 are associated with the sheath cell. These neurones originate from nerve fibres that run down to laterally positioned amphid ganglia, found posterior to the nerve ring. Similar structures to the amphids are present in the tail and are called the phasmids. These differ in that they expose only 2 neuronal endings, as opposed to the amphids 8, to the external environment. Neuronal architecture of the sensory neurones is mapped out in figure 5a.

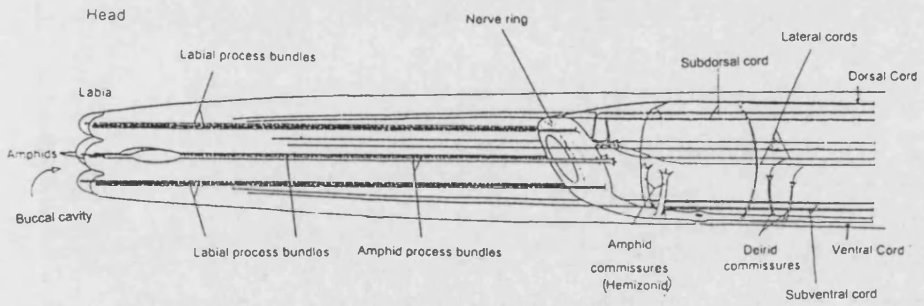

Figure 5a, Sensory neurones in the head. Labial and amphid process bundles are displayed running from the nerve ring to the labia and amphids respectively lining the buccal cavity of *C. elegans* . Adapted from White *et al.*, 1986.

Other sensilla include the 2 pairs of lateral receptors called the deirids or cervical papillae. These mechanosensory sensilla, having no external access, are situated in the lateral quadrants of the nematode, one pair posterior to the excretory pore and the other in the posterior portion of the body approaching the tail. They are believed to be responsible for determining whether the worms can pass through restricted gaps.

1.6.2.2 Central Nervous System (Nerve Ring)

The central nervous system surrounds the midpoint, or isthmus, of the pharynx and consists of ganglionated nerve tissue linked together by a circumoesphangeal commissure termed the nerve ring. This ring sits at an oblique angle with the dorsal side raised at a more anterior site than the oppositely located ventral side.

1.6.2.3 Peripheral Nervous system

Nerve processes connected to the cephalic sensillia, run in longitudinal tracts down to the front of the nerve ring where their cell bodies associate to form the anterior ganglion. Posterior to the nerve ring, ganglia are split by the basement membrane into four groups: a ventral ganglion, a small dorsal ganglion and two lateral ganglia. Nerve bundles connected

to amphids, run adjacent to laterally positioned tracts, bypassing the nerve ring completely and assembling their cell bodies in lateral ganglia. Amphid associated neurones are bipolar, with processes extending from lateral ganglia forming the amphid commissure which runs to the ventral midline.

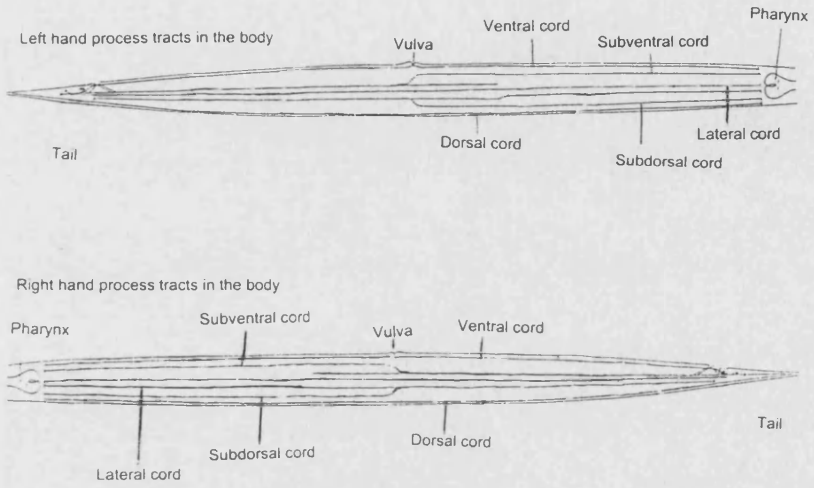

Figure 5b, The peripheral nervous system. Both left- and right-hand sections of the *C. elegans* body are displayed. Note that no detail of the head is given. Adapted from White *et al.*, 1986.

Ventral, dorsal and lateral nerve tracts project out of the respective ganglion and associate with longitudinal hypodermal ridges, extending posteriorly to the tail. The four tracts, shielded from the pseudocoelum by a layer of basal laminae, section the body symmetrically into quadrants. The ventral ganglion is separated into two groups by the presence of the excretory duct, cell bodies posterior to the duct overlap with the retrovesicular ganglion, but each ganglion remains an individual entity due to separation by the basal lamina. Nerve processes made up of interneurones and motor neurones, emerge from both ventral and retrovesicular ganglia forming a ventral cord (figure 5b). A single row of motor neurone cell bodies span the length of this cord before it terminates at the pre-anal ganglion in the tail. Seven main classes of motor neurones are present in the ventral cord of *C. elegans* denoted VAn, VBn and VDn innervating ventral muscle and DAn, DBn, ASn and DDn innervating dorsal muscle. These groups of motor neurone receive synaptic input from five types of interneurone denoted AVA, AVB, AVD, AVE and PVC. The cell bodies from the former 4 classes are situated in the lateral ganglia whilst PVC interneurones have cell bodies located in the lumbar ganglia, in the tail. Processes from AVA, AVB and AVD span the whole length of the ventral cord whereas the AVE set of neurones terminates in the mid-body region. Innervation of VAn, DAn, VBn, ASn and DBn results in the release of the excitatory neurotransmitter acetylcholine at neuromuscular junctions thus causing contraction of muscle

cells. Contraction of muscle groups in one quadrant coincides with the relaxation of the opposite quadrant. This is achieved by the release of GABA from VDn and DDn motor neurones, defined as VI and VD motor neurones in *Ascaris*, at neuromuscular junctions on to muscle (Johnson & Stretton, 1987).

The dorsal quadrant of *C. elegans* contains a dorsal ganglion and two small subdorsal ganglia. These are in close proximity to the nerve ring, and each comprises of two neuronal cell bodies. Dorsal cords extending from these ganglia contain no cell bodies but are predominantly made up of motor neurone axons that originate from the ventral cord. Connection of cords is achieved by motor neurones branching from the ventral cord to form commissures. These run around the circumference in contact with the hypodermis, to the dorsal cord (figure 5b).

Each lateral quadrant contains a lateral ganglion composed of cell bodies from interneurones, motor neurones and amphid associated sensory neurones. Processes from these neurones emanate from the ganglia forming lateral nerve cords, which terminate in the lumbar ganglia in the tail (figure 5b). As previously mentioned bipolar sensory neuronal processes branch away from each lateral cord, forming a commissure that connects to the ventral cord. Also spanning the lengths of the lateral cords are sensory neurones receptive to touch and are thus known as dendritic touch receptors.

1.6.2.4 Commissures

In whole mount preparations of the nematode, the hemizonid is identified as a biconcave, highly refractive band consisting of a tight bundle of axon processes. It is located in the vicinity of the excretory pore, its exact position depending on the species of nematode examined. In *C. elegans* it is located anterior to the pore whereas in L3 infective larvae of *Haemonchus contortus* it lies posterior to the pore (Rogers, 1968). This belt of nerve fibres extends from deirids in lateral fields, where present, around the circumference of the nematode to the ventral cord thus appearing semicircular in shape (figure 5c). Nerve endings from this structure are separated from the cuticle by a very narrow layer of hypodermal tissue. The cuticle directly above this structure appears to be modified in *H. contortus* having tightly packed annular striations in this area. It had originally been proposed that the hemizonid was a sensory receptor triggering the synthesis of neurosecretory granules. It had been hypothesised that these neurosecretions stimulated the production of enzymes present in the exsheathing fluid, thus initiating moulting (McLaren, 1976). A more recent report however has proposed that the hemizonid is more likely to be the amphid commissure (Bird & Bird, 1991). In 1986, White *et al.* identified a total of 44 nerve axons present in the *C. elegans* amphid commissure.

Directly neighbouring the amphid commissure is a sublateral commissure consisting of 10 axons, which run adjacent to the hypodermis until they reach sublateral lines. They then turn

to form longitudinal cords stretching down to the vulva. It is in this region that they merge with lateral cords (figure 5c). The deirid commissure is situated slightly further down stream from amphid and sublateral commissure and consists if 11 axon fibres (figure 5c). Commissures derived from motor neurones have cell bodies that are present in the ventral cord but have axons that branch out, crossing lateral lines and connecting to the dorsal nerve cord (figure 5c).

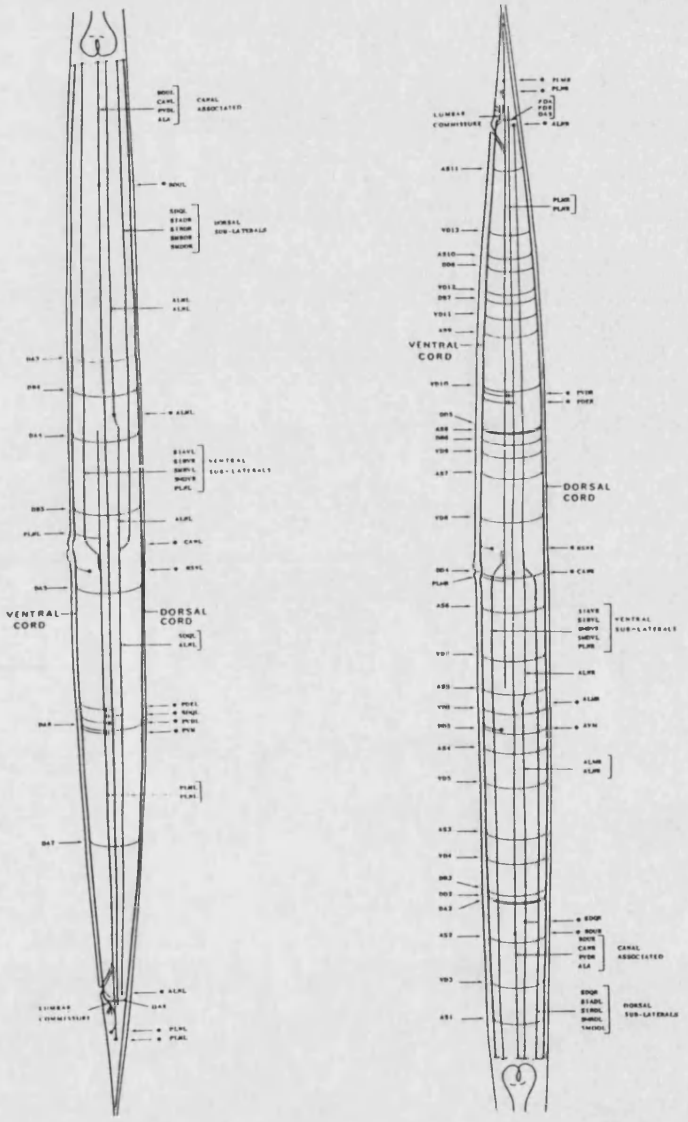

left hand right hand

Figure 5c, Commissures. This diagrams features the existing commissures mapped out in the *C. elegans* nervous system. Adapted from White *et al.*, 1986.

1.6.2.5 Neuromuscular organisation

Nematode somatic muscle cells are unusual in that they send out processes that form neuromuscular junctions with neurones in the nerve cord rather than neurones sending out processes that synapse on to muscles. Each somatic muscle cell has a longitudinal contractile region, known as the spindle, made of regularly arranged, thick myosin filaments and thin actin containing filaments aligned at an angle of 10° to the z-line (White *et al.*, 1986). This obliquely striated organisation runs beneath the epidermis of the worm. Each spindle is connected to a non-contractile muscle cell body containing a nucleus, cytoplasmic organelles including high levels of mitochondria, and glycogen. This bulbous bag-like structure projects into the pseudocoleum. The last feature, characteristic to these cells, is a thin process called

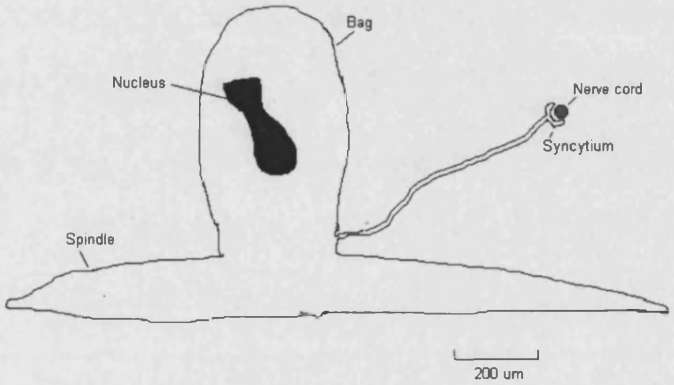

Figure 5d, The muscle cell structure and its neuromuscular junction.

the arm that emanates from the cell body to either dorsal or ventral nerve cords. The arm terminates in a structure called the syncytium which has a number of fine finger-like projections extending from its surface forming neuromuscular junctions on to a motor neurone axon (figure 5d).

The ventral, dorsal and lateral hypodermal ridges divide the body into four symmetric domains. *C. elegans* has a total of 95 somatic muscle cells, 24 cells lining each domain with the exception of the left ventral quadrant which contains 23 muscle cells. Cells from each quadrant are arranged in 2 parallel rows and are classified into three groups depending on the source of their synaptic input. An anterior group is located above the nerve ring containing 4 muscle cells per quadrant, a total of 16 cells, all sending arms that synapse on to the inside surface of the nerve ring. The next 16 cells, 4 in each quadrant are dually innervated by motor neurones present in the nerve ring and the ventral cord. Foraging movements made by the head results from the differential activation of muscle cells in adjacent quadrants as well as in adjacent rows creating lateral waves of muscle contraction

as well as dorso-ventral waves. The remaining muscle cells connect to motor neurones, which originate from the ventral cord and span both dorsal and ventral midlines. Stimulation of these muscles provokes sinusoidal waves that propagate along the length of the body.

1.6.3 Pharynx

Nematodes ingest nutrients via the buccal cavity, from where the nutrients are propelled by the pharynx into the intestine. Omission of this pumping action induced by blocking pharyngeal muscle action causes starvation. The pharynx of *C. elegans*, reviewed by Albertson & Thomson (1975), is a self contained, tubular organ having its own musculature and nervous system, with the exception of two interneurones, originating from the worm's central nervous system. These neurones, denoted RIP cells, are believed to mediate the overall control of pharyngeal pumping. The pharynx is separated from the rest of the nematode by a basement membrane and is composed of 34 muscle cells, 9 marginal cell, 9 epithelial cells, 5 gland cells and 20 neurones. The organ has three compartments: the corpus, isthmus and the terminal bulb (figure 6a). The corpus is located most anterior and functions to filter food from the buccal cavity. This compartment is subdivided into the procorpus and the metacorpus. Neighbouring this is the isthmus, which delivers food to the terminal bulb, where grinding takes place. Two types of motions induced by the muscle cells propel food through the pharynx by creating a pumping action. The first is a near simultaneous contraction of the corpus, anterior isthmus and terminal bulb, followed 200ms later by relaxation of parts. The second motion induces peristalsis whereby the isthmus drives a posteriorly directed wave of contraction, thus sending food towards the terminal bulb (Raizen & Avery, 1994). The lumen of both the buccal cavity and the pharynx are lined with cuticle that is continuous with the external body cuticle. Eight muscle types, denoted pm1 to pm8, line the pharynx and are innervated by motor neurones, M1 to M5 (figure 6b).

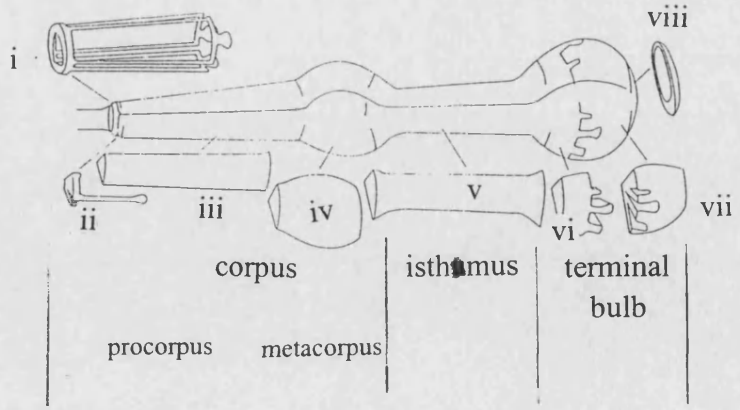

Figure 6a, Anatomy of the *C. elegans* pharynx. The three compartments 1) the corpus, which is split into procorpus and metacorpus chambers, 2) the isthmus and 3) the terminal bulb. These structures are composed of muscle cells as indicated. Key: i) pharyngeal muscle, pm1, ii) pm2, iii) pm3, iv) pm4, v) pm5, vi) pm6, vii) pm7 and viii) pm8. Adapted from Albertson & Thomson, 1976.

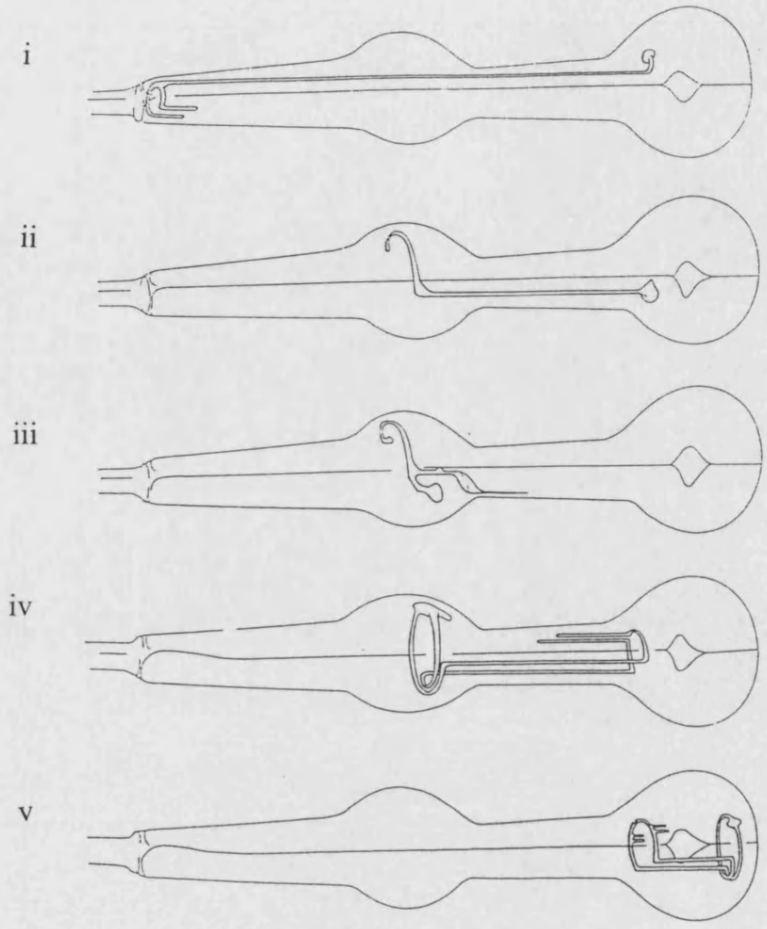

Figure 6b, Organisation of the pharyngeal motor neurones. The pm cells are innervated by 5 different motor neurones, M1-M5. Positions of these motor neurones are displayed. i) motor neurone M1, ii) M2, iii) M3, iv) M4, and v) M5. Adapted from Albertson & Thomson, 1976.

1.7 Nematode Fast Ion Channel Receptors, TGIC

This section details the superfamily of channels, localised to the nervous system, that are believed to be drug target sites. Knowledge of the function and mechanism by which drugs bind to these sites should help in the search for more effective drugs.

Sequence similarity between the polypeptide chains, coding nicotinic acetylcholine-, GABA-, glycine- and glutamate gated chloride-channels, forms a basis for classifying them as superfamily of transmitter-gated ion channels (TGICs). The following considers each of these channels and details on the known subunits that associate to form the receptor types. This includes the glutamate-gated chloride channels, denoted GluClRs that are targeted by

avermectin. Pharmacological properties of associated subunits are described as well as their localisation within the nematode's nervous system.

Identification of neurones that express GABA receptors in *C. elegans* is discussed as well as phenotypic observations form worms that no longer express them. These findings highlight the importance of a fully functional class of receptors that enable locomotion characteristic of wild type nematodes. The most characterised members of the ligand-gated ion channel superfamily are the nicotinic acetylcholine receptors (nAChRs). Topology of these receptors is outlined since this has provided a model for related receptors such as the GluClRs. Predicted binding sites for neurotransmitters such as GABA and glutamate are detailed along with possible sites for avermectin to bind to. These regions can be compared in subunits isolated from avermectin susceptible and resistant populations of nematodes including *H. contortus*. The current status of GluClR subunits isolated from the parasitic nematode *Haemonchus contortus* is discussed along with aims to further categorise this drug target.

1.7.1 Glutamate-gated chloride channels

The inhibitory glutamate receptor (GluClR) is a member of the ligand gated ion channel superfamily possessing a pharmalogical profile distict from glutamate gated cation channels, GABA and glycine gated channels (Cully *et al.*, 1994). As yet, no evidence supports their presence in vertebrates however they seem to be a common feature of invertebrates and have been described as H-receptors due to the hyperpolarising response induced by glutamate (Cully *et al.*, 1996a). The first report, identifying the existance of GluClRs or H-receptors, was by Cull-Candy & Usherwood on *Schistocerca gregaria* (locust) leg muscle, the extensor tibiae, in 1973. This was followed by their detection in insects, crustaceans and molluscs.

Studies into the mechanism of action of the anthelmintic drug avermectin on nematodes have led to the recognition of GluClRs as being their target (Arena *et al.*, 1991, 1992). This discovery has encouraged much study into the inhibitory class of glutamate receptors. Initially poly $(A)^+$ RNA from the free-living nematode *C. elegans* was injected into *Xenopus laevis* oocytes. Exposure of these ooctyes to the synthetic avermectin derivative, ivermectin 4'-O-phosphate ($IVMPO_4$), evoked inward membrane currents resulting from an influx of chloride into the cell having a dissociation constant K_d of 90 nM and a Hill coefficient of 1.1 (Arena *et al.*, 1991). Further work identified glutamate to be responsible for activating inward membrane currents, which were inhibited by the chloride channel blockers: picrotoxin and flufenamate. Co-application of avermectin with glutamate provided evidence of a glutamate receptor that was potentiated by avermectin shifting the glutamate dose response curve to the left, slowing receptor desensitisation (Arena *et al.*, 1992). A reduction in the Hill coefficient from approximately 2 to 1.0 was recorded, implying that in the presence of avermectin only one molecule of glutamate needs to bind in order to open the channel (Arena *et al.*, 1994).

The two insect species, *Drosophila melangastor* and the locust *Schistocerca americana* are also believed to possess a similar target. *D. melangastor* heads and the metathoracic ganglia from locusts are enriched with high affinity avermectin binding sites. A photoaffinity probe of (^{125}I)-arylazido-avermectin identified a 45 kDa protein from both sources of neuronal membranes (Rohrer *et al.*, 1995).

1.7.1.1 GluClR Subunits

To date, each of the GluClR subunits sequenced are typical of ligand gated ion channels with topology based on that observed for the nicotinic acetylcholine receptor (Unwin, 1993). They have long N-terminal extracellular domains coding one or more N-linked glycosylation sites and two highly conserved cysteine residues that form the characteristic cys-loop. In addition to these residues, a further 2 cysteines are located between the cys-loop and the first transmembrane region (TM1) that are also characteristic of vertebrate glycine gated chloride channels. Following the N-domain are four transmembrane domains, denoted TM1 to TM4. TM3 and TM4 are connected by a long intracellular loop of variable length containing consensus sites for phosphorylation such as those recognised by protein kinase C (Cully *et al.*, 1994).

The first two glutamate-gated chloride channel subunits to be isolated in nematodes were the GluCl-α and -β subunits from *Caenorhabditis elegans* (Cully *et al.*, 1994). The two subunits were expressed as homomeric channels following injection into *Xenopus* oocytes. GluCl-β channels were reversibly responsive to glutamate at a 1mM concentration whereas GluCl-α channels responded irreversibly to 1 μM of ivermectin. Co-expression of α and β subunits, resulted in the formation of heteromeric channels, responding to glutamate at μM concentrations and potentiated by 5 nM IVMPO$_4$. Simultaneous expression of the two subunits resulted in a shift in the EC_{50} value for glutamate from 380+/-20 (for the homomeric β channels) to 1,360+/-50 μM (for heteromeric channels). The Hill coefficient for GluCl-α and -β channels was calculated as 1.7+/-0.1 suggesting that more than one glutamate molecule was necessary to gate the channels. The GluClα sequence consisted of 1,383 bp coding for a 461 amino acid polypeptide, likewise GluClβ was 1,302 bp in size coding a polypeptide of 434 amino acids. Pharmacological properties differ in ooctyes injected with GluCl α and β to those injected with poly $(A)^+$ RNA indicating that additional subunits are required to form the wild type channel. Subsequent to these findings the GluClα sequence has been mapped to chromosome V (Dent *et al.*, 1997) and GluClβ to chromosome I (Laughton *et al.*, 1995).

Phylogenetic analysis has been aided by gene structure comparison (Vassilatis *et al.*, 1997). Several introns, specific to GluClRs, are absent in other ligand-gated ion channels, giving them a distinct evolutionary position. GluClα and GluClβ are thought to form a monophyletic sub-branch in the TGIC superfamily being most related to the vertebrate glycine receptors. In light of α and β sequence properties it has been suggested that these subunits may even represent genes orthologous to vertebrate glycine receptors. GluClRs share the feature of 2

conserved cys-cys pairs with the glycine receptors compared to GABA receptors, which only possess one of these pairs. A tyrosine residue at position 182 of GluClβ is conserved in both GABA and GluCl receptors. Glycine channels however, incorporate a phenylalanine at this site. Mutation of this residue alone was sufficient to change a glycine receptor into a GABA receptor (Schmieden *et al.*, 1993). This finding suggests that the tyrosine residue is responsible for the absence of glycine sensitivity among GluClRs and supports the possibility of these receptors being the othologues of the vertebrate glycine receptors.

Two further glutamate-gated chloride channel α subunits have been isolated from *C. elegans,* as a result the GluClα subunit isolated by Cully *et al.* (1994) will therefore now be described as GluClα1. The two novel subunits are products from the differentially spliced GluClα2 gene, which was found to map to the same position as the *avr-15* gene on chromosome I (Dent *et al.*, 1997). Worms possessing mutant *avr* genes confer resistance to avermectin. The two resulting alternatively spliced sequences differ only at the 5' extremity of the N-terminal extracellular domain with one variant coding 23 unshared amino acids (GluClα2A) and the second variant having an extra 202 amino acid chain (GluClα2B). Each stretch of amino acids is then followed by shared exons encoding a putative ligand binding domain and transmembrane spanning regions. Mature GluClα2A of 459 amino acids was 85 % identical to GluClα1 at the amino acid level followed by having a 45 % amino acid identity with GluClβ. The mRNA levels of GluClα2A (1.7 kbp) was twice that detected for GluClα2B (2.2 kbp). Expression of GluClα2A homomeric channels in *Xenopus* oocytes were activated by both ivermectin and glutamate.

A second set of alternatively spliced products, share the same 237 amino acid N-terminal extracellular sequence followed by different, though closely related, C-terminals (Laughton *et al.*, 1997b). These were denoted GBR-2A and GBR-2B, whose mRNA was 2.15 kbp long (coding a polypeptide of 416 amino acids) and 1250 bp (coding a 430 amino acid sequence) respectively. These putative sequences were most closely related to the GluClα1 subunit sharing an amino acid identity of about 55 %. This percentage is believed to be too low to qualify GBR-2A and -2B as alpha subunits, it has therefore been suggested that they form a third class of inhibitory glutamate gated receptor subunits of γ type.

Upon examination of the amino acid sequence for GBR-2A and -2B, variance occurs along the intracellular loop located between TM3 and TM4. Comparison reveals the presence of differing numbers of phosphorylation motifs with GBR-2A possessing 2 consensus sites for phosphorylation by protein kinase C contrasting with GBR-2B having 3 consensus sites for phosphorylation by protein kinase C, 2 for cAMP-dependent protein kinase and 2 for casein kinase 2. These differences infer that the two subunit-proteins are regulated by different mechanisms.

Additional partial sequences have been isolated from the filarial nematodes *Onchocera*

volvulus and *Dirofilaria immitis* and are both called GluClX, sequence obtained for the former codes for 330 amino acid residues (accession number U59745) whilst the translated sequence for the latter codes 141 residues (accession number U59744). These two filarial clones are believed to be orthologues of GBR-2. It is however uncertain as to whether the filarial forms of GBR-2 are the products of alternative splicing. The predicted sequences, C27H5.5 and ZC317.7, have been identified by the *C. elegans* genome sequencing project and are also predicted to be members of this family of inhibitory receptors.

Another GluClR subunit, denoted *Dros* GluCl-α (accession number U58776), has been isolated from *Drosophila melangastor,* by probing a cDNA library (Cully *et al.*, 1996b). This 456 amino acid protein was coded by a 3958 bp mRNA transcript and shares a 48 % amino acid identity with the *C. elegans* GluCl-α subunit. Responses were measured to gating by glutamate (EC_{50} of 23 μM, Hill coefficient of 2.0) and irreversible gating by avermectin when expressed as homomeric channels in *Xenopus* oocytes. Despite avermectins ability to bind to the channel it is unable to induce any potentiation.

1.7.1.2 Localisation of subunits in nematodes

To date only two receptor subunits have localised to specific cells in the nematode *C. elegans*. These are GluClβ (Laughton *et al.*, 1997a) and GluClα2A (Dent *et al.*, 1997) whose spatial expression was deciphered by using reporter gene constructs. Laughton *et al.* (1997a) designed a construct that encoded the GluClβ gene promoter along with the first 24 amino acid residues of the receptor subunit followed by the lac-Z reporter (Fire *et al.*, 1990). Stable lines of transformed *C. elegans* were assayed for β-galactosidase activity, resulting from the formation of the translational fusion. Expression of GluClβ was observed in the pm4 muscles situated in the metacorpus of the pharynx at all stages of development. Additional activity was also seen in the larval stages L1 to L3 towards the terminal bulb of the pharynx.

Dent *et al.* (1997) localised the receptor subunit GluClα2A by fusing the first three exons of the gene for green fluorescent protein, GFP (Chalfie *et al,* 1994). Stable lines of transformed *C. elegans* exhibited fluorescence in pm4 cells of the metacorpus as well as the isthmus pm5 muscle cells. A few neurones found in the head of the nematode were also found to express the GluClα2A-GFP fusion.

Both pm4 and pm5 pharyngeal muscle cells are innervated by the M3 neurone (Albertson & Thomson, 1975). The presence of post-synaptic GluClRs on muscle cells stimulated by the M3 neurone suggests that the neurone releases the neurotransmitter glutamate at the synapses. *C. elegans* pharyngeal preparations were utilised in a series of patch clamp experiments to monitor single channel currents produced as ion channels open and close (Li *et al.*, 1997). Biologically non-active neurotransmitters were synthesised possessing a N-(α-carboxy-2-nitrobenzyl) group, transforming then into photolabile or caged compounds. A pulse of ultra violet light was used to convert these compounds into active neurotransmitter.

This could be achieved at a localised area of the dissected pharynx within microseconds. Electropharyngeograms (EPGs) were recorded to establish the current transients associated with muscle contraction and relaxation. In between these two phases a small number of negative spikes, referred to as inhibitory post-synaptic potentials (IPSPs), can be detected. Removal of the two M3 neurones from the pharynx led to an absence of IPSPs resulting in a longer time interval between contraction and relaxation of muscle implying that M3 neurones are required to induce relaxation. Application of caged glutamate on pharynxes that have had their M3 neurones removed by laser ablation, followed by localised photolysis at the pm4 muscles of the metacorpus, generated the renewal of IPSPs. The pm5 muscles of the isthmus were also able to respond to a lesser extent to glutamate.

Avermectin receptors have been detected along *Ascaris suum* nerve cords preventing hyperpolarisation of somatic muscles from direct stimulation of the VI neurones, corresponding to VD and DD motor neurones in *C.elegans* (Kass *et al.*, 1980). Transmission between interneurones and motor neurones along the nerve cord was blocked by avermectin suggesting that GlUCIRs were present along this region, although to date no spatial expression has been published.

1.7.2 GABA receptors

1.7.2.1 Nematode subunits

A second set of inhibitory ion channel receptor is the GABA receptor. To date, only one gene in *C. elegans*, UNC-49, is known to encode a component of the GABA-gated chloride channel (MacIntire *et al.*, 1993a): moreover this gene has the potential to encode several proteins via splicing mechanisms that are members of this family of receptors (Bamber *et al.*, 1997). An excitatory GABAergic receptor may be present on the surface of enteric muscles. It is thought to play a role in the defecation cycle in *C. elegans*, consequently a gene has been identified denoted *exp-1* that may encode a component required in the regulation of this excitatory transmission (Avery & Thomas, 1997).

In *Haemonchus contortus*, isolation of a putative inhibitory amino acid receptor subunit having a 32 % homology to the rat $GABA_A$ receptor α-subunit was reported (Laughton *et al.*, 1994). Expression of homomeric channels in *Xenopus* oocytes gave no response to 1 mM GABA or acetylcholine, however application of 1 mM glycine invoked a small depolarisation in 5 out of 20 oocytes tested. To date, evidence of an inhibitory glycine receptor in nematodes does not exist therefore the recorded measurements may reflect an artefact resulting from the use of one subunit type in a multimeric channel.

1.7.2.2 Localisation in Nematodes

The locations of 26 neurones out of a total of 302, present in the *C. elegans* adult hermaphrodite, were identified using an antiserum raised against GABA. These GABAergic neurones comprised of 6 DD motor neurones, 13 VD, 4 RME, 1 DVB and 1 AVL as well as

one RIS interneurone (McIntire *et al.*, 1993b). The function of these cells was determined by selective laser beam microsurgery on each of the 26 neurones as well as characterising mutants that were defective in GABA expression. The sole use of these techniques however, was unable to determine the function of the RIS neurone, which was located in the nerve ring. Ablation of this neurone had no effect, with the resultant nematode possessing a wild-type phenotype. In accordance to *C. elegans* immunolocalisation, *Ascaris suum* GABA immunoreactivity appeared to be most concentrated at corresponding VD and DD motor neurones (Johnson & Stretton, 1987).

The GABAergic VD and DD motor neurones innervate body muscles required for the sinusoidal mode of locomotion. Innervation results in a wave of alternating contraction and relaxation on opposing ventral and dorsal muscles. An example of their action is when the excitatory motor neurones VA and VB release acetylcholine causing the ventral muscles to contract. These neurones simultaneously stimulate DD motor neurones, which respond by releasing GABA on to reciprocal dorsal muscle causing relaxation. Ablation of DD and VD motor neurones result in instant contraction of the dorsal and ventral body wall muscles due to the excitatory transmission becoming the sole form of muscle innervation (McIntire *et al.*, 1993b). The resulting "shrinker" phenotype observed in VD and DD ablated worms, is that the body shrinks in response to touch.

The four RME motor neurones control the extent of movement produced by the head necessary for foraging (McIntire *et al.*, 1993b). These innervate muscles in the head providing it with the ability to move rapidly from side to side within a restricted arc. This movement is grossly exaggerated when the RME cells are ablated; individuals following this treatment are described as having a loopy phenotype. GABA released by the RME cells is believed to limit the extent of head deflection during foraging.

The AVL and DVB motor neurones stimulate the enteric muscle required for defecation. These GABAergic cells are unusual in that they are excitatory, causing contraction of the intestinal, sphincter and anal repressors during the act of defecation. Ablation of these two neurones decreases the frequency of enteric muscle contraction (McIntire *et al.*, 1993b).

Mutations detected in five genes, *unc-25*, *unc-30*, *unc-46*, *unc-47* and *unc-49,* have been divided into three classes, depending at which stage GABA transmission is affected (McIntire *et al.*, 1993a). Three of the five genes, *unc-25*, *unc-46* and *unc-47* have defective presynaptic function. The *unc-25* mutant lacks the ability to synthesis GABA, as the gene encodes the enzyme glutamic acid decarboxylase or GAD, thus preventing production of GABA from glutamic acid. The observed phenotype of *unc-25* mutants is similar to that produced by ablation of all the GABAergic neurones, with shrinkage of loopy worms that are unable to defecate. Similarly, *unc-47* and *unc–46* mutants prevent the normal release of GABA into the synaptic cleft. These mutants displayed the same phenotype as *unc-25*

mutants although defects observed in *unc-46* were weaker. The *unc-47* mutant appeared to accumulate elevated amounts of GABA immunoreactivity suggesting that it coded for a GABA vesicular transporter. In both mutants, GABA functions do not differ to those found in wild type, therefore these genes may define components believed to contribute to packaging of GABA into synaptic vesicles, transport or fusion to the synaptic membrane.

The phenotype of *unc-30* mutants is that of a "shrinker", unlike the mutants that affect presynaptic function these do not have "loopy" or defecation defective phenotypes. This suggests that the presence of UNC-30 promotes the differentiation of type-D GABAergic neurones, VD and DD.

The *unc-49* gene is required for post-synaptic function coding for an inhibitory $GABA_A$-like receptor subunit. These mutants are both "loopy" and "shrinkers" but do not cause defective defecation, indicating its absence in AVL and DVB neurones.

Skinner (1997) localised the HG1 receptor subunit in both *H. contortus* and *A. suum.* An antiserum was raised to a synthetic peptide, the sequence of which corresponded to a site in the extracellular N-terminal domain of the protein. HG1 was found expressed on the postsynaptic membrane of neuromuscular junctions in both species. This result implies the presence of an HG1-like subunit in the parasitic nematode Ascaris suum. Additional staining was observed in *H. contortus,* specific to a number of cephalic neurones. A cell corresponding to the *C. elegans* sensory neurone AQR and two to four neurones similar to the RI and RM neurones all appear to express HG1.

1.7.3 The nicotinic Acetylcholine Receptor (nACR)

1.7.3.1 Topology

Advances into the three-dimensional structure of the nicotinic acetylcholine receptor isolated from the receptor rich electric tissue from the electric ray, *Torpedo californica,* has been accomplished. The receptor is heteropentameric in structure, composed of five subunit polypeptide chains. These include two α subunits of 437 amino acid residues, a β subunit of 469 residues, a δ subunit of 501 residues and a γ subunit of 489 residues (Noda *et al.*, 1982 & 1983a and Claudo *et al.*, 1983). Once the cDNA sequences coding for these polypeptides was established it became evident that they each possessed a signal sequence at the N-terminal enabling translocation across the ER membrane, and passage through the secretory pathway. Further more, upon examination of their hydropathy plots it was noted that each subunit had four transmembrane spanning domains, denoted TM1 to TM4 (Noda *et al,* 1983b).

Preceding the first transmembrane domain was a large hydrophilic extracellular domain of 210-224 amino acids carrying N-linked glycosylation sites. The purified receptor of 290kDa

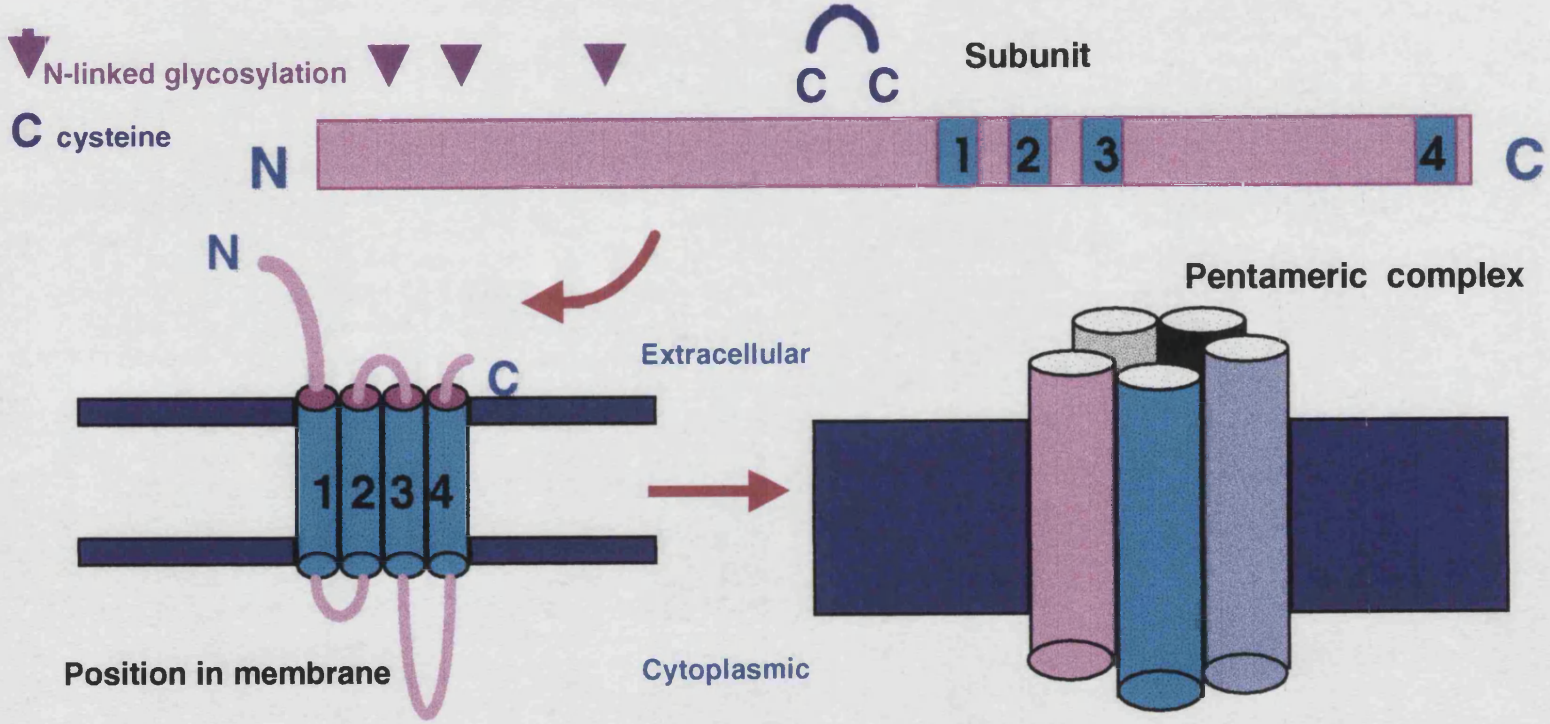

Figure 7, Topology of the nicotinic acetylcholine receptor

was found to consist of 20 kDa of carbohydrate obtained from N-linked glycosylation (Nomoto *et al.*, 1986). Also, within this domain a pair of cysteines can be found that link together via a disulphide bond. These two residues are located at fixed positions with 15 separating them.

The following three hydrophobic membrane spanning domains, TM1 to TM3, of 20-30 amino acids link together with short hydrophilic loops. Following TM3 is a longer hydrophilic loop of 109–142 residues, this connects to the fourth membrane-spanning domain. The loop encodes functional phosphorylation sites (Huganir & Greengard, 1987). Finally a short carboxy-terminal tail extends from TM4 and is exposed on the extracellular surface. Figure 7 displays the described topology of the nAChR presenting a typical subunit with its orientation in the membrane and its relationship with other subunits in a pentameric receptor complex.

Comparison of TM domains between different subunits reveals that TM2 is the most conserved and TM4 is the least conserved and most hydrophobic. When the subunits are assembled into a pentamer, TM2 is the most central, facing the lumen of the ion channel surrounding the receptors central axis (Revah *et al.*, 1990). In contrast, the TM4 domain of each of the subunits is exposed the most to the surrounding lipids of the membrane (Verall & Hall, 1992).

The receptor structure was established at 0.9 nm resolution using cryo-electron microscopy (Unwin, 1993). Each subunit in the complex appeared as elongated bodies of 12.5 nm, of which 6.0 nm extended out from the extracellular surface and 2.0 nm was left exposed on the cytoplasmic surface. It was calculated that 50 % of the subunit was distributed extracellularly and 33 % immersed within the membrane. A rough estimation of secondary and tertiary structure was ascertained at 0.9 nm resolution, with TM2 and TM4 believed to be α-helical and TM1 and TM3 most likely to be β-strands (Ortells & Lunt, 1994). Three α-helical rods from each subunit could be seen using electron microscopy (Unwin, 1993). Approximately 3.0 nm above the membrane bilayer and are believed to form cavities. Those produced by the α-subunit are the most pronounced of all subunits and are thus thought to represent the main constituent of the ligand-binding site. Further examination indicates that ligand binding sites are at the interfaces between α/γ and α/δ (Sine, 1993 & Kreienkamp *et al.*, 1995) as well as the pockets produced by the α-subunits.

As already mentioned TM2 is α-helical in nature and forms the wall lining of the pore. They do not form a straight path through the membrane but rather bend at a mid-point through the layer seen as a kink in the helix structure (Unwin, 1993). Each subunit codes a highly conserved leucine residue located at the level of the kink. The side chains of these residues project out into the pore creating a tight hydrophobic ring, acting as a barrier to hydrated ions. All five subunits arrange symmetrically around the central axis of the pore. A ring of negatively charged amino acids, such as glutamate, is found near the cytoplasmic surface of the pore lining. It is thought that this organisation repels negative ions surrounding the

intracellular opening. Deeper into the pore, three hydrophobic rings exist, one of threonines, one of serines and one of leucines, the latter being responsible for the kink in the tertiary structure. A final ring of negatively charged residues can be found close to the extracellular surface where negative ions are repelled (Revah *et al*, 1990).

In the absence of the ligand the receptor is in a closed confirmation with the leucine kinks pointing inwards. When ligand binds to the receptor a change in the configuration of the TM2 helices is observed altering the orientation of the kinks. In an open channel the leucine side chains have rotated over to the side drawing away from the central axis, permitting an influx of Na^+ and Ca^+ ions into the cell (Unwin, 1995).

1.7.3.2 Nematode Subunits

More than 20 nAChR subunits are present in *C. elegans,* including the α subunit coded by the gene *unc-38*, and the non-α subunits coded by *unc-29* and *lev-1* genes (Fleming *et al.*, 1997). Each is believed to be a component of the levamisole sensitive receptor found on body wall muscle. The *eat-18* gene encodes a third subunit, specific to the pharynx (Raizen *et al.,* 1995). To date, only one nAChR subunit has been identified in *Haemonchus contortus* and is denoted *Hca1* (Hoekstra *et al.*, 1997). This subunit has a 72 % amino acid identity with its counterpart in *Onchocerca volvulus* (Ajuh & Egwang, 1994).

1.7.3.3 Localisation in Nematodes

The localisation of *C. elegans* nAChRs have been determined by the production of antibodies against a choline acetyltransferase coded by the *cha-1* and a vesicular acetylcholine transporter molecule coded by the *unc-17* gene (Alfonso *et al.*, 1993 & 1994). The former enzyme is required to break down the released transmitter in the synaptic cleft or at the neuromuscular junction and the latter is responsible for the recycling of released transmitter from the cleft, back into the neurone. The presence of these two components would therefore suggest that acetylcholine receptors are in the vicinity. Immunolocalisation of *cha-1* and *unc-17* expressed proteins indicate that acetylcholine is released by the motor neurones VA, VB, VC, DA, DB and AS and three pharyngeal motor neurones M1, M2 and M5. Receptors are also present on the sublateral motor neurones SAA, SAB, SIA, SIB, SMB and SMD (Rand & Nonet, 1997).

1.7.4 Predicted Ligand Binding Sites

As already described: subunits of the ligand gated ion channel superfamily share related sequence homologies possessing the same predicted topological features. Subunits related to this superfamily each have a highly conserved TM2 region and a cys loop. A considerable amount of research has been covered to establish the amino acid residues coded by $GABA_A$ receptor subunits in vertebrates that are essential for agonist and modulator binding and has been reviewed by Smith and Olsen (1995). The GABA binding site is not just restricted to a

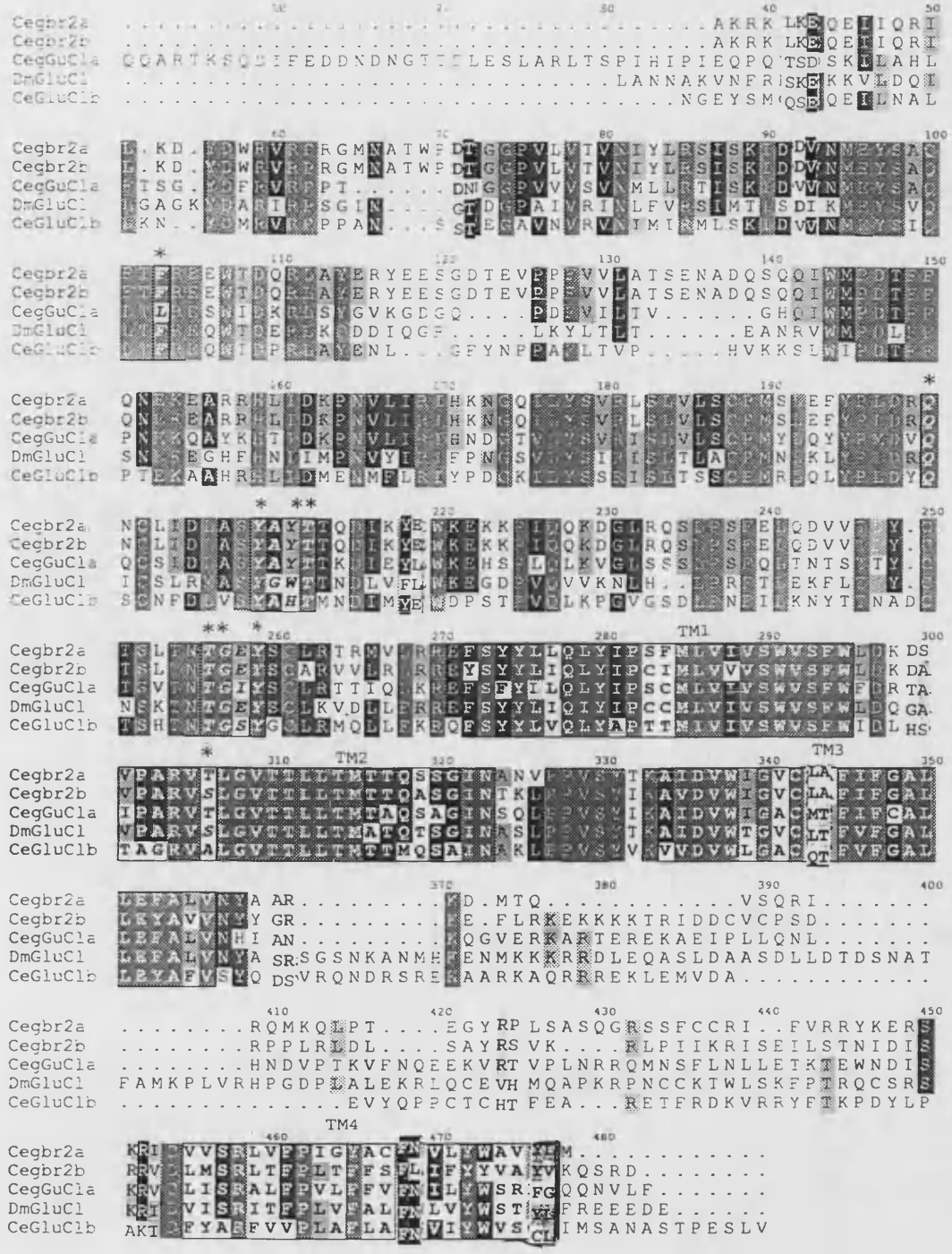

Figure 8. Amino acid alignment of nematode GluCl subunits. Comparison of *C. elegans* and *D. melangastor* subunits has been made with transmembrane domains marked TM1-4 amino acids predicted to play a role in ligand binding are indicated with an *. Homology is also summarised with different shades of grey.

pocket developed by the tertiary structure of one subunit but rather, is formed at the interfaces between adjacent subunits. Sequence alignment between subunits clarified highly conserved amino acids which when mutated prevented ligand binding.

A number of residues were also common to GluClRs and therefore have been predicted to play some role in ligand binding (Wolstenholme, 1997). In particular, the amino acid residues coded between position 209-212 (YAXT) and 256-259 (TGXY) seen in the alignment in figure 8 correspond to residues 157-160 and 202-205 of the $GABA_A$ β2 subunit isolated in rat are required for agonist binding. Mutation of tyrosine-157 or -205 to phenylalanine, or threonine-160 or -202 to serine in the β subunit significantly lowered the binding affinities for both GABA agonist and antagonists (Amin & Weiss, 1993). As these site are conserved in GluClRs they are not thought to be involved in discriminating between GABA and glutamate (Wolstenholme, 1997).

Other conserved residues between the GluClR subunits are glutamine-200, and phenyalanine-103, the latter corresponding to the F64 in the rat $GABA_A$ α1 subunit binding to GABA. The amino acid at position 223 of the *C. elegans* GluClβ varies between subunit types, the α-subunits coding a tyrosine and the β subunit a histidine. Interestingly, DrosGluClα codes a tryptophan at this position. Expression of GluClα homomeric channels in *Xenopus* oocytes is non-responsive to glutamate, however a point mutation of threonine-306 to proline in the TM2 domain creates a glutamate sensitive channel with an EC_{50} for glutamate of 1.4mM (Etter *et al.*, 1996). This suggests that the GluClα subunit has glutamate binding sites, which are unable to couple binding to channel gating.

1.7.5 Inhibitory TGIC subunits isolated from *H. contortus*

Amplification of inhibitory TGIC subunits from *Haemonchus contortus* was attempted by use of the Polymerase Chain Reaction (PCR). Degenerate primers were designed to conserved sequence present within the extracellular and first transmembrane spanning domain of $GABA_A$ and glycine receptor subunits (Laughton, 1993). Identification of 5 heterogeneous products of approximately 0.45 kbp was achieved in this manner using cDNA from *H. contortus* as template. Each of these partial sequences was related to inhibitory TGIC subunits. Partial sequences were denoted HG1 to HG5, the abbreviation for HG1 being *H*aemonchus GABA/Glycine receptor subunit 1. A PCR related method known as RACE (Rapid Amplification of cDNA Ends), devised by Frohman *et al.* in 1988, was utilised to isolate full-length sequences.

The first full-length copy of an inhibitory subunit from *H. contortus* was HG1 which when expressed in *Xenopus* oocytes responds to glycine (Laughton *et al.*, 1994). The absence of glycine receptors in helminths to date suggests that the homomeric expression of individual

member of the $GABA_A$-like receptors, sharing its highest amino acid identity with the *C. elegans* UNC-49 subunit. Expression of HG1 subunits occurs on several cephalic neurones that correspond to the *C. elegans* sensory cell AQR and RI & RM neurones (Skinner, 1997). Localisation was also specific to post-synaptic membranes at neuromuscular junctions in both *H. contortus* and *A. suum*.

Other full-length copies to be amplified by RACE-PCR include HG2 and HG3, a pair of alternatively spliced products (Jaggannathen *et al.*, in preparation). The high level of amino acid identity with GBR-2A and -2B, suggest that HG2 and HG3 may be parasitic orthologues, respectively, thus representing a third class of subunits of γ-type coded by *H. contortus* (Skinner, 1997). Following on from these findings a partial sequence lacking part of the N-terminal domain has been isolated from *Ascaris suum* and appears to orthologous to the GBR-2B and HG3 subunit amino acid sequences (Jaggannathan, pers. comm.).

Table 1. Inhibitory TGIC subunits PCR derived from *C. elegans* and parasitic species.

Species	Subunit name	Available sequence	References
C. elegans	GluClβ	Full-length cDNA EMBL, U41525	Cully *et al.*, 1994
	GBR2a	Full-length cDNA EMBL, U40573	Laughton *et al.*, 1997
	GBR2b	Full-length cDNA EMBL, U41113	
	GluClα1	Full-length cDNA EMBL, U42524	Cully *et al.*, 1994
	GluClα2a (long)	Full-length cDNA EMBL, AJ000538,	Dent *et al.*, 1997
	GluClα2b (short)	Full-length cDNA EMBL, AJ000537.	
H.contortus	HG1	Full-length cDNA EMBL, X73584	Laughton *et al.*, 1994
	HG2	Full-length cDNA	Laughton, 1993, & Jagernnathan *et al.*, un-published result
	HG3	Full-length cDNA	
	HG4	Partial sequence, 450 bp	Laughton, 1993
	HG5	Partial sequence, 450 bp	Laughton, 1993.
Ascaris suum	ASG2	Partial sequence, lacking~200bp of 5' terminus.	Jagernnathan *et al.*, un-published result
Dirofilaria immitis	GluClX	Partial sequence 423bp, EMBL U59744	Cully *et al*, un-published results.
Onchocerca volvulus	GluClX	Partial sequence, 990 bp EMBL, U59745	Cully *et al*, un-published results.

1.8 Aims of Study

Studies will be carried out on the nematode *Haemonchus contortus* to establish relevant drug targeting mechanisms within a parasitic species. HG4 and HG5 partial sequences share high amino acid identities with the glutamate-gated chloride channels. These receptors are targeted by the anthelmintic drug avermectin (Arena *et al.*, 1992). The first aim of this work is to derive full-length sequences for both HG4 and HG5 subunits. This will make expression studies in *Xenopus* oocytes possible, whereby expression of homomeric and heteromeric receptors can be analysed, including co-expression with HG2 and HG3.

Sequences isolated from avermectin-susceptible and –resistant isolates of the species, will be compared. This will determine whether resistance had developed as a result of an alteration in the coding sequence, such as a change in the ligand-binding site.

Another aim is to map the expression pattern of HG4 in adult *H. contortus* thus clarifying where drug targets exist. This will be established by raising antiserum to a peptide designed to a site along the N-terminal extracellular domain, sharing a low homology with related receptor subunits.

This work should contribute to defining the target of avermectin and the mechanism of drug resistance in the agriculturally important worm *H. contortus*.

2 Materials and Methods

2.1 General Materials

2.1.1 Molecular Biology Reagents

Molecular biology grade chemicals were purchased from BDH Chemicals (Poole, Dorset, UK), Sigma Chemical Company Ltd (Poole, Dorset, UK) or Fisons Scientific Equipment (Leicestershire, UK). Agarose was supplied by Biogene Ltd (Kimbolton, Cambridgshire, UK), ethidium bromide came from Sigma and radiochemicals from Amersham Life Sciences (Little Chalfort, Buckinghamshire, UK).

2.1.2 Enzymes

Restriction endonucleases, DNA polymerase 1 and Polynucleotide Kinase were supplied by NEB (Hitchin, Hertfordshire, UK), Calf intestinal alkaline phosphatase was purchased from Boehringer Mannheim UK (Diagnostics and Biochemicals) Limited, (East Sussex, UK) and T4 DNA ligase from Gibco BRL (Renfrewshire, Scotland).

2.1.3 Miscellaneous

λ DNA was purchased from NBL gene Sciences Ltd. (Cramlington, Northumberland, UK) and dNTPs from Pharmacia, Biotech UK (St Albans, Hertfordshire, UK). TEMED was supplied by Anachem Ltd. (Luton, Bedfordshire, UK) and Ammonium persulphate from Gibco BRL (Renfrewshire, Scotland).

2.1.4 Vectors

Table 2, List of vectors.

Plasmids	Genotype and Size	Supplier
pBluescript® II SK (+)	Amp^r, 2961 bp	Stratagene Ltd. (Cambridge, UK)
pALTER®-1	Amp^s, Tet^r, 5680 bp	Promega UK Ltd. (Southampton, UK)
pMAL-c2	Amp^r, 6646 bp	NEB (Hitchin, Hertfordshire, UK)

See Appendix 1 for vector maps

2.1.5 Buffer solutions

Table 3, Buffer compositions.

Buffer	Composition
TE	10 mM Tris-HCl, 1 mM EDTA, pH 7.6
10X TBE	0.89 M Tris-HCl, 0.89 M Boric Acid, 20 mM EDTA, pH 8.0
10X TTE	1.78 M Tris base, 0.57M Taurine, 10 mM Na EDTA
Phenol/Chloroform	50 % (v/v) Phenol equilibrated with 10 mM Tris-HCl pH7.6, 49% (v/v) chloroform, 1% (v/v) Isoamyl Alcohol
PBS	137 mM NaCl, 2.7 mM KCl, 4.3 mM $Na_2HPO_4.7H_2O$, 1.4 mM KH_2PO_4, pH 7.3

2.1.6 Microbiological reagents

Media reagents were supplied by Difco Laboratories (East Molesey, Surrey, UK) and Sigma (Poole, Dorset, UK), whilst Petri dishes came from Bibby Sterilin Ltd (Stone, Staffordshire, UK). Glycerol was purchased from BDH and both IPTG and X-Gal were supplied by Alexis Corporation (Bingham, Nottingham, UK). Ampicillin, tetracycline and dimethylformamide were ordered from Sigma.

2.1.7 Bacterial Media

Table 4, Media Composition

Media	Composition (in g/L)
Luria Bertani (LB) Broth	10 g bacto-tryptone, 5 g yeast extract, 10 g NaCl
LB agar	LB broth, 15 g agar
DYT Broth	16 g bacto-tryptone, 10 g yeast extract, 5 g NaCl
SOC medium	20 g bacto-tryptone, 5 g yeast extract, 10 ml 1 M NaCl, 2.5 ml 1 M KCl, 10 ml 2M Mg^{2+} Stock (1 M $MgCl_2.6H_2O$, 1M $MgSO_4.7H_2O$, sterile filtered), 10 ml 2M glucose (sterile filtered)

2.1.8 *E. coli* Strains

Table 5, List of *E. coli* strains.

Strain	Genotype	Supplier
XL1 - Blue	*supE44, hsdR17, recA1, endA1, gyrA46, thi, relA1 lac-, F' [ProAB+, LacIq, LacZΔM15,* Tn10(tetR)*]*	Stratagene Ltd. (Cambridge, UK)
XL2 - Blue	*supE44, hsdR17, recA1, endA1, gyrA96, thi-1, relA1 lac [F' proAB* $lac^qZ\Delta M15$ Tn 10 (Tet^r) Amy Cam^r*]*[a]	Stratagene Ltd
JM109	*endA1, recA1, gyrA96, thi, hsdR17* (r_K^-, m_K^+) *relA1, supE44,* Δ(*lac-proAB*), [*F',traD36, proAB,* $lacI^qZ\Delta M15$]	Promega (Southampton, UK)
BMH 71-18 *mutS*	*thi, supE,* Δ*(lac-proAB),* [*mutS*::Tn10] [F', *proAB,* $laqI^qZ\Delta M15$]	Promega

[a] chloramphenicol resistant at concentrations less than 40 μg/ml

Genotype definitions are detailed in Appendix 2.

2.2 Production of cDNA from *Haemonchus contortus*

2.2.1 *H. contortus* tissue

Adult *H. contortus* was kindly supplied by Dr Ed Munn (Babraham Institute, Cambridge, UK), eggs were provided by Dr. Ian Harrow (Pfizer Research, Sandwich,Kent, UK) and both eggs and adults of susceptible and resistant isolates, the latter being a White River isolate from South Africa (See Appendix 4 for further details), were generously donated by Dr Gerald Coles (School of Veterinary Medicine, Bristol, UK).

2.2.2 Isolation and purification of *H.contortus* eggs

Method 1

Sheep faeces infected with *H. contortus* eggs were collected in nappies. Faeces were stored at 4° C overnight and than mashed up by hand. Using a high-pressure water jet, the slurry was washed through a series of sieves of decreasing pore diameter (150 μm, 53 μm, 48 μm). The resulting sediment was filtered through a 38 μm sieve, the pore diameter being smaller than the size of the eggs, thereby concentrating the eggs on the top surface of the sieve. Eggs were then purified from remaining plant material by flotation. This was achieved by transferring the eggs to a 5-litre beaker containing a saturated salt solution filled up to the

brim. The resulting solution was stirred thoroughly and left for 10 min, enabling the eggs to rise up to the surface. These were then recovered by aspirating the top inch of the solution. The retrieved eggs were transferred to a 25 μm sieve and washed with tap water to remove the salt. The eggs were then transferred into 1 ml NUNC (GibcoBRL) cryovials and snap frozen for storage in liquid nitrogen.

Method 2

A handful of sheep dung infected with *Haemonchus contortus* was transferred to a food processor with an equal volume of water and homogenised by two 10 sec pulses. The mixture was sieved through a 158 μm pore sized sieve removing the majority of the debris and allowing the eggs to pass through for collection into a jug. 50 ml volumes were spun down in Falcon tubes at 1500 rpm for 2 min. The supernatant was extracted and another 50 ml was added and spun down as before. This was repeated until the pellet reached just above the 5 ml mark on the side of the tube. Flotation involved resuspending the eggs in a saturated NaCl solution and covering the top of the Falcon tube with a coverslip. With the absence of air bubbles existing at the interface, tubes were spun at 1000 rpm for 2 min. As a result of the salt concentration gradient produced from the spin, the eggs were able to float up to the top and coat the coverslip. Purified eggs were rinsed off the coverslip with distilled H_2O into a 17 ml Falcon tube and spun at 1500 rpm for 2 min. The supernatant was removed and the eggs were pipetted into NUNC cryovials and snap frozen for storage in liquid nitrogen.

2.2.3 Isolation of total RNA

Total RNA was isolated from frozen *H. contortus* eggs and adults using a single step, guanadinium thiocyanate-phenol-chloroform extraction technique (Chomczynski and Sacchi, 1987). Using a mortar and pestle, 1 g of nematode tissue was ground to a fine powder under liquid nitrogen. This was then added to 10 ml of denaturing solution (4 M guanadinium thiocyanate, 25 mM sodium citrate pH 7, 0.5 % sarcosyl, 0.1 M 2- mercaptoethanol) and homogenised using a glass-Teflon homogeniser. The solution was then poured into a 30 ml Corex tube and the following order of reagents were added, mixing after each addition: 1 ml of 2 M NaOAc, pH 4, 10 ml of water saturated phenol, and 2 ml of chloroform-isoamyl alcohol (49:1, v/v). The resulting mixture was shaken vigorously for 10 seconds and cooled on ice for 15 min followed by a 20 min spin at 10,000 g at 4 °C to separate the phases. RNA present in the aqueous phase was removed and added to 2-propanol followed by incubating at -20 °C for at least 2 h. RNA was sedimented at 10,000 g for 20 min at 4 °C and the pellet dissolved in 3 ml of denaturing solution. Addition of 3 ml of 2 - propanol precipitated the RNA at - 20° C for at least 1 h. Centrifuging at 10,000g for 20 min at 4 °C produced a pellet which was then resuspended in 75 % (v/v) DEPC treated ethanol, sedimented and vacuum dried. Finally 500 μl of RNase free 0.5 % (w/v) SDS was added to the total RNA and heated at 65 °C for 10 min.

2.2.4 Isolation of Poly-$[A]^+$ RNA from total RNA

This method uses Dynabead Oligo dT25 (Dynal, Wirral, UK) magnetic beads. These beads are 2.8 μm in diameter and have a 25 nt chain of deoxythymidylate which are covalently attached to the bead via a 3' linker group.

Dynabead Oligo dT beads were prepared first by placing a microcentrifuge tube containing 0.2 ml (1 mg) bead suspension into a Dynal MPC E-1 magnetic separator. The supernatant was removed and the beads were washed by adding 200 μl of 2x binding buffer (20 mM Tris-HCl pH 7.5, 1 M LiCl, 2 mM EDTA) and using the Dynal separator to remove the supernatant. Beads were then resuspended in 100 μl of 2x binding buffer. Total RNA (200 μg) was dissolved in 100 μl of DEPC-treated water and then heated for 2 min at 65 °C followed by addition to the washed beads. After a 5 min hybridisation at room temperature the tube was placed into the separator thus enabling the supernatant to be removed from the beads. Beads were washed twice with 200 μl of washing buffer (10 mM Tris-HCl pH 7.5, 0.15 M LiCl, 1 mM EDTA) and then resuspended in 30 μl of elution buffer (2 mM EDTA pH 8.0) before being heated at 65° C for 2 min. Eluted poly-$[A]^+$ RNA was extracted after separation from beads and used immediately for cDNA synthesis.

2.2.5 Synthesis of first strand cDNA

Poly-$[A]^+$ RNA from *H. contortus* was reverse transcribed into cDNA using the Superscript enzyme from Gibco BRL.

To 30 μl of eluted poly-$[A]^+$ RNA was added 10 μl of 5x Superscript buffer (0.25 M Tris-HCl pH 8.3, 0.375 M KCl, 15 mM $MgCl_2$), 5 μl of 0.1 M DTT, 2.5 μl of 10 mM dNTPs, 2 μl RNasin (40 U), 1 μl Oligo (RoRi) dT primer (1 μg/ μl) and 1 μl of Superscript enzyme (200 U). This mixture was incubated at 37° C for 90 min. The reaction was stopped by addition of 1 μl of EDTA (0.5 M) and aliquots of cDNA were then stored at -20° C.

2.3 Oligonucleotide Production

2.3.1 Synthesis and Deprotection

The Applied Biosystems 381A DNA Synthesiser was used to synthesis oligonucleotides using chemicals supplied by Cruachem, Glasgow, UK. Once synthesised the primers needed to be deprotected. This was achieved by first freeing the beads from the column and soaking them in ammonium hydroxide overnight at 55° C. Glacial acetic acid (1 ml) was added on ice followed by 6 ml of absolute ethanol. After incubating for 30 min on ice the primer was precipitated at 10,000 rpm (4° C). The pellet was washed with 85 % ethanol, vacuum dried and then resuspended in sterile double distilled water. The absorbance at 260 nm was taken and the oligonucleotide was diluted to appropriate working stock solutions (normally 20 μM).

2.3.2 Ordering

Oligonucleotides were purchased from Perkin Elmer's Biosystems Division, Cheshire, UK using the ABI 3948 Nucleic Acid Synthesis and Purification System. Primers were received ready to use in 20 % (v/v) acetonitrile/water.

2.4 The Polymerase Chain reaction, PCR

2.4.1 Expand™ Long template PCR System

PCR amplification of receptor subunit cDNA was performed using oligonucleotides designed to complement conserved areas (i.e. SL1 and RoRi sequences) and regions specific to the known partial sequences. The Expand™ PCR system from Boehringer Mannheim UK Ltd (East Sussex, UK) uses a combination of the thermostable *Taq* DNA polymerase and *Pwo* DNA polymerase. The presence of the latter enzyme allows 3'-5' exonuclease proof-reading to occur increasing the fidelity of DNA synthesis during the reaction. The long template PCR system is designed to give a high yield of PCR products from episomal DNA amplifying up fragments as long as 40 kbp from λ DNA.

A typical reaction would contain 5 µl of 10x PCR buffer 1 (500 mM Tris-HCl pH 9.2 (25° C), 160 mM $(NH)_2SO_4$, 17.5 mM $MgCl_2$), 350 µM dNTP, 300 nM of both sense and antisense primers, 500 ng of cDNA template and sterile double distilled H_2O to give a final volume of 50 µl. Reactions were then overlaid with 50 µl of mineral oil to prevent evaporation of components during the PCR. Thermocycling conditions included an initial denaturing step of 94° C for 2 min followed by addition of 2.5 U of Taq/Pwo mix. The cDNA template was then denatured for 30 sec at 94° C, primers were made to hybridise to the template at a previously calculated annealing temperature for 30 sec and then strands were elongated at 68° C for 2 min, this cycle profile was repeated for 45 cycles. Finally a 7 min step at 68° C was included to make sure that the PCR fragments were fully elongated.

The exact parameters of the temperature cycling however depends on the primers used i.e. their length and GC content. Optimal amounts of specific product were obtained by altering the annealing temperature and performing Mg^{2+} titrations with a concentration range of 0.5 mM to 4 mM.

2.4 2 Expand™ High Fidelity PCR System

The high fidelity system (supplied by Boehringer Mannheim UK Ltd, East Sussex, UK) uses the same DNA polymerases (*Taq* and *Pwo*) as the long template system but has been optimised to amplify up DNA fragments of up to 3 kbp having an error rate of 8.5 $x10^{-6}$ as opposed to 2.6 $x10^{-5}$ with just *Taq* DNA polymerase (detailed in supplied protocol). A typical reaction would contain 10 µl of 10x Expand HF buffer 2 (supplied with the kit, containing 15 mM $MgCl_2$), 200 µM dNTP, 300 nM of both sense and antisense primers, 100 ng of cDNA template and finally sterile double distilled water giving a total volume of 100 µl. Mixes were then overlaid with 50 µl of mineral oil and placed in a thermocycler ready to perform PCR. A

general cycle profile would commence with a denaturing step at 94° C for 2 min followed by a pause to add 2.6 U of *Taq/Pwo* enzyme mix. Initially 45 cycles were performed starting with a denaturing step for 30 sec at 94° C, followed by 30 sec at a calculated annealing temperature (AT), allowing hybridisation of primers to template and ending with an elongation step of 3 min at 72° C. The reaction was then stopped after a final elongation cycle of 72° C for 7 min.

2.4.3 Analysis by Agarose Gel Electrophoresis

A 1 % (w/v) agarose gel was made using 10 g of agarose and heating in 100 ml of 1x TBE buffer. Once dissolved, ethidium bromide (0.5 μg/ml) was added and poured into a gel cast. After the gel had set, DNA samples (containing 1/5th of the volume loading dye (15 % (v/v) ficoll, 0.25 % (w/v) bromo-phenol blue, 0.25 % (w/v) xylene cyanol)), and a standard (Lambda DNA digested with Pst1) were loaded into the wells and electrophoresed at 150 V for 1 h. Photographs of the gels were taken under uv light using a Polaroid camera with a yellow filter and Polaroid 667 black and white ISO3000/36 film.

For RNase free gels the gel tank, cast and comb were treated with 1 % v/v hydrogen peroxide (Sigma) to remove RNases. Loading dye was also made up to volume using DEPC treated water instead of double distilled sterile water.

2.4.4 Purification of DNA bands from Agarose Gels

PCR products were cut out of 1 % (w/v) agarose gels using a razor blade and purified using the Sephaglas™ Band Prep kit, supplied by Pharmacia. The purification procedure involved melting 0.25 g of agarose at 60° C in the presence of 250 μl of modified Gel Solubilizer (a buffered solution containing NaI and 5 μl of 50 % glacial acetic acid) for 10 min, vortexing periodically. 5 μl of Sephaglas™ BP suspension was then added per μg of DNA present in the agarose slice and vortexed gently every minute over a 5 min incubation at room temperature. The Sephaglas/DNA mix was then spun down for 30 sec and was discarded. 40 μl of Wash buffer (20 mM Tris-HCl pH 8.0, 1 mM EDTA, 0.1 mM NaCl and 18 ml absolute ethanol) was added to resuspend the pellet followed by a 30 sec pulse spin to enable removal of the supernatant. This washing procedure was repeated two more times. The pellet was left for at least 10 min to air dry followed by elution of he DNA by incubating at room temperature for 5 min in 10 μl (per μg of DNA) of Elution Buffer (10 mM Tris-HCl pH 8.0 and 1 mM EDTA). The sample was spun for 1 min and the supernatant containing the DNA was then transferred to a sterile microfuge tube and the elution procedure was repeated with another equal volume of Elution Buffer.

2.4.5 QIAquick™ Preparation

The QIAquick™ system supplied by QIAGEN Ltd (Crawley, West Sussex, UK.) was designed for a quick clean up of DNA. To DNA sample, 5 volumes of Buffer PB (supplied with kit) was added, mixed and pipetted into a QIAquick spin column fixed onto a 2 ml collection tube. The

DNA was bound to the column by spinning for 60 sec at 13,000 rpm. The flow-through was discarded and the column was washed with 0.75 ml of Buffer PE (supplied with kit) by spinning at 13,000 rpm for 60 sec. Flow-through was removed and the column was centrifuged for an additional 1 min at maximum speed to remove any residual ethanol present in the PE buffer. Elution of DNA was achieved by adding 30 µl of H_2O to column and incubating for 1 min at room temperature over a microfuge tube followed by centrifuging at 13,000 rpm for 1 min.

2.5 Vector Preparation for Cloning of Inserts

2.5.1 Linearising vector for Cloning in Blunt Ended products

The vector pBluescript® SK II (4 µg/µl) was digested with the restriction enzyme EcoRV (4U), 1/10 th of the final volume of 10x buffer B (100 mM Tris-HCl, 50 mM $MgCl_2$, 1 M NaCl, 10 mM 2-mercaptoethanol, pH 8.0) and sterile double distilled water giving a final volume of 50 µl. This was incubated at 37° C for at least 2 h. DNA extraction was performed by adding an equal volume of phenol/chloroform and then precipitating at -20° C for 15 min with 2 volumes of absolute ethanol. The pellet, produced by spinning at 13,000 rpm for 10 min at 4° C, was dissolved in 90 µl of 10 mM Tris-Cl pH 8.0.

2.5.2 Dephosphorylation of vector

Calf intestinal phosphatase (CIP) removes 5'-phosphate groups from linear DNAs thereby preventing the vectors circularising without an insert. 10 µl of 10x CIP buffer (10 mM $ZnCl_2$, 10 mM $MgCl_2$, 100 mM Tris-Cl pH 8.3) and 2 µl of CIP (1/2 unit / pmol of 5'-terminal phosphate residues) was added to the purified EcoRV cut vector. After a 15 min incubation at 37° C another 2 µl of CIP was added and incubated at 55° C for 45 min. To terminate the reaction 1 µl of 500 mM EDTA pH 8.0 was added along with incubating at 75° C for 10 min. DNA was purified using an equal volume of phenol/chloroform and precipitated with 0.1 volume of 3 M NaOAc pH 5.5 and 2x volume of absolute ethanol at -20° C. The pellet was washed with 70% (v/v) ethanol to remove salts and resuspended in TE pH 7.6 (10 mM Tris-Cl pH 7.6 and 1 mM EDTA) giving a final concentration of 100 µg/ml.

2.5.3 Linearising Vector for Cloning in Sticky Ended Products

pBluescript® SK II (4 µg/µl) was digested in a total volume of 50 µl with 4 Units of both Not1 and Xba1 restriction enzymes in the presence of BSA (100 µg/ml) and 5 µl of 10x NEBuffer 3 (50 mM Tris H-Cl, 10 mM $MgCl_2$, 100 mM NaCl, 1mM DTT (pH 7.9 at 25° C)). This reaction was placed at 37° C overnight. Vector DNA was then purified by vortexing with 1 volume of phenol/chloroform followed by a spin in the microfuge. The aqueous top layer was then transferred to a fresh microfuge tube and DNA was precipitated with 0.1 volume of NaOAc (pH 7.0) and 2 volumes of ice cold absolute ethanol, incubating at -20° C for 2 h. The DNA was spun down producing a pellet which was washed with 70% v/v ethanol to remove salts

and resuspended in TE pH 7.6 (10 mM Tris-Cl pH 7.6 and 1 mM EDTA) giving a final concentration of approximately 100 μg/ml.

2.6 Cloning of PCR Products into a Plasmid

2.6.1 Products generated using primers without restriction sites

This method was used when the PCR primers did not introduce restriction sites into the amplified product. Amplification products (100 ng-1 μg) were mixed with a 0.1 volume of 10x One-Phor-All buffer (100 mM Tris-acetate pH 7.5, 100 mM magnesium acetate and 500 mM potassium acetate), 0.4 mM ATP, 8U DNA Polymerase and 10U polynucleotide kinase. This was incubated at room temperature for 3 min during which time a stepwise degradation from free 3' hydroxyl ends occurs. Four x dNTP's (0.2 mM) were then added and incubated for 30 min at 37° C, allowing strand extension in the 5'-3' direction and enabling the phosphorylation of the 5' end by polynucleotide kinase. Addition of 2 μl of 0.5 M EDTA at pH8.0 stopped the reaction. DNA was then purified from the reaction mix by adding an equal volume of phenol/chloroform and precipitated with 0.1 volume of 3M NaOAc pH 5.5 and 2.5 volume of absolute ethanol at -20° C. The pellet was washed with 70% (v/v) ethanol to remove salts and resuspended in sterile double distilled water.

2.6 2 Products produced from primers with restriction sites

Sephaglas purified PCR products were cut with 20 units of Nsi1 and Not1 in a double digestion. This reaction was carried out in a total of 50 μl in the presence of 100μg/ml of BSA and 5 μl of 10x NEBuffer 3 (50 mM Tris H-Cl, 10 mM $MgCl_2$, 100 mM NaCl, 1mM DTT (pH 7.9 at 25° C)). A 50 μl double digest was also carried out on Sephaglas purified PCR products using 20 units of Xba1 and Nsi1 in the presence of 100μg/ml of BSA and 5 μl of 10x NEBuffer 2 (10 mM Tris H-Cl, 10 mM $MgCl_2$, 50 mM NaCl, 1 mM DTT (pH 7.9 at 25° C)). After incubating both double digests overnight at 37° C, DNA was purified using an equal volume of phenol/chloroform and precipitated with 0.1 volume of 3 M NaOAc pH 5.5 and 2x volume of absolute ethanol at -20° C. Finally 70% (v/v) ethanol was used to remove salts from the pellet and the DNA was resuspended in sterile double distilled water.

2.6.3 Ligation into vector

250 ng of vector was mixed with a 3 fold molar excess of amplified DNA purified from an agarose gel. To this 4 μl of 5x T4 DNA ligase buffer (250 mM Tris-Cl pH 7.6, 50 mM $MgCl_2$, 25 % (w/v) PEG8000, 5 mM ATP, 5 mM DTT) and 5 units of T4 DNA ligase were added, giving a final volume of 20 μl. The resulting reaction was left to incubate at room temperature overnight. A 1:4 (v/v) dilution was made with H_2O to dilute out the PEG and prevent it inhibiting transformation.

2.6.4 Transforming plasmids into competent XL1 Blue Cells

5 ml of LB broth was inoculated with XL1 Blue *E. coli* cells and shaken overnight at 37 °C. A 200 µl aliquot of this overnight culture was used to inoculate 40 ml of LB broth and shaken at 37 °C until the culture reached an absorbency of 0.3 at 550 nm. Cells were centrifuged at 3,000 rpm for 10 min at 4 °C and the pellet resuspended in 20 ml of ice cold 100 mM $CaCl_2$. Cells were incubated for 20 min on ice followed by a spin at 3,000 rpm for 5 min at 4 °C. The resulting pellet was resuspended in 4 ml of ice-cold 100 mM $CaCl_2$ that was then aliquoted (300 µl) for use. Half of the ligated DNA was added to the 300 µl aliquot of competent cells and placed on ice for 40 min. Cells were heat shocked at 42° C for 1 1/2 min, immediately followed by 2 min on ice. To each sample of heat shocked cells 0.7 ml of LB broth was added and left to incubate for 1 h at 37° C. The resulting XL1 Blue suspensions were spread out onto LB / ampicillin (100 µg/ml) plates coated with 50 µl of both 0.1 M IPTG and 2 % (w/v) X-Gal (dissolved in dimethylformamide). The vector pBluescript® II SK(+) contains the *lac-Z* selection marker encoding the enzyme β-galactosidase. Addition of the inducer, IPTG, and the substrate, X-Gal, to the surface of the agar distinguished successful transformation as white colonies.

2.7 Screening of Colonies

2.7.1 Small Scale Plasmid Preparation from *E. coli*

Single colonies of *E. coli* were used to inoculate 3 ml of LB broth containing ampicillin (100 µg/ml) and shaken overnight at 37° C. Cells were pelleted and resuspended in 100 µl GTE (50 mM glucose, 25 mM Tris-HCl pH 8.0, 10 mM EDTA) followed by the addition of 200 µl of 0.2 M NaOH containing 1 % (w/v) SDS. Samples were incubated on ice for 5 min and then 150 µl of ice cold 3 M KOAc pH 4.8 was added and vortexed. DNA extraction was performed with an equal volume of phenol/chloroform and then precipitated with 2 volumes of ice cold absolute ethanol by keeping at -20° C for 10 min. The pellet produced by spinning at 12,000g for 10 min at 4° C was washed with 70 % v/v of ethanol and spun as above prior to resuspending the pellet in 50 µl of TE pH 7.6 containing 10 µg/ml of RNase A.

2.7.2 Wizard™ Plus Minipreps DNA Purification System

E. coli colonies were inoculated into 3 ml of LB broth containing 100 µg/ml of ampicillin and shaken overnight at 37° C. Cells were harvested and DNA was extracted using the Promega Wizard™ Plus kit. This was done by first adding 200 µl of cell resuspension solution (50 mM Tris pH 7.6, 10 mM EDTA, 100 µg/ml RNaseA) to the harvested pellet of cells and then vortexing. Cells were lysed by using 200 µl of cell lysis solution (0.2 M NaOH, 1% w/v SDS) and inverting until the suspension went clear. 200 µl of neutralisation solution (1.32 M KOAc pH 4.8) was added and inverted causing coagulation. The resulting mix was spun down and the supernatant containing the plasmids was passed through a Wizard™ minicolumn via a 3 ml syringe containing 1 ml of Wizard™ Minipreps DNA purification resin. Plasmids present in the column were washed by gently pushing through 2 ml of column wash solution (80 mM

KOAc, 8.3 mM Tris-HCl pH 7.5, 40 μM EDTA and 55 % (v/v) ethanol) using a syringe followed by a 2 min spin to dry. Plasmids were eluted from the column by adding 50 μl of H_2O, incubating for 1 min at room temperature and spinning down for 20 sec.

2.7.3 Restriction Digests

Digests were performed in a total volume of 20 μl, which included 0.1 volume of the appropriate 10x reaction buffer along with 1 Unit/μg DNA of the relevant restriction endonuclease and 5 μl of plasmid DNA. For some restriction digests the presence of BSA was required in which case 2 μl of a 1 mg/ml solution was added. When larger quantities of DNA needed to be restricted, volumes were increased but the ratios of components in the reaction were kept the same. Digests were mixed and incubated at 37° C for 1 h. 5 μl of loading dye was then pipetted into each sample and loaded onto a 1 % (v/v) agarose gel.

2.7.4 Glycerol Stocks

Glycerol stocks were made by mixing 150 μl of glycerol with 850 μl of overnight culture which had been previously made by inoculating LB broth containing 100 μg/ml with an XL1 Blue colony and shaking overnight at 37 °C. Stocks were stored at -20 °C

2.7.5 Quantifying amount of plasmid DNA

The concentration of plasmid DNA was estimated visually on a 1 % w/v agarose gel by comparing the intensity of the ethidium bromide stained bands to those produced by plasmids with known concentrations. Samples of 1/4, 1/2 and 1 μg of pBluescript® II SK (+) were made up to 20 μl with 5 μl of loading dye and double distilled H_2O. Aliquots of 1 and 2 μl of plasmid DNA were also made up to 20 μl in the same way.

2.8 Sequencing

2.8.1 Direct sequencing of PCR products

The Sequenase™ PCR Product Sequencing Kit, supplied by Amersham Life Sciences (Little Chalfont, Buckinghamshire, UK), was used to sequence PCR products using the dideoxynucleotide chain termination method (Sanger *et al.,* 1977). To 5 μl of PCR amplification mixture were added 10 U of Exonuclease 1 and 2 U of Shrimp Alkaline Phosphatase. This was incubated for 15 min at 37° C, 15 min at 80° C and then placed on ice. An oligonucleotide designed to anneal internally to the sequence was added in excess (10 pmol). The reaction mixture was made up to 10 μl with H_2O, placed at 100° C for 3 min and then rapidly cooled to 0° C. To the annealed DNA, 2 μl of 5x Sequenase buffer (200 mM Tris-HCl pH 7.5, 100 mM $MgCl_2$, 250 mM NaCl), 1 μl of 0.1 M DTT, 5x labelling mix (5 μM dNTP, diluted down 1:5 v/v with H_2O), 5 μCi [α-^{35}S] dATP and Sequenase™ Version 2.0 T7 DNA polymerase (3.2 U) was added. This was incubated at room temperature for 5 min followed by aliquoting 3.5 μl into pre-warmed (37° C) tubes containing 2.5 μl ddNTP (8 μM) each and left at 37° C for 10 min. The reaction was stopped using 4 μl of stop solution (95 %

(w/v) formamide, 20 mM EGTA, 0.05% (w/v) Bromophenol Blue, 0.05% (w/v) Xylene Cyanol FF).

2.8.2 Sequencing of Plasmid constructs

The Sequenase™ Quick Denature™ Plasmid Sequencing Kit, supplied by Amersham Life Science uses the dideoxynucleotide chain termination method (Sanger *et al.,* 1977) to sequence PCR products that have been cloned into the vector pBluescript® II SK (+). Firstly, 8 µl of plasmid DNA was denatured in the presence of 10 pmol of primer by 2 µl of 1.0 M NaOH for 10 min at 37° C. The reaction was then neutralised by adding 2 µl of 1.0 M HCl and 2 µl of Plasmid Reaction Buffer (400 mM Tris-HCl pH 7.5, 100 mM $MgCl_2$, 250 mM NaCl), incubating at 37° C for 10 min then chilling on ice for 10 min. To the ice-cold mix 1 µl of 0.1 M DTT, 2 µl of diluted labelling mix (5 µM dNTP, diluted down 1:5 v/v with H_2O), 5 µCi [α-^{35}S] dATP and diluted Sequenase™ Version 2.0 T7 DNA polymerase (3.2 U) was added. This was incubated at room temperature for 3 min and 4.5 µl of this labelling mix was then transferred to pre-warmed (37° C) tubes containing 2.5 µl of ddNTP (8 µM) and left at 37° C for 5 min before stopping the reaction using 4 µl of Stop solution.

2.8.3 Preparation of poly-acrylamide sequencing gels

Front plates were washed with water and polished dry with 75 % (v/v) ethanol. Dichlorodimethylsilane (BDH Chemicals, Poole, Dorset, UK) was used to silanate the surface of the plate. After 5 min the plate was rinsed with water and polished with 75 % (v/v) ethanol. Back plates were cleaned by soaking for at least 5 h in 5M KOH followed by rinsing in water and polishing with 75 % (v/v) ethanol. To the surface of the plate a solution of 1.2 ml of 10 % acetic acid, 200 µl of silane A-174 adhesion promoter (BDH Chemicals) and 25 ml absolute ethanol was poured. This was left for 5 min after which time the plate was rinsed with water and polished dry with 75 % (v/v) ethanol. One 0.2 mm spacer was placed on each side of the back plate and the front plate was placed on top with the silanated surface face down and clamped loosely together. A 6 % (v/v) acrylamide solution was prepared using Sequagel reagents from Flowgen (Lichfield, Staffordshire, UK). Immediately before pouring, 300 µl of freshly prepared 16 % ammonium persulphate and 40 µl of TEMED were added to the acrylamide solution. Once poured the flat edge of a shark's tooth sequencing comb was inserted about 5 mm into the top of the gel, which was then clamped more tightly. The gel was left to set for 30 min after which the comb was removed and the residual unpolymerised acrylamide was washed away with 1x TTE, if running samples from the PCR Product Sequencing Kit, or 1x TBE for samples derived from the Plasmid Sequencing Kit. The comb was then reinserted so that the teeth could just pierce the surface of the gel. Immediately before the gel was ready for loading reaction samples were heated up to 80° C for 2 min. The gel was run vertically in the TTE or TBE buffer for 4 hours at 30 mA, 40 W and 1500 V. Gels were then fixed for 10 min in a solution containing 10 % v/v methanol and 10 % v/v acetic acid, then washed in water for 10 min followed by drying and exposing overnight on

Kodak X-ray film using a light tight cassette. The film was then passed through an X-Ograph Compact X2 X-ray processor.

2.8.4 Automated sequencing

Either 250 ng of Wizard™ Plus preparations or 50 ng of PCR product (both eluted in H_2O) were sequenced in a total volume of 6 µl in the presence of excess primer using the ABI Prism™, 377DNA Sequencer from Perkin Elmer.

2.9 Managing the Sequence Data via the Gnome GCG package

Sequence data was transferred to the GCG (Genetics Computer Group, Inc., Wisconsin, USA), suite of programs, accessible via the gnome work station, for analysis and comparison with existing sequences in the database.

2.10 Site Directed Mutagenesis

Selection of oligonucleotide-directed mutants were generated using the Altered Sites® II kit from Promega (Southampton, UK). The pALTER®-1 vector contains genes for ampicillin and tetracycline resistance, these selection markers were to be used as a way of obtaining a high frequency of mutants. The gene to be mutated was ligated into the multiple cloning site of pALTER®-1 and transformed into JM109 cells in the presence of tetracycline as the vector initially comes with an inactivated ampicillin gene. The mutagenesis reaction proceeded using an ampicillin repair oligo, a mutagenic oligo, and a tetracycline knockout oligo thus restoring ampicillin and inactivating tetracycline resistance to the mutant strand as well as incorporating the required mutation. To avoid selection against the desired mutation the mutagenesis reaction was transformed into a repair minus strain of *E. coli* (*BMH71-18 mutS*). A subsequent transformation of mutated plasmid into JM109 was plated out in the presence of ampicillin to ensure the correct segregation of mutant and wild type plasmids.

2.10.1 Subcloning into pAlter®-1 using *JM109 E. coli* strain

An HG4 cDNA clone in pBluescript® II SK (+) encoded a single nucleotide mismatch compared to the consenusus, 75 nt downstream from the fist nucleotide of the methionine start codon. This mismatch was to be mutated from a guanine to a thymine using the mutagenesis system. The HG4 cDNA was removed from the plasmid construct by digestion at 37 °C overnight with Sac1 and Xba1 (see section 2.7.3). An identical restriction digest was performed on pALTER®-1 which had been extracted via a Wizard Preparation (section 2.7.2) from a 3 ml culture of JM109s containing the vector. Each digest was electrophoresed on a 1 % (w/v) agarose gel. Cut pALTER®-1 and HG4 DNAs were excised out of the gel and purified using Sephaglas™ (section2.4.4) followed by an additional purification step of passing through a QIAquick column (section 2.4.5). The vector and HG4 insert were ligated together, as described in section 2.6.3, prior to transformation into competent *JM109* cells purchased from Promega. Ligation mix was diluted 1:4 and half of the sample was added to prechilled 15 ml Falcon tubes. Competent JM109s were thawed on ice and 50 µl aliquots were added

to Falcon tubes and left to incubate on ice for 30 min. Tubes were transferred to a 42 °C water bath and heat shocked for 50 sec and then returned to ice for 2 min. Addition of 900 µl of SOC medium to the heat shocked cells was followed by shaking (180 rpm) for 2 h at 37 °C. One tenth and nine tenths of the JM109 suspension were each spread out onto LB / tetracycline (12.5 µg/ml) plates coated with 50 µl of both 0.1 M IPTG and 2 % (w/v) X-Gal (in dimethylformamide) allowing blue/white selection to be made. Plates were incubated overnight at 37 °C after which time a number of white colonies were selected and inoculated into LB containing 10 µg/ml of tetracycline. These where grown up overnight, shaking at 180 rpm at 37 °C and then Wizard™ Plus minipreps (see section 2.7.2) were used to extract plasmids. Confirmation of successful cloning of HG4 was achieved by digestion with Not1 and Pst1 restriction enzymes (section 2.7.3) followed by automated sequencing (section 2.8.4) using the T7 primer (Appendix 3).

2.10.2 Design and Phosphorylation of Primers

For effective selection of mutated vector the mutagenic oligonucleotide was designed to hybridise to the same strand of pALTER as the antibiotic repair nucleotide. A sense primer (MUTs, Appendix 3) of 17 bases was designed with the mismatch located in the centre and 8 perfectly matched nucleotides present on either side. Production of mutants increases greatly when the oligonucleotides have been phosphorylated therefore all the primers supplied in the kit had been 5'-phosphorylated. This meant that only the mutagenic oligo needed to be phosphorylated. This was achieved by adding 100 pmol of MUTs to 2.5 µl of 10 x kinase buffer (700 mM Tris-HCl, pH 7.6, 100 mM $MgCl_2$, 50 mM DTT) 5 units of T_4 polynucleotide kinase, 2.5 µl of 10 mM ATP and H_2O giving a final volume of 25 µl. The 4 pmol/µl reaction mixture of phosphorylated MUTs was incubated at 37 °C for 30 min prior to kinase inactivation at 70 °C for 10 min.

2.10.3 Denaturation of Double-Stranded DNA Template

The double stranded DNA was alkali-denatured before it could undergo mutagenesis. 0.5 pmol (approximately 2 µg of HG4/pALTER®-1 construct) of double stranded DNA template was denatured with 2 µl of 2 M NaOH/2 mM EDTA in a final volume of 20 µl made up with H_2O. After incubating for 5 min at room temperature, 2 µl of 2 M ammonium acetate pH 4.6 and 75 µl of absolute ethanol were added and incubated at -70 °C for 30 min. Precipitated single stranded DNA was spun down at top speed for 30 min followed by washing with 70 % (v/v) ethanol and spinning for 15 min at top speed. The dried pellet was dissolved in 100 µl of TE pH 8.0.

2.10.4 Annealing Reaction and Mutant Strand Synthesis

Added 10 µl (0.05 pmol) of alkaline denatured double stranded DNA to 1 µl (0.25 pmol, 2.2 ng/µl) of both phosphorylated tetracycline knockout oligo & ampicilin repair oligo and 0.31 µl (1.25 pmol, 4 pmol/µl) of phosphorylated mutagenic oligo (MUTs). To this, 2 µl of 10 x

annealing buffer (200 mM Tris-HCl, pH 7.5, 100 mM $MgCl_2$, 500 mM NaCl) and H_2O was added to make up a total volume of 20 µl. Non-specific annealing of oligos was minimised by heating the reaction for 5 min at 75 °C and then allowing to cool slowly to room temperature (1 °C/min to 45 °C, then more rapidly). The sample was then placed on ice and 3 µl of 10 x synthesis buffer (100 mM Tris-HCl pH 7.5, 5 mM dNTPs, 10 mM ATP, 20 mM DTT), 1 µl (5-10 units) of T_4 DNA polymerase, 1 µl (1-3 units) T_4 DNA ligase and H_2O was added to give a total volume of 30 µl. The tube was then transferred to 37 °C for 90 min, allowing mutant strand synthesis and ligation to take place.

2.10.5 Transformation into BMH71-18 *mutS E. coli* strain

The 30 µl of mutagenesis reaction was transferred into prechilled 15 ml Falcon tubes followed by 150 µl of competent mismatch repair minus *E. coli*, BMH71-18 *mutS*. A 10 min incubation on ice was followed by a heat shock for 50 sec at 42 °C and then transferral to ice for 2 min. Cells were then shaken (180 rpm) at 37 °C in 900 µl of LB broth for 30 min, 500 µl of sample was then added to 4.5 ml LB / 125 µg/ml ampicillin in a 50 ml Falcon tube and shaken (180 rpm) overnight at 37 °C.

2.10.6 Transformation into JM109 *E. coli* strain

100 µl aliquots of competent JM109 cells were added to either 5 µl or 10 µl of chilled mutagenised pALTER®-1/HG4 construct obtained using the Wizard™ Plus miniprep (section 2.7.2) on all of the BMH71-18 *mutS* transformed cells. These were placed on ice for 30 min, heat shocked at 42 °C for 50 secs, transferred to ice for 2 min and finally shaken at 180 rpm in SOC medium for 2 h at 37 °C. 1/100, 1/10 and 9/10 aliquots were plated out onto LB plates containing 125 µg/ml of ampicillin and incubated overnight at 37 °C. A selection of colonies was screened by purifying plasmids with the Wizard™ Plus miniprep kit and digesting them with restriction enzymes (section 2.7.3). Correct constructs were then prepared for automated sequencing (section 2.8.4) in the presence of the T7 primer (Appendix 3).

2.11 Production of Peptide Antibodies to HG4

2.11.1 Coupling of Peptide to Carrier Protein

The HG4 synthetic peptide was prepared using the MilliGen 9050 PepSynthesizer (Millipore, Watford, Hertfordshire, UK). In order to generate a sufficient immunological response, it was necessary to conjugate the peptide to a carrier protein before immunisation. The carrier protein porcine thyroglobulin (Sigma) was coupled to the peptide using gluteraldehyde (Sigma). This enables cross-linking through free amino groups.

10 mg of both freeze-dried peptide and thyroglobulin were dissolved together in 0.1 M $NaHCO_3$ to give a final concentration of 2 mg/ml. 10 µl of a 25 % w/v solution of gluteraldehyde taken from a fresh ampoule was added. The mixture was left to rotate end over end in a glass vial overnight at room temperature. A 0.1 volume of 1 M glycine ethyl

ester, pH 8.0, was added and rotated as before for 30 min at room temperature. The sample was then left to dialyse overnight against PBS. Finally the volume was adjusted to give 1 mg of peptide conjugate / ml of solution.

2.11.3 Pre-immune Bleed

A pre-immune bleed of 5 ml was taken from the ear vein of the rabbit before injecting the adjuvant/immunogen complex. This sample was used as a pre-immune control.

2.11 4 Use of Adjuvant

Addition of an adjuvant to the hapten carrier conjugate induces a strong immune response to the immunogens when injected into the rabbit. A 250 µl aliquot of aluminium hydroxide based adjuvant, called Imject® Alum supplied by Pierce (Chester, UK), was added drop by drop to an equal amount of immunogen with stirring. This was left to mix for a further 30 min at room temperature.

2.11.5 Dose

Two 100 µl subcutaneous injections were given to an anaesthetised rabbit. Further boosts were given every ten days until an adequate antibody titre was reached.

2.11.6 Serum Collection by Test Bleeding

Samples of blood were taken from the ear vein of the rabbit before each injection to monitor the production of specific antibodies. Comparison of antibody titres isolated from successive injections allowed the antibody response to be monitored.

2.11.7 Serum Preparation

Each test bleed was allowed to clot for 1 h at 37 °C. The clot was then separated from the sides of the collection vessel with a spatula and placed overnight at 4 °C to retract. The resulting serum was removed at this stage and the remaining clot was spun at 3000 rpm at room temperature for 10 min to release any further serum. 1 ml aliquots of serum were stored at -20 °C.

2.11.8 Exanguination

Once the antibody titre had reached a satisfactory level the rabbit was terminated by exanguination. Blood was collected and left at room temperature for 5 h after which time the sample was spun at 3000 rpm at 4 °C for 10 min. This aided the extraction of the serum, which was then stored at -20 °C. Cutting of the clot into cubes preceded an incubation overnight at 4 °C, encouraging further retraction of the coagulated blood. A final spin was made at 3,000 rpm for 10 min at 4 °C, followed by removal of serum to a screw cap plastic tube, which was stored at -20 °C.

2.12 Antibody Quantification

2.12.1 Enzyme Linked Immunoabsorbant Assay (ELISA)

This technique (Schots *et al.,* 1978) was used to screen serum collected from bleeds so as to monitor antibody specificity and titre. 96-well Falcon Probind ELISA plates were coated with 100 µl of a 10 µg/ml solution of [redacted] coating buffer (15 mM Na_2CO_3, 35 mM $NaHCO_3$, 0.1% (w/v) NaN_3, pH 9.6). Plates were placed at 4 °C overnight, followed by washing three times with 300 µl/well of PBS/0.1 % v/v Tween-20. Non specific binding was blocked by addition of 300 µl/well of blocking buffer (PBS/0.1 % (v/v) Tween-20 / 1 % (w/v) Casein) and left for 2 h at room temperature. Plates were washed twice with PBS/0.1 % (v/v) Tween-20 followed by addition of test serum. Serial dilutions of serum were made starting with a 1/50 (v/v) dilution (in 200 µl of PBS) pipetted into the first well. Further 1:2 (v/v) dilutions were carried out in subsequent wells by transferring 100 µl of 1/50 (v/v) diluted serum to 100 µl of PBS present in the next well and so on. The plates were incubated at 4 °C overnight followed by washing three times with PBS/0.1 % (v/v) Tween-20 to remove unbound antibody. Incubation with a 1:1000 (v/v) dilution of goat anti-rabbit IgG conjugated with horse-radish peroxidase in PBS/0.1 % (v/v) Tween-20 at 4 °C overnight followed. PBS/0.1 % (v/v) Tween-20 was used to wash off antibody three times before washing a further two times with PBS. A 100 µl of freshly prepared substrate (50 mM sodium acetate/ citrate buffer, pH 6, 0.1 mg/ml tetramethylbenzidine, 0.006 % v/v hydrogen peroxide) was added to each well and left for 10-20 min until a blue colour could be visualised. Adding 50 µl of 1.84 M H_2SO_4 (1: 10 v/v dilution of concentrated H_2SO_4) stopped the reaction. The absorbance in each well was measured at 450 nm using a plate reader.

2.12.2 Protein Determination

The Bio-Rad Protein assay (supplied by Bio-Rad laboratories Ltd, Hemel Hemstead, Hertfordshire, UK) is based on the Bradford dye binding procedure (Bradford, 1976) in which the colour change of Coomassie brilliant blue G-250 dye to various concentrations of protein are measured at an absorbance of 595 nm. Protein assays were accomplished in microtitre plates by adding 200 µl of Bio-Rad reagent (supplied by the manufacturers) to a 10 µl (0.05 - 0.5 mg/ml protein) aliquot of protein sample. The absorbance was measured at 595 nm.

2.13 Purification of Polyclonal Antibodies by Affinity Chromatography

Peptide was first immobilised on a cyanogen bromide-activated Sepharose 4B gel (Pharmacia). 1g of CNBr-activated Sepharose 4B was suspended in 50 ml of 1 mM HCl pH 2.0, prior to washing on a sintered funnel with 1 mM HCl pH 2.0, 200 ml of distilled H_2O and 200 ml 0.1 M $NaHCO_3$ pH 8.3 respectively. 10 mg of peptide was dissolved in 5 ml of 0.1 M $NaHCO_3$/0.5 M NaCl pH 8.3. The swelled sepharose beads were spun down at 1500 rpm at room temperature for 2 min enabling extraction of residual $NaHCO_3$. The 5 ml sample of peptide was then added and left to rotate end over end overnight at 4 °C. Excess peptide was removed by washing with three gel volumes of 0.1 M $NaHCO_3$/0.5 M NaCl pH 8.3. Each

wash involved a centrifugation step of 1500 rpm for 2 min followed by removal of supernatant. The remaining active groups were blocked with 0.1 M Tris-HCl pH 8.0 rotating end over end overnight at 4 °C. Three cycles of alternating pH's were then used to wash the Sepharose. Each cycle consisted of a wash with 0.1 M sodium acetate/citrate buffer pH 4.0 containing 0.5 M NaCl followed by 0.1 M Tris-HCl pH 8.3 containing 0.5 M NaCl. The resin was then transferred to 5 ml of 20 mM Na_2HPO_4/0.5 M NaCl containing 0.01 % w/v sodium azide.

The slurry, of Sepharose immobilised with peptide, was packed into a column which had been linked up to a uvicord (LKB-Optical Unit UV-1 from Pharmacia) and graph plotter. In doing so the absorbance at 280 nm could be monitored to detect any proteins passing through the column at any given time. The beads were washed with 20 mM Na_2PO_4 pH 7.3 prior to addition of the elutant (0.05 M diethylamine pH 11.5), thus removing any unbound peptide from the column. Once a constant base level had been registered by the uvicord, 10 ml of serum was recycled through the column overnight at 4 °C. Washing with 20 mM Na_2PO_4 pH 7.3 followed this until the original base level had been reached. This ensured that no unbound serum remained in the column. Bound antibody was eluted with 0.05 M diethylamine pH 11.5. Fractions, corresponding to plotted peaks relating to protein detected by the uvicord, were immediately dialysed against PBS overnight at 4 °C. The resulting sample was concentrated by transferring the dialysis tube into polyethylene glycol-20,000. The sample was pipetted out of the tubing once the volume had been reduced to 2 ml, followed by storing 200 µl aliquots at -20 °C in the presence of 0.01 % v/v sodium azide. The column was washed with 20 mM Na_2PO_4 pH 7.3 before regenerating with three alternating cycles of 0.1 M Tris HCl / 0.5 M NaCl (pH 8.3) and 0.1 M sodium acetate/citrate buffer containing 0.5 M NaCl (pH 4.0). Storage in 20 mM Na_2PO_4 pH 7.3 and 0.01 % (v/v) sodium azide at 4 °C enabled the reuse of the column.

2.14 Production of Protein Antigens by Bacterial Over Expression

The protein fusion system, developed by NEB, was utilised to discover if purified antibody would bind to a folded form of the extracellular domain of HG4, along which the peptide epitope was located. Specific binding to the expressed protein would indicate whether the antibody epitope was exposed on the surface of the protein. This could be detected by running the expressed fusion protein on a SDS-PAGE gel followed by Western blot and probing with the purified antibody.

The DNA sequence coding for the N-terminal extracellular domain was inserted in-frame into the pMAL-c2 expression vector down-stream from the *malE* gene, which encodes maltose-binding protein (MBP). Cloning of this construct resulted in the periplasmic expression of an MBP-fusion protein upon induction with IPTG. This was carried out in the following manner:

2.14 1 Design of Primers

The sense primer pMALs and the antisense primer pMALa (Appendix3) were designed specifically to anneal to target sequences flanking the cDNA sequence that encoded the extracellular domain of HG4. The pMALs primer incorporated a Sal 1 restriction site whilst pMALa encoded a stop codon followed by a Pst1 site. Each restriction site was present in the polylinker found down stream from the *malE* gene thus allowing the PCR amplified product to insert in the correct orientation.

2.14.2 Isolation of Extracellular Domain of HG4 and ligation into the pMAL vector

A Wizard™ preparation of an HG4 cDNA clone in pBluescript® II SK (+) was prepared as described in section 2.7.2. 8 μg of plasmid was then digested with the restriction enzymes Not 1 and Xba 1 (section 2.7.3) and ran on a 1 % w/v agarose gel (section 2.4.3). HG4 cDNA was purified with the Sephaglas™ Band Prep (section 2.4.4) and used as template in a PCR reaction using the High Fidelity Expand Kit (section 2.4.2) with pMALs and pMALa primers. The sample was loaded onto a 1 % w/v agarose gel and a product corresponding to the correct size of the extracellular domain of HG4 (HG4-ex) was excised and purified using the Sephaglas™ Band Prep. A double digest, using Sal 1 and Pst 1 restriction enzymes, was performed on both pMAL vector and PCR product of HG4-ex followed by a QIAquick™ clean up (section 2.4.5). Restricted products were then ligated as described in section 2.6.3.

2.14.3 Transformation into XL2 Blue strain of *E. coli*

To 15 ml Falcon tubes containing 50 μl of ligation mix (previously diluted 1:4 with H_2O) 25 μl of ultra competent XL2 Blues were added. After incubating on ice for 30 min the cells were heated shocked at 42 °C for 30 sec followed by 2 min on ice. 0.9 ml of DYT, preheated to 42 °C, was added and left to cultivate for 2 h at 37 °C, shaking at 180 rpm. A tenth and nine tenths of the culture were plated out onto LB/ampicillin (100 μg/ml) plates and incubated overnight at 37 °C.

2.14.3 Replica Plating

The transformants were replica plated on a LB/ampicillin (100 μg/ml) master plate and on a LB/ampicillin (100 μg/ml)/IPTG (0.1 mM)/X-Gal (80 μg/ml) indicator plate and placed at 37 °C overnight. White colonies on the indicator plate were screened using the Wizard™ Plus kit and digested to confirm that HG4-ex had been successfully transformed into pMAL-c2.

2.14.4 Induction of Fusion Protein

100 μl of an overnight culture of HG4-ex/pMAL was inoculated into 5 ml LB/ampicillin (100 μg/ml) and grown to an optical density of 0.5 at 600nm. A 1 ml aliquot was transferred into a sterile microfuge tube and placed on ice whilst the remaining culture was induced with 15 μl of 0.1 M IPTG and incubated at 37 °C for a further 2 h shaking at 180 rpm.

2.15 SDS-PAGE

2.15.1 Sample Preparation

IPTG induced and uninduced cells were resuspended respectively in 100 µl and 50 µl of SDS-PAGE loading buffer (4 ml dH_2O, 1 ml 0.5 M Tris-HCl, pH 6.8, 0.8 ml glycerol, 1.6 ml 10 % w/v SDS, 0.4 ml 2-β mercaptoethanol and 0.2 ml of 0.05 % w/v bromophenol blue). These samples were then heated in a boiling water bath for 5 min. 15 µl of each sample was then loaded onto a 10 % v/v SDS-PAGE gel along with protein molecular weight markers (Bio-Rad). 5 µl/well of pre-stained marker was loaded on the gel used in Western blotting and 10 µl of 1:20 diluted standard marker in SDS-PAGE loading buffer was loaded on the gel to be stained with Coomassie brilliant blue R250 dye.

2.15.2 Preparation of a 10 % SDS-Polyacrylamide Gel

Two separating gels were made using 6 ml of Protogel™ (30 % w/v acrylamide stock solution, 29.2 g acrylamide, 0.8 g Bis (N, N'-methylenebisacrylamide), 100 ml H_2O, from Flowgen), 4.5 ml of solution B (1.5 M Tris-HCl, pH 8.8, 0.4 % w/v SDS), 100 µl of 10 % w/v ammonium persulphate, 20 µl of TEMED and 7.5 ml of H_2O. The solution was poured into Atto™ minigel rigs, overlaid with isopropanol and allowed to set. The solvent was removed and the gel interface was rinsed with distilled H_2O. A stacking gel (4.5 % v/v) was then prepared by mixing 0.9 ml of Protogel™ with 1.5 ml of solution C (0.5 M Tris-HCl, pH 6.8, 0.4 % w/v SDS), 50 µl of 10 % w/v ammonium persulphate, 20 µl of TEMED and 3.6 ml of H_2O. The solution was poured over the two separating gels and combs were inserted before leaving to set. The gels were placed into the electrophoretic chamber and 1x running buffer (5x stock: 15g/l tris base, 72g/l glycine, 5g/l SDS, for 1X: diluted 60 ml of 5x stock with 240 ml H_2O for electrophoresis) was added. Combs were removed and wells were washed out with buffer to remove any urea that may have collected there. Samples were then loaded and ran at 100 volts, at maximum current for 20 min followed by 150 volts, maximum current until the dye front had reached the bottom of the gel. Gels were removed from the apparatus, one was soaked overnight at room temperature by rotating in Coomassie Stain (0.5 g Coomassie Blue R-250, 200 ml methanol, 50 ml acetic acid, 249.5 ml H_2O), the other (loaded with prestained markers) was used for Western blotting. The Coomassie stained gel was put into destain solution (400 ml methanol, 100 ml acetic acid, 500 ml H_2O) and slowly rotated until background staining was removed.

2.16 Western Blot

2.16.1 Blotting

Two gel sized sets of 5 sheets of 3MM Whatman filter paper (supplied by Whatman Ltd, Maidstone, Kent, UK) were soaked in transfer buffer (2.92 g/l glycine, 5.8 g/l Tris, 0.375 g/l SDS, 200 ml methanol (20 % v/v)). The first set was aligned on the graphite transfer plate of a NovaBlot blotter (from Pharmacia) followed by nitrocellulose membrane (Amersham, Little Chalfont, Buckinghamshire, UK), that had previously been soaked in methanol and then

transfer buffer. The SDS-PAGE gel was rinsed in water and rolled out on top of the membrane. The stack was overlaid with the second set of soaked filter paper and any air bubbles, between layers, were removed by rolling a 10 ml pipette over the top of the sandwich. The upper graphite plate was lowered on top and the rig was then connected up to the power supply, set at 0.8 mA x surface area of gel for 2 h.

2.16.2 Probing with Primary and Secondary Antibodies

Western blots were rinsed in PBS for 10 min prior to an hour incubation on a rotating table (40 rpm) in blocking buffer at room temperature. Blots were washed three times with PBS/0.1 % v/v Tween-20 before incubating on a rotating table overnight at 4 °C with primary antiserum diluted 1:200 (v/v) in blocking buffer (10 % w/v Marvel™ non-fat milk powder in PBS, 0.01 % sodium azide). The membrane was washed three times as before, followed by rotating for 2 h at room temperature in the presence of secondary serum (horseradish peroxidase-conjugated goat anti-rabbit antibody) diluted 1:10,000 in blocking buffer. Unbound antibody was removed by washing three times in PBS/0.1 % v/v Tween-20.

2.16.3 Detection by ECL

The ECL detection kit was supplied by Amersham Life Science (Little Chalfont, Buckinghamshire, UK) and works on the principle that Horse Radish Peroxidase in the presence of H_2O_2 will oxidise luminol under alkaline conditions promoting chemiluminescence. In the presence of enhancers, such as phenol, the light emission can last up to 20 min during which time the reaction can be detected by overlaying the blot with autoradiography film.

An equal volume of detection solution 1 (supplied by Amersham) was mixed with detection solution 2 (supplied by Amersham) and poured onto the surface of the antibody bound blots followed by a 1 min incubation at room temperature. Excess detection fluid was drained off and the blot was wrapped in clingfilm before overlaying with X-ray film, protein side up in a film cassette over a series of exposure times. Films were developed using an X-Ograph Compact X2 processor.

2.17 Immunolocalisation Of HG4 in Whole Worms

2.17.1 Adult Worm Collection

A sheep, infected with avermectin-susceptible *Haemonchus contortus,* was slaughtered and its abomasum was removed during butchering. The stomach lining was cut through and water was used to rinse away the guts semi-digested contents. Adult *Haemonchus contortus* could be seen attached to the gut lining. The organ was placed into the isolation apparatus as depicted in figure 9 in the presence of DMEM, Dulbecco's Modified Eagle Medium supplied by Gibco BRL (Renfrewshire, Scotland) and kept at 37 °C using a heat-emitting lamp. Adults detach themselves from the gut lining and could thus be collected. Residual

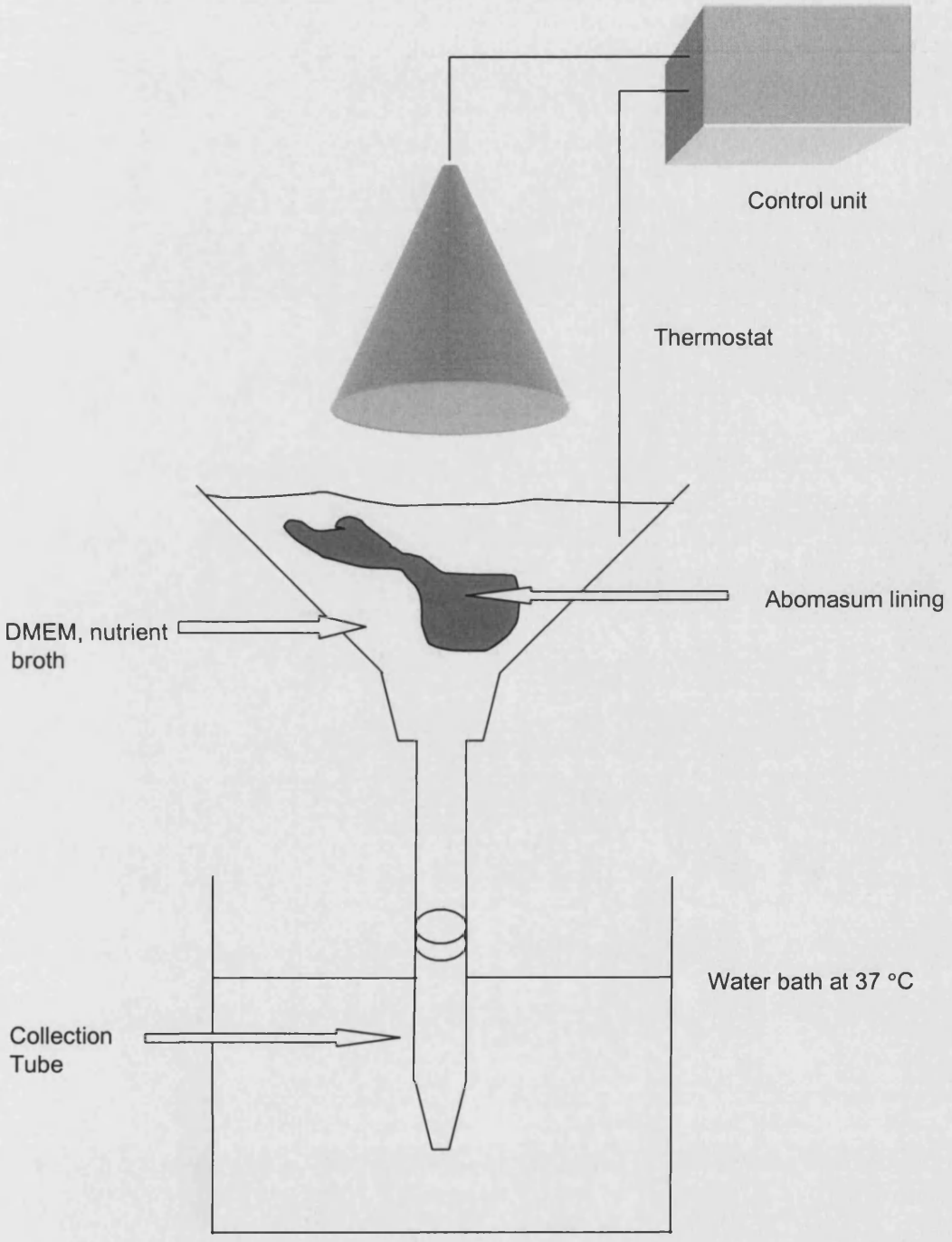

Figure 9. Apparatus set up to collect adult *H. contortus* from sheep abomasum.

debris was removed by washing the worms in broth kept at 37 °C. Once washing had been repeated several times the worms were transferred into fix.

2.17.2 Tissue Fixation and Permeabilisation

Haemonchus adults were incubated in freshly prepared fixative (4% w/v paraformaldehyde in PBS) for 8 h at 4°C. Worms were washed three times in PBS and transferred to storage buffer (0.1 % w/v paraformaldehyde in PBS), thus enabling long term storage at 4 °C.

In order to carry out immunolocalisation work, antibodies were required to enter the nematode via the cuticle. It was therefore a requirement that the multi-layered cuticle coating the worm was permeabilised. This was done by incubating the worms in BME solution (5% v/v β-mercaptoethanol, 1 % v/v Triton X-100 and 125 mM Tris pH 6.9) at 37 °C overnight, promoting the reduction of disulphide bonds, followed by briefly washing in PBS. Worms were then treated with 120 collagen digestion units/ml of collagenase in collagenase buffer (1 mM Ca_2Cl and 100 mM Tris pH 7.5) at 37 °C for either 10 h or 20 h rotating at 40 rpm, or still for 48 h. Once the cuticle had been digested the worms were washed in PBS before serum incubation.

2.17.3 Immunocytochemistry

Dilutions of Primary antibody in antibody dilution solution (0.1 % w/v BSA, 0.5 % v/v Triton X-100 and 0.05 % w/v NaN_3 in PBS) were pipetted onto the worms and incubated at 4 °C for 72 h. Unbound antibody was removed by washing three times with PBS. Worms were then exposed to a 1:200 dilution of secondary serum; TRITC-conjugated goat anti-rabbit IgG (Sigma) in antibody dilution solution. After incubating overnight at 4 °C, unbound IgG was removed with three 15 min washes, followed by an overnight wash of PBS/0.1 % v/v Triton X-100. Immunolabelled nematodes were mounted onto slides using VectaShield (Vector Laboratories, Bretton, Peterborough, UK) and viewed under an Olympus BHS Episcopic Fluorescence microscope. Microscope settings used were; green excitation region, exciter filter G (IF-545+BG36), Dichromic mirror G (DM-580+0.590) and barrier filter R-610. A more detailed examination was achieved using a Zeiss Axiovert 100M inverted confocal microscope from Zeiss (Germany).

2.17.4 Post-adsorption of Antibody with Peptide

A negative control was set up to confirm that the primary antibody was binding specifically. HG4 peptide (final concentration of 0.5 μg/ml) was incubated with 1:10 dilution (in antibody dilution solution) of primary antibody for 1 h at 37 °C. These samples were used directly on collagenase treated worms.

3. The Isolation of Full-Length HG4 cDNA

3.1 Introduction

This chapter describes the sequence of events leading to the identification of a full-length consensus sequence coding for the avermectin receptor subunit, HG4. The methods utilised to accomplish this are detailed as well as reasons for their preferential use over other existing methods. The production of a consensus sequence is also accomplished for further characterisation through expression in *Xenopus laevis* oocytes. Finally, an attempt is made at isolating HG4 from avermectin resistant *H. contortus* to determine whether resistance has developed from an alteration in the transcribed code.

3.1.1 Techniques to Isolate Genes of Interest

Isolation of genes provides the opportunity to establish the structure and function of expressed proteins in a living organism. Recombinant DNA technology has proven a useful tool in detecting these genes. The process of isolating and cloning such fragments begins with either construction of a DNA library or the use of the Polymerase Chain Reaction.

Screening of a genomic library enables the retrieval of a full-length gene including untranscribed 5' and 3' regions. For complex organisms, such as nematodes, a complete library will contain so many clones that identification of the desired gene may prove to be a lengthy task. A reduced number of clones can be catalogued in a cDNA library, produced from reverse transcribed mRNA. With this library, only the genes expressed at a particular stage of development are represented. cDNA libraries offer a method of obtaining a full-length clone of interest in one step. The success of isolation is however dependent on the relative abundance of the clone of interest. Highly abundant messages can represent 10 % or more of the total mRNA. In contrast, very rare messages, such as those coding transmitter-gated ion channel (TGIC) subunits, can be less than 1 part in 10^6 (Moore, 1987). Due to the scarcity of TGIC subunits it is essential that a high cloning efficiency must be maintained. Even with this considered, screening of millions of plaques may need to be accomplished before isolating the clone of interest (Harvey *et al,* 1991).

A relatively new technique, known as the Polymerase Chain Reaction (PCR), overcomes the problems encountered in screening cDNA libraries for clones of low abundance mRNAs. This method is so sensitive that it can amplify a single copy gene sequence from a single cell (Holding & Monk, 1990). It was therefore decided that PCR was to be used to amplify TGIC subunits specific to the avermectin receptor. This circumvents the inevitable lengthy process of screening millions of plaques, which follows the construction of a library.

PCR can amplify a segment of DNA that lies between two regions of known sequence. Two oligonucleotides are used as primers to anneal to opposite strands of template DNA with their 3' ends facing each other. This enables synthesis, by DNA polymerase, to extend across the

segment of DNA between the two primers, in a 5' to 3' direction. The template DNA is initially denatured with heating in the presence of buffer, Mg^{2+}, excess primers and dNTPs. Denaturation is followed by the addition of a thermostable DNA polymerase after which the reaction mixture is cooled to a temperature that allows the primers to hybridise to the target sequences (the annealing temperature). The temperature is then increased to ensure that the DNA polymerase synthesises a complementary strand under optimal conditions (the extension temperature). One cycle of denaturing, annealing and extension results in synthesis of a new strand of undefined length, a second cycle gives a single stranded product corresponding to the exact length of the stretch of DNA found between the two primers. Each strand synthesised is complementary to one of the two primers and can therefore participate as template in the exponential amplification produced by subsequent cycles (Coen & Scharf, 1990).

3.1.2 HG4 Partial Sequence

A partial 450 base pair cDNA fragment denoted HG4 had previously been isolated by PCR with cDNA produced from a population of *H. contortus* eggs (Laughton, 1993). This had been achieved using the degenerate primers DS and DA. These had been designed to conserved regions of $GABA_A$ and glycine receptor subunit sequences from both invertebrate and vertebrate species. One of the resulting partial sequences, denoted HG4 (Figure 10a/b), shared homology with the inhibitory amino acid receptor family. More specifically, it possessed a 66% amino acid identity with the glutamate-gated chloride channel beta subunit (GluClβ) isolated from *Caenorhabditis elegans*. This class of receptor is believed to be the target for the anthelmintic, avermectin. Administration of this drug to *H. contortus* infected livestock induces expulsion of nematodes from the host. Avermectin has been shown to target glutamate-gated chloride channels in the free-living nematode *C. elegans* (Arena *et al.*, 1991, 1992). Consequently, hyperpolarisation of receptor-expressing cells occurs which ultimately leads to paralysis of muscles (Geary *et al.*, 1993). Attempts to isolate full-length cDNAs from a parasitic nematode such as *H. contortus* were to be made using a variation of the PCR technique. Once this target has been obtained, further characterisation can be accomplished to determine the exact mechanism through which avermectin works. It will also be possible to establish why resistance to the drug has developed.

3.1.3 RACE PCR

Isolation of target cDNAs corresponding to TGIC subunits will be amplified using a variant of PCR known as RACE, an acronym for the Rapid Amplification of cDNA Ends (Frohman *et al.*, 1988). Unlike PCR, where amplification of DNA between two known or presumed sequences occurs, RACE can achieve amplification of the region between a short known sequence in a cDNA molecule and its unknown 3' and 5' end. In nematodes, this technique

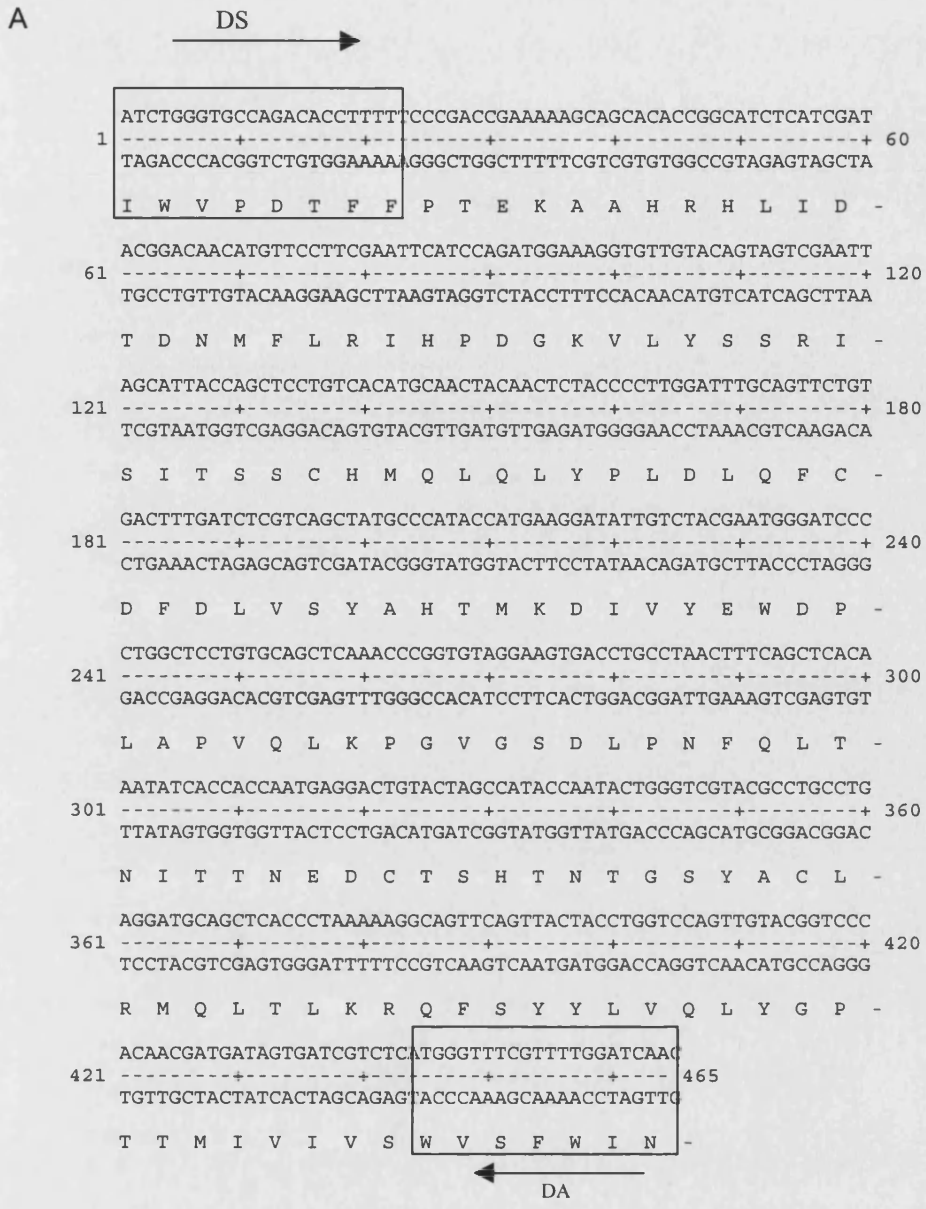

Primer	Nucleotide Sequence	Amino Acid Sequence
DS	5'(AC)T(CT)TGGGTGCCAGACACCT(AT)(CT)TT 3'	**(I/L)WVPDT(Y/F)F**
DA	5' (AG)(AG)(AG)TTNA(AGT)CCA(AG)AAN(CG)(AT)NACCCA 3'	**WVSFW(I/L)N**

N = For all nucleotides

Figure 10a, HG4 partial sequence. b, PCR approach. The 450 bp HG4 fragment was amplified using oligonucleotides DS and DA. Positions of these degenerate primers are depicted and nucleotide and **amino acid** composition is detailed. Five partial sequences were amplified using these primers and were denoted HG1-5.

exploits the presence of two ubiquitous stretches of sequence flanking 3' and 5' cDNAs ends.

The universal sequence present at 3' ends can be incorporated during reverse transcription of mRNA into cDNA by use of an adapter/primer known as RoRi$(dT)_{17}$. In the presence of reverse transcriptase the poly $(dT)_{17}$ anneals to the complementary poly (A) tail of the message initiating cDNA synthesis. The oligo (dT) adapter/primer is designed to allow the binding of two nested 17-mer primers: Ro (outer) and Ri (inner). This region also enables binding of a 28-mer RoRi that encompasses both inner and outer sequences.

In contrast, the majority of 5' ends possess a specific sequence derived from a trans-splicing event universal to nematodes. A spliced leader sequence (SL1) is donated from the 5' end of a small, non-polyadenylated RNA to primary transcripts thus forming a common 22 nt 5' terminal sequence on mature mRNAs (Davis, 1996). The leader sequence 'CTCAAACTTGGGTAATTAAACC' was originally identified in the free-living nematode *C. elegans* (Krause & Hirsh, 1987). Since then identical sequence to SL1 has been described at the 5' ends of a variety of parasitic nematodes including *Haemonchus contortus* (Bektesh *et al*, 1988).

Primers designed to hybridise to either RoRi or SL1 sites will be used in conjunction with gene specific primers (Appendix 3). The latter will be generated according to the previously isolated HG4 partial sequence to amplify both 3' and 5' ends respectively.

3.1.4 Semi-Nested PCR

A common occurrence when performing RACE PCR is that a significant amount of non-specific products can be amplified. These result from the presence of only one set of gene specific primer during the reaction. To overcome this problem a second round of PCR will be accomplished using first round amplification products as template. Included in this reaction will be the first round gene specific primer and a primer designed to hybridise to an internally located stretch of sequence (Frohman & Martin, 1989).

3.1.5 PCR induced Mutations

The most frequently used thermostable DNA polymerase in PCR reactions is the one isolated from *Thermus aquaticus* (*Taq* DNA polymerase). One drawback with *Taq* is that it lacks editing functions and incorporates an incorrect nucleotide at a rate of 2×10^{-4} nucleotides per cycle (Coen & Scharf, 1990). The low abundancy of mRNA coding for TGIC subunits makes it necessary to use high levels of cycling, which has the potential of introducing a high number of mutations. One step taken to reduce the error frequency will be to use a combination of thermostable polymerases with and without proof reading activity. The Expand™ PCR system suits this requirement as it uses both *Pwo* DNA polymerase isolated from *Pyrococcus wosei* as well as the traditional *Taq* polymerase. The former enzyme possesses a 3' exonuclease activity. Even with this added precaution individual clones from

an amplified pool may still contain unreliable sequence. It has therefore been decided that PCR amplification is to be done in triplicate yielding three individual sequences, which can then be aligned to give a consensus sequence.

3.1.6 Amplification of HG4 from Avermectin Resistant *H. contortus*

Current beliefs are that avermectin resistance has resulted from more than one alteration in the genetic make-up of the worm (Dent *et al*, 1997). Multiple genes appear to code for avermectin resistance in *C. elegans* including *avr-1, –5 and -15.* The former two are believed to play a role in avermectin uptake via the amphids (Perkins, 1986 and Starich, 1995). The *latter avr-15* mutant encodes a defective glutamate-gated chloride channel GluClα2 subunit. This defect is caused by a point mutation whereby the codon TGG at position 271 coding a tryptophan is mutated to an opal stop codon TGA (Dent *et al*, 1997). This alteration leads to the translation of a truncated protein that is no longer membrane spanning. It is possible that several other glutamate-gated chloride channel subunits carry mutations triggering avermectin resistance. The HG4 receptor subunit cDNA will be isolated from an avermectin resistant population and its sequence will be compared to HG4 from susceptible worms. This will be done to establish differences at the cDNA level, which may lead to avermectin resistance.

3.2 Results

3.2.1 Template Production

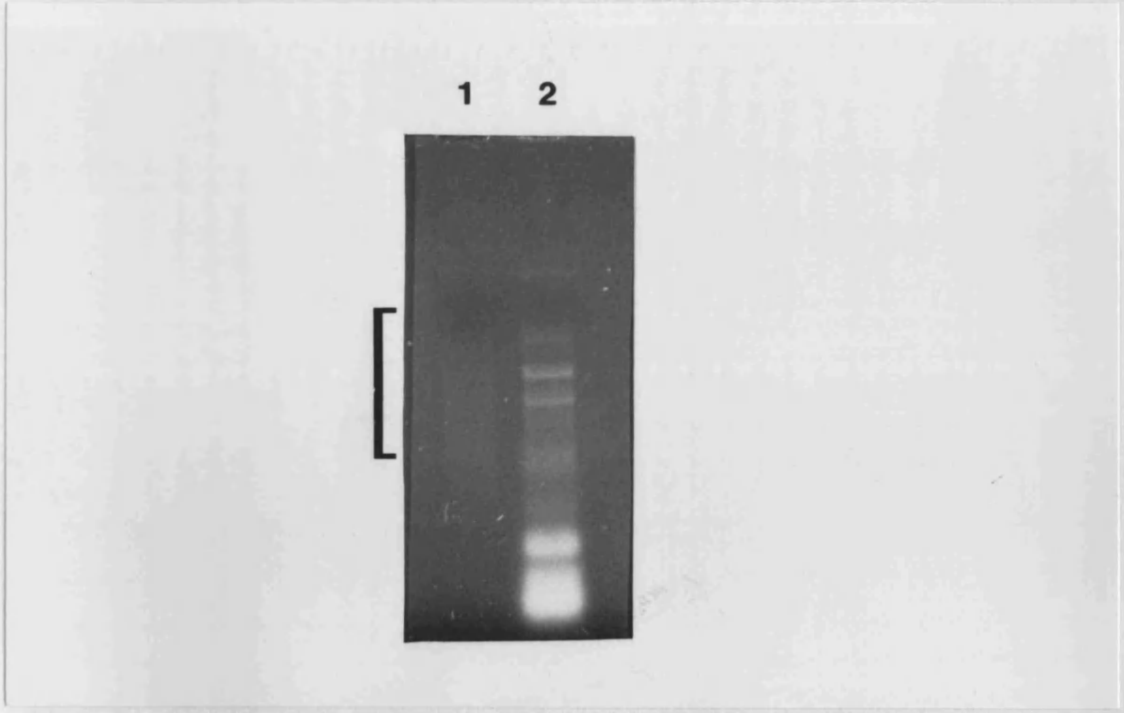

Figure 11, Total RNA and mRNA extraction from *Haemonchus contortus* eggs.
Lane 1, mRNA (260 ng) Lane 2, total RNA (1.55 μg)
Ran on a 1 % (w/v) RNase-free agarose gel.

Total RNA was extracted from two developmental stages of *H. contortus*, more specifically from 1g off adult worms or 1 g of eggs. The mRNA isolated from 200 µg aliquots of total RNA was reverse-transcribed, generating cDNA for utilisation in RACE-PCR. A 1 % (w/v) agarose gel loaded with total RNA and mRNA from eggs is depicted in figure 11. The faint smear of mRNA seen in lane 1 indicates that mRNA isolation was successful and that cDNA synthesis could proceed.

3.2.2 Isolation of the 3' Terminus of HG4 by RACE-PCR

A gene specific sense primer (HG4-GSSP1) was designed to hybridise to a stretch of 21 nts, specific to the partial fragment of HG4. RACE-PCR was carried out using HG4-GSSP1 in conjunction with the antisense RoRi primer in the presence of cDNA produced from adult *Haemonchus contortus*.

RACE-PCR has a tendency to yield significant amounts of non-specific products due to the universal sequence flanking the poly (T) tail that complements the RoRi primer. To overcome this problem a semi-nested PCR approach was developed. This required the design of a gene specific sense primer (HG4-GSSP2) which hybridises further down-stream of HG4-GSSP1. This technique enabled first round products to be screened using both RoRi and the internal HG4-GSSP2 in a second round of PCR as depicted in figure 12.

A potential 3' RACE product of HG4 was visualised after electrophoresis on a 1 % (w/v) agarose gel. Figure 13 depicts a set of PCR reactions yielding the expected size of fragments. Lane 2 was loaded with the products of a first round RACE reaction using adult cDNA template with HG4-GSSP1 and RoRi primers. A discrete band corresponding to a size of approximately 1.06 kbp had been amplified. A semi-nested second round of PCR was accomplished using this Sephaglas™ purified 1.06 kbp band as a template along with the terminal RoRi primer and the internal primer HG4-GSSP2. The resulting 1.03 kbp band seen in lane 5 suggested that the first round product was specific.

3.2.3 Direct Sequencing and Cloning Strategy for 3' end of HG4

The 1.06 kbp RACE product was primed with HG4-GSSP2 and sequenced using the Sequenase™ PCR Product Sequencing Kit. The sequence obtained confirmed that the product coded for the 3' end of HG4. The remaining 1.06 kbp Sephaglas™ purified band was treated with DNA polymerase and polynucleotide kinase forming blunt-ended cDNA. This was then ligated into an EcoRV cut pBluescript SK^+ vector. The resulting construct was transformed into the *E. coli* strain XL1-Blue, promoting blue/white selection. Plasmid DNA from white colonies was initially purified using the small-scale plasmid preparation. This technique offered a rapid step in which many clones could be purified at once. The screening of 18 individual clones was achieved by double digestion with the restriction enzymes Xba1 and Xho1. Digested clones were loaded onto a 1 % (w/v) agarose gel seen

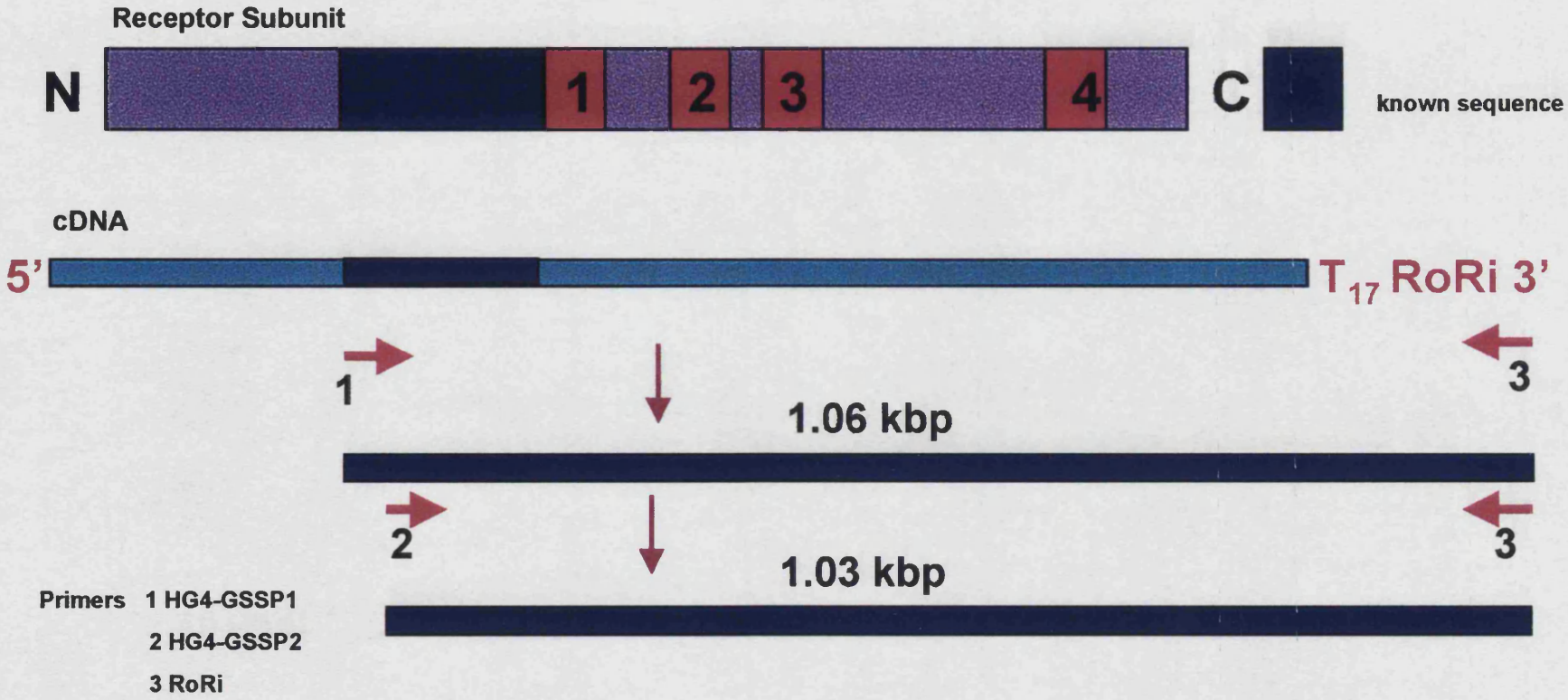

Figure 12, Strategy for Isolating the 3' end of HG4 using RACE-PCR.

in figure 14. The desired constructs released a 1.06 kbp fragment upon digestion as shown in lanes 3, 4, 5, 7, 8, 9, 11, 12, 14, and 18. The clone from lanes 7 was re-cultured and recombinant plasmids were purified using the Wizard™ Plus DNA purification kit.

Figure 13, Amplification of the 3' end of HG4 using RACE-PCR.
Lanes 1 & 8: λ DNA cut with the restriction enzyme Pst1, respective band sizes listed along the side of the gel.
Lane 2: First round PCR reaction using HG4-GSSP1 and RoRi amplifying a 1.06 kbp band (➔).
Lane 3: Single primer PCR control using HG4-GSSP1
Lane 4: Single primer PCR control using RoRi
Lane 5: Semi-nested PCR of 1.03 kbp using primers HG4-GSSP2 and RoRi with purified 1.06 kbp band seen in lane 2 as DNA template.
Lane 6: Single primer PCR control using the purified 1.06 kbp band shown in lane 2 as template and HG4-GSSP2.
Lane 7: Negative control using primers RoRi and HG4-GSSP2 and no template.

PCRs utilised the Expand™ Long Template PCR System in the presence of 1.75 mM $MgCl_2$ and 300 nM of each primer. Samples in lanes 1 to 4 were amplified from cDNA template synthesised from adult *H. contortus* mRNA. Cycling conditions: 94 °C denaturation for 2 min, followed by the addition of 2.5 U enzyme, after which 40 cycles of 94 °C for 30 sec, 60 °C for 30 sec and 68 °C for 2 min were run terminating with 7 min at 68 °C. 40 µl of reaction mix from each sample was separated by electrophoresis on a 1 % (w/v) agarose gel ran in TBE buffer.

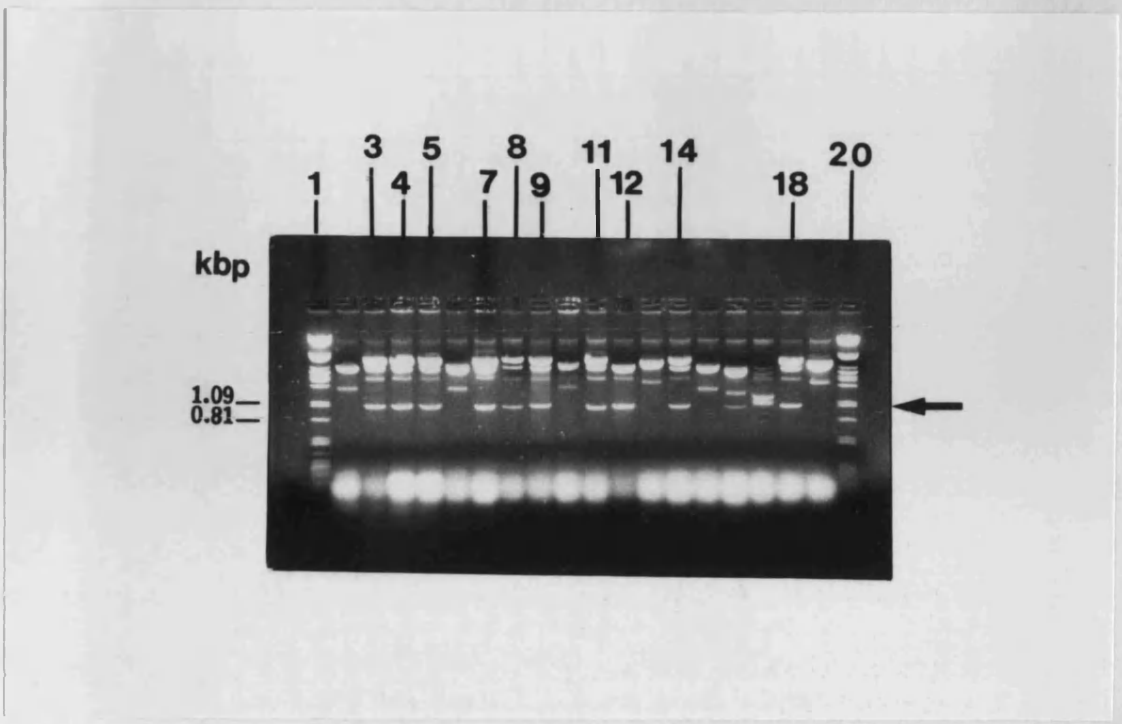

Figure 14, Restriction digests of HG4 3' plasmid constructs.
Lanes 1 & 20 contain λ cut with Pst1, band sizes are listed in kbp beside the gel.
Lanes 3, 4, 5, 7, 8, 9, 11, 12, 14, & 18 are loaded with constructs possessing the 1.06 kbp HG4 3' PCR product (➔).
Remaining lanes represent plasmids that do not contain the HG4 3' PCR insert.
Plasmids were previously purified from the *E. coli* strain XL1-Blue and then digested with the endonucleases Xba1 and Xho1 for 1 hour at 37 °C, restricted products were separated by electrophoresis on a 1 % (w/v) agarose gel in TBE buffer.

3.2.4 Sequence Analysis of the 3' end of HG4

Manual sequencing, employing the Sequenase™ Quick-Denature plasmid sequencing kit was performed on the Wizard™ Plus purified construct represented in lane 7 of figure 14. A preliminary sequence, displayed in figure 15, was obtained consisting of a coding region of 579 bp followed by a 3' untranslated region (3' UTR) of 431 bp, a poly (A) tail of 17 nts and the 28 nt RoRi sequence. This was transferred to the GCG package on the gnome workstation and a comparison was made with existing sequences listed in the GenEMBL database. The coding region was shown to have a 77.78 % amino acid identity with the *C. elegans* glutamate-gated chloride channel beta subunit, GluClβ.

3.2.5 Isolation of the 5' Terminal of HG4 by RACE-PCR

5' RACE required the use of a complementary SL1 primer, designed to the splice leader sequence, and a gene-specific antisense primer (HG4-GSAP1). As with the isolation of the 3' end, a semi-nested approach was taken, primers HG4-GSSP1 and HG4-GSAP1 (Appendix 3) were used in a second round of PCRs. The exact strategy used is illustrated in figure 16.

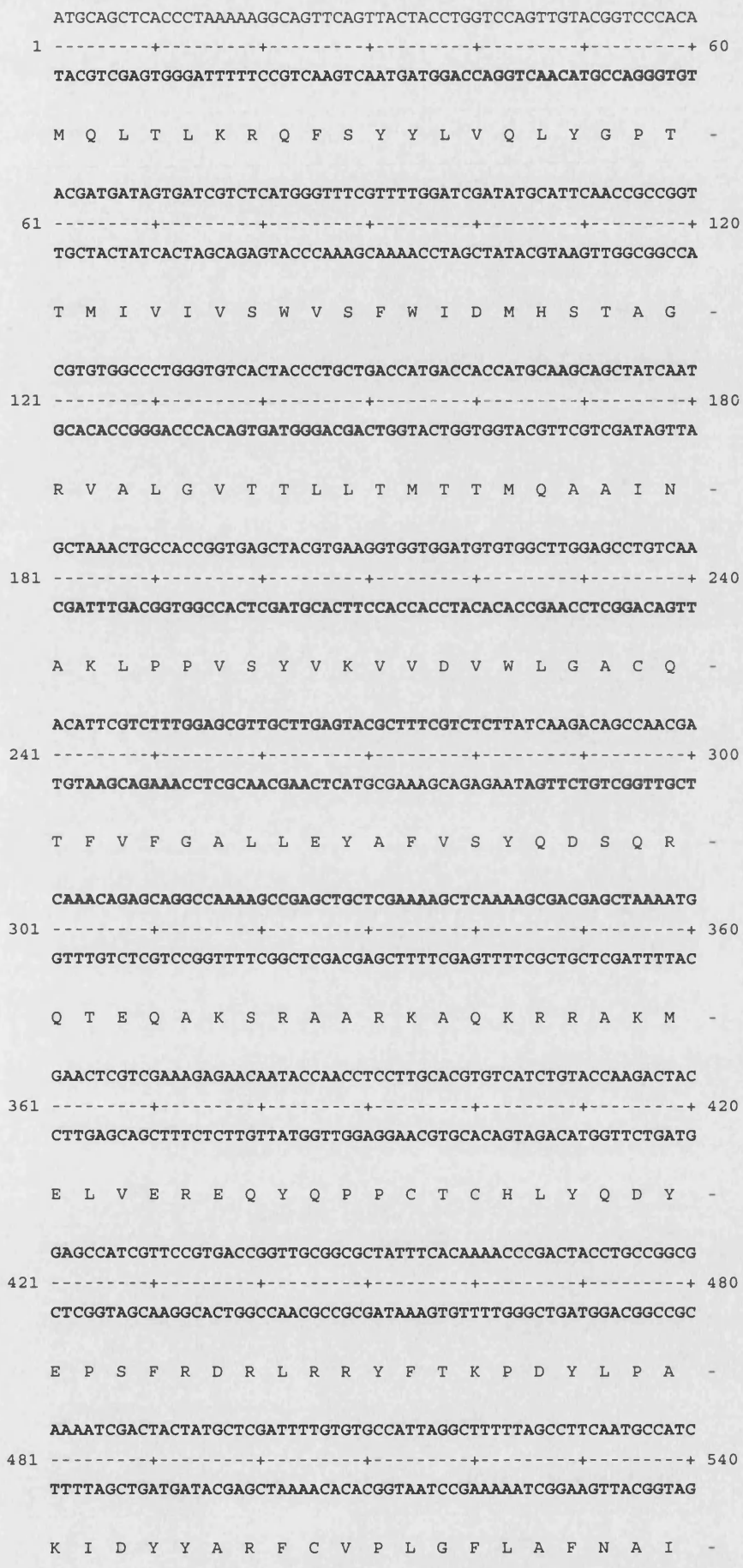

Figure 15, See legend see next page.

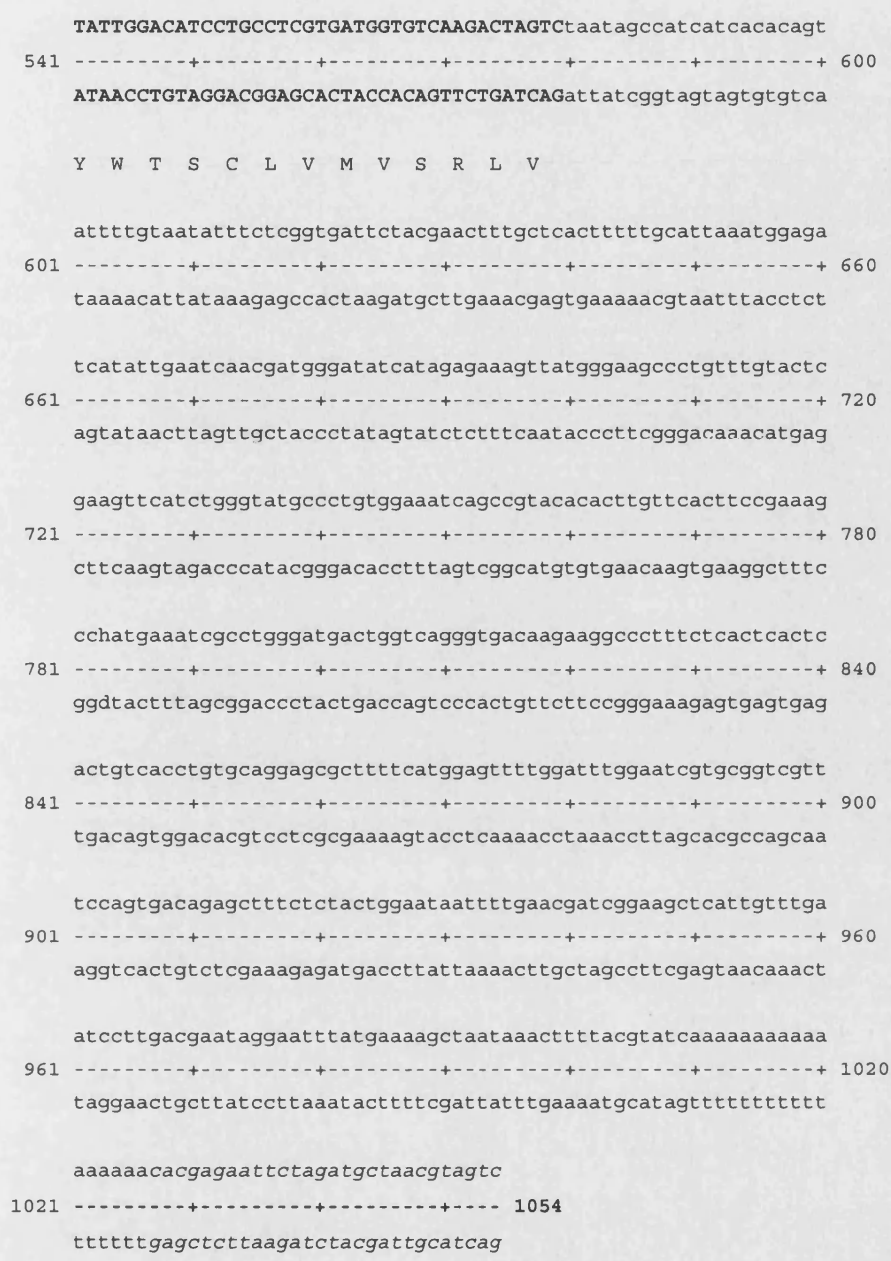

Figure 15, A preliminary 3'-RACE amplified sequence for HG4 cDNA. Includes the **coding sequence**, 3' utr, poly(A)$_{17}$ tail and *RoRi sequence.* The translated amino acid sequence is also displayed below the corresponding nucleotide sequence.

The 1 % (w/v) agarose gel in figure 17 reveals a set of PCR reactions amplifying the HG4 5' cDNA end. Lane 2 was loaded with a RACE-PCR done on adult *H. contortus* cDNA with primers SL1 and HG4-GSAP1. The band of interest, generated from this reaction, has an approximate size of 940 bp. Lane 3 was loaded with the reamplification products generated using the 940 bp product as template with SL1 and HG4-GSAP1 primers. A semi-nested

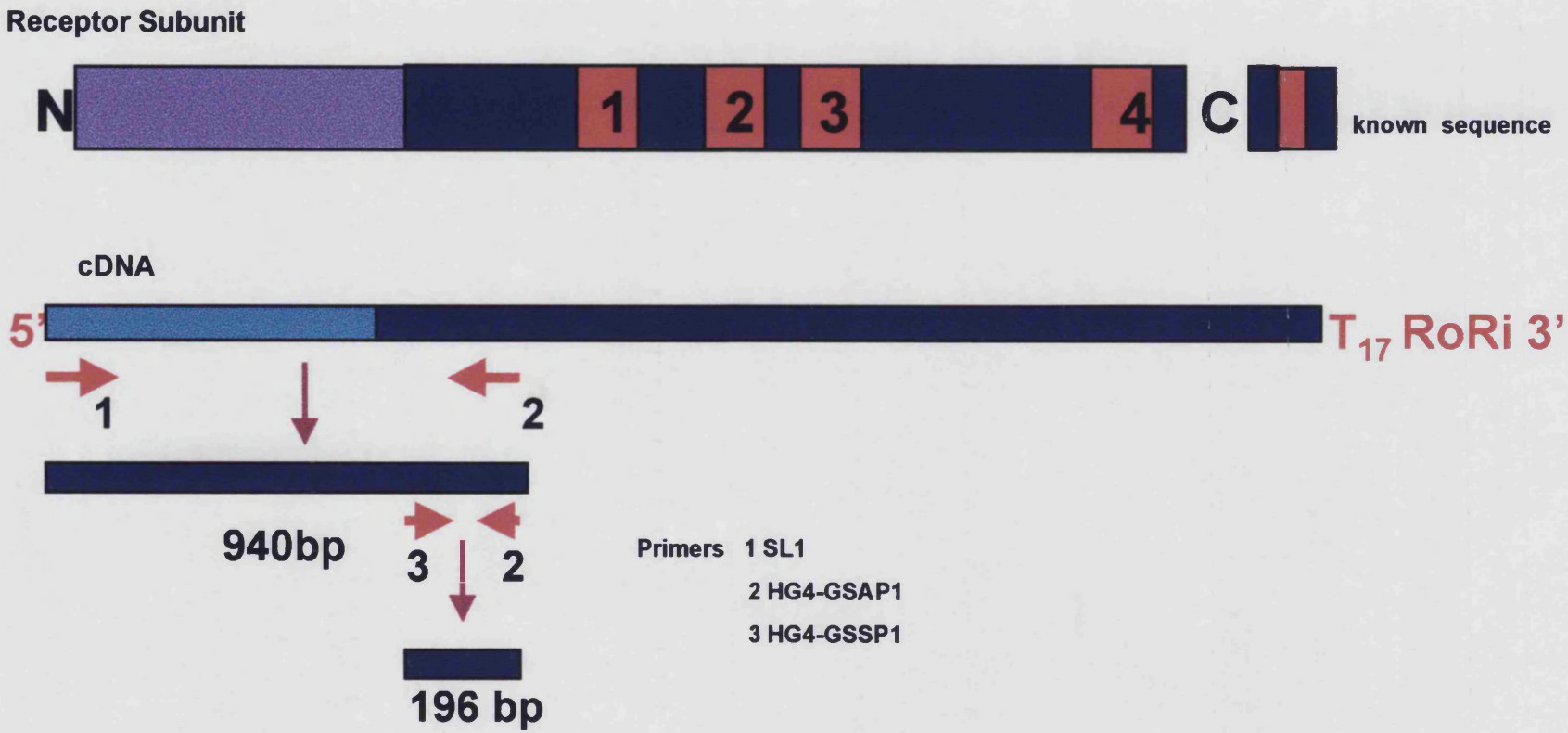

Figure16, Strategy for Isolating the 5' end of HG4 using RACE-PCR.

PCR, amplifying a 196 bp fragment, can be seen in lane 4 using the 940 bp product as template with the primers HG4-GSSP1 and HG4-GSAP1.

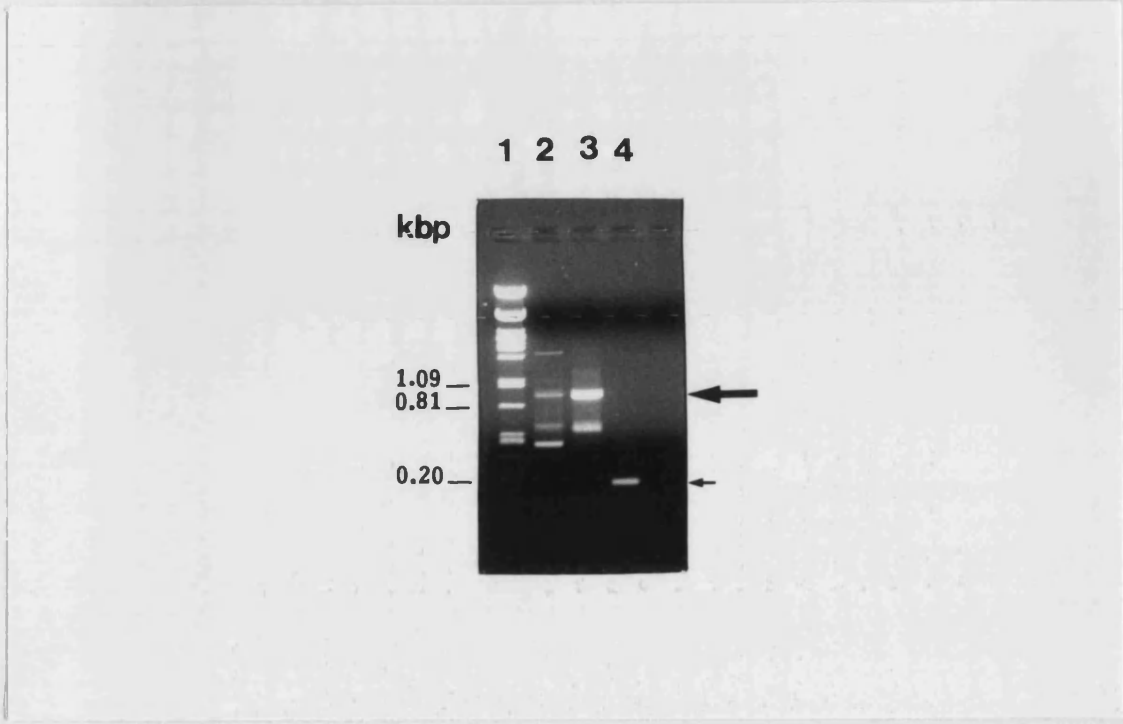

Figure 17 Amplification of the 5' end of HG4 cDNA.
Lane 1: λPst1 with equivalent band sizes listed beside the gel.
Lane 2: PCR product of 940 bp was obtained using the primers SL1 and HG4-GSAP1 (➔).
Lane 3: PCR reamplification using both SL1 and HG4-GSAP1 primers and purified template of the 940 bp product seen in lane 2.
Lane 4: Semi-nested PCR amplified a196 bp band using purified template of the 940 bp product seen in lane 2 with primers HG4-GSSP1 and HG4-GSAP1 (→).
The Expand™ Long Template PCR System was used in a series of PCRs in the presence of 1.75 mM $MgCl_2$ and 300nM of each primer. Adult *H. contortus* cDNA was used initially as template in the reaction run in lane 1.
Cycling conditions: 94 °C denaturation for 2 min, followed by the addition of 2.5 U enzyme, after which 45 cycles of 94 °C for 30 sec, 55 °C for 30 sec and 68 °C for 2 min were run terminating with 7 min at 68 °C. 10μl of reaction mix from each sample was analysed by separation via electrophoresis on a 1 % (w/v) agarose gel run in TBE.

3.2.6 Cloning Strategy used for the 5' end of HG4

The purified 940 bp fragment represented in lane 2 of figure 17 was blunt-ended using DNA polymerase and polynucleotide kinase and then ligated into a pBluescript SK^+ vector previously digested with EcoRV. This was followed by transformation into the XL1-Blue strain of *E. coli*. Positive white clones were then screened by purifying the plasmids and using the restriction enzymes Xba1 and Xho1 to release a 940 bp insert, this is shown in figure 18 where lanes 2, 6, 7, 8, 9, 10 and 14 have been loaded with successfully cloned constructs. The clone represented in lane 6 was re-cultured and plasmid DNA was purified using the Wizard™ Plus kit.

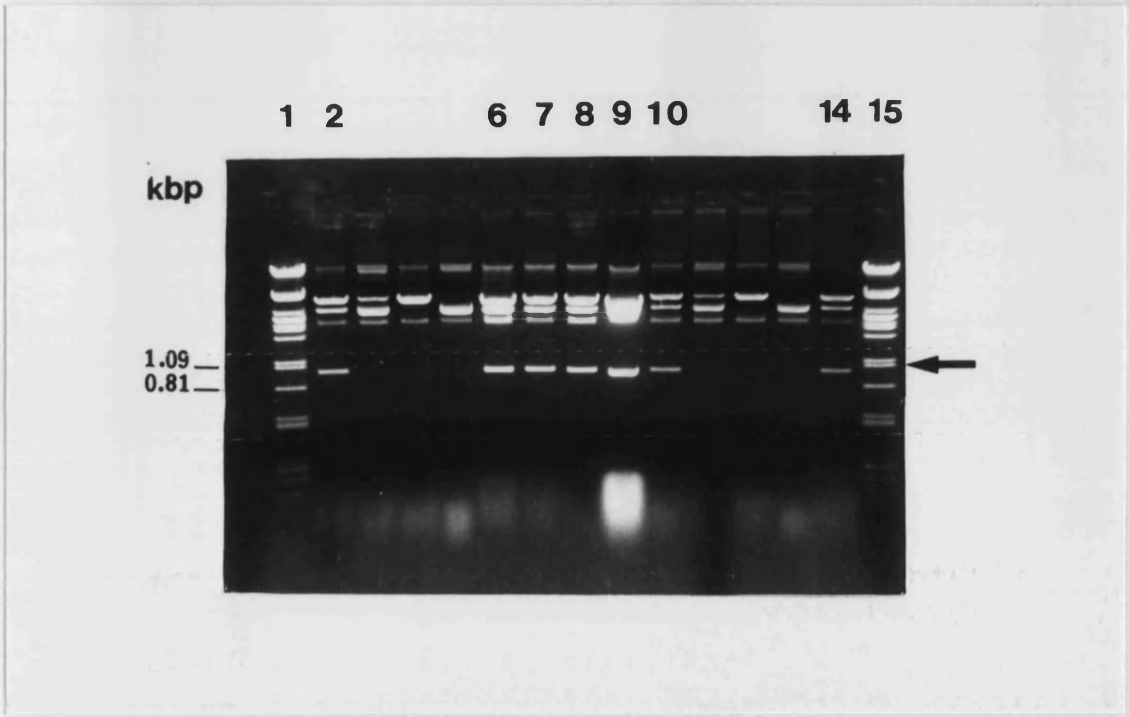

Figure 18, Restriction digests of the 5' end of HG4 plasmid.
Lanes 1 & 15: λ Pst1, relevant band sizes are indicated.
Lanes 2, 6, 7, 8, 9, 10 & 14 are loaded with purified plasmid containing the HG4 5' PCR product of 940 bp in size (➔).
Remaining lanes contained purified plasmids lacking 5' PCR product.
Previous to monitoring restriction patterns on a 1 % (w/v) agarose gel, recombinant plasmid constructs were purified from XL1-Blue colonies followed by digestion with Xho1 and Xba1 for h at 37 °C.

3.2.7 Sequence analysis of the 5' end of HG4

Manual sequencing with the Sequenase™ Quick-Denature plasmid sequencing kit produced a preliminary 5' sequence coding a 22 nt SL1 splice leader sequence followed by a 7 nt 5'UTR and a 914 bp HG4 coding domain, displayed in figure 19. The sequence was transferred to the GCG package on the gnome suite for analysis and comparison with existing sequences catalogued in the GenEMBL database. The 5' sequence of HG4 was 82.21 % identical at the amino acid level to the GluClβ 5' sequence from *C. elegans*.

```
      ggtttaattacccaagtttgagatcttgaATGTCACAGTATATGATGGTCGCCGTAGCGG
-30 ---------+---------+---------1---------+---------+---------+ 30
      ccaaattaatgggttcaaactctagaactTACAGTGTCATATACTACCAGCGGCATCGCC

                                  M  S  Q  Y  M  M  V  A  V  A  A -

      CCGTGGTCGCAGTGGCAGGTTCGTCCCAGATCTCGCGGCGATCCACTGGTGGCACTCAGG
 31 ---------+---------+---------+---------+---------+---------+ 90
      GGCACCAGCGTCACCGTCCAAGCAGGGTCTAGAGCGCCGCTAGGTGACCACCGTGAGTCC

        V  V  A  V  A  G  S  S  Q  I  S  R  R  S  T  G  G  T  Q  E -
```

Figure 19, See legend on next

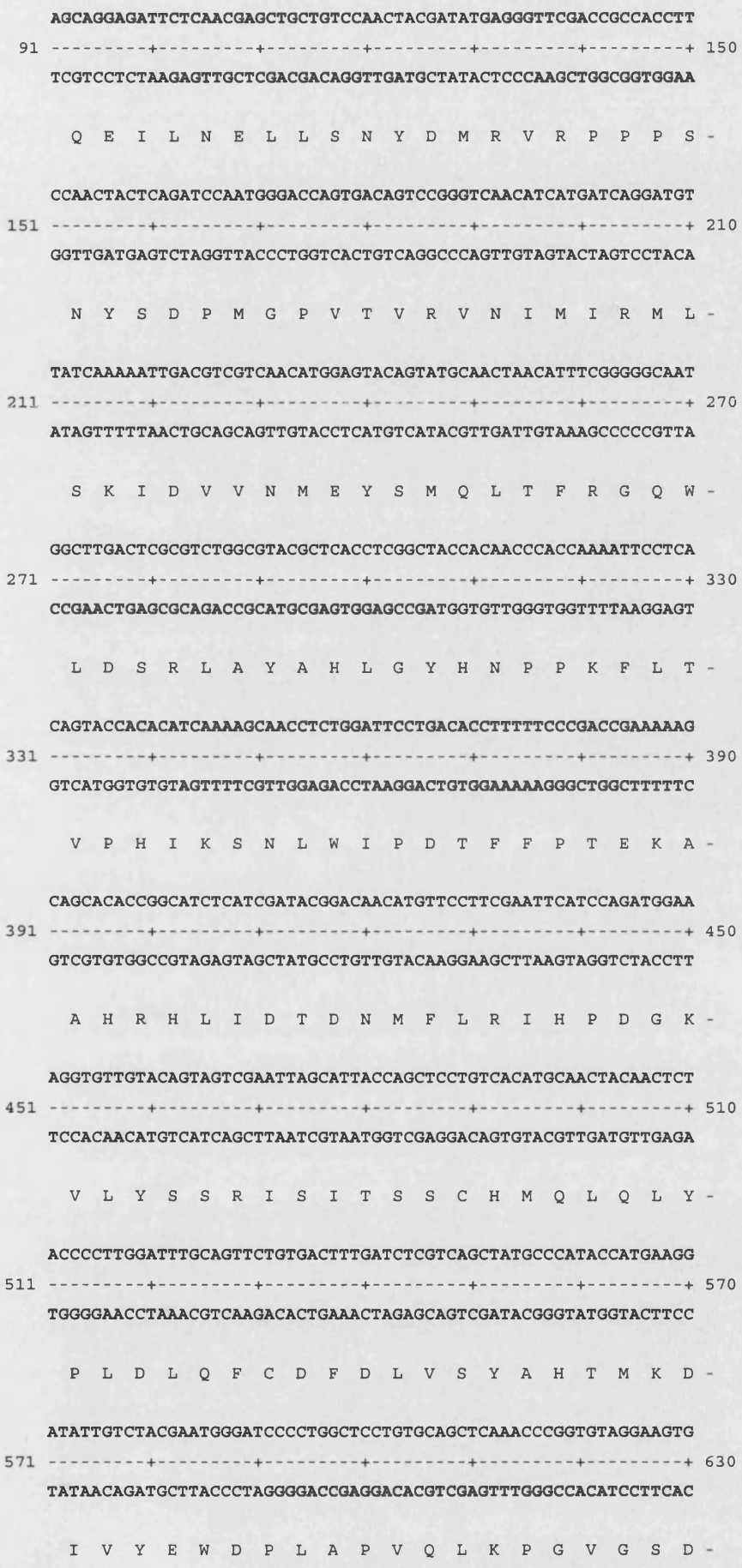

Figure 19, see figure legend next page.

```
    ACCTGCCTAACTTTCAGCTCACAAATATCACCACCAATGAGGACTGTACTAGCCATACCA
631 ---------+---------+---------+---------+---------+---------+ 690
    TGGACGGATTGAAAGTCGAGTGTTTATAGTGGTGGTTACTCCTGACATGATCGGTATGGT

      L  P  N  F  Q  L  T  N  I  T  T  N  E  D  C  T  S  H  T  N -

    ATACTGGGTCGTACGCCTGCCTGAGGATGCAGCTCACCCTAAAAAGGCAGTTCAGTTACT
691 ---------+---------+---------+---------+---------+---------+ 750
    TATGACCCAGCATGCGGACGGACTCCTACGTCGAGTGGGATTTTTCCGTCAAGTCAATGA

      T  G  S  Y  A  C  L  R  M  Q  L  T  L  K  R  Q  F  S  Y  Y -

    ACCTGGTCCAGTTGTACGGTCCCACAACGATGATAGTGATCGTCTCATGGGTTTCGTTTT
751 ---------+---------+---------+---------+---------+---------+ 810
    TGGACCAGGTCAACATGCCAGGGTGTTGCTACTATCACTAGCAGAGTACCCAAAGCAAAA

      L  V  Q  L  Y  G  P  T  T  M  I  V  I  V  S  W  V  S  F  W -

    GGATCGATATGCATTCAACCGCCGGTCGTGTGGCCCTGGGTGTCACTACCCTGCTGACCA
811 ---------+---------+---------+---------+---------+---------+ 870
    CCTAGCTATACGTAAGTTGGCGGCCAGCACACCGGGACCCACAGTGATGGGACGACTGGT

      I  D  M  H  S  T  A  G  R  V  A  L  G  V  T  T  L  L  T  M -

    TGACCACCATGCAAGCAGCTATCAATGCTAAACTGCCACCGGT
871 ---------+---------+---------+---------+--- 913
    ACTGGTGGTACGTTCGTCGATAGTTACGATTTGACGGTGGCCA

      T  T  M  Q  A  A  I  N  A  K  L  P  P    -
```

Figure 19, A preliminary 5'-RACE amplified sequence for HG4. The sequence includes the *SL1sequence*, the 5' UTR and the **coding sequence**. The translated amino acid sequence is also displayed underneath the corresponding nucleotide sequence.

3.2.8 Isolation of Full Length Clones of HG4

A complete sequence for HG4 can be compiled using the 5'-, 3'- and partially amplified PCR fragments. However, to ensure that these amplified products represented sequence from a single receptor subunit cDNA, a full-length HG4 cDNA was amplified directly from *H. contortus*.

Preliminary HG4 sequence was consulted to design two gene specific primers for use in a single step amplification of a full-length copy of the cDNA. Addition of restriction sites at the ends of each primer facilitated access of the insert when cloned. These sites were selected by screening the sequence for enzyme cleavage motifs using the GCG package. Absence of Not1 and Xba1 enzyme cleavage sites consequently meant that they could be incorporated into the primer sequence. This was confirmed by digesting both 5' and 3' clones with Not1 and Xba1 and then viewing resultant restriction products on a 1% (w/v) agarose gel.

A sense primer (HG4-CSP1), with an added Not 1 restriction site at its 5' end, was designed to hybridise to the 5' sequence downstream of SL1. Similarly, an antisense primer (HG4-CAP1) was designed to the 3' UTR sequence and included a Xba1 site at its 5' end. Primer sequences are listed in Appendix 3.

Full length HG4 was amplified in duplicate (Figure 20a and b) from first strand egg cDNA in the presence of sense and antisense primers giving a 1.3 kbp product. Each band was Sephaglas™ purified and restricted with Not1 and Xba1. The resulting sticky ended products were then ligated into a pBluescript SK^+ vector, which had previously been double digested with Not1 and Xba1. The new constructs from both PCRs were cloned into XL1-Blues and white colonies were selected from each construct for plasmid purification and restriction screening.

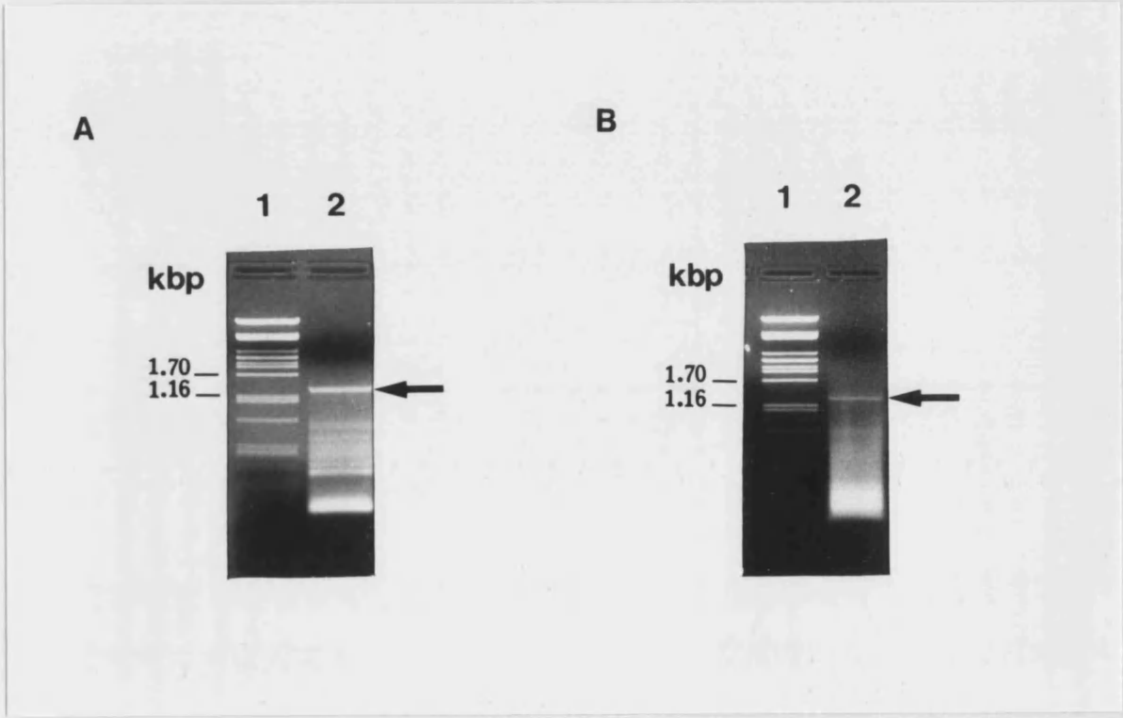

Figure 20, Amplification of Full-Length HG4 cDNA.
Lane 1: λ DNA restricted with Pst1, relevant sizes of bands are listed
Lane 2: Full-length HG4 PCR product of 1.3 kbp amplified using primers HG4-CSP1 and HG4-CAP1 (➔).
A, Product amplified using the Expand™ Long Template System in the presence of 1.75 mM $MgCl_2$. **B**, Amplification achieved using the Expand™ High Fidelity kit with 1.5 mM $MgCl_2$.
Each PCR required the use of cDNA reverse transcribed from *H. contortus* egg mRNA and 300 nM of each primer.
Cycling conditions: 94 °C denaturation for 2 min, followed by the addition of 2.5 U enzyme, after which 45 cycles of 94 °C for 30 sec, 43 °C for 30 sec and 68 °C (**A**) or 72 °C (**B**) for 2 min were run terminating with 7 min at 68 °C (**A**) or 72 °C (**B**). 40μl (**A**) and 80 μl (**B**) of reaction mix from each sample was separated by electrophoresis on a 1 % (w/v) agarose gel run in TBE.

Figure 21 displays successful transformations present in lanes 2, 3, 5 and 6. Automated sequencing of clones 8 (in lane 2) and 14 (in lane 6) was performed using the sense primers HG4-GSSP1, HG4-GSSP3, T3 and the antisense primers HG4-GSAP1, HG4-GSAP2 and KS. Primer sequences are detailed in Appendix 3 and their complementary sites along the constructs are illustrated in figure 22.

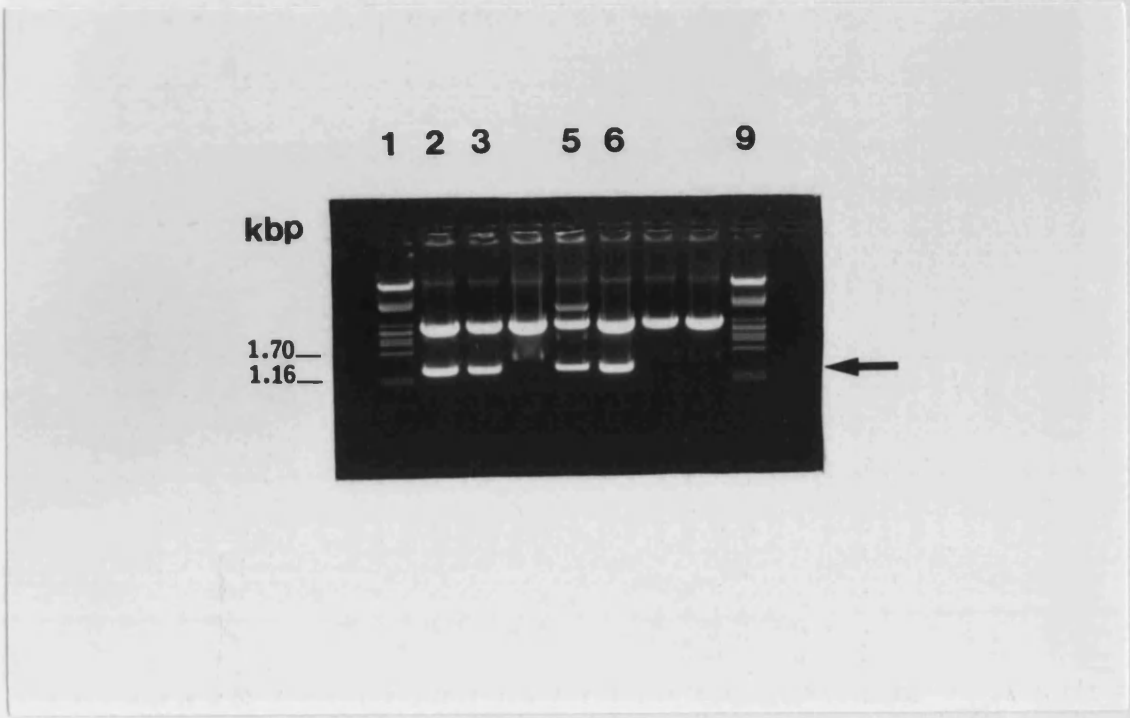

Figure 21, Restriction of plasmid constructs containing full-length HG4 DNA
Lanes 1 & 9: λ DNA digested with the Pst1 enzyme, relevant sizes of bands are noted next to the lane.
Lanes 2 & 3: Plasmid constructs possessing the 1.3 kbp insert amplified with the Expand™ Long Template PCR system (**figure 20a**). Lanes 5 & 6: Plasmid constructs encoding the 1.3 kbp insert produced using the High Fidelity system (**figure 20b**).
Remaining lanes were loaded with plasmids that did not encode the 1.3 kbp HG4 DNA.
Recombinant plasmids were purified from XL1-Blue colonies with the Wizard™ Plus kit followed by double digestion with the restriction enzymes Xho1 and Xba1 for 1 h at 37 °C. Restriction patterns were monitored on a 1 % (w/v) agarose gel by electrophoresis. Successful transformants released a 1.3 kbp fragment indicated by ➔.

Full length sequences from clones 8 and 14 were aligned with the preliminary 5' and 3' sequences to distinguish areas with nucleotide variation as shown in figure 22. Consequently, the percentage variation between each clone was calculated at both the nucleotide and amino acid levels and is listed in table 2 and 3 respectively.

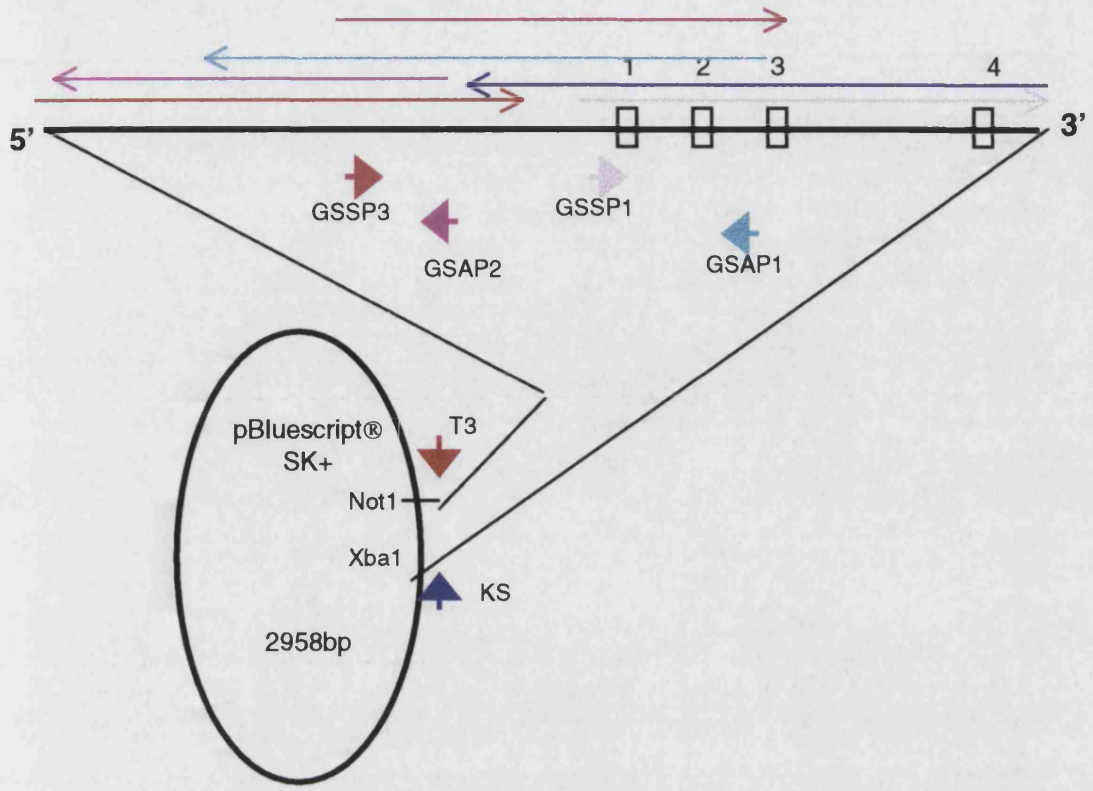

Figure 22, Sequencing strategy for Full-Length HG4
A schematic diagram representing the pBluescript vector with HG4 ligated into the multiple cloning site. Areas coding for transmembrane spanning regions are labelled 1 to 4. Sequencing involved the use of gene specific sense primers (HG4-GSSP), gene specific antisense primers (HG4-GSAP) and plasmid specific primers (KS and T3). Each of the primers used is listed with corresponding sites to which they hybridise to, indicated with an arrow, →. Regions of sequence obtained with primers were also shown by colour coded arrows →. For example the KS primer (→) was used to sequence the region marked by the → arrow.

```
            1                                                  50
      5'HG4 ggtttaatta cccaagtttg agatcttgaA TGTCACAGTA TATGATGGTC
      3'HG4 .......... .......... .......... .......... ..........
 Whole HG4(8) .......... .......... .........A TGTCACAGTA TATGATGGTC
Whole HG4(14) .......... .......... .........A TGTCACAGTA TATGATGGTC
 Whole HG4(3) .......... .......... .........A TGTCACAGTA TATGATGGTC
    Consensus ggtttaatta cccaagtttg agatcttgaA TGTCACAGTA TATGATGGTC

            51                                                 100
      5'HG4 GCCGTAGCGG CCGTGGTCGC AGTGGCAGGT TCGTCCCAGA TCTCGCGGCG
      3'HG4 .......... .......... .......... .......... ..........
 Whole HG4(8) GCCGTAGCGG CCGTGGTCGC AGTGGCAGGT TCGTCCCAGG TCTCGCGGCG
Whole HG4(14) GCTGTAGCGG CCGTAGTCGC AGTGGCACGT TCGTCCCAGA TCTCGCGGCG
 Whole HG4(3) GCCGTAGCGG CCGTGGTCGC AGTGGCAGGT TCGTCCCAGA TCTCGCGGCG
    Consensus GCYGTAGCGG CCGTRGTCGC AGTGGCASGT TCGTCCCAGR TCTCGCGGCG
```

Figure 23, See figure legend on following page.

```
              101                                                 150
       5'HG4 ATCCACTGGT GGCACTCAGG AGCAGGAGAT TCTCAACGAG CTGCTGTCCA
       3'HG4 .......... .......... .......... .......... ..........
 Whole HG4(8) ATCCACTGGT GGCACTCAGG AGCAGGAGAT TCTCAACGAG CTGCTGTCCA
Whole HG4(14) ATCCACTGGT GGCACTCAGG AGCAGGAGAT TCTCAACGAG CTGCTGTCCA
 Whole HG4(3) ATCCGCTGGT GGCACTCAGG AGCAGGAGAT TCTCAACGAG CTGCTGTCCA
    Consensus ATCCRCTGGT GGCACTCAGG AGCAGGAGAT TCTCAACGAG CTGCTGTCCA

              151                                                 200
       5'HG4 ACTACGATAT GAGGGTTCGA CCGCCACCTT CCAACTACTC AGATCCAATG
       3'HG4 .......... .......... .......... .......... ..........
 Whole HG4(8) ACTACGATAT GAGGGTTCGA CCGCCACCTT CCAACTACTC AGATCCAATG
Whole HG4(14) ACTACGATAT GCGTGTTCGA CCGCCACCTT CGAACTACTC AGATCCAATG
 Whole HG4(3) ACTACGATAT GAGGGTTCGA CCGCCACCTT CCAACTACTC AGATCCAATG
    Consensus ACTACGATAT GMGKGTTCGA CCGCCACCTT CSAACTACTC AGATCCAATG

              201                                                 250
       5'HG4 GGACCAGTGA CAGTCCGGGT CAACATCATG ATCAGGATGT TATCAAAAAT
       3'HG4 .......... .......... .......... .......... ..........
 Whole HG4(8) GGACCAGTGA CAGTTCGGGT CAACATCATG ATCAGGATGT TATCAAAAAT
Whole HG4(14) GGACCAGTGA CAGTTCGGGT CAACATCATG ATCAGGATGT TATCAAAAAT
 Whole HG4(3) GGACCAGTGA CAGTCCGGGT CAACATCATG ATCAGGATGT TATCAAAAAT
    Consensus GGACCAGTGA CAGTYCGGGT CAACATCATG ATCAGGATGT TATCAAAAAT
              251                                                 300
       5'HG4 TGACGTCGTC AACATGGAGT ACAGTATGCA ACTAACATTT CGGGGGCAAT
       3'HG4 .......... .......... .......... .......... ..........
 Whole HG4(8) TGACGTCGTC AACATGGAGT ACAGTATGCA ATTGACGTTT CGGGAGCAAT
Whole HG4(14) TGACGTCGTC AACATGGAGT ACAGTATGCA ACTGACATTT CGGGAGCAGT
 Whole HG4(3) TGACGTCGTC AACATGGAGT ACAGTATGCA ACTAACATTT CGGGAGCAAT
    Consensus TGACGTCGTC AACATGGAGT ACAGTATGCA AYTRACRTTT CGGGRGCART

              301                                                 350
       5'HG4 GGCTTGACTC GCGTCTGGCG TACGCTCACC TCGGCTACCA CAACCCACCA
       3'HG4 .......... .......... .......... .......... ..........
 Whole HG4(8) GGCTTGACTC GCGTCTGGCG TACGCTCACC TCGGCTACCA CAACCCTCCG
Whole HG4(14) GGCTTGACTC GCGTCTGGCG TACGCTCACC TCGGCTACCA CAACCCTCCG
 Whole HG4(3) GGCTTGACTC GCGTCTGGCG TACGCTCACC TCGGCTACCA CAACCCACCA
    Consensus GGCTTGACTC GCGTCTGGCG TACGCTCACC TCGGCTACCA CAACCCWCCR

              351                                                 400
       5'HG4 AAATTCCTCA CAGTACCACA CATCAAAAGC AACCTCTGGA TTCCTGACAC
       3'HG4 .......... .......... .......... .......... ..........
 Whole HG4(8) AAATTCCTCA CGGTACCACA CATCAAAAGC AACCTCTGGA TTCCGGACAC
Whole HG4(14) AAATTCCTCA CGGTACCACA CATCAAAAGC AACCTCTGGA TTCCTGACAC
 Whole Hg4(3) AAATTCCTCA CAGTACCACA CATCAAAAGC AACCTCTGGA TTCCTGACAC
    Consensus AAATTCCTCA CRGTACCACA CATCAAAAGC AACCTCTGGA TTCCKGACAC

              401                                                 450
       5'HG4 CTTTTTCCCG ACCGAAAAAG CAGCACACCG GCATCTCATC GATACGGACA
       3'HG4 .......... .......... .......... .......... ..........
 Whole HG4(8) CTTTTTCCCG ACCGAAAAAG CGGCACACCG GCATCTCATC GACACGGACA
Whole HG4(14) CTTTTTCCCG ACCGAAAAAG CAGCACACCG GCATCTCATC GACACGGACA
 Whole HG4(3) CTTTTTCCCG ACCGAAAAAG CAGCACACCG GCATCTCATC GATACGGACA
    Consensus CTTTTTCCCG ACCGAAAAAG CRGCACACCG GCATCTCATC GAYACGGACA
```

Figure 23, see figure legend on following page.

```
              451                                                 500
       5'HG4 ACATGTTCCT TCGAATTCAT CCAGATGGAA AGGTGTTGTA CAGTAGTCGA
       3'HG4 .......... .......... .......... .......... ..........
 Whole HG4(8) ACATGTTCCT TCGGATTCAT CCAGATGGAA GGGTGTTGTA CAGTAGTCGA
Whole HG4(14) ACATGTTCCT TCGAATTCAT CCAGATGGAA AGGTGCTGTA CAGTAGTCGA
 Whole HG4(3) ACATGTTCCT TCGAATTCAT CCAGATGGAA AGGTGTTGTA CAGTAGTCGA
    Consensus ACATGTTCCT TCGRATTCAT CCAGATGGAA RGGTGYTGTA CAGTAGTCGA

              501                                                 550
       5'HG4 ATTAGCATTA CCAGCTCCTG TCACATGCAA CTACAACTCT ACCCCTTGGA
       3'HG4 .......... .......... .......... .......... ..........
 Whole HG4(8) ATTAGCATTA CCAGCTCCTG TCACATGCAA CTACAACTCT ACCCCTTGGA
Whole HG4(14) ATTAGCATTA CCAGCTCCTG CCATATGCAA CTACAACTCT ACCCCTTGGA
 Whole HG4(3) ATTAGCATTA CCAGCTCCTG TCACATGCAA CTACAACTCT ACCCCTTGGA
    Consensus ATTAGCATTA CCAGCTCCTG YCAYATGCAA CTACAACTCT ACCCCTTGGA

              551                                                 600
       5'HG4 TTTGCAGTTC TGTGACTTTG ATCTCGTCAG CTATGCCCAT ACCATGAAGG
       3'HG4 .......... .......... .......... .......... ..........
 Whole HG4(8) TTTGCAGTTC TGTGACTTTG ATCTCGTCAG CTATGCCCAT ACCATGAAGG
Whole HG4(14) TTTGCAATTC TGTGACTTTG ATCTCGTCAG CTATGCCCAT ACGATGAAGG
 Whole HG4(3) TTTGCAGTTC TGTGACTTTG ATCTCGTCAG CTATGCCCAT ACCATGAAGG
    Consensus TTTGCARTTC TGTGACTTTG ATCTCGTCAG CTATGCCCAT ACSATGAAGG

              601                                                 650
       5'HG4 ATATTGTCTA CGAATGGGAT CCCCTGGCTC CTGTGCAGCT CAAACCCGGT
       3'HG4 .......... .......... .......... .......... ..........
 Whole HG4(8) ATATTGTCTA CGAATGGGAT CCCCTGGCTC CTGTGCAGCT CAAACCCGGT
Whole HG4(14) ACATTGTCTA CGAATGGGAC CCCCTGGCTC CTGTGCAGCT CAAACCCGGT
 Whole HG4(3) ATATTGTCTA CGAATGGGAT CCCCTGGCTC CTGTGCAGCT CAAACCCGGT
    Consensus AYATTGTCTA CGAATGGGAY CCCCTGGCTC CTGTGCAGCT CAAACCCGGT

              651                                                 700
       5'HG4 GTAGGAAGTG ACCTGCCTAA CTTTCAGCTC ACAAATATCA CCACCAATGA
       3'HG4 .......... .......... .......... .......... ..........
 Whole HG4(8) GTAGGAAGTG ACCTGCCTAA CTTTCAGCTC ACAAATATCA CCACCAATGA
Whole HG4(14) GTAGGAAGTG ACCTGCCTAA CTTCCAGCTC ACAAATATCA CCACCAATGA
 Whole HG4(3) GTAGGAAGTG ACCTGCCTAA CTTTCAGCTC ACAAATATCA CCACCAATGA
    Consensus GTAGGAAGTG ACCTGCCTAA CTTYCAGCTC ACAAATATCA CCACCAATGA

              701                                                 750
       5'HG4 GGACTGTACT AGCCATACCA ATACTGGGTC GTACGCCTGC CTGAGGATGC
       3'HG4 .......... .......... .......... .......... ......ATGC
 Whole HG4(8) CGACTGTACT AGCCATACCA ATACTGGGTC ATACGCCTGT CTGAGGATGC
Whole HG4(14) CGACTGCACT AGCCATACTA ATACTGGGTC ATACGCCTGT CTGAGGATGC
 Whole HG4(3) CGACTGTACT AGCCATACCA ATACTGGGTC GTACGCCTGC CTGAGGATGC
    Consensus SGACTGYACT AGCCATACYA ATACTGGGTC RTACGCCTGY CTGAGGATGC

              751                                                 800
       5'HG4 AGCTCACCCT AAAAAGGCAG TTCAGTTACT ACCTGGTCCA GTTGTACGGT
       3'HG4 AGCTCACCCT AAAAAGGCAG TTCAGTTACT ACCTGGTCCA GTTGTACGGT
 Whole HG4(8) AGCTCACCCT AAAACGACAG TTCAGTTACT ACCTGGTCCA GTTGTACGGT
Whole HG4(14) AACTCACCCT AAAAAGGCAG TTCAGTTACT ACCTAGTCCA ATTGTACGGT
 Whole HG4(3) AGCTCACCCT AAAAAGGCAG TTCAGTTACT ACCTGGTCCA GTTGTACGGT
    Consensus ARCTCACCCT AAAAMGRCAG TTCAGTTACT ACCTRGTCCA RTTGTACGGT
```

Figure 23, See figure legend on following page.

```
              801                                                  850
       5'HG4 CCCACAACGA TGATAGTGAT CGTCTCATGG GTTTCGTTTT GGATCGATAT
       3'HG4 CCCACAACGA TGATAGTGAT CGTCTCATGG GTTTCGTTTT GGATCGATAT
 Whole HG4(8) CCCACAACGA TGATAGTGAT CGTCTCATGG GTTTCGTTTT GGATCGATAT
Whole HG4(14) CCCACAACGA TGATAGTGAT CGTCTCATGG GTTTCATTTT GGATCGATAT
 Whole HG4(3) CCCACAACGA TGATAGTGAT CGTCTCATGG GTTTCGTTTT GGATCGATAT
    Consensus CCCACAACGA TGATAGTGAT CGTCTCATGG GTTTCRTTTT GGATCGATAT

              851                                                  900
       5'HG4 GCATTCAACC GCCGGTCGTG TGGCCCTGGG TGTCACTACC CTGCTGACCA
       3'HG4 GCATTCAACC GCCGGTCGTG TGGCCCTGGG TGTCACTACC CTGCTGACCA
 Whole HG4(8) GCATTCAACG GCCGGTCGTG TGGCCCTGGG TGTCACTACC CTGCTGACCA
Whole HG4(14) GCATTCAACG GCCGGTCGTG TGGCCCTGGG TGTCACTACC CTGCTAACCA
 Whole HG4(3) GCATTCAACG GCCGGTCGTG TGGCCCTGGG TGTCACTACC CTGCTAACCA
    Consensus GCATTCAACS GCCGGTCGTG TGGCCCTGGG TGTCACTACC CTGCTRACCA

              901                                                  950
       5'HG4 TGACCACCAT GCAAGCAGCT ATCAATGCTA AACTGCCACC GGT.......
       3'HG4 TGACCACCAT GCAAGCAGCT ATCAATGCTA AACTGCCACC GGTGAGCTAC
 Whole HG4(8) TGACCACCAT GCAAGCAGCT ATCAATGCTA AACTGCCACC GGTGAGCTAC
Whole HG4(14) TGACCACCAT GCAAGCAGCC ATCAATGCTA AACTGCCCCC TGTGAGCTAC
 Whole HG4(3) TGACCACCAT GCAAGCAGCC ATCAATGCTA AACTGCCCCC TGTGAGCTAC
    Consensus TGACCACCAT GCAAGCAGCY ATCAATGCTA AACTGCCMCC KGTGAGCTAC

              951                                                 1000
       5'HG4 .......... .......... .......... .......... ..........
       3'HG4 GTGAAGGTGG TGGATGTGTG GCTTGGAGCC TGTCAAACAT TCGTCTTTGG
 Whole HG4(8) GTGAAGGTGG TGGATGTGTG GCTTGGAGCC TGTCAAACAT TCGTCTTTGG
Whole HG4(14) GTGAAGGTAG TAGATGTGTG GCTCGGAGCC TGTCAAACGT TCGTGTTTGG
 Whole HG4(3) GTGAAGGTAG TAGATGTGTG GCTCGGAGCC TGTCAAACGT TCGTGTTTGG
    Consensus GTGAAGGTRG TRGATGTGTG GCTYGGAGCC TGTCAAACRT TCGTSTTTGG

              1001                                                1050
       5'HG4 .......... .......... .......... .......... ..........
       3'HG4 AGCGTTGCTT GAGTACGCTT TCGTCTCTTA TCAAGACAGC CAACGACAAA
 Whole HG4(8) AGCGTTGCTT GAGTACGCTT TCGTCTCTTA TCAAGACAGC CAACGACAAA
Whole HG4(14) AGCGCTGCTC GAATACGCGT TCGTCTCTTA TCAAGACAGC CAACGACAAG
 Whole HG4(3) AGCGCTGCTC GAATACGCGT TCGTCTCTTA TCAAGACAGC CAACGACAAA
    Consensus AGCGYTGCTY GARTACGCKT TCGTCTCTTA TCAAGACAGC CAACGACAAR

              1051                                                1100
       5'HG4 .......... .......... .......... .......... ..........
       3'HG4 CAGAGCAGGC CAAAAGCCGA GCTGCTCGAA AAGCTCAAAA GCGACGAGCT
 Whole HG4(8) CAGAGCAGGC CAAAAGCCGA GCTGCTCGAA AAGCTCAAAA GCGACGAGCT
Whole HG4(14) CAGAGCAGGC CAAAAGCCGA GCTGCTCGAA AAGCTCAAAA GCGACGTGCC
 Whole HG4(3) CAGAGCAGGC CAAAAGCCGA GCTGCTCGAA AAGCTCAAAA GCGACGTGCC
    Consensus CAGAGCAGGC CAAAAGCCGA GCTGCTCGAA AAGCTCAAAA GCGACGWGCY

              1101                                                1150
       5'HG4 .......... .......... .......... .......... ..........
       3'HG4 AAAATGGAAC TCGTCGAAAG AGAACAATAC CAACCTCCTT GCACGTGTCA
 Whole HG4(8) AAAATGGAAC TCGTCGAAAG AGAACAATAC CAACCTCCTT GCACGTGTCA
Whole HG4(14) AAAATGGAAC TCGTCGAAAG AGAACAATAC CAACCTCCTT GCACGTGTCA
 Whole HG4(3) AAAATGGAAC TCGTCGAAAG AGAACAATAC CAACCTCCTT GCACGTGTCA
    Consensus AAAATGGAAC TCGTCGAAAG AGAACAATAC CAACCTCCTT GCACGTGTCA
```

Figure 23, See figure legend on following page.

```
              1151                                                1200
       5'HG4 .......... .......... .......... .......... ..........
       3'HG4 TCTGTACCAA GACTACGAGC CATCGTTCCG TGACCGGTTG CGGCGCTATT
 Whole HG4(8) TCTGTACCAA GACTACGAGC CATCGTTCCG TGACCGGTTG CGGCGCTATT
Whole HG4(14) TCTGTACCAA GACTATGAGC CGTCGTTCCG TGACCGGTTA CGGCGCTATT
 Whole HG4(3) TCTGTACCAA GACTATGAGC CGTCGTTCCG TGACCGGTTA CGGCGCTATT
    Consensus TCTGTACCAA GACTAYGAGC CRTCGTTCCG TGACCGGTTR CGGCGCTATT

              1201                                                1250
       5'HG4 .......... .......... .......... .......... ..........
       3'HG4 TCACAAAACC CGACTACCTG CCGGCGAAAA TCGACTACTA TGCTCGATTT
 Whole HG4(8) TCACAAAACC CGACTACCTG CCGGCGAAAA TCGACTACTA TGCTCGATTT
Whole HG4(14) TCACAAAACC CGACTACCTG CCAGCGAAAA TCGACTACTA TGCTCGATTT
 Whole HG4(3) TCACAAAACC CGACTACCTG CCAGCGAAAA TCGACTACTA TGCTCGATTT
    Consensus TCACAAAACC CGACTACCTG CCRGCGAAAA TCGACTACTA TGCTCGATTT

              1251                                                1300
       5'HG4 .......... .......... .......... .......... ..........
       3'HG4 TGTGTGCCAT TAGGCTTTTT AGCCTTCAAT GCCATCTATT GGACATCCTG
 Whole HG4(8) TGTGTGCCAT TAGGCTTTTT AGCCTTCAAT GCCATCTATT GGACATCCTG
Whole HG4(14) TGTGTGCCAT TAGGCTTTTT AGCCTTCAAT GCCATCTACT GGACATCCTG
 Whole HG4(3) TGTGTGCCAT TAGGCTTTTT AGCCTTCAAT GCCATCTACT GGACATCCTG
    Consensus TGTGTGCCAT TAGGCTTTTT AGCCTTCAAT GCCATCTAYT GGACATCCTG

              1301                                                1350
       5'HG4 .......... .......... .......... .......... ..........
       3'HG4 CCTCGTGATG GTGTCAAGAC TAGTCtaata gccatcatca cacagtattt
 Whole HG4(8) CCTCGTGATG GTGTCAAGAC TAGTC..... .......... ..........
Whole HG4(14) CCTCGTGATG GTGTCAAGAC TAGTC..... .......... ..........
 Whole HG4(3) CCTCGTGATG GTGTCAAGAC TAGTC..... .......... ..........
    Consensus CCTCGTGATG GTGTCAAGAC TAGTCtaata gccatcatca cacagtattt

              1351                                                1400
       3'HG4 tgtaatattt ctcggtgatt ctacgaactt tgctcacttt ttgcattaaa
    Consensus tgtaatattt ctcggtgatt ctacgaactt tgctcacttt ttgcattaaa

              1401                                                1450
       3'HG4 tggagatcat attgaatcaa cgatgggata tcatagagaa agttatggga
    Consensus tggagatcat attgaatcaa cgatgggata tcatagagaa agttatggga

              1451                                                1500
       3'HG4 agccctgttt gtactcgaag ttcatctggg tatgccctgt ggaaatcagc
    Consensus agccctgttt gtactcgaag ttcatctggg tatgccctgt ggaaatcagc

              1501                                                1550
       3'HG4 cgtacacact tgttcacttc cgaaagccga tgaaatcgcc tgggatgact
    Consensus cgtacacact tgttcacttc cgaaagccga tgaaatcgcc tgggatgact

              1551                                                1600
       3'HG4 ggtcagggtg acaagaaggc cctttctcac tcactcactg tcacctgtgc
    Consensus ggtcagggtg acaagaaggc cctttctcac tcactcactg tcacctgtgc

              1601                                                1650
       3'HG4 aggagcgctt ttcatggagt tttggatttg gaatcgtgcg gtcgtttcca
    Consensus aggagcgctt ttcatggagt tttggatttg gaatcgtgcg gtcgtttcca
```

Figure 23, See figure legend on next page.

```
          1651                                                  1700
    3'HG4 gtgacagagc tttctctact ggaataattt tgaacgatcg gaagctcatt
Consensus aggagcgctt ttcatggagt tttggatttg gaatcgtgcg gtcgtttcca

          1701                                                  1750
    3'HG4 gtttgaatcc ttgacgaata ggaatttatg aaaagctaat aaacttttac
Consensus gtttgaatcc ttgacgaata ggaatttatg aaaagctaat aaacttttac

          1751
    3'HG4 gtatct
Consensus gtatct
```

Figure 23, Sequence alignment of HG4 from different PCR amplifications. Sequence for HG4 3', HG4 5', whole HG4(8) and whole HG4(14) were derived from PCR amplifications displayed in figures 13, 17, 20a and 20b respectively. The production of HG4 whole(3) is described in the next section with details of its amplification in figures 25 and 26. Shaded regions highlight nts that vary between the clones. A consensus sequence is also displayed with a summary of possible nts highlighted in bold. **Y** codes either a C or a T, **M** codes either an A or a C, **R:** an A or a G, **S:** a G or a C, **K:** a G or a T and **W:** an A or a T. Nucleotides in uppercase are coding sequence whilst lower case nucleotides represent the UTRs.

Table 6, Percentage variation between the HG4 RACE amplified cDNA clones at the nucleotide level. 3' HG4, 5' HG4', clone 8 and clone 14 were derived by PCR detailed in figures 13, 17, 20a and 20b respectively. The production of clone 3 is described in the next section with details of its amplification in figures 25 and 26. Values are calculated by dividing the number of mismatches by the length of overlapping sequence. These details are noted in brackets.

	3' HG4 (579 nt)	Clone 8 (1296 nt)	Clone 14 (1296 nt)	Clone 3 (1296 nt)
5' HG4 (914nt)	0.00% (0/197)	2.08% (19/914)	3.94% (36/914)	0.55% (5/914)
3' HG4 (579nt)		0.35% (2/579)	4.49% (26/579)	3.45% (20/579)
Clone 8 (1296 nt)			4.01% (52/1296)	2.93% (38/1296)
Clone 14 (1296 nt)				2.47% (32/1296)

Table 7, Percentage variation between the HG4 PCR amplifications at the amino acid level. 3' HG4, 5' HG4', clone 8 and clone 14 were derived by PCR detailed in figures 13, 17, 20a and 20b respectively. The production of clone 3 is described in the next section with details of its amplification in figures 25 and 26. Values are calculated by dividing the number of amino acid mismatches by the length of overlapping sequence. These details are noted in brackets.

	3'HG4 (193 aa)	Clone 8 (432 aa)	Clone 14 (432aa)	Clone 3 (432 aa)
5'HG4 (304 aa)	0.00% (0/64)	1.32% (4/304)	0.99% (3/304)	0.99% (3/304)
3'HG4 (192 aa)		0.00% (0/192)	0.52% (1/192)	0.00% (0/192)
Clone 8 (432 aa)			0.93% (4/432)	0.69%(3/432)
Clone 14 (432aa)				0.69% (3/432)

Nucleotide variation may be a direct result of the introduction of errors during the 45 rounds of PCR. It is also probable that variation may be attributed to polymorphism existing between mRNA transcripts extracted from different nematodes. Sequences from clones 8 and 14 were compared with existing sequences present in the GenEMBL database and were found to have a 79.41 % and 79.66 % amino acid identity respectively with GluCl β. Comparison at the nucleotide level showed that the respective clones were 70.24 % and 70.15 % identical to GluCl β.

3.2.9 Ligation of 5' and 3' PCR Products

The independently amplified clones 8 and 14 each possessed 2 codon alterations, which gave rise to a change in the amino acid sequence coding for the receptor subunit as summarised in table 3. These differences may be a consequence of polymorphism or they may have been introduced by PCR. The enzyme used in the reaction has been calculated to have a 8.5 x 10^{-6} error rate as detailed in the Expand™ protocol. Clones 8 and 14, approximately 1.3 kbp in size have undergone 45 cycles thus increasing the likelihood of mutations occurring. To eliminate the possibility that the variation seen was PCR induced, attempts to amplify the whole HG4 cDNA were made with a reduced number of cycles. Reactions using less than 45 cycles however yielded bands of very low intensity which could not be used for ligation.

Table 8, Amino Acid variation between HG4 clones 8 and 14.

Clone	Consensus amino acid sequence	Mutation
8	I21	V21
8	K152	R152
14	G17	R17
14	T341	A341

An alternate approach whereby 5' and 3' fragments, amplified using the least number of PCR cycles, were ligated together. A unique Nsi1 endonuclease restriction site located approximately 850 nucleotides into the sequence was exploited to link both ends together, this strategy is displayed in figure 24.

The 5' fragment was amplified using the primers HG4-CSP1 and HG4-GSAP1 (Appendix 3) using a number of different cycles. This was done to try and optimise the level amplified possessing the least amount of PCR induced mutations. An approximate 930 bp fragment was amplified after 35, 40 and 45 cycles and is shown in figure 25.

Further PCRs were performed to amplify a 3' end with the least amount of PCR induced mutations. The primers HG4-CSAP1 and HG4-GSSP1 were used to amplify a 610 bp fragment using 35, 40 and 45 cycles, these products were analysed on a 1% (w/v) agarose gel and are seen in figure 26.

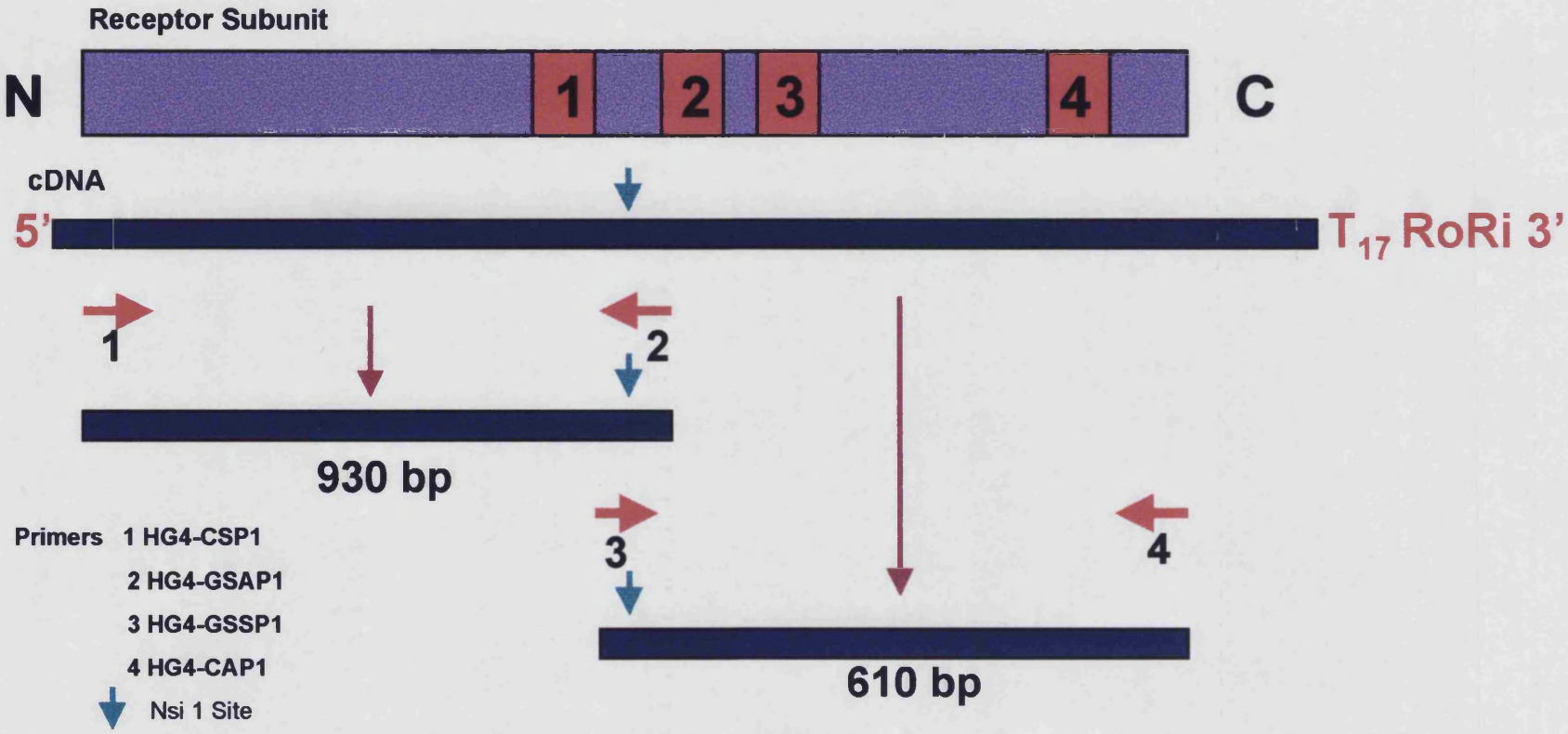

Figure 24, Production of a full-length HG4 clone using a three-way ligation

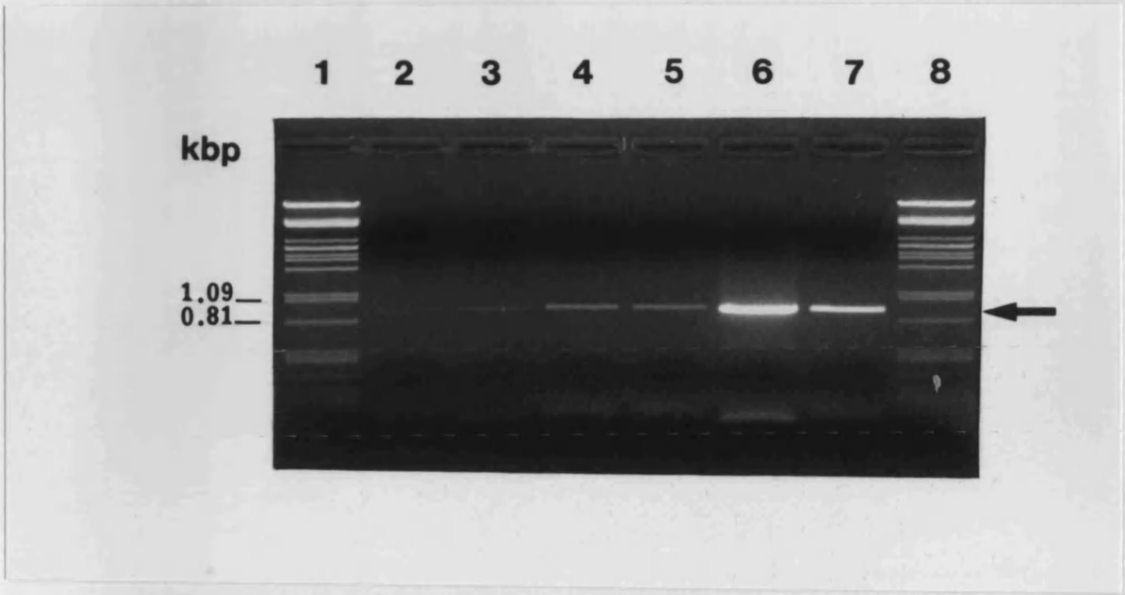

Figure 25, Amplification of the 5' end of HG4 using a range
Lanes 1& 8: λ DNA cut using Pst1 with relevant band sizes noted in parallel.
Duplicate PCRs were done to amplify the 930 bp 5' end of HG4. Lanes 2 & 3: products amplified after 35 cycles. Lanes 4 & 5: after 40 cycles. Lanes 6 & 7: after 45 cycles.
The Expand™ High Fidelity System was utilised requiring the presence of 300 nM of HG4-GSAP1 and HG4-CSP1 primer, *H. contortus* cDNA template reverse transcribed from eggs and 1.5 mM $MgCl_2$.
Cycling conditions: 94 °C denaturation for 2 min, followed by the addition of 2.5 U enzyme, after which 35, 40 or 45 cycles of 94 °C for 30 sec, 55 °C for 30 sec and 72 °C for 2 min were run terminating with 7 min at 72 °C. 80μl of reaction mix from each sample was analysed by separation via electrophoresis on a 1 % (w/v) agarose gel run in TBE. The arrow (➔) indicates the amplified band of interest.

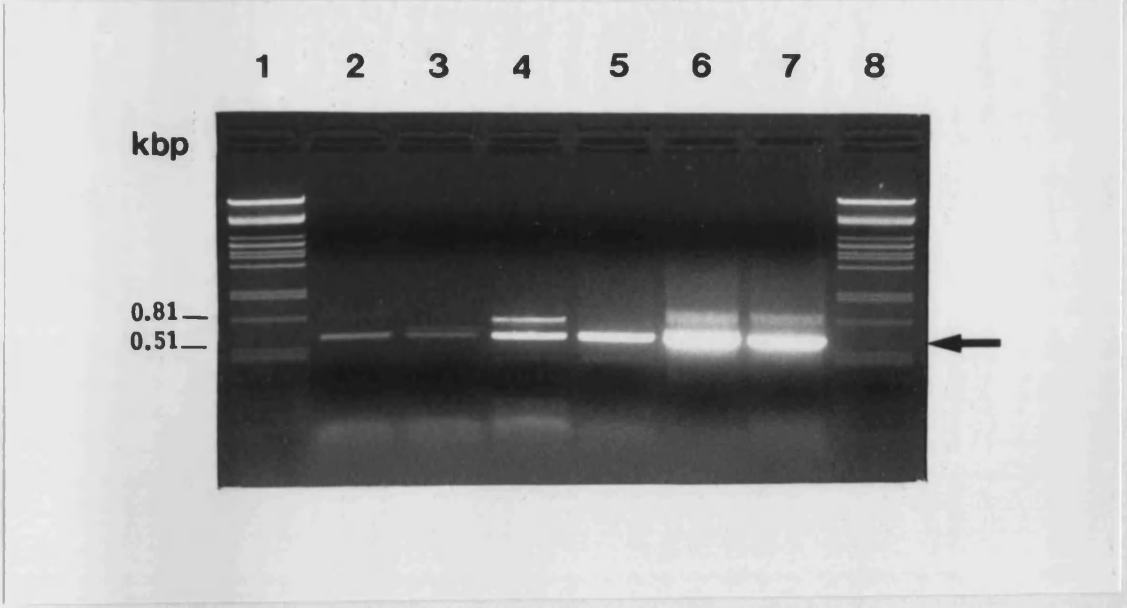

Figure 26, Amplification of the 3' end of HG4 using a range PCR cycles,
Lanes 1& 8: λ DNA cut using Pst1 with relevant band sizes noted in parallel.
Duplicate PCRs were done to amplify the 610 bp 3' end of HG4. Lanes 2 & 3: products amplified after 35 cycles. Lanes 4 & 5: after 40 cycles. Lanes 6 & 7: after 45 cycles.
The Expand™ High Fidelity System was utilised requiring the presence of 300 nM of HG4 GSSP1 and HG4 CAP1 primer, *H. contortus* cDNA template reverse transcribed from eggs and 1.5 mM $MgCl_2$. Cycling conditions as in figure 25.

The 5' and 3' products were Sephaglas™ purified and digested with Not1/Nsi1 and Xba1/Nsi1 respectively. Figure 27 shows a 1% (w/v) agarose gel resolving the resultant fragments prior to ligation into Not1/Xba1 cut pBluescript SK$^+$ vector.

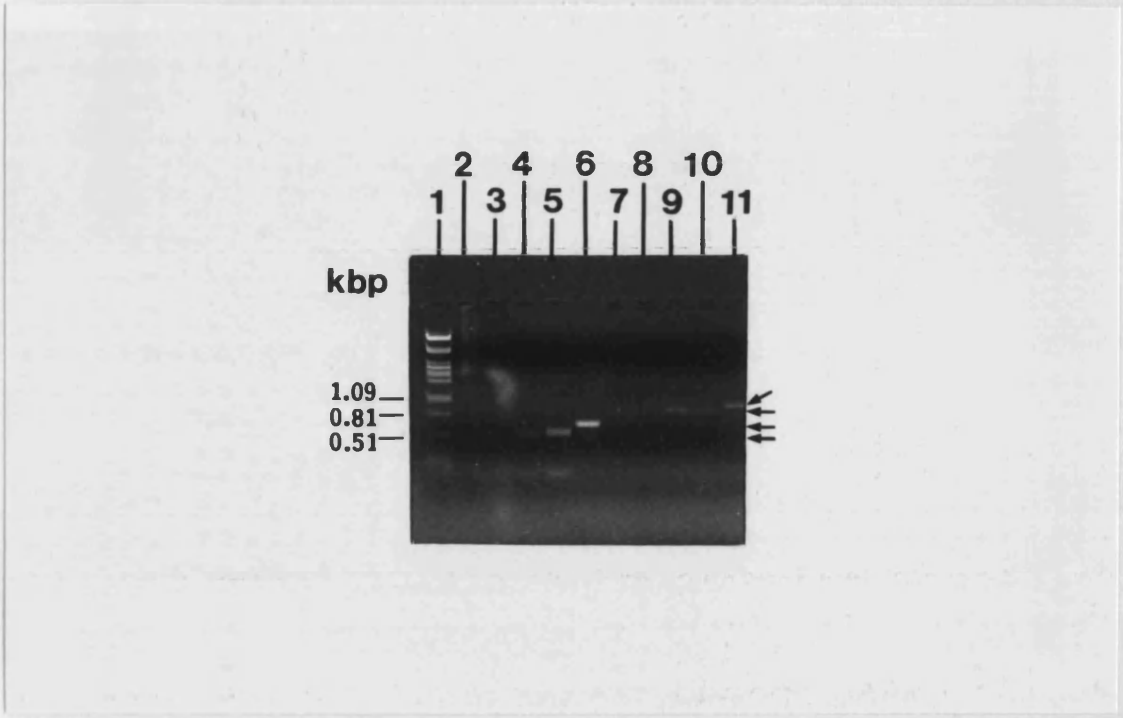

Figure 27, PCR amplified fragments before and after digestion
Lane 1: λ DNA cut using Pst1 with relevant band sizes listed along side.
Lanes 2 & 3: Nsi1 and Xba1 restricted 3' RACE product produced after 35 cycles.
Lanes 4 & 5: Nsi1 and Xba1 restricted 3' RACE product produced after 40 cycles of 500 bp .
Lane 6: 3' RACE product of 610 bp before digestion.
Lanes 7 & 8: Not1 and Nsi1 restricted 5' RACE product after 35 cycles.
Lanes 9 & 10: Not1 and Nsi1 restricted 5' RACE product after 40 cycles of 890 bp.
Lane 11: 5' RACE product of 930 bp before digestion.
An arrow indicates each of the above bands. PCR amplified fragments were purified from the agarose gels seen in figures 25 & 26 using the Sephaglas™ kit and then digested with the specified enzymes for 1 h at 37 °C. 4 μl of each sample were analysed by running on a 1 % (w/v) agarose gel to establish whether digestion was successful.

Both 5' and 3' products, produced after 40 cycles, were ligated together in the presence of pBluescript SK$^+$, which had previously been digested with Not1 and Xba1. These were then transformed into XL1 Blues. Resulting colonies were selected for plasmid DNA purification and screened by digesting with Not1 and Xba1 enzymes. Restricted fragments were analysed on an agarose gel depicted in figure 28. Successful release of a 1.3 kbp fragment upon digestion can be seen in lanes 2, 3, 4, 5, 6, 10 and 11. Clone 3, in lane 3, was re-cultured and plasmid DNA was purified using the Wizard™ Plus kit for automated sequencing.

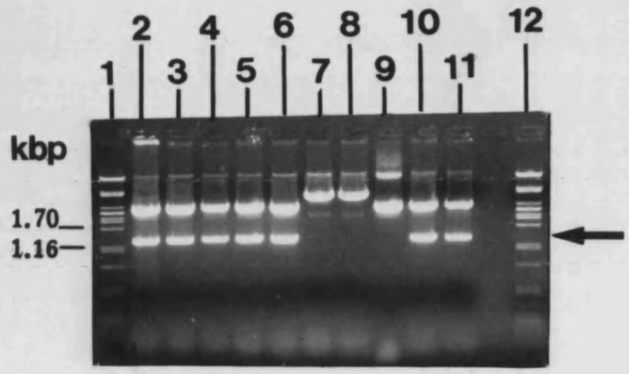

Figure 28, Restriction of constructs produced from a three-way ligation
Lanes 1 & 12: λ DNA cut using Pst1 with relevant band sizes listed along side.
Lanes 2, 3, 4, 5, 6, 10 & 11: Transformed plasmid digested with Not1 and Xba1 releasing a 1.3 kbp HG4 fragment.
Lane 7: Control of purified plasmid equivalent to that seen in lane 6, digested with Not1.
Lane 8: Control of purified plasmid equivalent to that seen in lane 6, digested with Xba1.
Lane 9: control of undigested plasmid.
Recombinant plasmids were purified from XL1-Blue colonies with the Wizard™ Plus kit followed by double or single digestion, as noted above, with the restriction enzymes Not1 and/or Xba1 for 1 h at 37 °C. Restriction patterns were monitored on a 1 % (w/v) agarose gel by electrophoresis. Full-length HG4 products are indicated by ➔.

Each full-length sequence was aligned with the previously obtained clones, in figure 23 and the percentage of variation was calculated as summarised in Table 6 and 7. Clone 3 appears to possess a single bp difference, which results in an amino acid substitution of alanine for threonine at position 26. This result suggests that a reduction of thermocycles used in the PCR has minimised the possible introduction of mutations relative to that seen for clones 8 and 14. By running the sequence through the GCG package on the gnome workstation, clone 3 was found to have a 79.66 % amino acid identity with GluClβ. With three full-length and two RACE sequences for HG4 elucidated a final consensus sequence was produced and found to have an 80.25 % amino acid identity with GluClβ. This consensus sequence has been aligned with that of GluClβ in figure 29. Table 9 highlights the amino acid identity of HG4 with other closely related members from the inhibitory TGIC family.

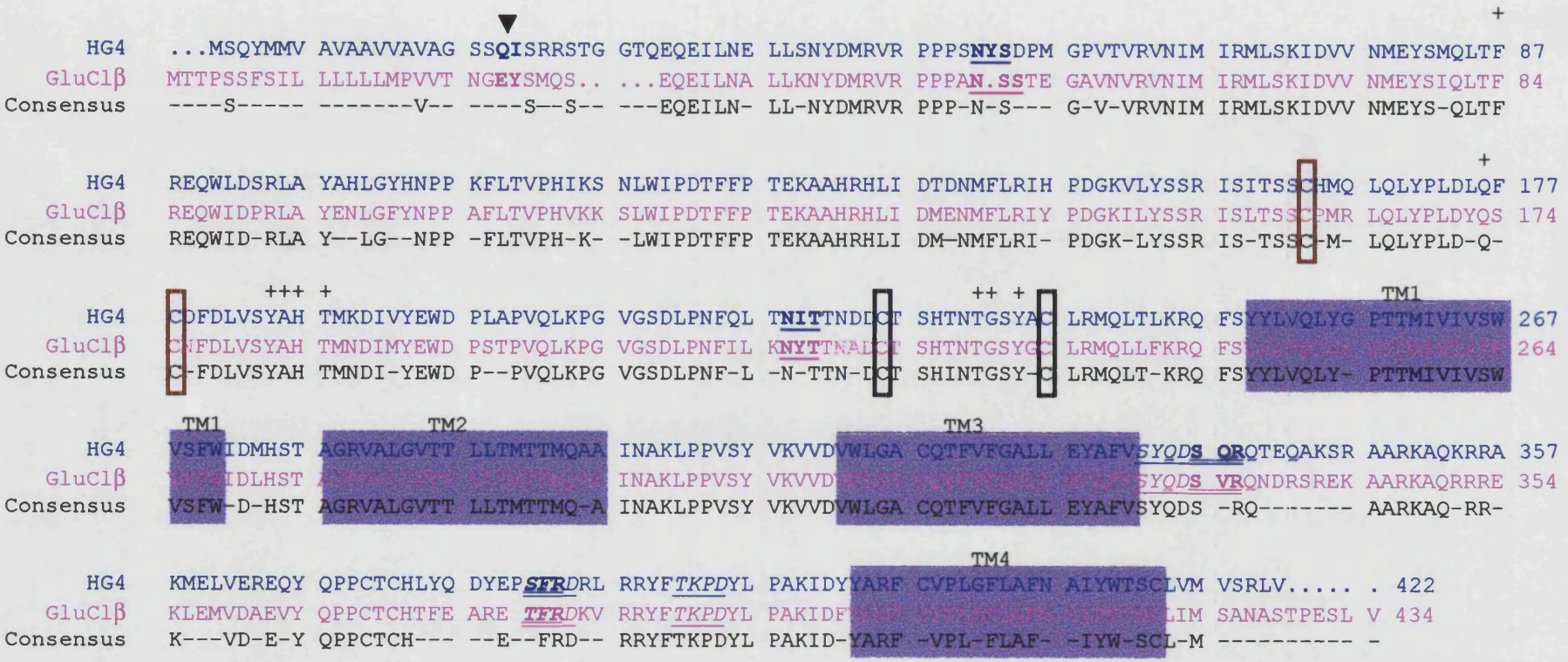

Figure 29, Alignment of HG4 with GluClβ

KEY: Predicted signal cleavage sites are between the residues ***QI*** (indicated by ▼) for HG4, ***EY*** for GluClβ,

NX(T/S) are predicted N-linked Glycosylation sites,

SYQD & ***SFRD*** *and* *SYQD* & ***TFRD*** are predicted casein kinase II phosphorylation sites, **SQR** & **SFR**,and **SVR** & **TFR** are predicted protein kinase C phosphorylation site

, C cysteines forming the cysteine loop, C cysteine characteristic of glycine receptors, Transmembrane domains (TM1-4). + marks the residues believed to be involved in ligand binding.

			GluCLR													
	GABA R	Glycine R	Beta, β-like subunits		Gamma, γ-like subunit						Alpha, α-like subunits					
	HG1	Glyα	GluCl β	HG4	Gbr-2a	Gbr-2b	HG2	HG3	GluClX	GluCl X	Zc317.3	C27h55	GluCl α1	GluCl α2s	GluCl α2l	GluCl α
$GABA_A$	28%	38%	31%	31%	36%	35%	33%	35%	42%	40%	33%	27%	31%	32%	32%	31%
HG1	-	33%	26%	27%	26%	28%	25%	27%	32%	29%	29%	24%	28%	30%	29%	28%
Glyα			40%	41%	43%	42%	42%	42%	47%	47%	43%	36%	40%	41%	41%	46%
GluClβ				80%	48%	47%	46%	48%	57%	57%	49%	39%	45%	47%	47%	44%
HG4					48%	47%	45%	48%	53%	57%	47%	38%	47%	46%	46%	42%
Gbr2a						79%	79%	74%	81%	91%	60%	41%	57%	57%	57%	52%
Gbr2b							72%	87%	88%	86%	58%	40%	54%	54%	55%	50%
HG2								75%	81%	89%	55%	37%	52%	53%	54%	45%
HG3									88%	85%	59%	40%	54%	55%	55%	49%
GluClX										91%	68%	55%	63%	63%	68%	55%
GluClX											72%	53%	72%	72%	72%	59%
Zc317.3												40%	61%	67%	67%	50%
C27h55													38%	38%	38%	37%
GluClα1														77%	77%	46%
GluClα2s															96%	48%
GluClα2l																47%

Key; *H contortus* *C. elegans* *O. volvulus* *D. immitis* *D. melangastor* *R. norvegicus* Partial sequence

Table 9, Comparison of the Amino Acid Identities of HG4 with Related TGIC Subunits.

3.2.10 Analysis of HG4 Full-Length Consensus Sequence

As depicted in figure 29, the HG4 receptor subunit has four transmembrane spanning domains and two N-linked glycosylation sights, residues NYS (position 52-54) and NIT (219-221) positioned along the N-terminal extracellular domain. The characteristic cys-loop is also present with cysteine residues at position 164 and 178. A further two cysteines are located downstream from the cys-at sites 226 and 237. These are characteristic of glycine receptor subunits found in mammals. The presence of phosphorylation sites has been predicted along the intracellular loop between TM3 and TM4. These include the protein kinase C phosphorylation sites SQR (residues 337-339) and SFR (382-384). Casein kinase II phosphorylation sites are also predicted, these motifs being SYQD (amino acids 233-236), SFRD (337-340) and TKPD (382-385).

Predicted ligand binding sites common to GluClRs (Wolstenholme, 1997) are encoded by the HG4 cDNA. These include the amino acid residues YAHT at positions 185-188 and TGSY at positions 232-235, seen in figure 29. Likewise, the amino acid residue glutamine-176 and phenylalanine-87 are also conserved in HG4. These residues are predicted to play a role in agonist binding.

3.2.11 Production of a Consensus Sequence

In order to characterise the protein expressed by HG4 cDNA, a consensus clone needed to be constructed. Expression of a consensus sequence in *Xenopus laevis* oocytes would enable the screening of homomeric HG4 channels with potential agonists and antagonists. A technique introducing point mutations to revert PCR amplified sequence to the consensus sequence was adopted. This procedure involved the hybridisation of single stranded DNA to a complementary synthetic oligonucleotide possessing the desired mutation of a single nt mismatch in the centre. Double stranded DNA was then made in the presence of DNA polymerase. Nicks present in the duplex were sealed by DNA ligase and transformed into an *E. coli* host (Hutchinson, 1978).

To obtain an HG4 construct coding the consensus sequence, the Altered Sites® II *in vivo* Mutagenesis system was utilised to convert A26 to T26. This required a mutation to be made converting the G in codon GCT to an A. This was achieved by designing a sense oligonucleotide (MUTS), incorporating ACT at its centre (Appendix 3).

HG4 was cut out of clone 3 using the restriction enzymes Sac1 and Xba1 and ligated into a Sac1 / Xba1 digested pALTER®-1 vector. This vector carries gene sequences for both ampicillin and tetracycline resistance, thus antibiotic selection could be used to dictate an increase in mutant yield. The resulting construct was transformated into JM109 competent cells in the presence of tetracycline. Purified plasmid was denatured into single stranded template and used in a mutagenesis reaction with 5' phosphorylated primers: ampicillin repair oligonucleotide (ARO), tetracylcine knockout oligonucleotide (TKO) and the MUTS primer.

Resultant mutant strands, synthesised using T4 DNA polymerase and T4 DNA ligase, were transformed into BMH71-18 mutS under no antibiotic selection. A Wizard™ Plus purification of plasmid from BMH71-18 mutS cells was transformed into JM109 *E. coli* cells and plated out onto LB/ ampicillin plates. Plasmids from 4 colonies were purified and sequenced with the T7 primer to confirm incorporation of the point mutation. Figure 30 displays two electrophoretograms before and after mutagenesis, the point mutation is highlighted. Mutated HG4 was finally re-transformed into the pBluescript SK$^+$ for expression studies in *Xenopus* oocytes, which are yet to be completed.

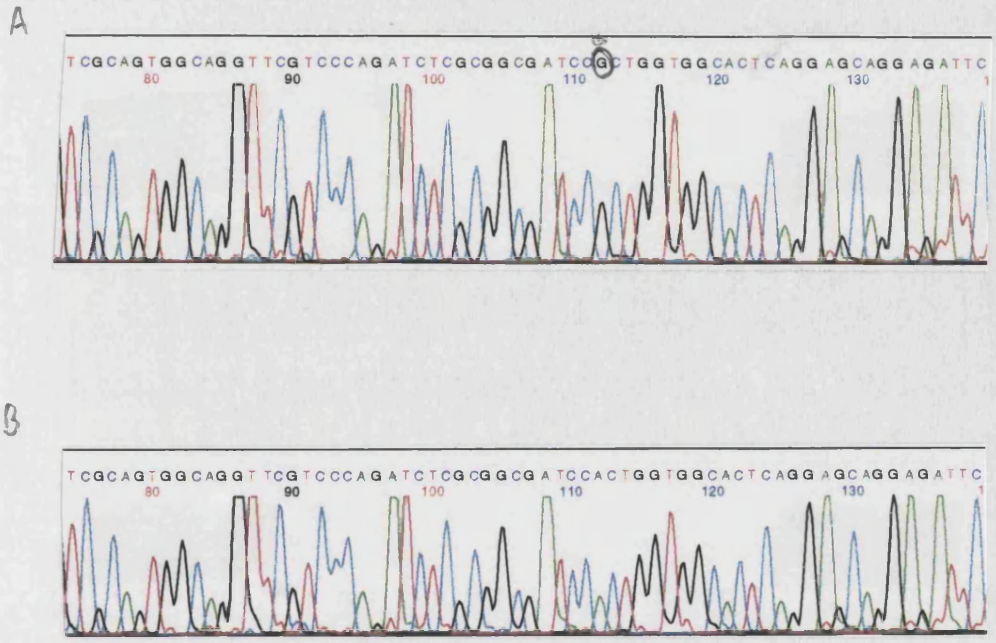

Figure 30, Electrophoretograms of HG4 Sequence A]Before, and B]After, mutagenesis.

3.2.12 Isolation of HG4 from Avermectin Resistant *H. contortus*

mRNA extracted from 1g of avermectin resistant *H. contortus* eggs was reverse transcribed into cDNA. RACE-PCR to amplify HG4 cDNA was carried out to enable comparison of its nucleotide sequence with that obtained from a susceptible population. This was done to detect variations in the amino acid sequence between the two isolates, which may contribute to the switch to avermectin resistance. Both 5' and 3' ends were amplified using 35 cycles to minimise the possible occurrence of mutations introduced by PCR. Two individual 5' and 3' ends were amplified using primers HG4-CSP1 with HG4-GSAP1 and HG4-GSSP1 with HG4-CAP1 respectively. These were then blunt-ended and cloned into EcoRV cut pBluescript SK$^+$ vectors for sequencing. The sequence derived for these clones has been aligned with the consensus sequence compiled from clones isolated from avermectin susceptible worms and can be seen in figure 31. The percentage variation was calculated by comparison with the avermectin susceptible HG4 clones and is summarised in Table 10. Whilst differences are

observed at the nucleotide level no sequence alterations are seen at the amino acid level. This suggests that avermectin resistance has not developed due to a change in the genetic make up of HG4.

Figure 31, see figure legend on next page.

```
                351                                                 400
Susceptible Con AAATTCCTCA CRGTACCACA CATCAAAAGC AACCTCTGGA TTCCKGACAC
Resistant 5'(1) AAATTCCTCA CAGTACCACA CATCAAAAGC AACCTCTGGA TTCCTGACAC
Resistant 5'(2) AAATTCCTCA CAGTACCACA CATCAAAAGC AACCTCTGGA TTCCTGACAC
Resistant 3'(1) .......... .......... .......... .......... ..........
Resistant 3'(2) .......... .......... .......... .......... ..........

                401                                                 450
Susceptible Con CTTTTTCCCG ACCGAAAAAG CRGCACACCG GCATCTCATC GAYACGGACA
Resistant 5'(1) CTTTTTCCCG ACCGAAAAAG CAGCACACCG GCATCTCATC GATACGGACA
Resistant 5'(2) CTTTTTCCCG ACCGAAAAAG CAGCACACCG GCATCTCATC GATACGGACA
Resistant 3'(1) .......... .......... .......... .......... ..........
Resistant 3'(2) .......... .......... .......... .......... ..........

                451                                                 500
Susceptible Con ACATGTTCCT TCGRATTCAT CCAGATGGAA RGGTGYTGTA CAGTAGTCGA
Resistant 5'(1) ACATGTTCCT TCGAATTCAT CCAGATGGAA AGGTGTTGTA CAGTAGTCGA
Resistant 5'(2) ACATGTTCCT TCGAATTCAT CCAGATGGAA AGGTGTTGTA CAGTAGTCGA
Resistant 3'(1) .......... .......... .......... .......... ..........
Resistant 3'(2) .......... .......... .......... .......... ..........

                501                                                 550
Susceptible Con ATTAGCATTA CCAGCTCCTG YCAYATGCAA CTACAACTCT ACCCCTTGGA
Resistant 5'(1) ATTAGCATTA CCAGCTCCTG TCACATGCAA CTACAACTCT ACCCCTTGGA
Resistant 5'(2) ATTAGCATTA CCAGCTCCTG TCACATGCAA CTACAACTCT ACCCCTTGGA
Resistant 3'(1) .......... .......... .......... .......... ..........
Resistant 3'(2) .......... .......... .......... .......... ..........

                551                                                 600
Susceptible Con TTTGCARTTC TGTGACTTTG ATCTCGTCAG CTATGCCCAT ACSATGAAGG
Resistant 5'(1) TTTGCAGTTC TGTGACTTTG ATCTCGTCAG CTATGCCCAT ACCATGAAGG
Resistant 5'(2) TTTGCAGTTC TGTGACTTTG ATCTCGTCAG CTATGCCCAT ACCATGAAGG
Resistant 3'(1) .......... .......... .......... .......... ..........
Resistant 3'(2) .......... .......... .......... .......... ..........

                601                                                 650
Susceptible Con AYATTGTCTA CGAATGGGAY CCCCTGGCTC CTGTGCAGCT CAAACCCGGT
Resistant 5'(1) ATATTGTCTA CGAATGGGAT CCCCTGGCTC CTGTGCAGCT CAAACCCGGT
Resistant 5'(2) ATATTGTCTA CGAATGGGAT CCCCTGGCTC CTGTGCAGCT CAAACCCGGT
Resistant 3'(1) .......... .......... .......... .......... ..........
Resistant 3'(2) .......... .......... .......... .......... ..........

                651                                                 700
Susceptible Con GTAGGAAGTG ACCTGCCTAA CTTYCAGCTC ACAAATATCA CCACCAATGA
Resistant 5'(1) GTAGGAAGTG ACCTGCCTAA CTTTCAGCTC ACAAATATCA CCACCAATGA
Resistant 5'(2) GTAGGAAGTG ACCTGCCTAA CTTTCAGCTC ACAAATATCA CCACCAATGA
Resistant 3'(1) .......... .......... .......... .......... ..........
Resistant 3'(2) .......... .......... .......... .......... ..........

                701                                                 750
Susceptible Con SGACTGYACT AGCCATACYA ATACTGGGTC RTACGCCTGY CTGAGGATGC
Resistant 5'(1) CGACTGTACT AGCCATACCA ATACTGGGTC GTACGCCTGC CTGAGGATGC
Resistant 5'(2) CGACTGTACT AGCCATACCA ATACTGGGTC GTACGCCTGC CTGAGGATGC
Resistant 3'(1) CGACTGTACT AGCCATACCA ATACTGGGTC GTACGCCTGC CTGAGGATGC
Resistant 3'(2) .......... .......... .......... .......... ..........
```

Figure 31, See figure legend on next page.

```
                751                                                 800
Susceptible Con ARCTCACCCT AAAAMGRCAG TTCAGTTACT ACCTRGTCCA RTTGTACGGT
Resistant 5'(1) AGCTCACCCT AAAAAGGCAG TTCAGTTACT ACCTGGTCCA GTTGTACGGT
Resistant 5'(2) ACCTCACCCT AAAAAGGCAG TTCAGTTACT ACCTGGTCCA GTTGTACGGT
Resistant 3'(1) AGCTCACCCT AAAAAGGCAG TTCAGTTACT ACCTGGTCCA GTTGTACGGT
Resistant 3'(2) .......... .......... ...AGTTACT ACCTGGTCCA GTTGTACGGT

                801                                                 850
Susceptible Con CCCACAACGA TGATAGTGAT CGTCTCATGG GTTTCRTTTT GGATCGATAT
Resistant 5'(1) CCCACAACGA TGATAGTGAT CGTCTCATGG GTTTCGTTTT GGATCGATAT
Resistant 5'(2) CCCACAACGA TGATAGTGAT CGTCTCATGG GTTTCGTTTT GGATCGATAT
Resistant 3'(1) CCCACAACGA TGATAGTGAT CGTCTCATGG GTTTCGTTTT GGATCGATAT
Resistant 3'(2) CCCACAACGA TGATAGTGAT CGTCTCATGG GTTTCGTTTT GGATCGATAT

                851                                                 900
Susceptible Con GCATTCAACS GCCGGTCGTG TGGCCCTGGG TGTCACTACC CTGCTRACCA
Resistant 5'(1) GCATTCAACC GCCGGTCGTG TTGCCTTGGG TGTCACTACC ..........
Resistant 5'(2) GCATTCAACG GCTGGTCGTG TTGCTTTGGG TGTCACCACC CTGCTGACCA
Resistant 3'(1) GCATTCGACG GCCGGCCGAG TGGCCTTGGG TGTCACTACC CTACTGACCA
Resistant 3'(2) GCATTCAACG GCTGGTCGTG TTGCTTTGGG TGTCACCACC CTGCTGACCA

                901                                                 950
Susceptible Con TGACCACCAT GCAAGCAGCY ATCAATGCTA AACTGCCMCC KGTGAGCTAC
Resistant 5'(1) .......... .......... .......... .......... ..........
Resistant 5'(2) TGACCACCAT GCAAGCAGCT ATCAATGCTA AACTGCCACC GGT.......
Resistant 3'(1) TGACCACTAT GCAAGCAGCC ATCAATGCTA AATTGCCACC GGTGAGCTAC
Resistant 3'(2) TGACCACCAT GCAAGCAGCC ATCAATGCTA AACTGCCCCC GGTGAGCTAC

                951                                                1000
Susceptible Con GTGAAGGTRG TRGATGTGTG GCTYGGAGCC TGTCAAACRT TCGTSTTTGG
Resistant 5'(1) .......... .......... .......... .......... ..........
Resistant 5'(2) .......... .......... .......... .......... ..........
Resistant 3'(1) GTGAAGGTAG TAGATGTGTG GCTTGGAGCC TGTCAAACAT TCGTGTTTGG
Resistant 3'(2) GTGAAGGTGG TAGATGTGTG GCTTGGAGCC TGTCAAACAT TCGTCTTTGG

               1001                                                1050
Susceptible Con AGCGYTGCTY GARTACGCKT TCGTCTCTTA TCAAGACAGC CAACGACAAR
Resistant 5'(1) .......... .......... .......... .......... ..........
Resistant 5'(2) .......... .......... .......... .......... ..........
Resistant 3'(1) AGCGTTGCTT GAGTACGCGT TCGTCTCTTA TCAAGACAGC CAACGGCAAA
Resistant 3'(2) AGCGTTGCTT GAGTACGCGT TCGTCTCTTA TCAAGACAGC CAACGACAAA

               1051                                                1100
Susceptible Con CAGAGCAGGC CAAAAGCCGA GCTGCTCGAA AAGCTCAAAA GCGACGWGCY
Resistant 5'(1) .......... .......... .......... .......... ..........
Resistant 5'(2) .......... .......... .......... .......... ..........
Resistant 3'(1) CAGAGCAAGC TAAAAGCCGA GCTGCTCGAA AAGCTCAAAA GCGACGAGCC
Resistant 3'(2) CAGAGCAGGC CAAAAGCCGA GCTGCTCGAA AAGCTCAAAA GCGACGCGCT

               1101                                                1150
Susceptible Con AAAATGGAAC TCGTCGAAAG AGAACAATAC CAACCTCCTT GCACGTGTCA
Resistant 5'(1) .......... .......... .......... .......... ..........
Resistant 5'(2) .......... .......... .......... .......... ..........
Resistant 3'(1) AAAATGGAAC TCGTTGAAAG AGAACAATAC CAACCTCCCT GCACGTGTCA
Resistant 3'(2) AAAATGGAAC TCGTCGAAAG AGAACAATAT CAACCTCCTT GCACGTGTCA
```

Figure 31, See figure legend on next page.

```
                1151                                                1200
Susceptible Con TCTGTACCAA GACTAYGAGC CRTCGTTCCG TGACCGGTTR CGGCGCTATT
Resistant 5'(1) .......... .......... .......... .......... ..........
Resistant 5'(2) .......... .......... .......... .......... ..........
Resistant 3'(1) TCTGTACCAA GACTACGAGC CGTCGTTCCG TGACCGGTTG CGGCGCTACT
Resistant 3'(2) TCTGTACCAA GACTACGAGC CGTCGTTCCG TGACCGGTTG CGGCGCTACT

                1201                                                1250
Susceptible Con TCACAAAACC CGACTACCTG CCRGCGAAAA TCGACTACTA TGCTCGATTT
Resistant 5'(1) .......... .......... .......... .......... ..........
Resistant 5'(2) .......... .......... .......... .......... ..........
Resistant 3'(1) TCACAAAACC CGATTACCTG CCTGCGAAAA TCGACTACTA TGCTCGATTT
Resistant 3'(2) TTACAAAACC CGACTACCTG CCTGCGAAAA TCGACTACTA TGCTCGATTT

                1251                                                1300
Susceptible Con TGTGTGCCAT TAGGCTTTTT AGCCTTCAAT GCCATCTAYT GGACATCCTG
Resistant 5'(1) .......... .......... .......... .......... ..........
Resistant 5'(2) .......... .......... .......... .......... ..........
Resistant 3'(1) TGTGTGCCAT TAGGCTTTTT AGCCTTCAAT GCCATCTATT GGACATCCTG
Resistant 3'(2) TGTGTGCCAT TAGGCTTTTT AGCCTTCAAT GCCATCTACT GGACATCCTG

                1301                  1325
Susceptible Con CCTCGTGATG GTGTCAAGAC TAGTC
Resistant 5'(1) .......... .......... .....
Resistant 5'(2) .......... .......... .....
Resistant 3'(1) CCTCGTGATG GTGTCAAGAC TAGTC
Resistant 3'(2) CCTCGTGATG GTGTCAAGAC TAGTC
```

Figure 31, Alignment of HG4 from an avermectin-resistant *H. contortus*. Resistant 5' (1) and (2) are 5' RACE products whilst Resistant 3' (1) and (2) are 3' RACE products. These are compared with susceptible con, the consensus sequence created from clones isolated from a susceptible population of *H. contortus*, detailed in figure 23. Shaded regions highlight nts that vary between the clones. Key: **Y** codes either a C or a T, **M** codes either an A or a C, **R:** an A or a G, **S:** a G or a C, **K:** a G or a T and **W:** an A or a T. Nucleotides in uppercase are coding sequence whilst lower case nucleotides represent the 5' UTR.

Table 10, Percentage variation between avermectin-susceptible and -resistant populations of *Haemonchus contortus*. Resistant 5' (1) and (2) and resistant 3' (1) and (2) nucleotide sequences are compared with each of the clones amplified from avermectin-susceptible nematodes. Values are calculated by dividing the number of mismatches by the length of overlapping sequence. These details are noted in brackets.

Clones from avermectin susceptible isolate	Clones from the avermectin resistant isolate			
	5' RACE products		3' RACE products	
	1 (861 nt)	2 (914 nt)	1 (625 nt)	2 (532 nt)
5' end (914nt)	0.58% (5/861)	0.86% (8/914)	4.12% (10/243)	4.71% (8/170)
3' end (579 nt)	1.39% (2/144)	3.55% (7/197)	3.97% (23/579)	3.08% (17/552)
8 (1296 nt)	2.44% (21/861)	2.52% (23/914)	4.16% (26/625)	2.72% (15/552)
14 (1296 nt)	3.83% (33/861)	4.16% (38/914)	4.16% (26/625)	1.09% (6/552)
3(1296 nt)	0.58% (5/862)	1.20% (11/914)	3.52% (22/625)	4.00% (22/552)

Table 11, Percentage variation at the amino acid level between avermectin-susceptible and -resistant populations of *Haemonchus contortus*. Resistant 5' (1) and (2) and resistant 3' (1) and (2) are compared with each of the clones amplified from avermectin-susceptible nematodes. Values are calculated by dividing the number of mismatches by the length of overlapping sequence. These details are noted in brackets.

Clones from avermectin susceptible isolate	Clones from the avermectin resistant isolate			
	5' RACE products		3' RACE products	
	1	2	1	2
5' end	0.7 % (2/287)	0.7 % (2/304)	0/81	0.0 % (0/81)
3' end	0.0 % (0/48)	0.0 % (0/65)	0/193	0.0 % (0/193)
8	0.7 % (2/287)	0.7 % (2/304)	1/198	0.0 % (0/123)
14	0.3 % (1/287)	0.3 % (1/304)	1/198	0.8% (1/123)
3	0.0% (0/287)	0.0 % (0/304)	0.0 % (0/198)	0.0 % (0/123)
Consensus	0.0 % (0/287)	0.0 % (0/304)	0.0 % (0/198)	0.0 % (0/123)

3.3 Discussion

A total of 3 full-length HG4 cDNAs and 2 partial clones were amplified from a susceptible population of *H. contortus*. These were sequenced and aligned with each other to obtain a consensus sequence for this receptor subunit. Comparison of sequences revealed as high as 4.49% variation existed at the nucleotide level. Alignment of clone 14 with the HG4 3' partial clone (figure 23) identified 26 nucleotide mismatches from a total of 579 overlapping base pairs (Table 6). Upon examination of these mismatches the majority appeared to be third base changes which do not alter the amino acid sequence. This variation may be a consequence of polymorphism resulting from the extraction of mRNA from a population of *H. contortus*. Polymorphism is a common feature detected in nematodes and has been noted by Emmons *et al.* (1979) using restriction patterns to estimate the degree of polymorphism to be 1 % in *C. elegans*. Likewise, in *H. contortus* a 1.5 % difference was established between PCR amplified clones of the HG1 receptor subunit (Laughton *et al.*, 1994). Similarly up to 4 % variation between cDNAs encoding a levamisole resistant acetylcholine receptor subunit, HCA1, was calculated from various *H. contortus* populations (Hoekstra *et al.*, 1997). Another possible but less likely explanation for this level of variation may be that there is more than one closely related sequence in the nematode genome.

Comparison of clone 14 with the HG4 3' partial clone at the amino acid level revealed that 1 amino acid difference existed over the overlapping 193 amino acid translated sequence (Table 7). This alteration may be a result of polymorphism at the coding level or a PCR induced artefact. Percentage variation at the amino acid level exists between each clone. Two differences are present both in clone-8 and -14 (table 8) when compared to the consensus sequence. To reduce the possibility of PCR induced variation; a further PCR was done using a reduced number of cycles. Clone 3 was derived from 40 cycles of PCR rather than 45 used previously to amplify clones 8 and 14. The resulting sequence was 99.77 %

identical to the predicted amino acid consensus sequence. This clone possessed one amino acid difference at position 26, encoding an alanine instead of a threonine.

The consensus sequence for HG4 was calculated to have an 80.25 % amino acid identity and a 69.98 % nucleotide identity with the glutamate gated chloride channel beta subunit, GluClβ (Cully *et al.*, 1994) present in *C. elegans*. It is therefore reasonable to suggest that the HG4 receptor subunit is the parasitic orthologue of GluClβ. Homomeric GluClβ channels in *Xenopus* oocytes respond reversibly to glutamate at concentrations equal to or greater than 1 mM with more than one glutamate-binding site present (Hill coefficient of 1.9 +/- 0.2). Accordingly, if HG4 is a parasitic orthologue of GluClβ, expression of homomeric HG4 channels in *Xenopus* oocytes is also predicted to yield a reversible response to glutamate at equivalent concentrations. In order to express consensus HG4 homomeric channels in *Xenopus* oocytes the alanine present at position 26 of clone 3 was mutated to a threonine, expression studies have yet to be completed.

It has also been established that GluClβ subunits are located in the pm4 and pm5 pharyngeal muscles cells of *C. elegans* (Laughton *et al.*, 1997a) both of which are innervated by the M3 motor neurone which releases glutamate at its synapses. It is therefore expected that HG4 receptor subunits localise to equivalent cells in the pharynx of *H. contortus*. To examine this theory, spatial expression was to be determined by utilising an immuncytological approach and has been detailed in future chapters. Co-expression in *Xenopus* oocytes of GluClβ with GluClα1, a related receptor alpha-subunit isolated from *C. elegans,* results in a glutamate-gated chloride channel potentiated by avermectin at nanomolar concentrations (Cully *et al.*, 1994). Further to these findings, a second alpha related receptor subunit, GluClα2 localises to pm4 and pm5 cells in the pharynx (Dent *et al.*, 1997). It can therefore be suggested that both subunit types assemble together with other like subunits in *C. elegans* to form an avermectin sensitive receptor.

The HG4 receptor subunit cDNA was isolated from an avermectin resistant population of *H. contortus* to establish whether it conveys a specific mutation preventing binding of the drug. Sequencing of two 5'- and two 3'-RACE products revealed identical translated sequences to the HG4 consensus sequence previously isolated from the avermectin susceptible population. Therefore, no mutation in transcribed HG4 was responsible for the switch in phenotype to avermectin resistance. This result is not surprising as homomeric GluClβ channels do not bind avermectin when expressed in *Xenopus* oocytes (Cully *et al.,* 1994). In retrospect, an alteration at the ligand-binding domain of α-subunits is more likely to cause avermectin resistance. This is because the α-subunit has been shown to bind the drug when expressed as homomeric channels in *Xenopus* oocytes (Cully *et al.*, 1994 & Dent *et al.*, 1997).

4 Production of Polyclonal Antibodies

4.1 Introduction

Further characterisation of HG4 is to be accomplished by determining its expression pattern within the parasitic nematode, *Haemonchus contortus*. Sequence comparison of HG4 with related proteins suggests that it is the GluClβ orthologue. Therefore, localisation of HG4 within *H. contortus* is believed to be on pm4 and pm5 muscles cells of the pharynx, as is the case for *C. elegans* (Laughton *et al.*, 1997a). If this were true, then avermectin may effect pharyngeal function in the parasite. In order to define HG4 expressing cells, anti-HG4 antibodies were generated. This chapter details possible approaches taken to determine spatial expression of proteins. It also discusses the advantages of using an immunohistochemical approach, which is the route that will be taken. Results using this method are displayed as well as corroboration that the antibodies bind specifically to a defined epitope.

4.1.1 Techniques employed for localisation of nematode genes

Temporal and spatial expression patterns within nematodes have been studied using a variety of techniques such as histochemistry, *in-situ* hybridisation, gene reporter constructs and immunohistochemistry. These methods offer sensitive routes to localise proteins such as transmitter-gated ion channel (TGIC) subunits to a minority of cells where levels of mRNA may vary with the nematode's stage of development.

4.1.1.1 Histochemisrty

A histochemical approach is useful when studying the localisation of an enzyme within a tissue. Substrate for the required enzyme is catalysed into a visible product upon addition; thus highlighting enzyme saturated areas within the tissue of interest. The expression pattern of NADPH diaphorase in whole worm mounts of *Ascaris suum* was achieved with this method converting the substrate tetrazolium to an insoluble, visible formazan in the presence of NADPH (Bascal *et al.*, 1996). However, as TGIC subunits possess no specific enzyme activity this technique is of no use to this project.

4.1.1.2 *In-situ* hybridisation

In-situ hybridisation relies upon the hybridisation of a specifically labelled nucleic acid probe to the cellular mRNAs within the nematode tissues. Probes may be DNA or RNA but use of the former increases the sensitivity of the method. Ribonucleotide probes are detected by incorporating nucleotides labelled with radioisotope, biotin or digoxigenin. Radioactivity can be monitored by autoradiographic detection whilst biotin and digoxigenin labelled probes can be detected by either a fluorescent or enzymatic system. Amplification and localisation of low copy RNA can be achieved by amplifying target mRNAs using *in-situ* PCR. This method has been

used to screen neonatal heart for the protozoan parasite *Trypanosoma cruzi* (Taleton *et al.*, 1997). Detection of intracellular PCR products can either be achieved indirectly by hybridising with labelled probe after amplification or through direct detection using labelled nucleotides during amplification.

4.1.1.3 Reporter gene constructs

Gene expression can be studied in the free-living nematode *Caenorhabditis elegans* by using vectors containing reporter molecules. These include β-galactosidase, encoded by the *Escherichia coli lac-z* gene, or green fluorescent protein (GFP) isolated from the jelly-fish *Aequorea victoria* (Fire *et al.*, 1990 & Chalfie *et al.*, 1994).

C. elegans is an ideal candidate for this technique as it is well characterised and can be grown successfully *in vitro*. In contrast the *in vitro* culturing of *Haemonchus contortus* has not yet developed to an equivalent level. Free-living stages (egg to L3 larvae) can be grown by incubation in dung but survival of adult worms depends on the simulation of conditions experienced in the sheep abomasum. These include the presence of gastric secretions and host blood, which as yet have not been fully optimised for *in vitro* culturing (Stringfellow, 1986). However, *C. elegans* has been used as a model system into which parasitic genes are transformed (Kwa *et al.*, 1995). Some debate still exists as to whether this technique reflects the exact location of target proteins as it does not consider control elements that may be present in intronic or downstream sequences. This method should therefore be used in combination with other related techniques.

Typical experiments involve the cloning of reporter fusions where the promoter elements for the gene of interest are linked to the reporter gene. The generation of transgenic nematodes is achieved by microinjection of the recombinant construct with a plasmid containing a marker gene. Selection of F1 progeny displaying the marker phenotype are then assayed for reporter activity. For *lac-z* fusions the chromogenic substrate X-Gal (5-bromo-4-chloro-3-indolyl-β-D-galactopyranoside) is added to permeabilized whole worms (Fire *et al.*, 1990). A more recent report described by Laughton *et al.* (1997) utilised the *lac-z* reporter gene for looking at the expression pattern of the inhibitory glutamate receptor β subunit. Likewise, expression of GFP tagged proteins such as β-tubulin coded by the *mec-7* gene (Chalfie *et al.*, 1994) can be monitored under ultra violet light.

Some reporter constructs contain a 5' nuclear localisation sequence leading to accumulation of the reporter molecules in the nuclei. Concentration of these molecules facilitates the identity of expressing cells in complex nematode tissues, but does not reveal the exact intracellular distribution.

4.1.1.4 Immunohistochemistry

The main advantage of immunohistochemical localisation is that exploits the ability of antibodies to bind to specific protein epitopes, thus localising antigens to subcellular compartments within the cell. Neuronal protein distribution has been deduced in a variety of parasitic nematodes including *H. contortus* (Keating *et al.*, 1995) and *Ascaris suum* (Brownlee *et al*, 1994) by exposure to a primary antibody. Detection of bound primary antibody is achieved by addition of a secondary antibody labelled either with a fluorochrome, an electron dense particle (such as gold) or an enzyme. The disadvantage of this approach is that it is the most time consuming of all the methods discussed in this section. Not only does the antigen need to be synthesised from the target consensus sequence but antibodies must then also be raised specifically against it once injected into the host rabbit.

Apart from the time restraints it was considered that localisation of HG4 will be best achieved by selecting the latter approach, requiring the production of anti-HG4 antibodies. Subunit proteins from the TGIC family have many highly conserved regions. Hence, production of antisera to a whole receptor subunit would generate antibodies exhibiting affinities for many antigenic determinants over the entire protein surface. This would increase the probability of cross-reaction with related subunits. It has therefore been decided that anti-HG4 antibodies will be raised against a peptide specific to the HG4 subunit rather than using the whole subunit.

A polyclonal serum will be raised in a rabbit rather than producing a monoclonal serum from a rodent. This route is preferred, as monoclonal antiserum against peptide-antigens produce low titres. Also, conformational changes in the antigenic determinant between the peptide and parent protein can reduce binding affinity thus decreasing titre even further. In contrast, a high titre of antibodies can be retrieved from raising polyclonal anti-serum. This is because the anti-serum is able to recognise a whole range of epitopes spread over the target peptide.

4.2 Results

4.2.1 Design of a Peptide

The first step, when selecting a peptide to raise antibodies against, was to determine whether it's predicted location in the proteins three-dimensional structure would be exposed on the surface. This was accomplished by predicting the conformation of the whole subunit. This in turn dictated whether individual residues were found, exposed on the surface or buried within the molecule. An ideal peptide sequence needed to span mobile regions on the surface of the molecule possessing high flexibility and that were hydrophilic in nature.

The predicted secondary structure of HG4 was determined using the computer program command "peptidestructure" in the GCG program suite on the gnome workstation. Measures of

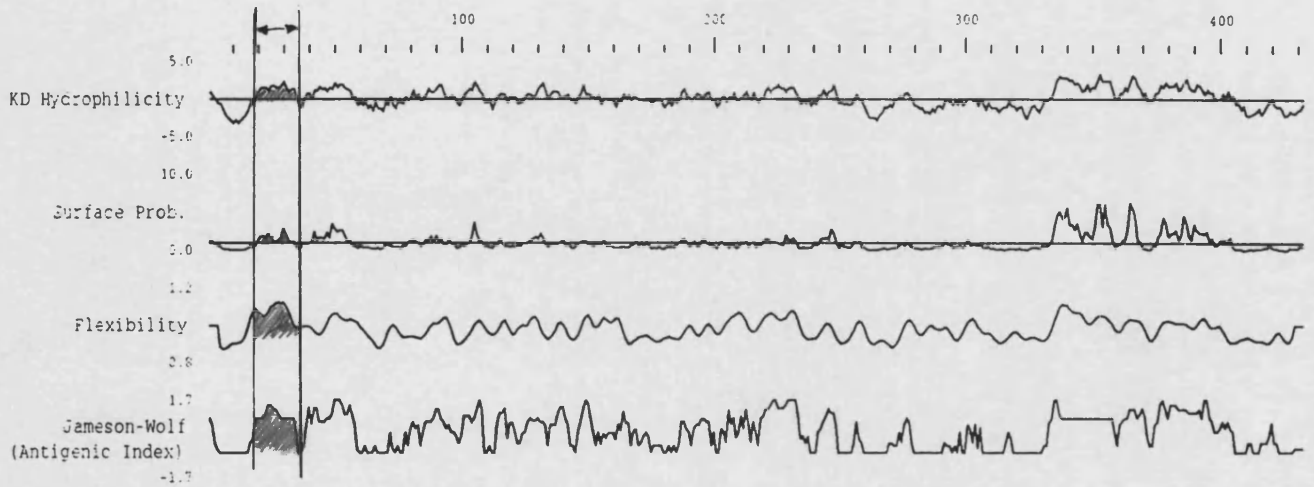

Figure 32, Predicted secondary structure of HG4. A hydrophilicity plot of HG4 is displayed with measures of flexibility, surface probability, secondary structure and the antigenic index for each amino acid. This was generated using the command "peptidestructure" in the GCG suite accessed via the gnome workstation. The shaded region defines the section from which an antigenic peptide was designed to.

hydrophilicity, flexibility, surface probability, secondary structure as well as antigenic index for each amino acid within the protein were calculated by the program and are represented as a graphic plot in figure 32.

A sequence alignment of HG4 with related subunits distinguished an area of little homology present at the N-terminal extracellular domain (figure 33). In light of secondary structure predictions and the sequence-alignment, a peptide corresponding to the amino acid sequence RSTGGTQEQEILNELLSN, starting 24 amino acids downstream from the start methionine, was synthesised.

4.2.2 Coupling to Carrier Protein

To elicit an antibody response in the rabbit, the HG4 immunogen needed to contain an epitope for both B-cell binding and for class II-T-cell receptor binding. To ensure both of these sites were present a carrier protein was conjugated to the peptide. Several methods exist to couple peptide to a carrier protein and rely on the presence of free amino, sulphydryl, phenolic or carboxylic acid groups. Free amino groups are found on lysine side chains or on the amino-terminal residue. Sulphydryl groups are present on cysteine side chains, phenolic groups on tyrosines and carboxylic acid groups on aspartic acids, glutamic acids and the carboxy-terminal residue. As the peptide sequence (RSTGGTQEQEILNELLSN) contains no sulphydryl or phenolic groups, coupling to carrier protein could not be accomplished using m-Maleimidobenzoyl-N-Hydroxysuccinamide Ester or Bis-diazotived benzidine reagents. It was also not ideal to couple via carboxylic acid groups, as many of these sites were present along the peptide sequence. As the peptide only possessed one free amino group, present at the N-terminus, it was decided to use gluteraldehyde as a coupling reagent. Thyroglobulin was selected as a carrier protein as it is not found in nematodes and thus any antibodies made towards this protein are unlikely to cross-react when immunolabelling.

4.2.3 Immunisation and determination of Antibody Titre

The peptide carrier conjugate was mixed with the adjuvant Imject Alum, which contains aluminium hydroxide precipitates. Once injected subcutaneously into the rabbit the adjuvant acts as a depot from which antigen is protected from rapid catabolism and is released gradually. Adjuvant also acts as a non-specific stimulator of the immune response by raising the level of lymphokines. These cells stimulate the activity of antigen processing-cells and cause a local inflammatory reaction at the site of injection.

Before each injection, samples of serum were taken to check the production of specific antibodies. Comparison of antibody titre using the enzyme linked immunosorbant assay (ELISA) after successive injections enabled antibody response to be monitored (Schots *et al.*, 1988).

Figure 33, Alignment of TGIC Subunit N-terminal domains

HG4, HG2, HG1 are inhibitory TGIC subunits from *H. contortus*. GluClβ, GluClα1, GluClα2s, GBR2A and zc3173 are from TGIC subinits from *C. elegans*. O. cGluClX is a TGIC subunit fron *O. volvulus* and D.mGluClα is from *D. melanogastor*. Finally Rnglyα is a glycine gated alpha TGIC subunit from *R. norvegicus*.

Test bleeds were taken every 10 days just before the administration of immunogen/adjuvant mix.

ELISA pro-bind plates were coated with 3 different types of antigen: HG4 peptide, HG4 peptide conjugated to thyroglobulin and thyroglobulin. A serial dilution of serum was added to each well followed by exposure to a secondary antibody conjugated with horseradish peroxidase. The substrate 3,3',5,5'-tetrmethylbenzidine (TMB) was added and the reaction was stopped by addition of sulphuric acid. This converted the blue colour of the TMB breakdown products into a yellow hue, which was measured at an absorbance of 450 nm. Figure 34 displays readings from an ELISA using samples taken over 60 days during which time 6 boosts were carried out, one every 10 days. A pre-immune bleed was taken as a control to monitor antibody levels before administration of immunogen acting as a base line of antibody levels.

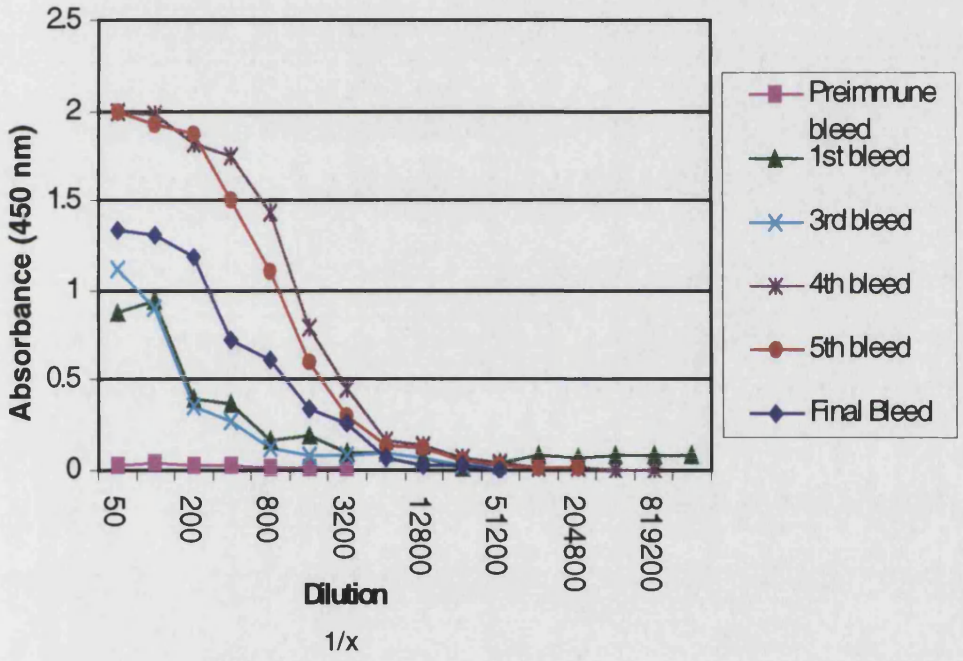

Figure 34, Serum response to the HG4 peptide. An ELISA plate was coated with HG4 peptide and titres of anti-HG4 antibody were measured by adding serial dilutions of 1) pre-immune bleed, 2) 1st bleed, 3) 3rd bleed, 4) 4th bleed, 5) 5th bleed and 6) final bleed. From this graph fourth and fifth bleeds contain the highest anti-HG4 antibody titres.

The antibody titre specific to the HG4 peptide had reached a sufficiently high level in the fifth bleed with a half-maximal response at 1:1200 dilution. It was therefore decided that the rabbit was to be terminated by exsanguination 10 days following the 6th boost. 160 ml of serum was extracted from the collected blood and an ELISA was carried out to determine the final anti-HG4 antibody titre. Unfortunately the antibody titre had dropped giving a half-maximal response at 1:600, thus making the serum collected on the 5th bleed (a total of 10 mls) a more ideal sample to purify initially.

Due to the use of the carrier protein thyroglobulin, a high titre of antibodies had been raised specific to the epitopes present on the protein. To check that no cross-reaction of these antibodies to the HG4 peptide has occurred, the HG4 peptide was used to coat wells exposed with a previously made anti-thyroglobulin antibody (kindly donated by Dr A. Rogers). Results of this ELISA are shown in figure 35. Non-specific binding of anti-thyroglobulin antibodies to HG4 peptide was negligible with levels equivalent to pre-immune serum recognising HG4 peptide. In contrast, anti-thyroglobulin antibodies recognised the antigen HG4/thyroglobulin complex and thyroglobulin at half-maximal responses of 1:22400 and 1:70400 respectively. This meant that purifying anti-HG4 antibody on an affinity column would be specific, ruling out the possibility of anti-thyroglobulin antibodies cross-reacting. Antibodies recognising thyroglobulin epitopes would pass through the column with out binding non-specifically.

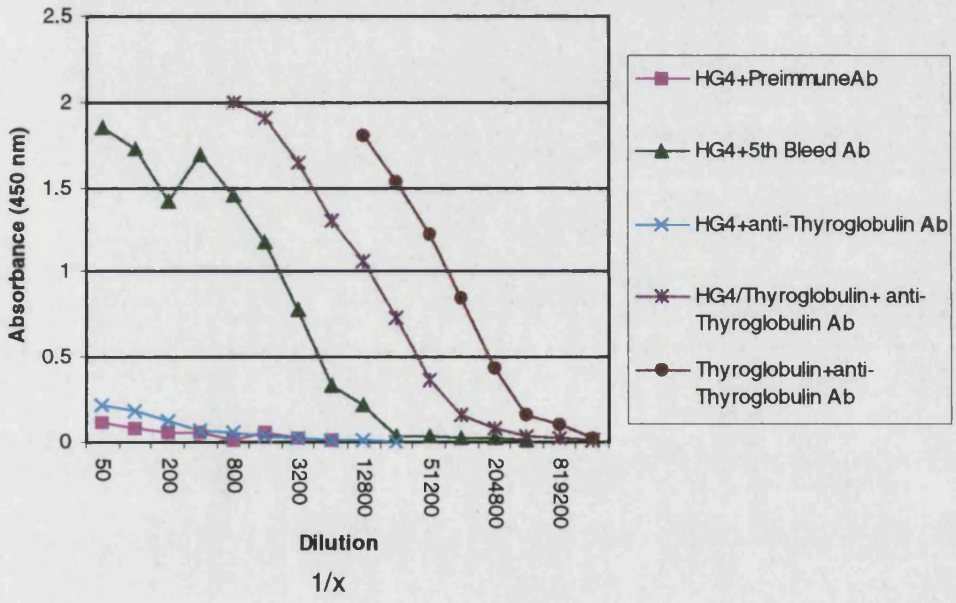

Figure 35, The response of anti-thyroglobulin antibodies on different antigens. An ELISA plate was coated with the following antigens: 1) HG4 peptide, 2) HG4 peptide conjugated to thyroglobulin, 3) thyroglobulin. Serial dilutions of Pre-immune, 5th bleed and anti-thyroglobulin samples were added to antigen 1. Absorbencies from these samples were compared to the response measured for anti-thyroglobulin antibodies against antigen 2 and 3.

4.2.4 HG4 Peptide Affinity Column

The column was made using cyanogen bromide activated Sepharose 4BA beads coupled with HG4 peptide. 10 ml of 5th bleed serum was recycled overnight followed by elution with diethlyamine at pH 11.5. Elution was tracked using a UVI cord and a trace is displayed in figure 36. The two peaks represent the elution of two groups of antibodies each possessing different

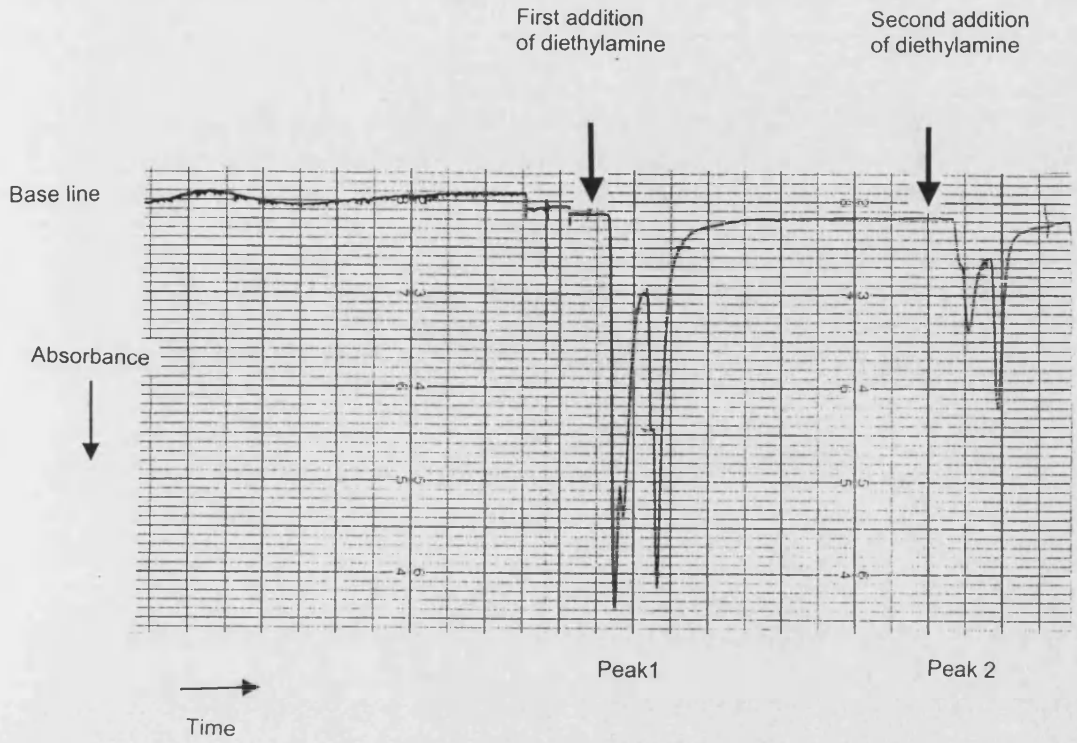

Figure 36, Elution of anti-HG4 antibodies from an affinity column. A UVI cord, attached to a chart recorder, was used to monitor the elution of anti-HG4 antibodies off an affinity column. Two peaks labelled 1 and 2 were eluted, each possessing a different affinity to the column. Peak 1 was eluted initially followed by peak 2 hence antibodies collected in the peak 2 fractions have a higher affinity for HG4 peptide epitopes.

affinity to the peptide. Purified anti-HG4 antibodies were dialysed overnight to remove the diethylamine and concentrated using PEG-20,000. Bradford assays quantified the levels of antibody collected via the column. The collected fraction from peak one had a concentration of 150 ng/ml whilst the fraction corresponding to peak two contained 40 ng/ml of anti-HG4 antibody. An ELISA was done to examine how efficient the column was at binding specific antibodies and to look at the efficiency of elution with diethylamine. The antigens HG4 and HG4/thyroglobulin were used to coat the wells of a Falcon Pro-bind plate for ELISA analysis. Samples of fifth bleed serum, recycled serum, wash collected after recycling and fractions collected from first and second peaks after elution were tested. The results are summarised in figure 37a and b. The majority of anti-HG4 peptide antibodies were found to bind to the column with a half-maximal response for peak 1 and peak 2 of 1:3200 (v/v) and 1:10400 (v/v) dilutions respectively compared to a negligible value recorded for the left over recycled serum.

Figure 37b illustrates that the majority of anti-thyroglobulin antibodies remain in the recycled- and wash-solutions. A relatively low amount of anti-thyroglobulin antibodies however, remains present in peak 1 and peak 2 samples having half-maximal responses of 1:800 (v/v) and 1:200 (v/v) respectively.

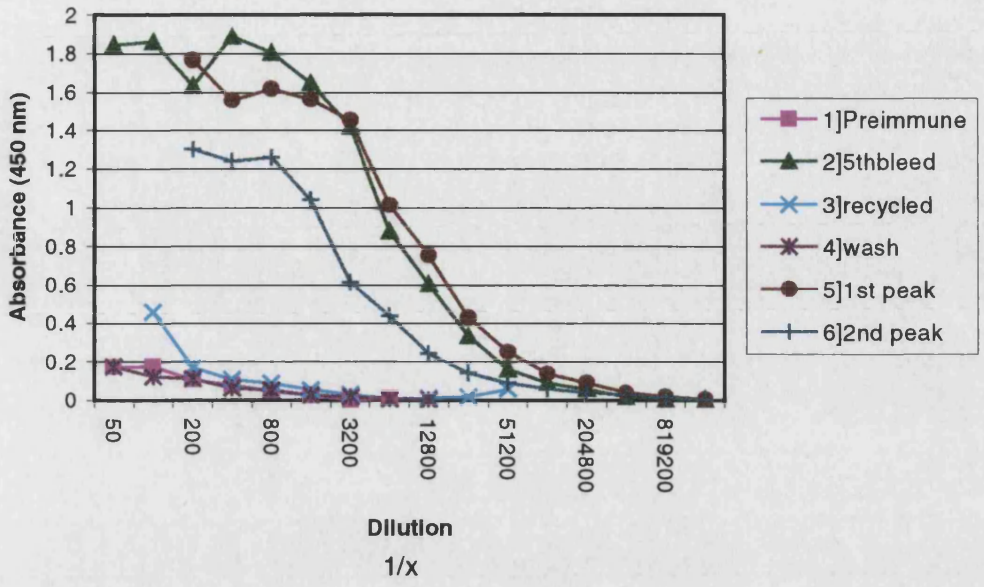

Figure 37a, ELISA of anti-HG4 antibody titres from different stages of purification. An ELISA was carried out using a plate coated with HG4 peptide to establish anti-HG4 antibody titres at the different stages of affinity purification. Blood samples taken from 1) the pre-immune bleed and 2) the 5th bleed were compared 3) 5th bleed sample that had been recycled though the column, 4) buffer used to wash column before elution, 5) eluted product from the first peak and 6) eluted product from the second peak. Serial dilutions of these samples were added to the plate and resulting absorbencies were measured It is clear from this graph that the majority of anti-HG4 antibodies has been purified and eluted in peaks 1 and 2, with negligible amounts in recycled and wash solutions.

4.2.5 Recognition of the HG4 Extracellular Domain

ELSIA assays showed that affinity purified anti-HG4 antibodies, corresponding to peak 1 and 2 in figure 36, recognise the HG4 peptide sequence. However, confirmation that both types have an affinity to a folded form of the HG4 protein needed to be obtained, as the chosen epitope may have been buried in the tertiary structure of the native protein. This was achieved by using a prokaryotic over expression system, requiring the use of a pMAL™-2 vector (refer to Appendix 1). HG4 was to be inserted into pMAL-2, downstream from the *malE* gene of *E. coli,* which encodes a maltose binding protein (MBP). Fusion of the two sequences would therefore give rise to a MBP fusion protein. Two variations of the vector exist; pMAL™-p2 possesses a signal sequence whilst the other, pMAL™-c2, does not. The former is required if the protein to be over expressed passes through the secretary pathway and the latter could be used if the protein is cytoplasmic in nature. The *malE* gene in each of the vectors is fused to a *lacZα* gene via a polylinker. An in-frame insertion of the HG4 gene into the polylinker site inactivates the β-galactosidase activity of the *malE-lacZα* fusion. Subsequently, colonies transformed with pMAL-

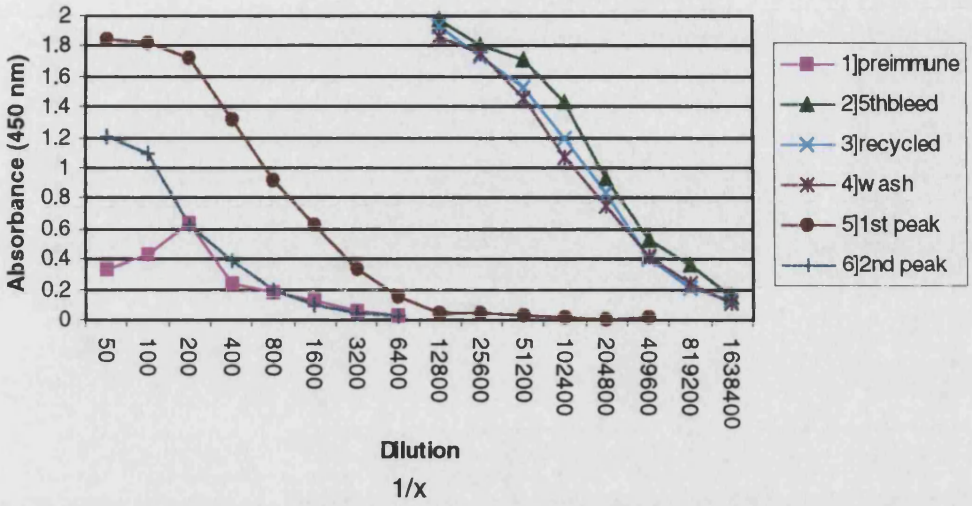

Figure 37b, ELISA of anti-thyroglobulin antibody titres during purification. An ELISA plate was coated with thyroglobulin to establish anti-HG4 antibody titres at the different stages of affinity purification. Blood samples tested from 1) the pre-immune bleed and 2) the 5th bleed were compared 3) 5th bleed sample that had been recycled though the column, 4) buffer used to wash column before elution, 5) eluted product from the first peak and 6) eluted product from the second peak. Serial dilutions of these samples were added to the plate and resulting absorbencies were measured. This graph illustrates that the majority of anti-thyroglobulin antibodies remain in the recycled and wash samples.

2/HG4 will be white in colour as opposed to blue pMAL™-2 transformed colonies. It was advantageous to use the pMAL-c2 vector, as the resulting expressed fusion protein constitutes 20-40 % of the total cellular protein compared with 5-10 % levels when expressing pMAL-p2. It was therefore decided to express the first 5' 693 bp (231 residues) of extracellular sequence cytoplasmically using pMAL-c2.

4.2.5.1 Cloning of the HG4 Extracellular Domain

A PCR was conducted to amplify the first 693 bp of HG4, coding the N-terminal extracellular domain, for cloning into the pMAL™-c2 vector. Primers were designed so that the 5' HG4 sequence would insert in the correct orientation, in frame with the *malE* gene. A stop codon was also introduced at the 3' end, preventing expression of the neighbouring *lacZα* gene. Sense primer pMALs and antisense primer pMALa were designed, the former incorporating a Sal1 restriction site and the latter a stop codon followed by a Pst1 restriction site, the exact sequences of which are detailed in Appendix 3. Template for PCR was prepared by digestion of a pBluescript/HG4 construct with Not1 and Xba1 restriction enzymes. Isolation of the released HG4 insert was achieved by running a 1 % (w/v) agarose gel from which it was cleaned using the Sephaglas™ Band Prep and then a QIAquick™ column. A PCR reaction using HG4 template,

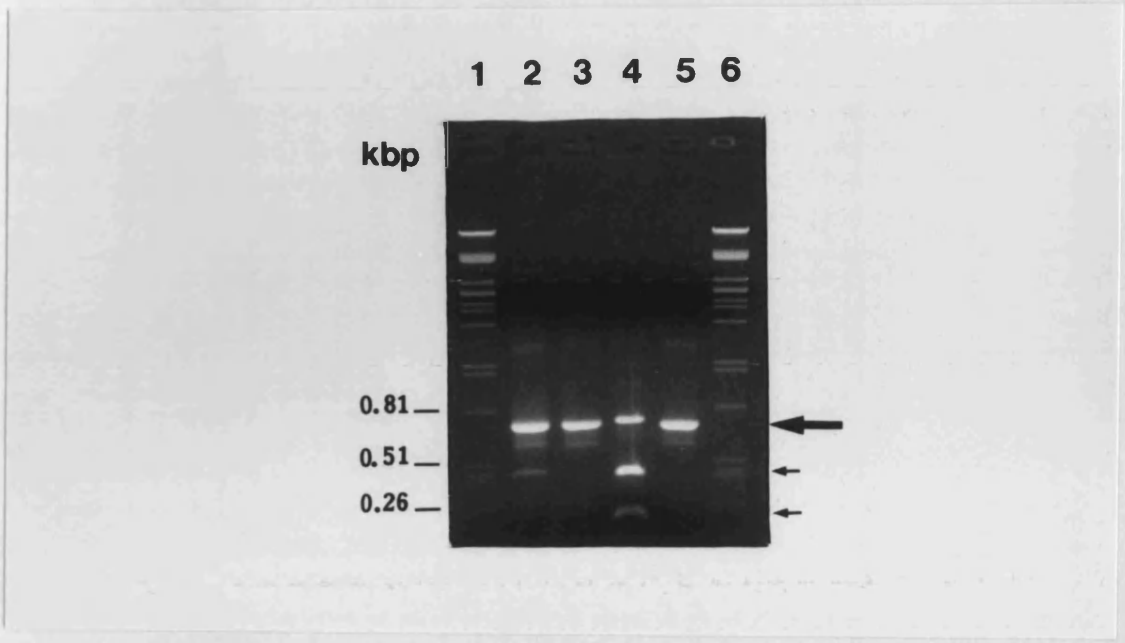

Figure 38, Amplification of HG4-ex using PCR.
Lanes 1 & 6: λ DNA cut with the restriction enzyme Pst1, respective band sizes listed along the side of the gel.
Lane 2: PCR using pMALs and pMALa primers in the presence of HG4 cDNA, which had previously been released by Not1/Xba1 digestion of a pBluescript/HG4 construct. This amplifies a specific HG4-ex band of 720 bp, which is indicated with a large arrow.
Lane 3: PCR product represented in lane 2 has been purified using Sephaglas and passed through a Qiagen QIAquick™ column.
Lane 4: The purified 720 bp fragment represented in lane 3 has been digested with EcoR1 to give bands of 434 bp and 259 bp, indicated by the small arrows.
Lane 5: The purified 720 bp HG4-ex fragment represented in lane 3 has been restricted with Sal1 and Pst1 for ligation into pMAL-c2.
Amplification of HG4-ex was achieved using the Expand™ High Fidelity kit with 1.5 mM $MgCl_2$. Each PCR required the use of 300 nM of pMALs and pMALa primers. Cycling conditions: 94 °C denaturation for 2 min, followed by the addition of 2.5 U enzyme, after which 45 cycles of 94 °C for 30 sec, 40 °C for 30 sec and 72 °C for 2 min were run terminating with 7 min at 72 °C. The reaction was separated by electrophoresis on a 1 % (w/v) agarose gel run in TBE.

pMALs and pMALa primers with High Affinity Expand™ amplified a 720 bp product (HG4-ex) and is seen in the 1 % (w/v) agarose gel in figure 38.

Confirmation that the amplified product was specific was accomplished by digestion using the restriction enzyme EcoR1. This gave 2 products of 434 bp and 259 bp in size, seen in lane 4 of figure 38. Sequencing also confirmed the specificity of the products. Both HG4-ex and the pMAL-c2 vector were restricted with Sal1 and Pst1 enzymes, also shown in figure 38, enabling ligation of HG4-ex into the plasmid. This was then transformed into *the E. coli* strain XL2 Blue and cultured on LB/ampicillin agar plates.

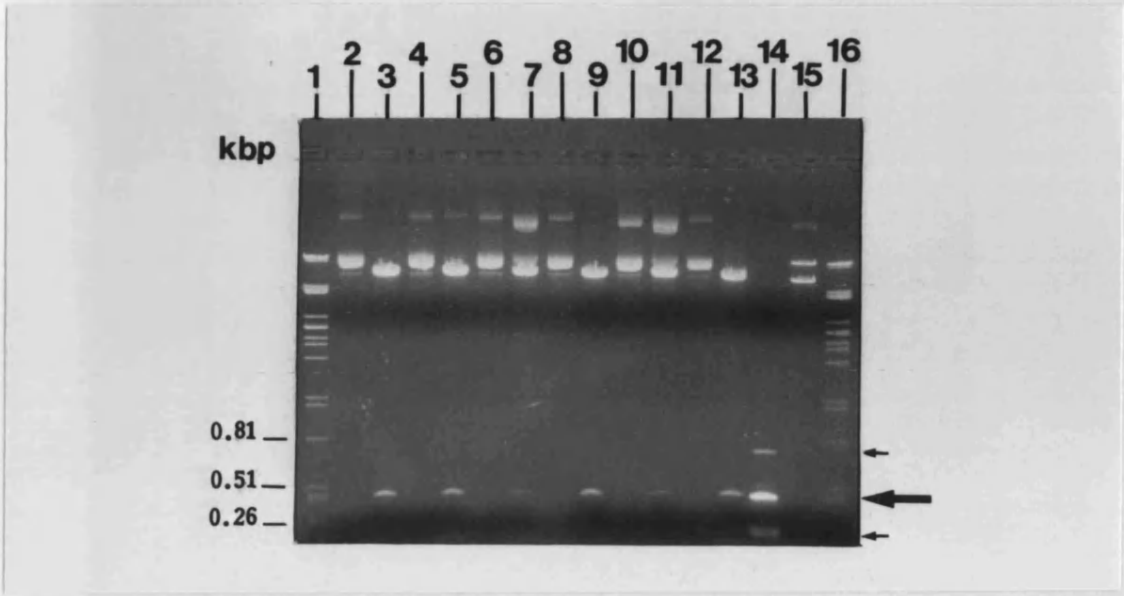

Figure 39, Restriction digests of HG4-ex plasmid constructs.
Lanes 1 & 16 contain λ cut with Pst1: band sizes are listed in kbp beside the gel.
Lanes 2, 4, 6, 8, 10 and 12 are uncut pMAL constructs carrying HG4-ex.
Lanes 3, 5, 7, 9, 11 and 13 are loaded with the respective EcoR1 digested constructs possessing a 259 bp HG4 specific product. The large arrow indicates these bands.
Lane 14: The 720 bp HG4-ex (little arrow) has been digested with EcoR1, the resulting bands of 434bp and 259 bp are also indicated.
Lane 15: Uncut pMAL-c2 vector.
Plasmids were previously purified from the *E. coli* strain XL2-Blue and then digested with the endonuclease EcoR1 for 1 hour at 37 °C, restricted products were separated by electrophoresis on a 1 % (w/v) agarose gel in TBE buffer.

Resultant colonies were replica plated with one of the plates supplemented with IPTG and X-Gal. The presence of IPTG suppresses the Lac repressor, encoded by the *lacI*^{q} gene carried by pMAL, inducing expression. Constructs possessing HG4-ex were distinguished by colonies being white in colour due to their inability of X-Gal breakdown. A selection of 6 colonies corresponding to white colonies grown on a LB/Amp plate, containing IPTG and X-Gal, were taken from the replica LB/Amp plate. Plasmids were purified using Wizard Plus™ Mini-Preps and digested using Sal1 & Pst1 restriction enzymes followed by electrophoresis through a 1 % (w/v) agarose gel (Figure 39). Each of the 6 colonies selected had successfully been transformed with constructs encoding HG4-ex.

4.2.5.2 Expression of Recombinant HG4 Fusion Protein

Clone 4, containing HG4-ex/pMAL-c2 (seen in lanes 7 and 8 of figure 39) and a clone carrying the pMAL-c2 vector were inoculated each into 5 ml of LB/ampicillin broth. These were grown to a density of 2 X10^8 cells/ml (A_{600} of 0.5) at which point 1 ml of both were retained and IPTG was added, inducing protein expression of the remaining culture. IPTG induced and un-induced samples from both pMAL-c2 +/- HG4-ex were run on a SDS-PAGE gel (Figure 40a and 41a). A

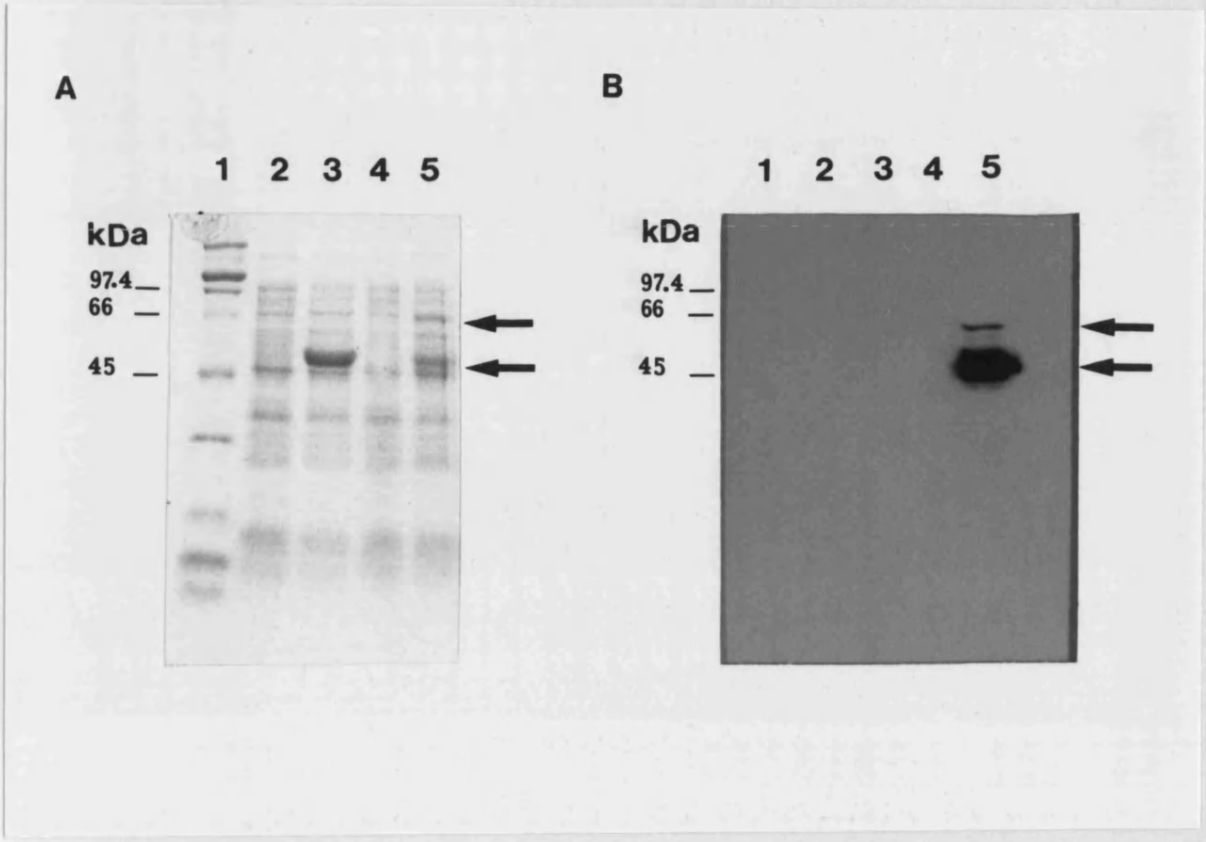

Figure 40, Recognition of HG4-ex by Peak 1 purified antiserum.
Lane 1: A) Bio-Rad Molecular weight marker, B) Bio-Rad pre-stained marker. Corresponding band sizes are detailed beside the gel.
Lane 2: un-induced XL2-Blue *E. coli* carrying the pMAL-c2 vector.
Lane 3: IPTG induced XL2-Blue *E. coli* carrying the pMAL-c2 vector. Gives over-expressed MBP of 51 kDa
Lane 4: un-induced XL2-Blue *E. coli* carrying the pMAL-c2/HG4-ex construct.
Lane 5: IPTG induced XL2-Blue *E. coli* carrying the pMAL-c2/HG4-ex construct. Top arrow indicates a 68 kDa HG4-ex protein, bottom arrow highlights degraded Hg4-ex.
A] 10% (v/v) SDS-PAGE loaded with respective sample previously resuspended in SDS-PAGE loading buffer and boiled for 5 min. The gel was run 100 volts for 20 min and then at 150 volts each at maximum current until the dye front had reached the bottom of the gel. . The gel was soaked overnight in Coomassie Stain and then destain was used to remove background staining. seen in lane 5.
B] Western Blot probed with 1:200 diluted, peak1 purified, anti-HG4 antibodies followed by exposure to a 1:10,000 dilution of horseradish peroxidase-conjugated goat anti-rabbit antibody. The ECL detection kit was then used to promote chemiluminescence, which was detected on X-ray film.

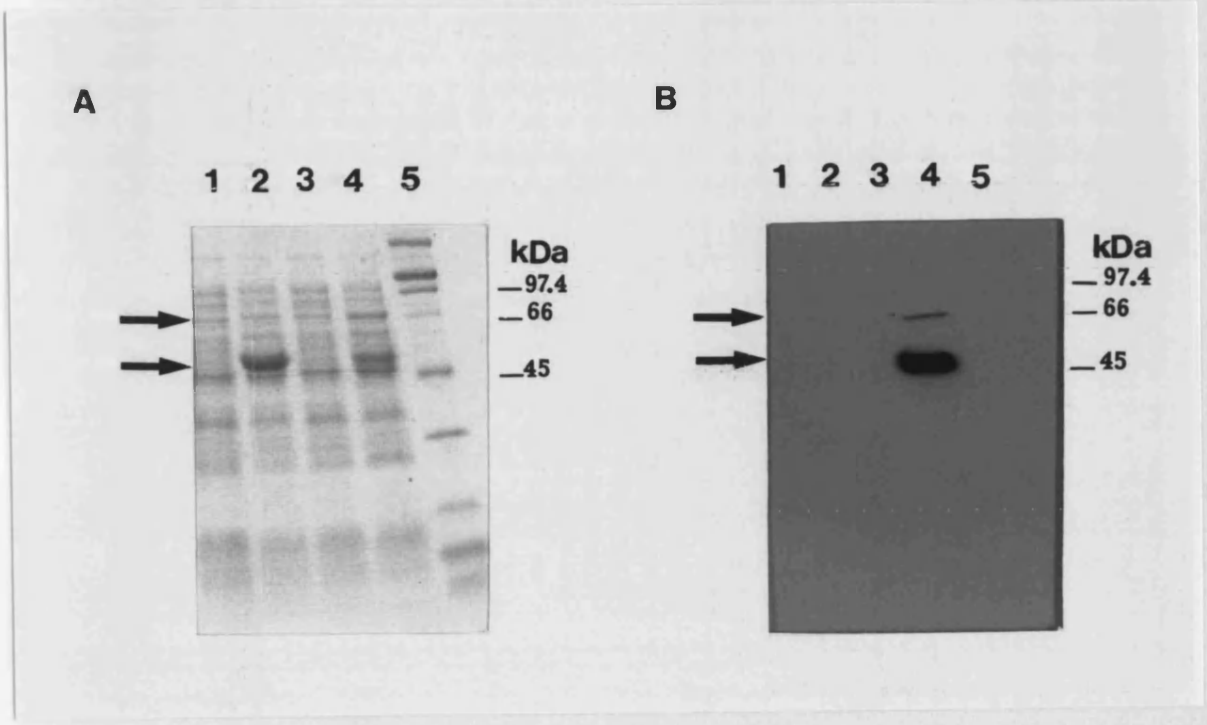

Figure 41, Recognition of HG4-ex by Peak 2 purified antiserum.
Lane 1: un-induced XL2-Blue *E. coli* carrying the pMAL-c2 vector.
Lane 2: IPTG induced XL2-Blue *E. coli* carrying the pMAL-c2 vector. Gives over-expressed MBP of 51 kDa
Lane 3: un-induced XL2-Blue *E. coli* carrying the pMAL-c2/HG4-ex construct.
Lane 4: IPTG induced XL2-Blue *E. coli* carrying the pMAL-c2/HG4-ex construct. Top arrow indicates a 68 kDa HG4-ex protein, bottom arrow highlights degraded Hg4-ex.
Lane 5: A) Bio-Rad Molecular weight marker, B) Bio-Rad pre-stained marker. Corresponding band sizes are detailed beside the gel.
A] SDS-PAGE, B] Western Blot probed with a 1:200 dilution of peak 2 purified anti-HG4 antibodies followed by secondary antiserum. See figure legend 40 for details concerning the loading and running of SDS-PAGE and Western Blot.

MBP/β-galactosidase fusion protein of 51 kDa from the pMAL-c2 culture can be a seen upon induction with IPTG. Moreover, an approximate 68 kDa fusion of MBP and HG4-ex is produced from the pMAL-c2 /HG4-ex culture after IPTG induction.

4.2.5.3 Probing with Purified Anti-HG4 Antibody

Western Blots were carried out to establish whether the affinity-purified antibodies would recognise a folded form of the extracellular domain of HG4. IPTG induced and un-induced constructs were run on a 10 % (v/v) SDS-PAGE gel and transferred to nitro-cellulose. These

blots were probed with anti-HG4 antibodies from either peak-1 (figure 40b) or –2 (figure 41b), previously obtained during elution from the affinity column. Western blots displayed in figures 40b & 41b show that the 68 kDa protein, corresponding to the MBP/HG4-ex fusion, is recognised along with smaller polypeptides by both anti-HG4 antibodies. It is possible that these smaller proteins may be degradation products derived from the fusion protein.

4.3 Discussion

Localisation of HG4 within the whole worm was to be studied following production of anti-HG4 antibodies raised against the peptide sequence RSTGGTQEQEILNELLSN. This amino acid sequence had been chosen due to its heterogeneity with related subunits within the inhibitory ligand-gated ion channel family. It was also necessary to select a peptide, which would be exposed on the surface of the folded native protein. The peptide also had to be flexible in nature and possess a high antigenic index. ELISAs were used to monitor antibody titre during a series of boosts (Figure 34); a higher titre was recorded for the fifth bleed compared to that measured for the sixth bleed. This meant that the former bleed was a more suitable sample to purify. Before proceeding to purify anti-HG4 antibodies on an affinity column, an ELISA was done confirming that any anti-thyroglobulin antibodies that may have been generated would not cross react with the HG4 epitope (figure 35). Anti-HG4 antibodies were then affinity purified on a column bound with HG4 peptide. Addition of diethylamine to the column eluted 2 peaks (figure 36) corresponding to 2 groups of antibody possessing different affinities to the HG4 peptide. The larger of the peaks had a lesser affinity for the HG4 peptide than the smaller peak. ELISA results displayed in figure 37a revealed that antibodies eluted in peak 1 and peak 2 give a half-maximal response at a 1:3200 and a 1:10400 dilution respectively.

Confirmation that affinity purified antibodies would recognise the peptide when present in the folded native protein was achieved by using the prokaryotic pMAL over-expression system. This enabled generation of the folded N-terminal extracellular domain of HG4 fused to a maltose binding protein when induced with IPTG. Western blots using antibodies eluted in either peak 1 or peak 2 revealed specific binding solely to folded HG4-ex and its degradation products (figure 40 b & 41b). Such specificity made antibodies eluted in each fraction ideal candidates for immunohistochemical studies on whole worm preparations.

5. Localisation of HG4 in *H. contortus.*

5.1 Introduction

The translated HG4 sequence is 80.25 %identical to the glutamate gated-chloride channel subunit, GluClβ (Cully *et al.*, 1994). Such a high amino acid identity suggests that HG4 is a parasitic orthologue of GluClβ. The latter subunit has been localised to pm4 and pm5 muscle cells situated in the pharynx of *C. elegans* by construction of a *lac-z* fusion protein (Laughton *et al.*, 1997a). It therefore seems reasonable to assume that HG4 is expressed in equivalent cell types in *Haemonchus contortus.* This hypothesis will be tested out using the purified anti-HG4 antibodies described in Chapter 4. If HG4 localisation is consistent with GluClβ findings, it is suspected that it assembles with a subunit equivalent to GluClα2A, which has also been localised to the pm4 and pm5 cells of *C. elegans* using green fluorescent protein (Dent *et al.*, 1997).

Affinity purified anti-HG4 antibodies will be utilised in the immunolabelling of HG4 in whole mount preparations of *Haemonchus contortus.* This chapter describes the preferred approaches taken to optimise the quality of immunohistochemical labelling. Particular reference is made to the preparation of whole worms, involving fixation followed by permeablisation and exposure to antisera. Examination of these slides will be achieved using a fluorescent and confocal microscope. Results obtained whilst optimising the technique are discussed along with HG4 specific localisation.

5.1.1 Whole Worms Preparations

Adult H. contortus is translucent permitting, its anatomy to be easily visualised under the microscope. Localisation studies utilising fluorescently conjugated antibodies can therefore be detected with ease in such an organism. Consequently, whole worms will be examined to establish which cells express HG4.

5.1.2 Fixation

Fixation is an essential requirement necessary for retaining the morphology of the tissue, thus preventing gradual degradation of the antigen. Optimum levels of fixation permit the ability of antibody both to penetrate the helminth and to bind to the fixed antigen. Over-fixation denatures antigenic sites and blocks their accessibility by excessive cross-linking, resulting in a loss of antigen/antibody binding. Prolonged fixation also tends to obscure weak signals produced by the antibody. Careful consideration needs to be made on the type of fix used and the time given to fix the tissue.

Aldehydes such as gluteraldehyde and paraformaldehyde are generally used in fixation protocols and can be used together or individually. Aldehydes fix tissue by way of cross-linking antigens, gluteraldehyde being the harshest in nature causing a higher degree of antigen damage with over fixing. Recent studies of whole mount preparations of *H. contortus* have pointed to gluteraldehyde causing a higher degree of auto-fluorescence compared to

that seen when fixing with paraformaldehyde alone (T. Skinner, personnel communication). It was therefore decided to fix solely in 4% w/v paraformaldehyde made up in PBS.

5.1.3 Permeablisation

The cuticle of a nematode is a physiologically active structure that acts as a protective barrier to environment assault such as attacks by the host's immune system and extremes of desiccation or salinity. Its rigid structure is due to the hydrostatic pressure produced by the body fluids within the pseudocoelom and exhibits selective permeability. The chemical composition of nematode cuticle consists largely of collagen rich lipids cross-linked by disulphide bonds that were originally secreted by the hypodermis. Other cuticular components include insoluble structural proteins called cuticlins as well as a small set of highly antigenic hydrophilic proteins that are not cross-linked (Blaxter *et al.*, 1992).

In order for antibodies to make contact with their target, the cuticular barrier needs to be degraded to such an extent that allows penetration by the antiserum. Either mechanical manipulation or enzymatic methods can accomplish this. The former is achieved by following a freeze-crack approach whereby the coat is physically torn off of the worm through the force of quickly popping off a frozen coverslip from the slide on which the worm is mounted (Miller & Shakes, 1995). Nematodes in the following set of experiments however, will be subjected to the enzymatic method. An added control handle exists with this method in that the level of cuticular degradation is proportionally regulated with the collagenase incubation times. The cuticle becomes more susceptible to collagenase treatment after it has been subjected to β-mercaptoethanol. This chemical induces the reduction of disulphide bonds between cuticular proteins. Nematodes will therefore be incubated in β-mercaptoethanol overnight followed by collagenase treatment for periods of 10 h, 20 h, and 42 h.

5.1.4 Controls and blocking techniques

The presence of blocking agents can improve the degree of specific staining to the antigen expressing cells while minimising non-specific background fluorescence. For this reason the following experiments use BSA and TritonX-100, the latter being a mild non-ionic detergent which also conveniently reduces the tendency of worms sticking to each other in a tangled bulk.

A range of antibody concentrations will be tested to optimise the quality of the specific signal. Addition of excessive antibody concentrations will increase non-specific background staining whereas exposure to too diluted amount of antibody will fail to produce a signal. As the primary antiserum to be used for immunohistochemical studies is polyclonal in nature the choice of controls is critical. Controls include worms treated with no antibodies, secondary antibody alone, pre-immune serum, and post-absorbed (with HG4 peptide) anti-HG4 antiserum.

The post-absorbed control is used to establish the presence of any contaminating non-specific antibodies. These may have been raised in response to either a contamination of the innoculant or infection of the host rabbit with nematodes during the immunisation period. In the likelihood of these events occurring the post-absorbed control will be able to distinguish non-specific staining induced by this nature of immune response. Similarly, preimmune serum will be used to identify the presence of antibodies that have been produced in response to previous nematode infections experienced by the rabbit. This control is less significant compared to the post-absorbed control, as binding seen with this sample will not represent antibodies present in anti-HG4 antiserum, as the majority will have been removed during the affinity purification procedure.

5.1.5 Direct and Indirect Immunochemistry

Two types of immunochemistry are available; one involves the direct use of a primary antibody conjugated with a marker such as an enzyme or fluorochrome on a tissue sample. This approach is quick but insensitive, as the signal produced by the antibody is not amplified. In contrast the indirect approach no longer requires that primary antibody be labelled with marker. Rather, an additional set of secondary anti-rabbit antibodies is conjugated with marker, which recognise primary antibody. These commercially bought antibodies amplify the signal, as multiple copies are able to bind to a single primary antibody.

5.1.6 Secondary Antibody

The indirect technique will be adopted; requiring the use of affinity purified antisera raised against rabbit IgG for detection of the primary antiserum. Fluorescently conjugated secondary antibodies will be used rather antibodies tagged with enzyme. The former gives optimum results under a confocal microscope, enabling the generation of a three dimensional interpretation. The use of enzymes such as Horseradish peroxidase or alkaline phosphatase requires the presence of a chromogenic substrate to produce a coloured reaction product. The disadvantage with this choice of markers is that it produces a high level of background staining and enables the diffusion of coloured reaction products. The fluorescent TRITC label has been chosen for use in the following set of experiments as recent localisation studies in whole preparations of *H. contortus* give greater levels in background fluorescence when using FITC (T. Skinner, personnel communication).

Images studied using fluorescent microscopy can be limiting as a result of stray light from fluorescent objects situated out of the plane of focus. A more precise representation is obtained using a confocal scanning microscope using a laser to scan a single optical section in the z-axis plane. Sharp images are produced with greater resolution and significantly reduced levels of focus fluorescence.

5.2 Results

5.2.1 Immunocytochemistry following 42 hours of collagenase treatment

The cuticles of paraformaldehyde fixed *H. contortus,* were treated with collagenase following reduction of disulphide bonds by β-mercaptoethanol. It was initially decided to monitor collagenase digestion under a light microscope. The collagenase was removed from the worms after 42 hours, when a form of surface blebbing was visualised. At this point, it was assumed that the cuticle was successfully stripping away from the hypodermis-enveloped body. Further exposure to Triton X-100 during washing steps, leading up to the final viewing of antibody bound tissue, contributed to further degradation of the nematode's surface.

Worms were exposed to 1:10 (v/v), 1:50 (v/v), 1:100 (v/v), and 1:200 (v/v) dilutions of primary antibody dilutions. Following this a 1:200 (v/v) dilution of secondary anti-rabbit antiserum was added to each sample. Background fluorescence levels did not appear to be a problem, which could be attributed to the sole use of paraformaldehyde as a fixative. Upon viewing nematodes treated with each of the listed antisera dilutions, fluorescence was localised to an organ specific to the female reproductive system in each case. Figure 42a represents a sketch of the female reproductive system and its position within the worm. The pars ejectrix (Veglia, 1915), more recently referred to as the ovijector (Lichtenfels *et al.*, 1994) is also depicted. This organ consists of a vestibule sac sandwiched between two cylindrical sphincters. It is heavily muscularised to aid in its action of expelling fertilised eggs that are stored in the connecting uteri. A phase contrast image of this structure in *Haemonchus contortus* is presented in figure 42b.

Figure 43 depicts a fluorescence image of a female treated with a 1:200 (v/v) dilution of primary antiserum followed by a 1:200 dilution of secondary antibody. Localisation of fluorescence appears to be restricted mainly to each of the ovijector's sphincters. Apart from the ovijector lighting up in all examined females, no other fluorescent labelling existed in either males or females.

A negative control was performed, studying whole worms that had not been exposed to either primary or secondary antiserum. An identical fluorescence was produced to that seen in figure 43, a higher magnification of one of the sphincters is displayed in figures 44. The intricate network observed on the surface of the ovijector is therefore not a true presentation of HG4 expression but rather an artefact of auto-fluorescence. In figures 43 and 44 the fluorescence pattern is confined to the ovijector and could represent a fine network of folds from where the lining naturally undulates. This unique pattern may be highly refractive when placed under direct light thus resulting in the observed auto-fluorescence.

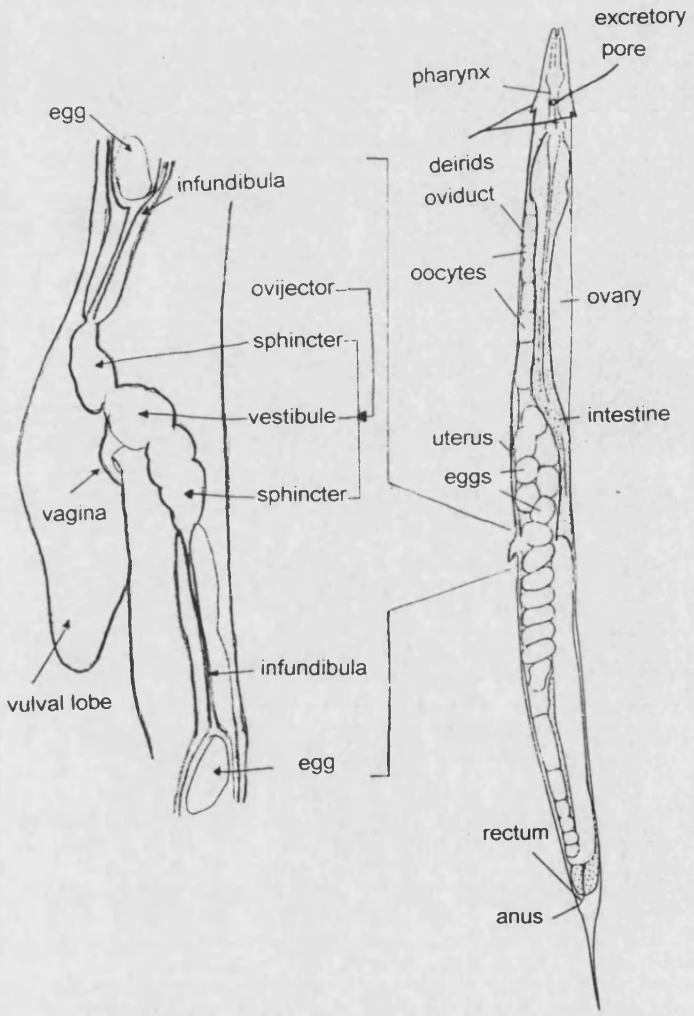

Figure 42a, The female reproductive system of *H. contortus*. Positions of the different organs are marked including the ovijector, a muscular organ used to eject eggs, stored in the uteri, out of the female via the vagina.

In summary, the 'no-antibody' control proved that fluorescence specific to the ovijector is not due to the presence of HG4 in this region. However, absence of fluorescence in the rest of the worm suggested that the protocol had not been fully optimised. As HG4's predicted role is neurone related, the 42 hours of cuticular digestion may have been too harsh, thus stripping away its presence. In accordance, the blebbing originally thought to be the stripping of cuticle, could have been the removal of vesicles from the somatic musculature. If this were the case then the nematodes nervous system, which is sandwiched between the hypodermis and the basolateral membrane would have been removed. It was therefore decided that worms were to be digested with collagenase for a shorter length of time. It should be noted that future studies of worms consistently revealed the existence of an auto-fluorescing ovijector but will not be mentioned any further.

Figure 42b, A phase contrast image of the ovijector. Adult female worm previously fixed in 4% w/v paraformaldehyde was mounted on a slide for viewing under phase contrast. Scale bar approximately 100 μm.

Figure 43, Fluorescence seen in the female adult ovijector of *H. contortus*. Whole mount of a female adult nematode: view of the ovijector. A 1:10 (v/v) dilution of anti-HG4 antibody from peak 1 purified antiserum was used followed by a 1:200 (v/v) dilution of secondary antibody. Scale bar approximately 50 μm

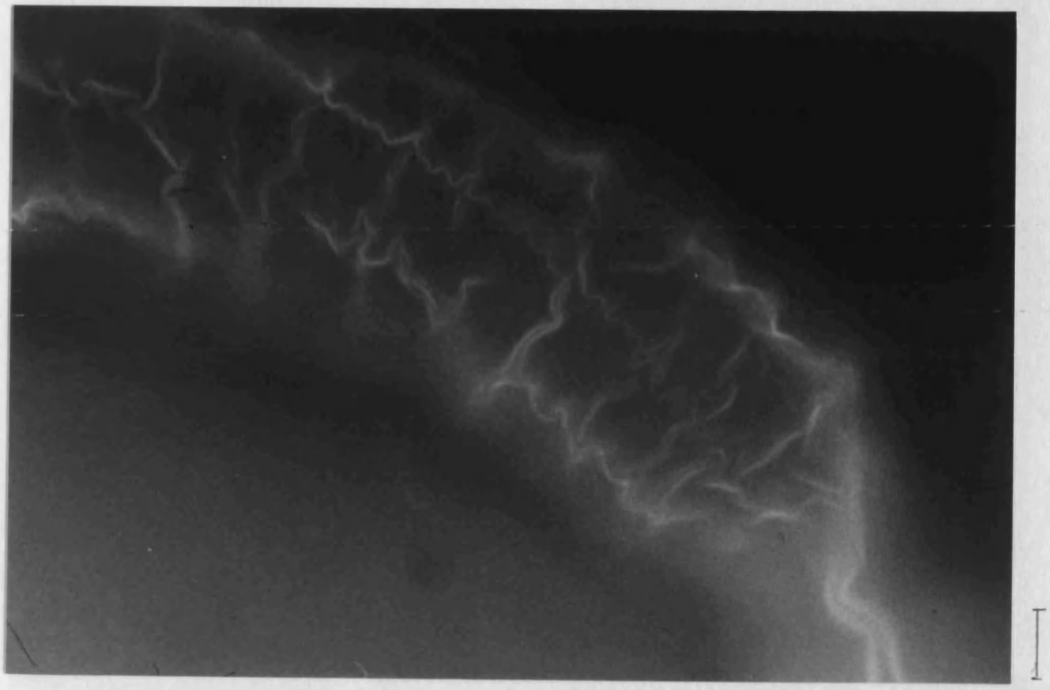

Figure 44, Auto-fluorescence observed on an ovijector sphincter. Adult female nematode, one of the ovijector sphincters has been magnified. Displays the auto-fluorescence obtained when no antibody is added. Scale bar approximately 25 μm.

5.2.2 Immunolabelling after 10 hours of collagenase digestion

Worms were treated with collagenase for 10 hours in an attempt to allow antibody penetration and at the same time preserve the underlying neuronal architecture. Primary anti-HG4 antiserum was added to collagenase treated worms at 1:10 (v/v), 1:50 (v/v), 1:100 (v/v) and 1:200 (v/v) dilutions followed by a 1:200 (v/v) dilution of secondary TRITC conjugated antibody. Examination of each of these preparations under the fluorescence microscope revealed staining solely in worms exposed to a 1:10 (v/v/) dilution of primary antiserum. A structure in the anterior portion of the worm repeatedly labelled with TRITC. Upon close inspection, labelling was present at the same level as the pair of mechanosensory flaps termed the deirids situated posterior to the excretory pore. Figure 45a sketches the position of the deirids in relation to the pharynx and the excretory system in the head of the worm. Figure 45b represents a phase contrast image of head with the deirid flaps clearly indicated. Figure 45c reveals the fluorescence obtained surrounding this region. As fluorescence microscopy yields information on a single plane, a lot of the anatomical structure is hidden out of view. To obtain more of an appreciation for the total structure that has been

recognised by the antibody, confocal microscopy was used.

Figure 46 displays a three-dimensional confocal image of this structure labelled with the antiserum. Staining appears as a semi-circular fibrous sheet that commences at one of the laterally located deirids and extends around the ventral quadrants to the oppositely positioned deirid (McLaren, 1976). It has been described as a biconcave cluster of highly refractive bodies consisting of a ventro-lateral commissure of tightly packed nerve axons. These extend around the ventral sides of the nematode and terminate at the lateral fields. In accordance with the image seen in figure 46, previous studies have reported that deirids, if present, are located more or less opposite the ends of the structure. In 1968, Rogers reported a structure called the hemizonid in *H. contortus* infective larvae, posterior to the excretory pore, in a similar position to that seen in figure 46. More recently the hemizonid has been given the name amphid commissure (Bird & Bird, 1991).

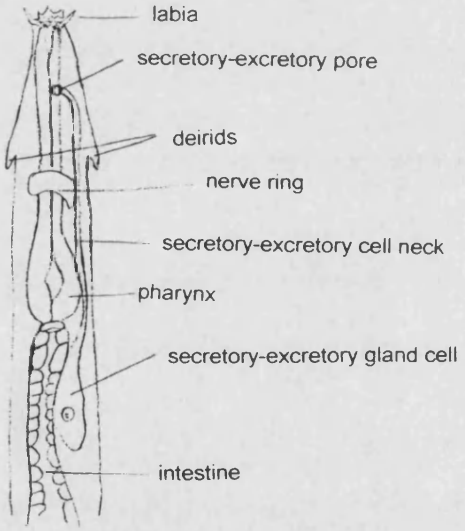

Figure 45a, The head of *Haemonchus contortus*. Particular reference has been made to the pharynx and its position relative to the excretory system and the mechanosensory organs, the deirids.

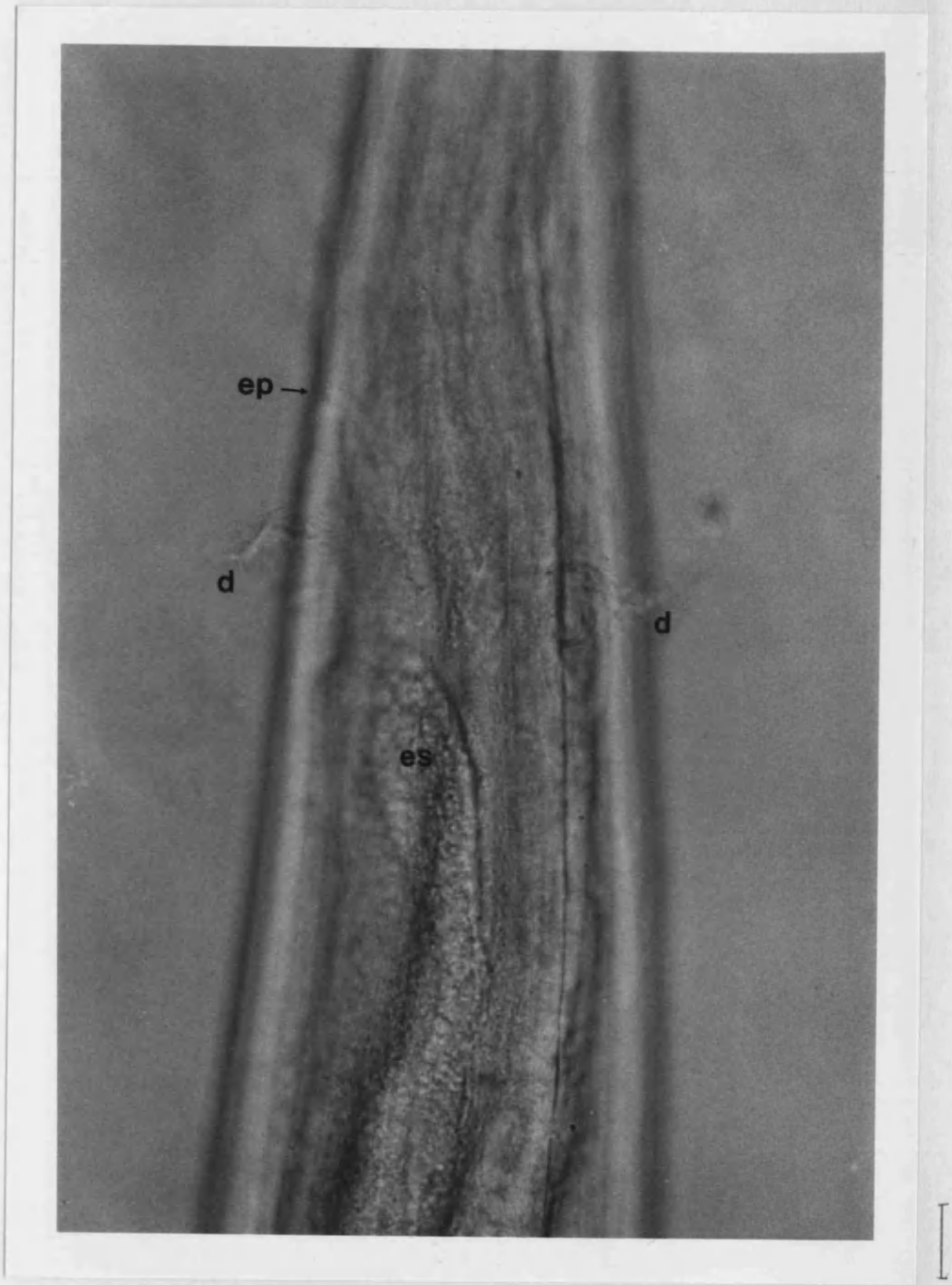

Figure 45b, A Phase contrast image of the *H. contortus* head. A view of the head of a whole mounted adult male, previously digested with collagenase for 10 h. es: excretory sac, ep: excretory pore and d: deirids. Scale bar approximately 50 μm.

Figure 45c, Immunolabelling seen after 10 h of collagenase digestion. A fluorescent image of the adult male depicted in the phase contrast in figure 45b. Following 10 h of collagenase digestion, the nematode has been exposed to a 1:10 (v/v) dilution of anti-HG4 antibody (eluted in peak one) followed by a 1:200 (v/v) dilution of TRITC conjugated secondary antiserum. A fluorescent ring found in line with the deirids can be seen. Scale bar approximately 50 μm.

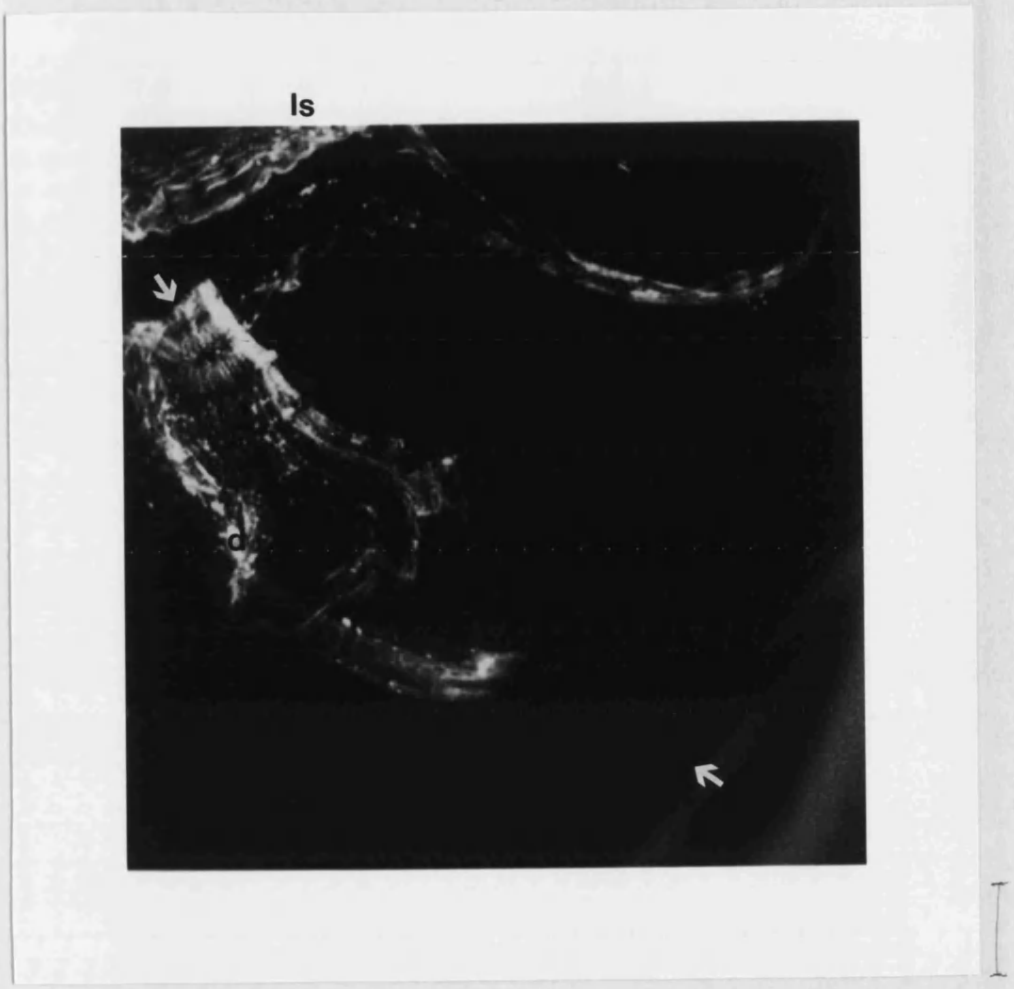

Figure 46, A confocal image of the head of *H. contortus*. Nematodes, treated with collagenase for 10 h, were then exposed to a 1:10 (v/v) dilution of anti-HG4 antibody (eluted in peak one) followed by a 1:200 (v/v) dilution of TRITC conjugated secondary antiserum. These were then viewed under the confocal microscope. A refractive sheet can be seen wrapping around the nematode in the vicinity of the deirids. d: deirid, ls: loose strand, arrows define diameter of body. Scale bar approximately 50 µm

When collagenase treated worms that had not had been incubated with antisera were examined, no fluorescence was detected in the head region. This finding indicates that the structure had been recognised by the antibodies and was not an artefact of auto-fluorescence. Exposure to TRITC-conjugated anti-rabbit IgG alone gave similar non-fluorescing results. This suggested that the fluorescence observed in figure 46 was due to the specific binding of primary antiserum rather than the non-specific binding of anti-rabbit IgG.

Worms were then subjected to post-absorbed primary antiserum followed by secondary antiserum. Anti-HG4 antiserum was incubated at 37 °C with HG4 peptide for an hour and

then transferred to collagenase treated worms. During the hour incubation, anti-HG4 bound to the HG4 peptide epitopes. The remaining unbound antibodies therefore represented a population of antibodies that may bind non-specifically. A similar staining pattern to that viewed in figure 46 could be seen (result not shown).

A preimmune control was carried out whereby preimmune serum at a 1:10 (v/v) dilution was added to whole *H. contortus* followed by secondary anti-rabbit IgG. Figure 47 portrays a nematode with a fluorescing ring-like structure in an equivalent region to that observed in figure 46. A more intense fluorescence is observed using the preimmune serum. This is believed to be due to a combination of background fluorescence from stained tissue present in other planes of vision as well as viewing the structure from a different angle. Labelling is also seen just below the semi-ring structure, along longitudinal tracts called cuticular ridges that encompass the cylindrical body. Ridges tend to be very pronounced in members of the Trichstrongyloidae family in the order Strongylida. *Haemonchus contortus* has 30 of these ridges that arrange into a pattern known as the synlophe (Lichtenfels *et al.*, 1994). Ridges are raised areas that commence anterior of the excretory pore and span the length of the worm. Their function is to help maintain the nematodes position on the gut wall and are composed from both cortical and median layers of the cuticle in the presence of collagen fibrils (Bird & Bird, 1991). The presence of these ridges, therefore, may suggest that the cuticle has not been removed and thus the semicircular structure in this control may in fact be cuticular staining. During examination of infective larvae Rogers noticed that the outer cuticle, overlaying the hemizonid, was modified having annular striations that were positioned 0.3 μm apart rather than the normal 0.9 μm separation (1968). He also noticed that the modified cuticle was 1.3 μm from the posterior edge of the excretory pore and spanned slightly beyond the hemizonid structure. A change in cuticle texture may therefore have led to the non-specific binding of preimmune serum seen in figure 47.

Non-specific labelling as seen in the negative controls may have resulted from the rabbit previously being infected with nematodes. This would have stimulated the production of an array of anti-nematode antibodies, which would therefore cross react with epitopes presented by *H. contortus*. It is possible that the fraction of bound antibodies in the preimmune control, represented a population of antibodies that were co-eluted with the anti-HG4 antibodies during affinity purification. Labelling of the hemizonid in the post-absorbed control confirmed that co-elution had taken place and that the result was a non-HG4 related artefact.

Figure 47, Cuticular fluorescence of *H. contortus*. Preimmune serum at a 1:10 (v/v) dilution was added to 10 h collagenase treated worms followed by a 1:200 (v/v) dilution of TRITC conjugated IgG. d: deirid, cr: cuticular ridges. Scale bar approximately 100 μm.

5.2.3 Immunological staining seen after 20 hours of digestion

As cuticle had not been totally removed after 10 hours of collagenase treatment a further batch of nematodes were digested for a total of 20 hours followed by the standard immunolabelling protocol. A 1:10 (v/v) dilution of anti-HG4 antiserum was added to collagenase treated worms and viewed under the fluorescence microscope. Figure 48a reveals labelling of a neuronal network, stretching from the anterior to the mid-body region of the helminth. When viewed under higher magnifications, as seen in figures 48b and 48c, this network appears to be confined to commissures that project from both dorsal and ventral cords. In females, commissure labelling occurred from just below the mid-region of the pharynx and stopped anterior of the vulva. The latter organ was easily located due to its connection with the auto-fluorescent ovijector; equivalent fluorescence was detected in males. Upon close inspection of figure 48b and c an intermittent fine line between commissures is seen to fluoresce, this was believed to be nerve cord staining. A further magnification displayed in figure 48d illustrates a clear image of nerve cord. Figure 49a and b represent two confocal images in which commissures branch out from a nerve cord situated parallel to the pharynx.

A

Figure 48, See legend on next page.

B

C

Figure 48, See legend on next page.

D

Figure 48, A neuronal network recognised by anti-HG4 antibodies. Nematodes were treated with collagenase for 20 h. A 1:10 (/v/) dilution of anti-HG4 antibody (eluted in peak 1) was added followed by a 1:200 (v/v) dilution of secondary antibody conjugated with TRITC. Labelling highlights neurones that span the anterior portion of the nematode. nc: nerve cord c: commissures. A] scale bar approximately 200 μm. B] scale bar approximately 100 μm. C] scale bar approximately 100 μm. D] scale bar approximately 10 μm .Arrows in figures b and c identify where commissures fold over thus producing a double layer of fluorescence.

A

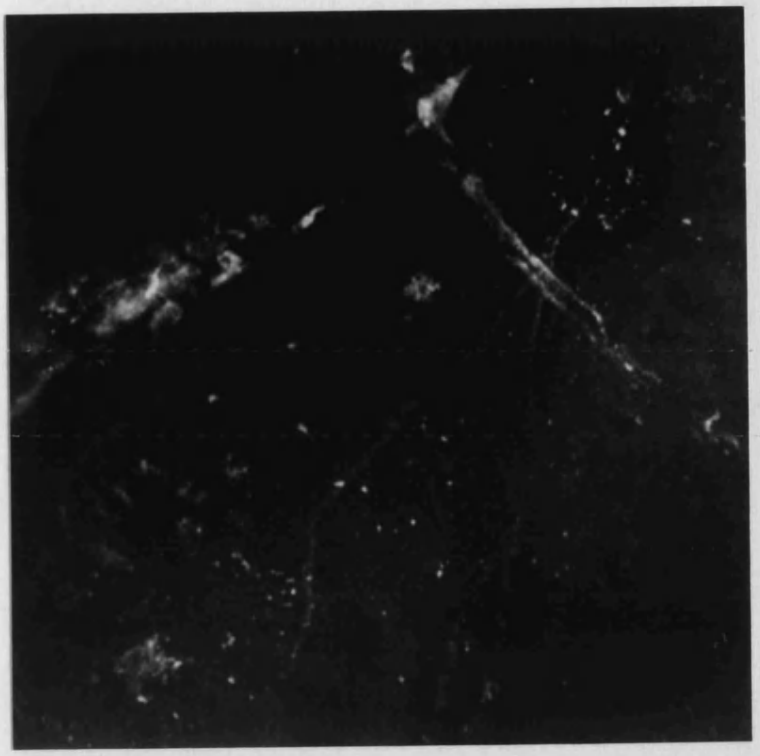

B

Figure 49, Confocal images of commissure and nerve cord staining. 20 h collagenase treated *H. contortus* were exposed to a 1:10 (v/v) dilution of purified anti-HG4 antibody followed by addition of a 1:200 (v/v) dilution of TRITC conjugated IgG. a] a view of a single commissure branching out from the nerve cord present near the pharynx, scale bar is approximately . b] Several commissures are depicted originating from nerve cord which also appears to be possess axons that express HG4 subunits, scale bar approximately represents 50 µm

The junction between commissures and nerve cord has been compared with those found in *Ascaris suum*. Dr Richard Martin kindly donated slides mounted with *A. suum*. Dr Carl Johnson had previously prepared these by injecting ligatured worms with crude bacterial collagenase. This was done to induce the dissociation of muscle cells from the hypodermis. Worms were then cut along the lateral line and pinned open, allowing the removal of muscles and internal organs and leaving the cuticle and the hypodermal layer intact. The latter of which, being embedded with the nervous system. The exposed nervous system was then labelled using antibodies to a neurofilament protein. Figures 50a, b and c represent various commissure projections from dorsal and ventral cords in *A. suum*. Comparison of these branching structures with fluorescence patterns obtained in *H. contortus* in figures 49a and b confirms that fluorescence is localised to commissures. In each case, the nerve fibre leaves the cord at right angles, looping over the cord to stem off in the opposite direction. It is this change in direction that causes the axon to retrace its path, producing a double layer of fluorescence which is seen in figures 48c and 48d marked out by the arrows.

A

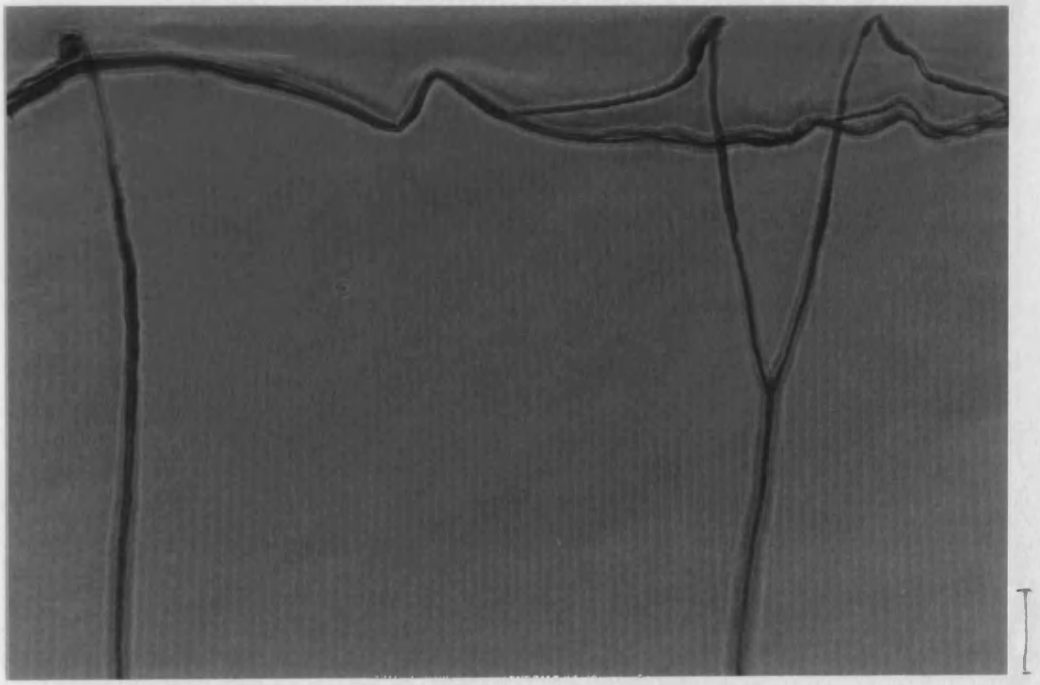

Figure 50, See legend on next page.

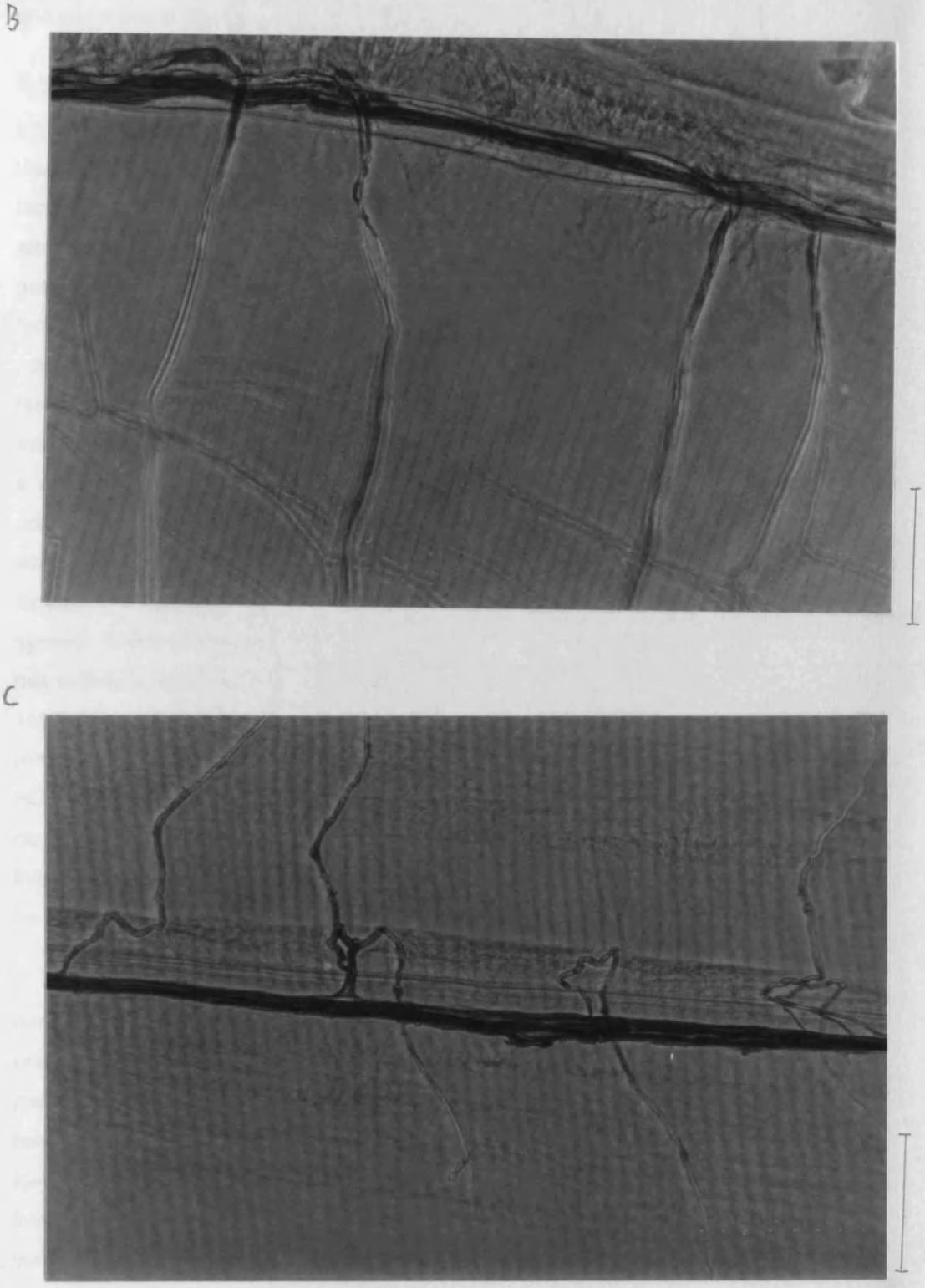

Figure 50, Nerve cord and commissure staining observed in the parasitic pig parasite *Ascaris suum*. a], b] and c] illustrate the different types junctions produced from axons branching out of the cords. The scale bars for each of these images represent 100 μm.

Worms that were not exposed to antibodies and ones that were incubated in only secondary antibody gave no labelling of neuronal anatomy. Both post-absorbed and pre-immune

controls gave no commissure or nerve cord staining. These findings indicate that nerve cord and commissure staining is specific to anti-HG4 antiserum recognising HG4 expression.

5.3 Discussion

Immunohistological labelling of whole *Haemonchus contortus* has proven successful in localising HG4 expression to specific neurones within its nervous system. Optimisation the techniques used has lead to evidence for three types of fluorescence, only one of which is attributable to HG4 expression. Firstly, it has been shown that the female nematode possesses an auto-fluorescing ovijector (Figure 43). This was observed consistently in all female specimens, including the controls where no antibodies had been added. Secondly, cuticular fluorescence was achieved after ten hours of collagenase treatment. This may be a result of non-specific trapping of primary antibodies in the tightly packed annular striations that occur directly above the hemizonid. Alternatively, it is possible, although less likely, that a sub-population of antibodies had been co-purified with anti-HG4 antibodies. This sub-population may therefore recognise the cuticular antigens overlaying the hemizonid on worms treated with collagenase (Figure 37). The final set of experiments using worms digested for 20 hours yielded evidence of HG4 expression occurring within the nervous system. This is an unexpected result since localisation of the *C. elegans* orthologue (GluClβ) has previously been confined to the pharyngeal pm4 and pm5 muscle cells (Laughton *et al.*, 1997a). No HG4 localisation to the pharynx was observed in any of the worms studied. This raises the question as to whether HG4 is the GluClβ orthologue or a novel beta-2 subunit. If HG4 is the parasitic orthologue of GluClβ, the apparent difference in subunit distribution in nematodes cast doubts to the suitability of *C. elegans* as a model system. Following from this, the establishment of avermectin action and mechanisms recorded for *C. elegans* can not be assumed to be identical to those in parasite equivalents.

C. elegans and *A. suum* neuronal architecture are very similar, both possessing ventral and dorsal nerve cords containing seven classes of motor neurones of analogous shape and orientation (Stretton & Johnson, 1991 & White *et al.,* 1986). It is therefore possible that a matching organisation occurs in *H. contortus.* As the entire nervous system of *C. elegans* has been mapped out (White *et al.*, 1986), an attempt at localising HG4 expression to identifiable neuronal types has been made. In the free living nematode a pair of interneurones called AVE neurones are unique in that they span an equivalent length of the ventral nerve cord that is specified by HG4 expression. AVE cell bodies are situated in the lateral ganglion. Their axons leave the ganglia and run around the nerve ring via the dorsal mid-line to the ventral cord, where they leave the ring. The paired axons run close to the centre of the ventral nerve cord and terminate prior to reaching the vulva. In adults, AVE interneurones receive many synapses from mechanosensory neurones as well as synapsing onto the interneurone AVA and the excitatory motor neurones VAn, DAn and ASn. Each of the latter excitatory neurones releases the neurotransmitter acetylcholine.

There are 12 members in the VAn group of motor neurones that innervate ventral muscles, out of these VA1, VA2 and VA3 each receive synaptic input from the AVE neurone. Nine DAn motor neurones exist in *C. elegans* of which DA1, DA2, DA3 and DA4 receive synaptic input from the AVE neurones. Eleven ASn motor neurones span the length of the nematode of which AS1 to 3 are innervated by AVE interneurones. Out of all the classes of motor neurones mentioned, only the VAn family remains along the ventral cord and innervates muscles in the ventral quadrants. DA1 to 4 and AS1 to 6 neurones each have a cell body in the ventral cord with axons that branch out at right angles. These form commissures, which lead to the dorsal cord. DA1, DA3 and DA4 are left-handed commissures whilst DA2 is right handed. AS1 to 3 are right-handed commissures. DAn and ASn processes run anteriorly in the dorsal cord and form many excitatory neuromuscular junctions with muscle in the dorsal quadrants.

AVE interneurones communicate with VAn, DAn and ASn motor neurones, which in turn produce neuromuscular junctions with somatic muscle as well as synapsing with inhibitory motor neurones VD1-7 and DD1-4. The latter two neuronal types release GABA at neuromuscular junctions.

It seems likely that each of the motor neurones mentioned i.e. VA1-3, DA1-4, AS1-6, VD1-7 and DD1 to 4 express HG4 subunits and these co-assemble with other related subunit proteins to form surface receptors. The network whereby the AVE interneurones send signals to VAn, DAn and ASn neurones, which in turn synapse with VDn and DDn neurones, may be achieved by glutamate transmission. These signals may be received via HG4 associated glutamate gated chloride channels. Transmission via glutamate at synapses along the discussed neurones may therefore achieve a modulatory action on the potential produced along the axons.

Some commissures spanning from the anterior to the mid-body region of *A. suum* have been found to possess protruding branches that join either ventral-sublateral or dorsal-sublateral cords (Johnson & Stretton, 1987). It is possible that this characteristic occurs in *H. contortus*. The above studies show HG4 expression occurring on commissures which cross sublateral cords. It therefore seems plausible that the synaptic input received by the HG4 associated receptors may provide a more refined potential. This in turn may modulate transmitter release or gap junction transmission at synapses with the sublateral cords. Motor neurones present in the sublateral cords enhance the movement in the anterior part of the worm occurring in the right-left plane.

These findings suggest that glutamate transmission via HG4 associated receptors contributes to the movement in the anterior of the nematode. If this is correct, then the action of avermectin on these parasites would be to inhibit locomotion rather than to cause paralysis of the pharynx where avermectin sensitive receptors exist in *C. elegans* (Arena *et al.*, 1994).

6 PCR Amplification of HG5 cDNA

6.1 Introduction

A full-length consensus sequence coding HG4 has successfully been isolated using the polymerase chain reaction (PCR) as detailed in chapter 3. This chapter describes attempts made to isolate a second full-length glutamate-gated chloride channel (GluClR) subunit using an identical approach. This was done to further characterise the GluClR family; establishing its role as a target for avermectin and whether avermectin-resistance has resulted from an alteration in its genetic make-up.

6.1.1 The Partial HG5 sequence

Laughton (1993) was able to amplify a total of 5 PCR products denoted HG1 to HG5, each consisting of 450 bp. He achieved this by designing the degenerate primers, DA and DS to highly conserved regions of vertebrate and invertebrate $GABA_A$ and glycine receptor subunits. The HG5 partial nucleotide sequence was compared to existing sequences in the EMBL database and was found to be 74 % and 71 % identical at the amino acid level to GBR2A and GluCl-α1 receptor subunits respectively (accession numbers U40573 and U14524). Both of these subunits are members of the GluClR family isolated from the nematode *C. elegans.*

6.1.2 Obtaining a Full Length HG5 cDNA Sequence

Rapid Amplification of cDNA Ends (RACE) using PCR will be used to amplify the 5' end and the 3' end of HG5. This method requires the use of the splice leader sequence, SL1, and the RoRi sequence. The former is located at the 5' terminus, upstream from the 5' untranslated region. In contrast, the latter, having been incorporated during cDNA synthesis, is found downstream from the Poly $(T)_n$ tail. A gene specific antisense primer designed to the partial sequence was used in conjunction with SL1 to amplify the 5' end and a sense primer was made for use with RoRi for isolation of the 3' end.

6.1.3 HG5 5' Terminus Comparisons

The HG5 receptor subunit is believed to be a component of the glutamate-gated chloride channel as it has a 71 % amino acid identity with the GluCl-α receptor subunit. Expression of homomeric GluCl-α channels in *Xenopus* oocytes were selectively responsive to the anthelmintic drug ivermectin at μM concentrations, binding irreversibly to the N-terminal extracellular domain of the receptor (Cully *et al.* 1994). Avermectin resistance may have developed as a result of a genetic mutation at the site of ligand binding, preventing coupling which in turn impedes the entrance of chloride ions into the cell. As HG5 was predicted to be alpha-like in nature, amplification of the N-terminal avermectin-binding domain of HG5 from an avermectin resistant isolate was attempted by RACE-PCR. This will establish whether the cDNA sequence differs from that isolated from the susceptible isolate. If any discrepancies are detected then expression in *Xenopus* oocytes will determine whether they induce avermectin resistance.

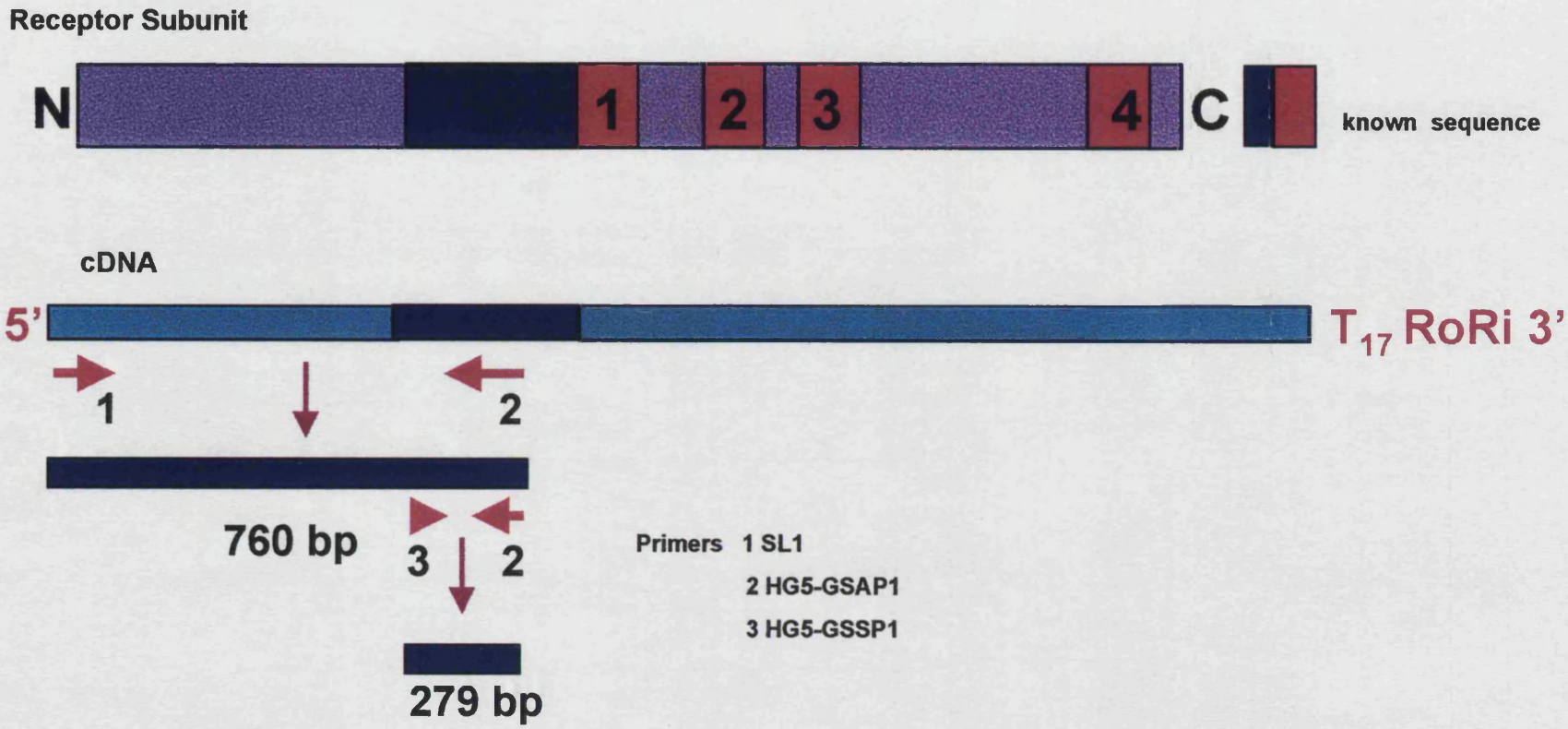

Figure 51, Strategy for Isolating the 5' end of HG5 using RACE-PCR.

6.2 Results

6.2.1 Template

Haemonchus contortus eggs were used as a source from which total RNA was isolated. From this pool of RNA, mRNA was extracted using Dynabeads, aliqouts from both total RNA and mRNA samples are displayed in figure 11 in Chapter 3. The rest of the mRNA was reverse transcribed into cDNA for use as template in RACE-PCR.

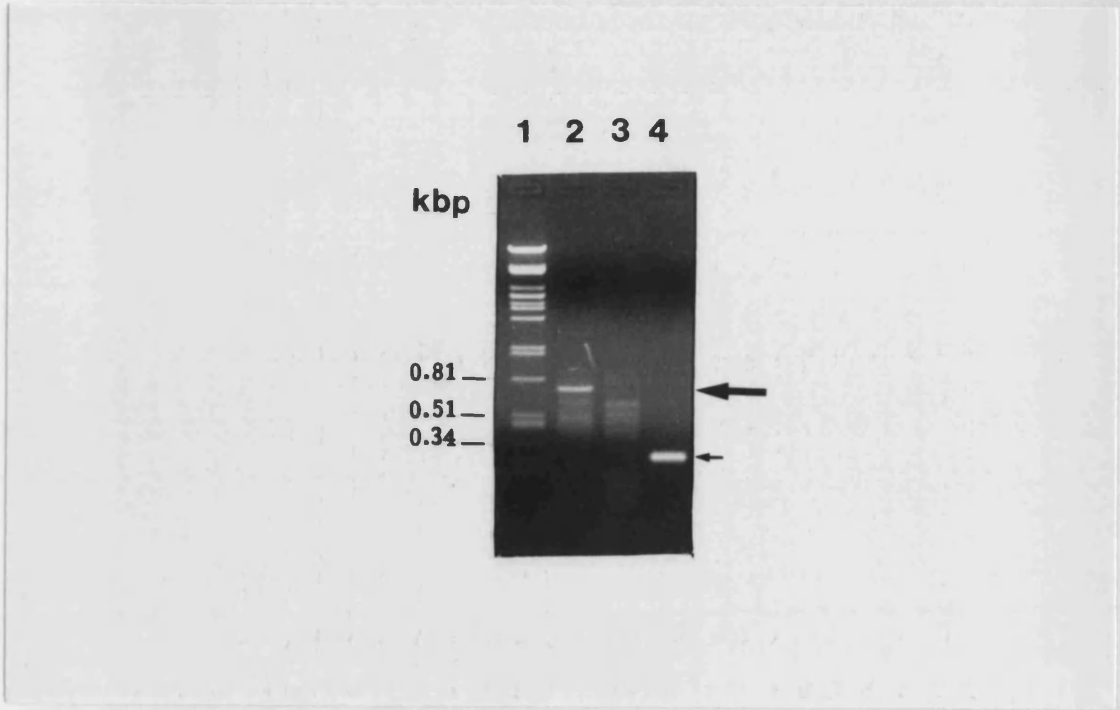

Figure 52, Amplification of a 5' end of HG5 product by RACE-PCR.
Lane1: λ DNA cut with the restriction enzyme Pst1, relevant band sizes are detailed along the side of the gel.
Lane 2: PCR using primers HG5-GSAP1 and SL1 amplifying a 760 bp fragment (➔),using an annealing temperature of 55 °C.
Lane 3: PCR using primers HG5-GSAP1 and SL1 with an annealing temperature of 50 °C.
Lane 4: Semi-nested PCR of 279 bp (→) using primers HG5-GSAP1 and HG5-GSSP1with purified 760 bp PCR product seen in lane 2 as DNA template.
Each PCR sample had been amplified using the Expand™ High Fidelity system, in the presence of 1.5 mM $MgCl_2$ and 300nM of each primer with cDNA reverse transcribed from *H.contortus* egg mRNA.
PCR Cycling conditions: 94 °C denaturation for 2 min, after which time 2.5 U of enzyme was added. 45 cycles of 94 °C for 30 sec, 55 °C for 30 sec and 72 °C for 2 min followed and was terminated by a further 7 min at 72 °C.
10 μl of each PCR sample was separated on 1 % (w/v) agarose gel using electrophoresis.

6.2.2 Isolation of the 5' end of HG5

RACE-PCR was used to amplify the 5' terminus of HG5, the strategy of which is illustrated in figure 51. A complementary antisense primer, HG5-GSAP1 (detailed in Appendix 3), was designed to the HG5 partial sequence and used along with SL1 in RACE-PCR with the goal of amplifying up an approximate 760 bp product. The arrow in figure 52 indicates a

promising PCR product in lane 2 of the agarose gel. The 760 bp band was excised from the gel for Sephaglas™ purification and then used as template in a semi-nested PCR. A perfect match sense primer, HG5-GSSP1, was designed to anneal to an internal region of the sequence and was used in conjunction with HG5-GSAP1. Amplification of a 279 bp fragment can be seen in lane 4 of figure 52. RACE-PCR was repeated two further times to amplify two other individual copies of the 760 bp HG5 5' end product.

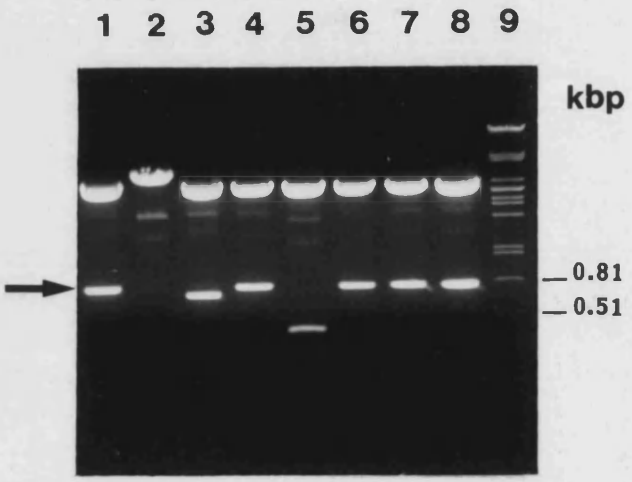

Figure 53, Digests of HG5 5' RACE products ligated into pBluescript II SK (+).
Lanes 1, 3, 4, 6, 7 & 8 are loaded with constructs possessing the 760 bp HG5 5' PCR product (➔).
Lane 9: λ DNA cut with the restriction enzyme Pst1, relevant band sizes are detailed along the side of the gel.
Remaining lanes represent plasmids that do not contain theHG5 5' PCR fragment.
Transformed colonies were cultured for plasmid purification using the Wizard™ Plus kit. Purified DNA was then digested with the endonucleases Xba1 and Xho1for an hour at 37 °C, restricted products were then separated by electrophoresis on a 1 % (w/v) agarose gel ran in TBE buffer.

6.2.3 Cloning of the 5' end

The three 760 bp PCR products were treated with DNA polymerase 1 and polynucleotide kinase to produce blunt-ended products. These were ligated into EcoRV-cut pBluescript SK^+ vectors. Constructs were then transformed into the XL1-Blue strain of *E. coli* and grown on LB agar supplemented with ampicillin, IPTG and the chromogenic substrate X-Gal. This enabled the differentiation between white colonies, transformed with recombinant plasmid, and blue colonies, transformed with wild-type plasmid. A selection of white colonies produced from ligations of each of the three PCR amplified 5' ends were cultured overnight and plasmids were purified using the Wizard™ Plus kit. Screening of the plasmids was achieved by digestion with Xba1 and Xho1, followed by examination on an agarose gel.

Figure 53 illustrates the digestion of purified plasmid constructs from 8 white colonies. Lanes 1, 3, 4, 6, 7 & 8 were loaded with recombinant plasmids, each encoding a 760 bp HG5-5' RACE product, these inserts are indicated by the arrow. Constructs represented in lanes 1 & 2 were ligated with one 5' amplification, lanes 3, 4 & 5 with another amplification and lanes 6, 7 & 8 another. Each of the three individually amplified 5'-RACE products, were thus successfully cloned ready for sequencing. Lane 3 is loaded with a construct carrying a slightly smaller 5'-PCR product than the others. The difference in size is believed to be a consequence of the 'blunt ending procedure', whereby flanking sequence is exposed to the exonuclease activity of DNA Polymerase 1.

The constructs represented in lanes 1, 4 and 8 were re-cultured for sequencing on the ABI Prism™ 377DNA Sequencer using the primers T3 and KS (appendix 3). Figure 54a displays an alignment of the nucleotide sequences amplified from three individual cDNAs, with differences shaded in grey. The amino acid variation between the sequences is also displayed in figure 54b. The percentage variation between these clones has been summarised in table 12. A translated consensus sequence was derived from the comparison of all three sequences and can be seen in figure 54b. This was transferred to the GCG package accessed via the gnome workstation. Using the 'pileup' command an alignment with related sequences was achieved and the percentage identity was calculated. The 5' end of HG5 was 67 % identical at the amino acid level with the partial sequence isolated from *Dilofilaria immitis* followed by 62 % identical to GBR-2A & -2B from *C. elegans,* both of which are predicted to be GluCl receptors (accession numbers U59744 and U40573 respectively).

A

```
                    1                                                   25
          HG55'(3)  gtcagtatctatgtgatcgacacta ATGTTCGCCT TAATTCTGCC ATTTC
          HG55'(8)  attagtatctatgtgatcgacacta ATGTTCGCCT TGATTCTGCC ATTTC
          HG55'(12) attagtatctatgtgatcgacacta ATGTTCGCCT TGATTCTGCC ATTTC
          Consensus rtyagtatctatgtgatcgacacta ATGTTCGCCT TRATTCTGCC ATTTC

          26                                                          85
HG55'(3)  TGTTGCATTT CACACGGTCC GAAGGTTTTG GTTACGAGAA GCTATTGGAT GAGCAGAAAA
HG55'(8)  TGTTGCATTT CACGCGGTCC GAAGGTTTTG GTTACGAGAA GCTATTGGAT GAGCAGAAAA
HG55'(12) TGTTGCATTT CACGCGGTCC GAAGGTTTTG GTTACGAGAA GCTATTGGAT GAGCAGAAAA
Consensus TGTTGCATTT CACRCGGTCC GAAGGTTTTG GTTACGAGAA GCTATTGGAT GAGCAGAAAA

          86                                                         145
HG55'(3)  TTATCAAACA TCTATTGGAA AGTCCCTATA GCGATTACGA TTGGCGGGTT CGTCCCCGTG
HG55'(8)  TTATCAAGCA TCTATTGGAA AGTCCCTATA GCGATTACGA TTGGCGGGTT CGTCCCCGTG
HG55'(12) TTATCAAGCA TCTATTGGAA AGTCCCTATA GCGATTACGA TTGGCGGGTT CGTCCCCGTG
Consensus TTATCAARCA TCTATTGGAA AGTCCCTATA GCGATTACGA TTGGCGGGTT CGTCCCCGTG
```

Figure 54, see legend on next page.

```
          146                                                                 205
HG55'(3)  GTCGTCTTGG TCCCGCTGAC GACGACGATT ACGATAGTGA ACCAGTATTC ATTACAGTCA
HG55'(8)  GTCGTCTTGG TCCCGCTGAC GACGACGATT ACGATAGTGA ACCAGTATTC ATTACAGTCA
HG55'(12) GTCGTCTTGG TCCCGCTGAC GACGACGATT ACGATAGTGA ACCAGTATTC ATTACAGTCA
Consensus GTCGTCTTGG TCCCGCTGAC GACGACGATT ACGATAGTGA ACCAGTATTC ATTACAGTCA

          206                                                                 265
HG55'(3)  ACATGTACTT GAGGAGTATT TCTAAAGTCG ACGATGTTAA TATGGAATAT TCATTGCATT
HG55'(8)  ACATGTACTT GAGGAGTATA TCTAAAGTCG ATGATGTTAA TATGGAGTAT TCGTTGCACT
HG55'(12) ACATGTACTT GAGGAGTATA TCTAAAGTCG ATGATGTTAA TATGGAGTAT TCGTTGCACT
Consensus ACATGTACTT GAGGAGTATW TCTAAAGTCG AYGATGTTAA TATGGARTAT TCRTTGCAYT

          266                                                                 325
HG55'(3)  TTACATTTCG AGAAGAGTGG ATTGACGAGA GGCTATATTT CAACAGCCCG ACGTTGAAAC
HG55'(8)  TCACATTTCG AGAAGAATGG ATTGACGAAA GGCTGTATTT CAATAGCCCG ACGTTGAAAC
HG55'(12) TCACATTTCG AGAAGAATGG ATTGACGAAA GGCCGTATTT CAATAGCCCG ACGTTGAAAC
Consensus TYACATTTCG AGAAGARTGG ATTGACGARA GGCYRTATTT CAAYAGCCCG ACGTTGAAAC

          326                                                                 385
HG55'(3)  ATATCGTTCT GTCACCTGGA CAACGAATCT GGGTGCCCGA CACATTCTTC CAAAACGAGA
HG55'(8)  ATATTGTGCT GTCACCTGGA CAACGAATCT GGGTGCCCGA CACCTTCTTC CAGAATGAGA
HG55'(12) ATATTGTGCT GTCACCTGGA CAACGAATCT GGGTGCCCGA CACCTTCTTC CAGAATGAGA
Consensus ATATYGTKCT GTCACCTGGA CAACGAATCT GGGTGCCCGA CACMTTCTTC CARAAYGAGA

          386                                                                 445
HG55'(3)  AAAATGGCAA GAAACATGAC ATCGATACTC CGAACATTTT GATTCGGATA CATAACGGTA
HG55'(8)  AAGATGGCGA GAAACATGAC ATCGATACTC CGAATATTCT AATTCGGATA CATAATGGCA
HG55'(12) AAGATGGCAA GAAACATGAC ATCGATACTC CGAATATTCT AATTCGGATA CATAATGGCA
Consensus AARATGGCRA GAAACATGAC ATCGATACTC CGAAYATTYT RATTCGGATA CATAAYGGYA

          446                                                                 505
HG55'(3)  CAGGAAAGAT ACTGTATTCC TGTCGGCTTA CTCTGACCCT GAGCTGTCCG ATGAGGTTGG
HG55'(8)  CAGGAAAGAT TCTTTATTCA TGTCGGCTTA CTTTGACCCT GAGCTGTCCA ATGAGGTTGG
HG55'(12) CAGGAAAGAT TCTTTATTCA TGTCGGCTTA CTTTGACCCT GAGCTGTCCA ATGAGGTTGG
Consensus CAGGAAAGAT WCTKTATTCM TGTCGGCTTA CTYTGACCCT GAGCTGTCCR ATGAGGTTGG

          506                                                                 565
HG55'(3)  CCGATTATCC CCTTGATGTA CAGACATGTG TTGTGGATTT TGCTTCATAC GCCTATACTA
HG55'(8)  CCGATTATCC GCTTGATGTA CAGACATGTG TAGTGGATTT TGCTTCATAC GCCTATACTA
HG55'(12) CCGATTATCC GCTTGATGTA CAGACATGTG TAGTGGATTT TGCTTCATAC GCCTATACTA
Consensus CCGATTATCC GCTTGATGTA CAGACATGTG TWGTGGATTT TGCTTCATAC GCCTATACTA

                    566                                 597
HG55'(3)  CGAAAGACAT AGAATACGGA TGGAAAGAGG AG
HG55'(8)  CGAAAGACAT CGAATACGGA TGGAAAGAGG AA
HG55'(12) CGAAAGACAT CGAATACGGA TGGAAGAAGG AA
Consensus CGAAAGACAT MGAATACGGA TGGAARRAGG AR
```

Figure 54, See legend on next page.

B

```
           1                                                          60
HG55'(3)   MFALILPFLL HFTRSEGFGY EKLLDEQKII KHLLESPYSD YDWRVRPRGR LGPADDDDYD
HG55'(8)   MFALILPFLL HFTRSEGFGY EKLLDEQKII KHLLESPYSD YDWRVRPRGR LGPADDDDYD
HG55'(12)  MFALILPFLL HFTRSEGFGY EKLLDEQKII KHLLESPYSD YDWRVRPRGR LGPADDDDYD
Consensus  MFALILPFLL HFTRSEGFGY EKLLDEQKII KHLLESPYSD YDWRVRPRGR LGPADDDDYD

           61                                                         120
HG55'(3)   SEPVFITVNM YLRSISKVDD VNMEYSLHFT FREEWIDERL YFNSPTLKHI VLSPGQRIWV
HG55'(8)   SEPVFITVNM YLRSISKVDD VNMEYSLHFT FREEWIDERL YFNSPTLKHI VLSPGQRIWV
HG55'(12)  SEPVFITVNM YLRSISKVDD VNMEYSLHFT FREEWIDERP YFNSPTLKHI VLSPGQRIWV
Consensus  SEPVFITVNM YLRSISKVDD VNMEYSLHFT FREEWIDERL YFNSPTLKHI VLSPGQRIWV

           121                                                        180
HG55'(3)   PDTFFQNEKN GKKHDIDTPN ILIRIHNGTG KILYSCRLTL TLSCPMRLAD YPLDVQTCVV
HG55'(8)   PDTFFQNEKD GEKHDIDTPN ILIRIHNGTG KILYSCRLTL TLSCPMRLAD YPLDVQTCVV
HG55'(12)  PDTFFQNEKD GKKHDIDTPN ILIRIHNGTG KILYSCRLTL TLSCPMRLAD YPLDVQTCVV
Consensus  PDTFFQNEKD GKKHDIDTPN ILIRIHNGTG KILYSCRLTL TLSCPMRLAD YPLDVQTCVV

                     181             199
HG55'(3)   DFASYAYTTK DIEYGWKEE
HG55'(8)   DFASYAYTTK DIEYGWKEE
HG55'(12)  DFASYAYTTK DIEYGWKKE
Consensus  DFASYAYTTK DIEYGWKEE
```

Figure 54, Alignment of three 5' RACE-PCR amplifications a] nucleotide sequence, b] peptide sequence. Shaded regions highlight nts that vary between the clones. A consensus sequence is also displayed with a summary of possible nts highlighted in bold. For part **a]** only: **Y** codes either a C or a T, **M** codes either an A or a C, **R:** an A or a G, **S:** a G or a C, **K:** a G or a T and **W:** an A or a T. Nucleotides in uppercase are coding sequence whilst lower case nucleotides represent the 5' UTR.

Table 12, Percentage variation between the HG5 5' RACE. Comparison of amplified cDNA clones at both nucleotide and amino acid levels from an avermectin susceptible isolate of *H. contortus* has been addressed.

		HG5 5' ends isolated from avermectin susceptible *H. contortus*	
		Clone 3	Clone 8
Variation at the nucleotide level, over a length of 613 bp	Clone 8	5.53% (33/597nt)	
	Clone 12	5.86% (35/597nt)	0.67% (4/597nt)
Variation at the amino acid level, over a length of 209 residues	Clone 8	1.01% (2/199aa)	
	Clone 12	1.51% (3/199aa)	1.51% (3/199aa)

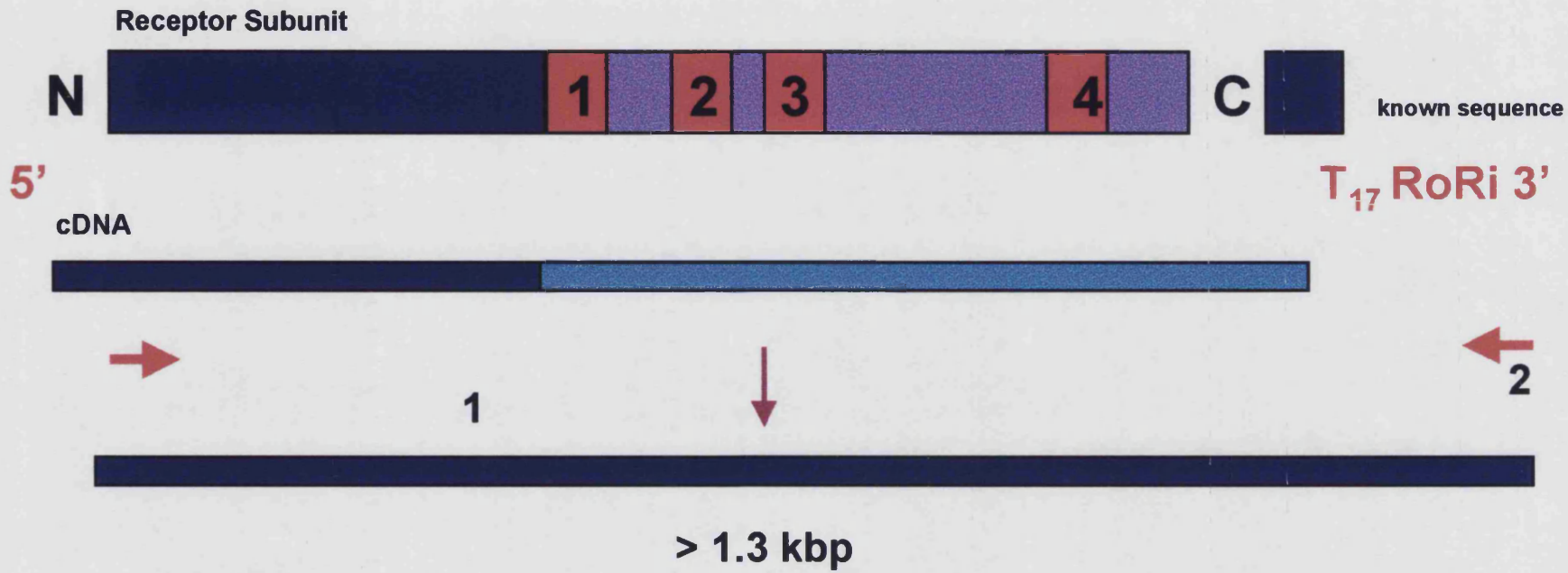

Figure 55, Strategy for Isolating the 3' end of HG5 using RACE-PCR.

6.2.4 Isolation and cloning of the 3' end of HG5

With the 5' sequence of HG5 established, a gene specific sense primer, HG5-GSSP2 (Appendix 3), was designed for use in a 3' RACE-PCR with the RoRi oligonucleotide. The exact strategy is illustrated in figure 55, with the successful amplification yielding a PCR product of greater than 1.3 kbp in length. The exact length could not be predefined, as although the coding domain had been predicted to be approximately 1.29 kbp, the length of the 3' untranslated region could not be determined.

Figure 56 depicts a 3' PCR amplification using HG5-GSSP2 and RoRi primers with avermectin-susceptible *H. contortus* as template. The resulting 1.65 kbp product was amplified following 45 cycles. The concentration of this product was too low to sequence directly, so 1 µl of the Sephaglas™ purified band was used as template to re-amplify the product in a second PCR. The same primers, RoRi and HG5-GSSP2, were added to the template and a further 45 rounds of thermal cycling was carried out with the same cycle temperatures used for the previous amplification.

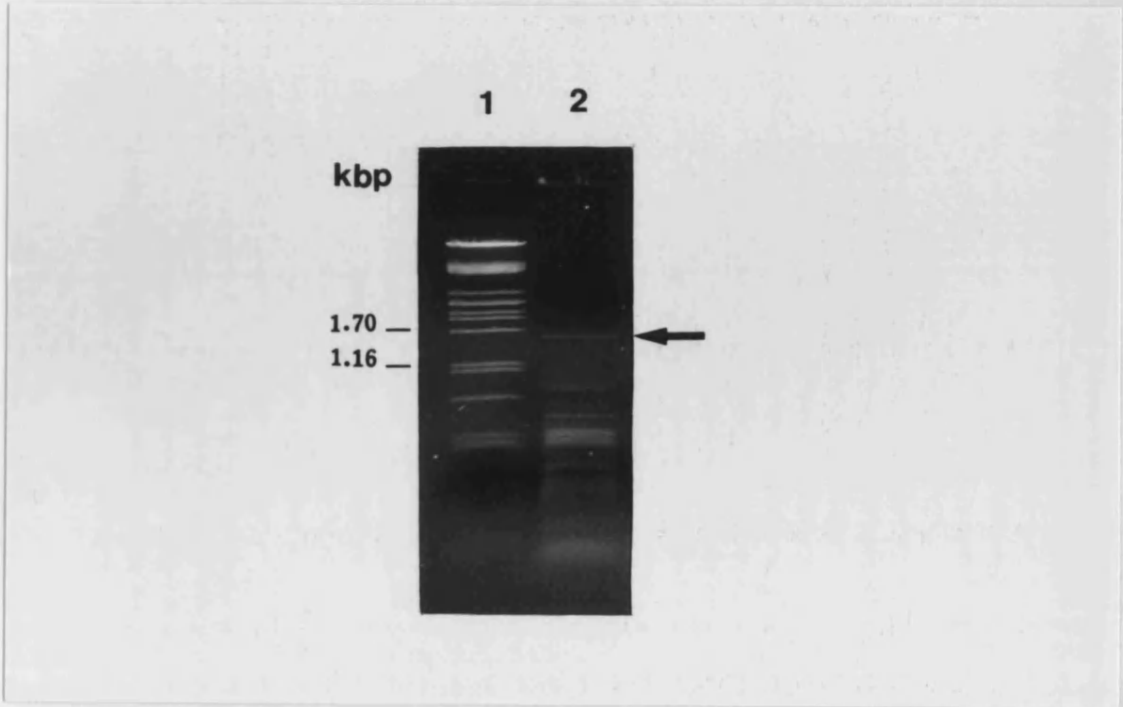

Figure 56, Amplification of a 3' RACE Product.
Lane1: λ DNA digested with the restriction enzyme Pst1, relevant band sizes are shown along the side of the gel.
Lane 2: 3' RACE using primers HG5-GSSP2 and RoRi amplifying a 1.65 kbp fragment (➔).
The PCR sample had been amplified using the Expand™ High Fidelity system, in the presence of 1.5 mM $MgCl_2$ and 300nM of each primer with cDNA reverse transcribed from *H.contortus* egg mRNA.
Cycling conditions: 94 °C denaturation for 2 min, after which time 2.5 U of enzyme was added. 45 cycles of 94 °C for 30 sec, 61 °C for 30 sec and 72 °C for 2 min followed and was terminated by a further 7 min at 72 °C.
80 µl of PCR sample was separated on 1 % (w/v) agarose gel using electrophoresis.

The resulting 1.65 kbp amplification was sequenced directly, confirming that it was HG5 specific. To obtain a consensus sequence of the 3' end of HG5, a further two PCR reactions were carried out using cDNA from avermectin susceptible *H. contortus* as template. This yielded an extra two individual products of 1.65 kbp in size which were re-amplified in an identical manner to that described for the first 3' PCR product (Figure 56). All three 1.65 kbp cDNAs were treated with DNA polymerase 1 and polynucleotide kinase to create blunt-ended products for ligation into pBluescript II SK (+) via the EcoRV restriction site. These were then transformed into the *E. coli* strain XL1-Blue and colonies were grown up on LB agar in the presence of ampicillin, X-Gal and IPTG. Plasmids purified from a selection of white colonies were restricted with Xba1 and Xho1 in a double digestion to determine whether the 1.65 kbp insert had been successfully ligated into the vector. Figure 57 represents an agarose gel loaded with digested plasmids. Lanes 4, 5, 6 & 7 contain constructs carrying one 3' end amplified from the first set of PCRs. Similarly constructs in lanes 9, 10 & 11 have been ligated with the second PCR amplified 3' end and lanes 12, 13, 14 & 15 with the third individually amplified insert.

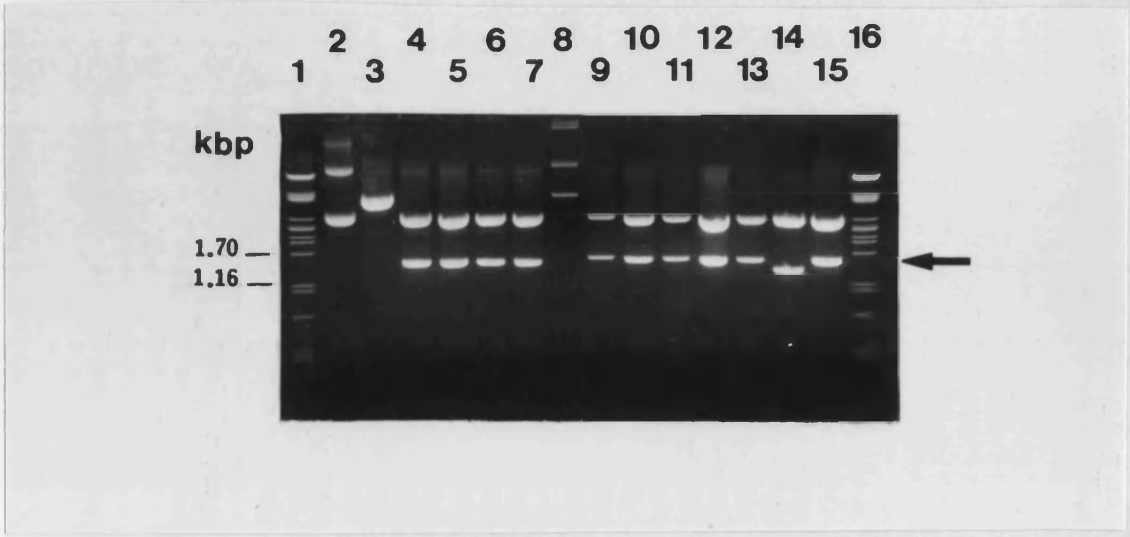

Figure 57, Clones containing HG5 3'RACE products.
Lane1 & 16: λ DNA cut with the enzyme Pst1, relevant band sizes are noted along the side of the gel.
Lane 2: Uncut construct carrying 1.65 kbp fragment, previously represented in lane 2 of figure 55.
Lane 3: Same construct used as in lane 2 of this figure but cut with the enzyme Xba1.
Lane 4: A single Xho1 digest using construct represented in lane 2, this releases a 1.65 kbp fragment indicating that there is an extra Xho1 site near the Xba1 motif.
Lanes 5, 6 & 7: loaded with double digested constructs possessing the 1.65 kbp HG5 3' end product seen in lane 2 of figure 55.
Lanes 8, 9, 10 & 11: double digested constructs ran in these lanes comprise a separately amplified 1.65 kbp insert using the same RACE-PCR conditions as detailed in figure 6.
Lanes 12, 13, 14 & 15: a third PCR identical to that described in figure 6 was achieved with the resulting 1.65 kbp fragment cloned successfully into plasmids run in these lanes.
Lane 8 represents a plasmid that does not contain the HG5 3' end insert. Plasmids, previously purified with the Wizard Plus™ kit were double digested with the restriction enzymes Xba1 and Xho1 for 1 hour at 37 °C unless otherwise stated. Digested products were then separated by electrophoresis on a 1 % (w/v) agarose gel in TBE buffer for analysis.

Plasmid-constructs from clones seen in lanes 4, 10 & 15 were sequenced using the primers T3, KS, HG5-GSAP1, HG5-GSAP2 and HG5-GSSP3. These sequences were then aligned to establish the degree of variation between the three individually amplified PCR products displayed in figure 58a and b. Table 13 lists the calculated percentage of variation between the clones and the percentages of the consequent amino acid discrepancies seen at the translated level respectively. The 3' end was 66 % identical to the partial GluCIX sequence isolated from *O. volvulus* and 62 % identical to the GBR-2A from *C. elegans* (accession numbers U59745 and U40573 respectively). These results consistent with the identities calculated for the partial and 5' end clones of HG5.

A

```
           1                                                   50
HG53'(4)   TTGCATTTCA CGCGTTCCGA AGGTTTTGGT TACGAGAAGC TATTGGATGA
HG53'(10)  TTGCATTTCA CGCGGTCCGA AGGTTTTGGT TACGAGAAGC TATTGGATGA
HG53'(15)  TTGCATTTCA CGCGGTCCGA AGGTTTTGGT TACGAGAAGC TATTGGATGA
Consensus  TTGCATTTCA CGCGKTCCGA AGGTTTTGGT TACGAGAAGC TATTGGATGA

           51                                                  100
HG53'(4)   GCAGAAAATA ATCAAACATC TACTGGAAAG TCCCTATAGC GATTACGATT
HG53'(10)  GCAGAAAATT ATCAAGCATC TATTGGAAAG TCCCTATAGC GATTACGATT
HG53'(15)  GCAGAAAATT ATCAAACATC TATTGGAAAG TCCCTATAGC GATTACGATT
Consensus  GCAGAAAATW ATCAARCATC TAYTGGAAAG TCCCTATAGC GATTACGATT

           101                                                 150
HG53'(4)   GGCGGGTTCG TCCCCGTGGT CGTCTGGGTC CAGCTGACGA CGACGATTAC
HG53'(10)  GGCGGGTTCG TCCCCGTGGT CGTCTTGGTC CCGCTGACGA CGACGATTAC
HG53'(15)  GGCGGGTTCG TCCCCGTGGT CGTCTTGGTC CCGCTGACGA CGACGATTAC
Consensus  GGCGGGTTCG TCCCCGTGGT CGTCTKGGTC CMGCTGACGA CGACGATTAC

           151                                                 200
HG53'(4)   GATAGTGAAC CAGTATTCAT TACAGTCAAC ATGTACTTAA GGAGTATTTC
HG53'(10)  GATAGTGAAC CAGTATTCAT TACAGTCAAC ATGTACTTGA GGAGTATATC
HG53'(15)  GATAGTGAAC CAGTATTCAT TACAGTCAAC ATGTACTTGA GGAGTATTTC
Consensus  GATAGTGAAC CAGTATTCAT TACAGTCAAC ATGTACTTRA GGAGTATWTC

           201                                                 250
HG53'(4)   CAAAGTCGAT GATGTTAATA TGGAGTATTC ATTGCACTTT ACATTTCGAG
HG53'(10)  TAAAGTCGAT GATGTTAATA TGGAGTATTC GTTGCACTTC ACATTTCGAG
HG53'(15)  TAAAGTCGAC GATGTTAATA TGGAATATTC ATTGCATTTT ACATTTCGAG
Consensus  YAAAGTCGAY GATGTTAATA TGGARTATTC RTTGCAYTTY ACATTTCGAG

           251                                                 300
HG53'(4)   AAGAATGGAT TGACGAGAGG CTGTATTTCA ATAGCCCAAC GTTGAAACAT
HG53'(10)  AAGAATGGAT TGACGAAAGG CTGTATTTCA ATAGCCCGAC GTTGAAACAT
HG53'(15)  AAGAGTGGAT TGACGAGAGG CTATATTTCA ACAGCCCGAC GTTGAAACAT
Consensus  AAGARTGGAT TGACGARAGG CTRTATTTCA AYAGCCCRAC GTTGAAACAT
```

Figure 58, see legend on next page.

```
            301                                                 350
HG53'(4)    ATTGTGCTGT CACCTGGACA ACGAATATGG GTGCCCGACA CTTTCTTCCA
HG53'(10)   ATTGTGCTGT CACCTGGACA ACGAATCTGG GTGCCCGACA CCTTCTTCCA
HG53'(15)   ATCGTTCTGT CACCTGGACA ACGAATCTGG GTGCCCGACA CATTCTTCCA
Consensus   ATYGTKCTGT CACCTGGACA ACGAATMTGG GTGCCCGACA CYTTCTTCCA

            351                                                 400
HG53'(4)    GAACGAGAAA GATGGCAAGA AGCATGACAT CGATACTCCG AACATTCTGA
HG53'(10)   GAATGAGAAA GATGGCAAGA AACATGACAT CGATACTCCG AATATTCTAA
HG53'(15)   AAACGAGAAA GATGGCAAGA AACATGACAT CGATACTCCG AACATTTTGA
Consensus   RAAYGAGAAA GATGGCAAGA ARCATGACAT CGATACTCCG AAYATTYTRA

            401                                                 450
HG53'(4)    TTCGGATACA TAACGGCACA GGAAAGATCC TGTATTCGTG CCGGCTTACT
HG53'(10)   TTCGGATACA TAATGGCACA GGAAAGATTC TTTATTCATG TCGGCTTACT
HG53'(15)   TTCGGATACA TAACGGTACA GGAAAGATAC TGTATTCATG TCGGCTTACT
Consensus   TTCGGATACA TAAYGGYACA GGAAAGATYC TKTATTCRTG YCGGCTTACT

            451                                                 500
HG53'(4)    CTGACCCTGA GCTGTCCAAT GAGGTTGGCC GATTATCCGC TTGATGTACA
HG53'(10)   TTGACCCTGA GCTGTCCAAT GAGGTTGGCC GATTATCCGC TTGATGTACA
HG53'(15)   CTGACCCTGA GCTGTCCGAT GAGGTTGGCC GATTATCCGC TTGATGTACA
Consensus   YTGACCCTGA GCTGTCCRAT GAGGTTGGCC GATTATCCGC TTGATGTACA

            501                                                 550
HG53'(4)    GACATGTGTA GTGGATTTCG CTTCATACGC CTATACTACA AAAGATATCG
HG53'(10)   GACATGTGTA GTGGATTTTG CTTCATACGC CTATACTACG AAAGACATCG
HG53'(15)   GACATGTGTT GTGGATTTTG CTTCATACGC CTATACTACG AAAGACATAG
Consensus   GACATGTGTW GTGGATTTYG CTTCATACGC CTATACTACR AAAGAYATMG

            551                                                 600
HG53'(4)    AATATGGATG GAAAGAAGAA AAACCGATCC AGATCAAAGA TGGCCTTCGA
HG53'(10)   AATACGGATG GAAAGAAGAA AAACCGATCC AGATCAAAGA TGGCCTTCGA
HG53'(15)   AATACGGATG GAAAGAGGAG AAACCGATCC AGATCAAAGA TGGCCTTCGA
Consensus   AATAYGGATG GAAAGARGAR AAACCGATCC AGATCAAAGA TGGCCTTCGA

            601                                                 650
HG53'(4)    CAATCATTGC CTTCGTTTTT GCTCAGTAAT GTAAAAACCG GTAATTGTAC
HG53'(10)   CAATCATTGC CTTCATTTTT GCTCAGTAAT GTAAAAACCG GTAATTGTAC
HG53'(15)   CAATCATTGC CTTCGTTTTT GCTCAGTAAT GTAAAAACCG GTAATTGTAC
Consensus   CAATCATTGC CTTCRTTTTT GCTCAGTAAT GTAAAAACCG GTAATTGTAC

            651                                                 700
HG53'(4)    GTCAGTTACC AATACGGGCG CTTATTCATG CCTTCGAACT ATCATCGAAC
HG53'(10)   GTCAGTTACC AATACGGGCG CTTATTCATG CCTTCGAACC ATCATCGAAC
HG53'(15)   GTCAGTTACC AATACGGGCG CTTATTCATG CCTTCGAACC ATCATCGAAC
Consensus   GTCAGTTACC AATACGGGCG CTTATTCATG CCTTCGAACY ATCATCGAAC
```

Figure 58, see legend on next page.

```
            701                                                 750
HG53'(4)    TCAAGAGGGA ATTCAGTTAT TATCTTTTAC AGCTTTATAT TCCATCTTTT
HG53'(10)   TCAAGAGGGA ATTCAGTTAC TACCTTTTAC AGCTTTATAT TCCATCTTTT
HG53'(15)   TCAAGAGGGA ATTCAGTTAC TACCTTTTAC AGCTTTACAT TCCATCTTTT
Consensus   TCAAGAGGGA ATTCAGTTAY TAYCTTTTAC AGCTTTAYAT TCCATCTTTT

            751                                                 800
HG53'(4)    ATGCTAGTGG CAGTATCGTG GGTGTCTTTT TGGCTAGACA AAGATTCTGT
HG53'(10)   ATGCTAGTCG CAGTATCGTG GGTGTCTTTT TGGCTAGACA AAGATTCTGT
HG53'(15)   ATGTTGGTCG CAGTATCATG GGTGTCATTT TGGCTAGACA AAGATTCTGT
Consensus   ATGYTRGTSG CAGTATCRTG GGTGTCWTTT TGGCTAGACA AAGATTCTGT

            801                                                 850
HG53'(4)    CCCGGCTCGT GTAACGCTAG GAGTAACCAC CTTACTAACT ATGACTACAC
HG53'(10)   CCCGGCTCGG GTTACGCTAG GAGTAACTAC CTTACTCACT ATGACCACAC
Hg53'(15)   CCCGGCTCGG GTTACGCTAG GAGTAACGAC CTTACTCACT ATGACCACGC
Consensus   CCCGGCTCGK GTWACGCTAG GAGTAACXAC CTTACTMACT ATGACYACRC

            851                                                 900
HG53'(4)    AAGCATCAGG TGTAAATGCG AATTTGCCGC CAGTCAGCTA TACCAAGGCA
HG53'(10)   AAGCATCGGG TGTAAATGCG AATTTGCCTC CAGTCAGTTA CACAAAGGCA
HG53'(15)   AAGCATCGGG TGTAAACGCG AATTTGCCTC CAGTCAGCTA TACAAAGGCA
Consensus   AAGCATCRGG TGTAAAYGCG AATTTGCCKC CAGTCAGYTA YACMAAGGCA

            901                                                 950
HG53'(4)    ATTGACATAT GGATTGGTGT CTGTCTAGCA TTTATTTTTG GTGCTCTTTT
HG53'(10)   ATTGACATAT GGATCGGTGT CTGTCTAGCA TTTATTTTTG GTGCTCTTTT
Hg53'(15)   ATTGACATAT GGATCGGTGT CTGTCTAGCA TTTATTTTTG GTGCTCTTTT
Consensus   ATTGACATAT GGATYGGTGT CTGTCTAGCA TTTATTTTTG GTGCTCTTTT

            951                                                1000
HG53'(4)    GGAATTTGCA TTAGTGAATT GGGCAGCACG GCAGGATCTC GTAGCCCACA
HG53'(10)   GGAATTTGCA TTAGTGAATT GGGCAGCACG GCAGGATCTC GTAGCACACA
HG53'(15)   GGAATTTGCA TTAGTGAATT GGGCAGCACG GCAGGATCTC GTAGCACACA
Consensus   GGAATTTGCA TTAGTGAATT GGGCAGCACG GCAGGATCTC GTAGCMCACA

            1001                                               1050
HG53'(4)    GTCGGGCCCG ATATCGACAA TCACCTTTGT TCTTTAGGAA TCCTGATTCA
HG53'(10)   GTCGGGCCCG ATATCGACAG CTACCTTTGT TCTTTAGGAA TCCAGATTCA
HG53'(15)   GTCGGGCCCG ATATCGACAG TCACCTTTGT TCTTTAGGAA CCCTGATTCA
Consensus   GTCGGGCCCG ATATCGACAR YYACCTTTGT TCTTTAGGAA YCCWGATTCA

            1051                                               1100
HG53'(4)    CGACAAGAAA ACTCCCATCA TTTCTATGCA CCTATACAAC AAGAGGTTAC
HG53'(10)   CGACAAGAAA ACTCCCATCA TTTCTATGCA CCTATACAAC AAGAGGTTAC
HG53'(15)   AGACAAGGAA ACTCCCATCA TTTCTATGCA CCTATACAAC AAGAGGTTAC
Consensus   MGACAAGRAA ACTCCCATCA TTTCTATGCA CCTATACAAC AAGAGGTTAC
```

Figure 58, See legend on next page.

```
           1101                                                1150
HG53'(4)   GTTGGAAGAT TTGCCGTTCA GTTGGTGGGA TAAAATATGG AAAATACGCT
HG53'(10)  GTTGGAAGAT TTACCGTTCA GTTGGTGGGA TAAAATATGG AAAATACGCT
HG53'(15)  GTTAGAAGAT TTGCCATTCA GTTGGTGGGA TAAAATATGG AAAATACGCT
Consensus  GTTRGAAGAT TTRCCRTTCA GTTGGTGGGA TAAAATATGG AAAATACGCT

           1151                                                1200
HG53'(4)   ATAAGGAACG GAGTCGAAGG ATAGATCTTA TATCGAGAGT GATGTTTCCG
HG53'(10)  ATAAGGAACG GAGTCGGAGG ATTGATCTTA TATCGAGAGT GATGTTTCCG
HG53'(15)  ATAAGGAACG GAGTCGAAGA ATTGATCTTA TATCGAGAGT GATGTTCCCG
Consensus  ATAAGGAACG GAGTCGRAGR ATWGATCTTA TATCGAGAGT GATGTTYCCG

           1201                                                1250
HG53'(4)   CTGTGCTTCA TTATTTTCAA TATTATGTAC TGGTGGCGAT ATCTGATACC
HG53'(10)  CTGTGCTTCA TTATTTTCAA TATCATGTAC TGGTGGCGAT ATCTGATACC
HG53'(15)  CTGTGCTTCA TTATTTTCAA TATAATGTAC TGGTGGCGAT ATCTGATACC
Consensus  CTGTGCTTCA TTATTTTCAA TATXATGTAC TGGTGGCGAT ATCTGATACC

           1251                                                1300
HG53'(4)   GTACATGGCA GTACAAGCAC AGTTGGAATG Atgaggcctt ccaatatgga
HG53'(10)  GTACATGGCA GTCCAGGCAC AGTTGGAGTG Atga..cttt ccaatgtgga
HG53'(15)  GTACATGGCA GTGCAAGCGC AGTTGGAATG Atga..ctgt tcattatgga
Consensus  GTACATGGCA GTHCARGCRC AGTTGGARTG Atga..ctwt ycawtrtgga

           1301                                                1350
HG53'(4)   ggcttgtctt tttacggaaa aattctattt atgtgataca aaaactcggg
HG53'(10)  ggcttgtctt tctacgg.aa aattctattg atgtgatacg aaaactcggg
HG53'(15)  ggcttgtctt tctacgc.aa aattctatcg atgtgatacg aaaattcggg
Consensus  ggcttgtctt tctacgs.aa aattctatyk atgtgatacg aaaaytcggg

           1351                                                1400
HG53'(4)   gatttgatac agtattgttg tagatgcctt catattcatt ttgtaatgtg
HG53'(10)  ggtttgatac agtattgttg tagatgcctt tatatttatc ttgtaagatg
HG53'(15)  gatttgatac agtattgttg tagatgcctt tatatttatc ttgtaatatg
Consensus  grtttgatac agtattgttg tagatgcctt yatattyaty ttgtaawatg

           1401                                                1450
HG53'(4)   accaattgat tctcaaaaag tgctgatctc aaaagaaaag tataaactgt
HG53'(10)  accaattgat tctcaaaaag tgctgatctc aaaagaatta tataaactgt
HG53'(15)  accaattgat tctcaaaaag tgctgatct caaaagaaaaa tataaactgt
Consensus  accaattgat tctcaaaaag tgctgatct caaaagaaaar tataaactgt

           1451                                                1500
HG53'(4)   gaaatc.... .......... .......... .......... ..........
HG53'(10)  gaaatcattc .......... .......... .......... ..........
HG53'(15)  ggaatcattc atttgtgcgt ttacggacca atttaatcca ttgtagtatg
Consensus  ggaatcattc atttgtgcgt ttacggacca atttaatcca ttgtagtatg
```

Figure 58, See legend on next page for details.

```
            1501                                1536
HG53'(15)   tcacattttg aaagacgaat aaatgtcagg gtcatt
Consensus   tcacattttg aaagacgaat aaatgtcagg gtcatt
```

B

```
            1                                                    50
HG53'(4)    LHFTRSEGFG YEKLLDEQKI IKHLLESPYS DYDWRVRPRG RLGPADDDDY
HG53'(10)   LHFTRSEGFG YEKLLDEQKI IKHLLESPYS DYDWRVRPRG RLGPADDDDY
HG53'(15)   LHFTRSEGFG YEKLLDEQKI IKHLLESPYS DYDWRVRPRG RLGPADDDDY
Consensus   LHFTRSEGFG YEKLLDEQKI IKHLLESPYS DYDWRVRPRG RLGPADDDDY

            51                                                  100
HG53'(4)    DSEPVFITVN MYLRSISKVD DVNMEYSLHF TFREEWIDER LYFNSPTLKH
HG53'(10)   DSEPVFITVN MYLRSISKVD DVNMEYSLHF TFREEWIDER LYFNSPTLKH
HG53'(15)   DSEPVFITVN MYLRSISKVD DVNMEYSLHF TFREEWIDER LYFNSPTLKH
Consensus   DSEPVFITVN MYLRSISKVD DVNMEYSLHF TFREEWIDER LYFNSPTLKH

            101                                                 150
HG53'(4)    IVLSPGQRIW VPDTFFQNEK DGKKHDIDTP NILIRIHNGT GKILYSCRLT
HG53'(10)   IVLSPGQRIW VPDTFFQNEK DGKKHDIDTP NILIRIHNGT GKILYSCRLT
HG53'(15)   IVLSPGQRIW VPDTFFQNEK DGKKHDIDTP NILIRIHNGT GKILYSCRLT
Consensus   IVLSPGQRIW VPDTFFQNEK DGKKHDIDTP NILIRIHNGT GKILYSCRLT

            151                                                 200
HG53'(4)    LTLSCPMRLA DYPLDVQTCV VDFASYAYTT KDIEYGWKEE KPIQIKDGLR
HG53'(10)   LTLSCPMRLA DYPLDVQTCV VDFASYAYTT KDIEYGWKEE KPIQIKDGLR
HG53'(15)   LTLSCPMRLA DYPLDVQTCV VDFASYAYTT KDIEYGWKEE KPIQIKDGLR
Consensus   LTLSCPMRLA DYPLDVQTCV VDFASYAYTT KDIEYGWKEE KPIQIKDGLR

            201                                                 250
HG53'(4)    QSLPSFLLSN VKTGNCTSVT NTGAYSCLRT IIELKREFSY YLLQLYIPSF
HG53'(10)   QSLPSFLLSN VKTGNCTSVT NTGAYSCLRT IIELKREFSY YLLQLYIPSF
HG53'(15)   QSLPSFLLSN VKTGNCTSVT NTGAYSCLRT IIELKREFSY YLLQLYIPSF
Consensus   QSLPSFLLSN VKTGNCTSVT NTGAYSCLRT IIELKREFSY YLLQLYIPSF

            251                                                 300
HG53'(4)    MLVAVSWVSF WLDKDSVPAR VTLGVTTLLT MTTQASGVNA NLPPVSYTKA
HG53'(10)   MLVAVSWVSF WLDKDSVPAR VTLGVTTLLT MTTQASGVNA NLPPVSYTKA
HG53'(15)   MLVAVSWVSF WLDKDSVPAR VTLGVTTLLT MTTQASGVNA NLPPVSYTKA
Consensus   MLVAVSWVSF WLDKDSVPAR VTLGVTTLLT MTTQASGVNA NLPPVSYTKA

            301                                                 350
HG53'(4)    IDIWIGVCLA FIFGALLEFA LVNWAARQDL VAHSRARYRQ SPLFFRNPDS
HG53'(10)   IDIWIGVCLA FIFGALLEFA LVNWAARQDL VAHSRARYRQ LPLFFRNPDS
HG53'(15)   IDIWIGVCLA FIFGALLEFA LVNWAARQDL VAHSRARYRQ SPLFFRNPDS
Consensus   IDIWIGVCLA FIFGALLEFA LVNWAARQDL VAHSRARYRQ SPLFFRNPDS

            351                                                 400
HG53'(4)    RQENSHHFYA PIQQEVTLED LPFSWWDKIW KIRYKERSRR IDLISRVMFP
HG53'(10)   RQENSHHFYA PIQQEVTLED LPFSWWDKIW KIRYKERSRR IDLISRVMFP
HG53'(15)   RQGNSHHFYA PIQQEVTLED LPFSWWDKIW KIRYKERSRR IDLISRVMFP
Consensus   RQGNSHHFYA PIQQEVTLED LPFSWWDKIW KIRYKERSRR IDLISRVMFP

            401                         426
HG53'(4)    LCFIIFNIMY WWRYLIPYMA VQAQLE
HG53'(10)   LCFIIFNIMY WWRYLIPYMA VQAQLE
HG53'(15)   LCFIIFNIMY WWRYLIPYMA VQAQLE
Consensus   LCFIIFNIMY WWRYLIPYMA VQAQLE
```

Figure 58, Alignment of three individually amplified 3' RACE-PCR products a] nucleotide sequence: Variation between the different clones is shaded in grey. A consensus sequence is also displayed with a summary of possible nts highlighted in bold. For part a] only **Y** codes either a C or a T, **M** codes either an A or a C, **R:** an A or a G, **S:** a G or a C, **K:** a G or a T, **W:** an A or a T and **H**: an A, C or T. Nucleotides in uppercase are coding sequence whilst lower case nucleotides represent the UTRs. **b] peptide sequence:** Variation between the amino acid sequence is indicated with grey shading.

Table 13, Percentage variation between the HG5 3' RACE cDNA clones. This has been calculated at both the nucleotide and amino acid levels with clones amplified from an avermectin susceptible isolate.

		HG5 3' ends isolated from avermectin susceptible *H. contortus*	
		Clone 4	Clone 10
Variation at the nucleotide level, over a length of 1281 bp	Clone 10	4.45% (57/1281nt)	
	Clone 15	5.31% (68/1281nt)	4.45% (57/1281nt)
Variation at the amino acid level, over a length of 426 residues	Clone 10	0.23% (1/426aa)	
	Clone 15	0.00% (0/426aa)	0.23% (1/426aa)

6.2.5 HG5 Sequence from Avermectin Susceptible *H. contortus*

The consensus full-length sequence for HG5 was transferred to the GCG package on the gnome workstation and was compared with known sequences present in the EMBL database. The identity of HG5 with related sequences has been summarised in Table 14.

Figure 59 illustrates an alignment of HG5 with the two most similar full-length protein sequences GBR2A (U40573) and GluClα1 (U142524), both isolated from *C. elegans*. The four transmembrane regions (denoted TM1-4) have been highlighted and the signal cleavage site is indicated by the arrow. Two N-linked glycosylation sites exist at residues 148-150 (NGT) and residues 225-227 (NCT). The two cysteines at positions 165 and 179 are believed to form the cys-loop, which is the signature of TGICs. The two conserved cysteines (C2226 & C237) situated further downstream from the loop are a common feature of glycine receptor subunits. Several predicted phosphorylation sites have been identified along the intracellular loop spanning between transmembrane domain 3 and 4 of HG5. These include 2 casein kinase II phosphorylation motifs, TLED (residues 377-380) and SWWD (residues 384-387), and a phosphorylation site specific to protein kinase C, SKR (residues 398-900).

Predicted ligand binding sites are also present including residues YAXT and TGXY at positions 186-189 and 232-235 respectively. Phenlyalanine (residue 91) and glutamine (residue 177) are also thought to play a role in agonist binding. Finally the tyrosine residue at position 185 appears to be highly conserved in α-like subunits compared to β-like subunits which tend to have a histadine at this site.

			GluClR														
	GABA R	Glycine R	Beta, β-like subunits		Gamma, γ-like subunit						γ/α-like	Alpha, α-like subunits					
	HG1	Glyα	GluClβ	HG4	Gbr2a	Gbr2b	HG2	HG3	GluClX	GluClX	HG5	Zc317.3	C27h55	GluClα1	GluClα2s	GluClα2l	GluClα
$GABA_A$	28%	38%	31%	31%	36%	35%	33%	35%	42%	40%	33%	33%	27%	31%	32%	32%	31%
HG1	-	33%	26%	27%	26%	28%	25%	27%	32%	29 %	28%	29%	24%	28%	30%	29%	28%
Glyα			40%	41%	43%	42%	42%	42%	47%	47%	42%	43%	36%	40%	41%	41%	46%
GluClβ				80%	48%	47%	46%	48%	57%	57%	43%	49%	39%	45%	47%	47%	44%
HG4					48%	47%	45%	48%	53%	57%	43%	47%	38%	47%	46%	46%	42%
Gbr2a						79%	79%	74%	81%	91%	62%	60%	41%	57%	57%	57%	52%
Gbr2b							72%	87%	88%	86%	57%	58%	40%	54%	54%	55%	50%
HG2								75%	81%	89%	55%	55%	37%	52%	53%	54%	45%
HG3									88%	85%	56%	59%	40%	54%	55%	55%	49%
GluClX										91%	66%	68%	55%	63%	63%	68%	55%
GluClX											71%	72%	53%	72%	72%	72%	59%
HG5												53%	44%	56%	55%	55%	48%
Zc317.3													40%	61%	67%	67%	50%
C27h55														38%	38%	38%	37%
GluClα1															77%	77%	46%
GluClα2s																96%	48%
GluClα2l																	47%

Key; *H contortus* *C. elegans* *O. volvulus* *D. immitis* *D. melangastor* *R. norvegicus* Partial sequence

Table 14, Comparison of Amino Acid Identities of HG5 with related receptor subunits.

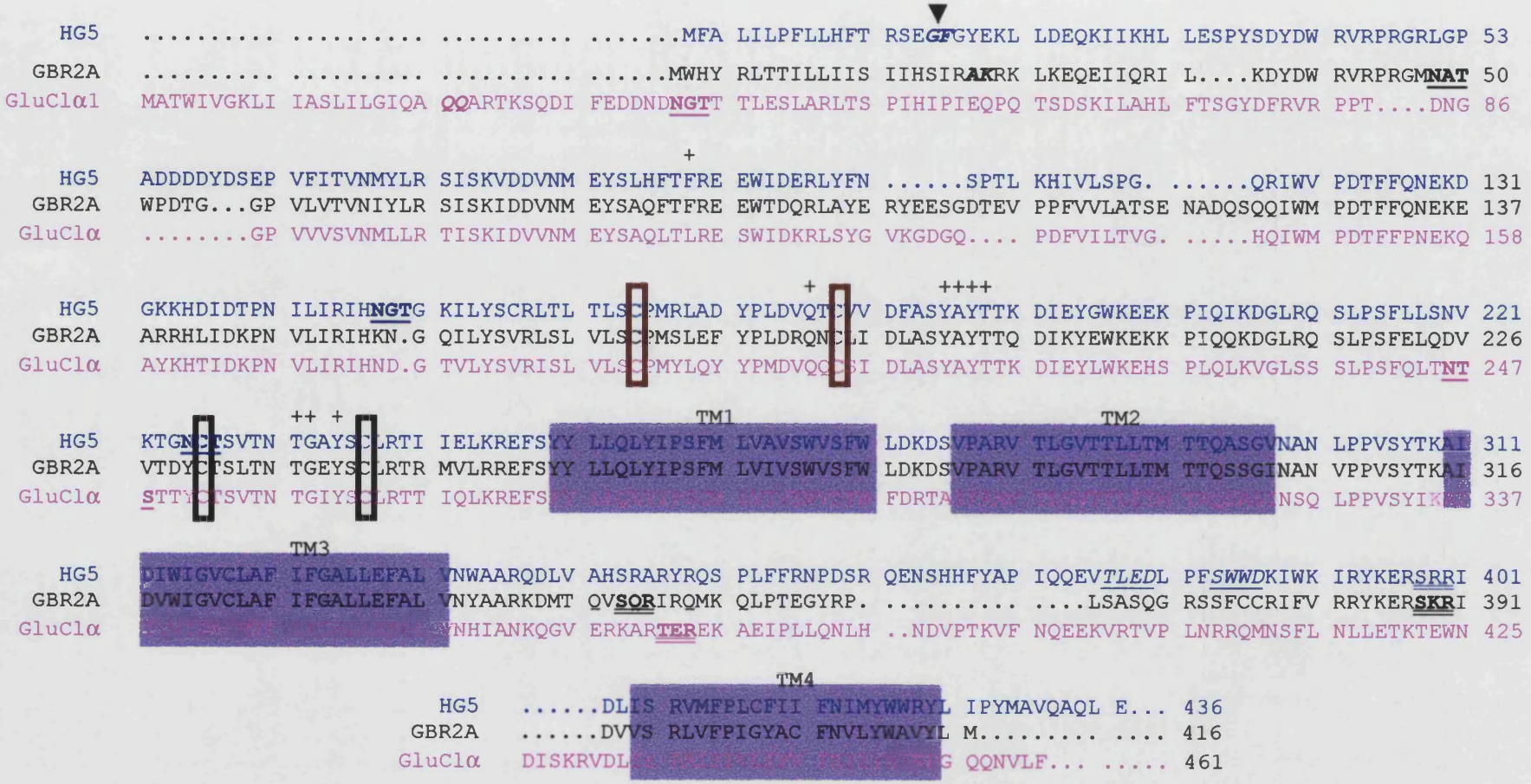

Figure 59 Alignment of HG5 with GBR2A and GluClα receptor subunits

KEY: Predicted signal cleavage sites are between the residues *GF* (indicated by ▼) for HG5, *AK* for GBR2A, *QQ* for GluClα, NX(T/S) are predicted N-linked Glycosylation sites. Transmembrane domains (TM1-4). + marks the residues believed to be involved in ligand binding. *TLED* *SWWD* are predicted casein kinase II phosphorylation sites, SRR, SQR, SKR and TER are predicted protein kinase C phosphorylation site, C cysteines forming the cysteine loop, C cysteine characteristic of glycine receptors.

6.2.6 Isolation of the 5' end of avermectin resistant HG5

The mRNA from avermectin resistant *Haemonchus contortus* eggs was extracted for cDNA synthesis. The resulting cDNA was used in RACE-PCR to amplify two individual copies of the 5' end of HG5. The exact conditions required to amplify the 5' end of HG5 from avermectin susceptible worms were used. The alignment of the two 5' end, HG5 sequences, from resistant nematodes and the consensus 5' sequence from susceptible worms can be seen in figure 60. Variation of sequence between the clones is shaded in grey and has been summarised in table 15. The 5' consensus sequence for HG5 from avermectin susceptible and resistant *H. contortus* was identical. It can therefore be concluded that avermectin resistance has not resulted from a genetic mutation coded within the N-terminal domain of HG5.

```
                                          1                          25
          SConsensus rtyagtatctatgtgatcgacacta ATGTTCGCCT TRATTCTGCC ATTTC
           RHG55'(1) gtcagtatctatgtgatcgacacta ATGTTCGCCT TAATTCTGCC ATTTC
           RHG55'(2) aattcgatctatgtgatcgacacta ATGTTCGCCT TGATTCTGCC ATTTC

                     26                                                  85
SConsensus TGTTGCATTT CACRCGGTCC GAAGGTTTTG GTTACGAGAA GCTATTGGAT GAGCAGAAAA
 RHG55'(1) TGTTGCATTT CACACGGTCC GAAGGTTTTG GTTACGAGAA GCTATTGGAT GAGCAGAAAA
 RHG55'(2) TGTTCCATTT CACACGGTCC GAAGGTTTTG GTTACGAGAA GCTATTGGAT GAGCAGAAAA

                     86                                                 145
SConsensus TTATCAARCA TCTATTGGAA AGTCCCTATA GCGATTACGA TTGGCGGGTT CGTCCCCGTG
 RHG55'(1) TTATCAAACA TCTATTGGAA AGTCCCTATA GCGATTACGA TTGGCGGGTT CGTCCCCGTG
 RHG55'(2) TTATCAAACA TCTATTGGAA AGTCCCTATA GCGACTACGA TTGGCGAGTT CGTCCCCGTG

                    146                                                 205
SConsensus GTCGTCTTGG TCCCGCTGAC GACGACGATT ACGATAGTGA ACCAGTATTC ATTACAGTCA
 RHG55'(1) GTCGTCTTGG TCCCGCTGAC GACGACGATT ACGATAGTGA ACCAGTATTC ATTACAGTCA
 RHG55'(2) GTCGTCTGGG TCCCGCTGAC GACGACGATT ACGATAGCGA ACCAGTATTC ATTACAGTCA

                    206                                                 265
SConsensus ACATGTACTT GAGGAGTATW TCTAAAGTCG AYGATGTTAA TATGGARTAT TCRTTGCAYT
 RHG55'(1) ACATGTACTT GAGGAGTATT TCTAAAGTCG ACGATGTTAA TATGGAATAT TCATTGCATT
 RHG55'(2) ACATGTACCT AAGGAGTATA TCAAAAGTCG ACGATGTTAA TATGGAGTAT TCATTGCACT

                    266                                                 325
SConsensus TYACATTTCG AGAAGARTGG ATTGACGARA GGCYRTATTT CAAYAGCCCG ACGTTGAAAC
 RHG55'(1) TTACATTTCG AGAAGAGTGG ATTGACGAGA GGCTATATTT CAACAGCCCG ACGTTGAAAC
 RHG55'(2) TTACATTTCG AGAAGAATGG ATTGACGAGA GGCTGTATTT CAATAGCCCG ACGTTGAAAC

                    326                                                 385
SConsensus ATATYGTKCT GTCACCTGGA CAACGAATCT GGGTGCCCGA CACMTTCTTC CARAAYGAGA
 RHG55'(1) ATATCGTTCT GTCACCTGGA CAACGAATCT GGGTGCCCGA CACATTCTTC CAAAACGAGA
 RHG55'(2) ATATCGTGCT GTCACCTGGA CAACGAATAT GGGTGCCCGA CACTTTCTTC CAGAACGAGA
```

Figure 60, See legend on next page.

```
          386                                                    445
SConsensus AARATGGCRA GAAACATGAC ATCGATACTC CGAAYATTYT RATTCGGATA CATAAYGGYA
 RHG55'(1) AAGATGGCAA GAAACATGAC ATCGATACTC CGAACATTTT GATTCGGATA CATAACGGTA
 RHG55'(2) AAGATGGCGA GAAACATGAC ATCGATACTC CGAACATTCT GATTCGGATA CATAACGGCA

          446                                                    505
SConsensus CAGGAAAGAT WCTKTATTCM TGTCGGCTTA CTYTGACCCT GAGCTGTCCR ATGAGGTTGG
 RHG55'(1) CAGGAAAGAT ACTGTATTCA TGTCGGCTTA CTCTGACCCT GAGCTGTCCG ATGAGGTTGG
 RHG55'(2) CAGGAAAGAT ACTGTATTCG TGTCGGCTTA CTCTAACCCT GAGCTGTCCA ATGAGGTTGG

          506                                                    565
SConsensus CCGATTATCC GCTTGATGTA CAGACATGTG TWGTGGATTT TGCTTCATAC GCCTATACTA
 RHG55'(1) CCGATTATCC GCTTGATGTA CAGACATGTG TTGTGGATTT TGCTTCATAC GCCTATACTA
 RHG55'(2) CCGATTATCC GCTTGATGTA CAGACATGTG TAGTGGATTT TGCTTCATAC GCCTATACTA

                              566                              597
SConsensus CGAAAGACAT MGAATACGGA TGGAARRAGG AR
 RHG55'(1) CGAAAGACAT AGAATACGGA TGGAAGGAGG AA
 RHG55'(2) CAAAAGACAT CGAATACGGA TGGAAGGAGG AA
```

Figure 60, Alignment of HG5 5'-RACE products from avermectin-resistant *H. contortus*. The sequence of two individually amplified HG5 5' RACE products, from an avermectin-resistant population of *H. contortus*, were aligned together with the consensus sequence from an avermectin susceptible population. Key: **Y** codes either a C or a T, **M** codes either an A or a C, **R:** an A or a G, **S:** a G or a C, **K:** a G or a T and **W:** an A or a T. Nucleotides in uppercase are coding sequence whilst lower case nucleotides represent the 5' UTR.

Table 15, Variation between the 5' end RACE products amplified from avermectin susceptible and resistant isolates. Note that these values are for coding region only.

		HG5 5' ends isolated from avermectin resistant *H. contortus*			
		Clone 1		Clone 2	
		Nts (coding)	aa	Nts (coding)	Aa
Avermectin susceptible *H. contortus*	Clone 3	1.0 % (6/597)	0.50% 1/199	4.7 % (28/597)	1.51% 3/199
	Clone 8	5.2 % (31/597)	0.50% 1/199	4.5 % (27/597)	0.00% 0/199
	Clone 12	5.2 % (31/597)	1.01% 2/199	4.9% (29/597)	1.51% 3/199
Avermectin resistant *H. contortus*	Clone 1	-	-	-	-
	Clone 2	4.5 % (27/597)	0.50% 1/199	-	-

6.3 Discussion

The derivation of a consensus sequence for HG5 came from six individual HG5 cDNAs. This was achieved by amplifying three 5'- and three 3'-ends using a RACE-PCR technique. Comparison of sequences revealed as high as 5.86 % and 5.53 % nucleotide variation existed between 5' and 3' termini respectively. These values are slightly higher than the 4.49 % variation observed for the different HG4 amplified cDNAs (Chapter 3). The

translated 5' end HG5 sequence encoded by clones 8 & 3 each have one amino acid differing from the consensus whilst clone 12 has two. These may either represent polymorphic sites or PCR induced artefacts.

Similarly, the translated 3' end sequence is identical for two of the amplified clones with the third clone (seen in lane 10 of figure 57) conferring one amino acid mismatch with the consensus sequence. It may also be noted that even though clones 4 and 15 differ by having 68 nt mismatches across a sequence of 1281 nts, none of the variation is carried over to the translated sequence. Since the majority of variation is present at the nucleotide level it is likely that they are a result of polymorphism existing between the individual nematodes used to synthesis the cDNA.

The HG5 consensus sequence was found to be most similar to the *C. elegans* full-length glutamate-gated chloride channel subunits GBR-2A (62 % identical at the amino acid level), GBR-2B (57 %) and GluClα1 (56 %) (Laughton *et al.*, 1997b & Cully *et al.*, 1994). Two partial sequences, catalogued in the EMBL database, also show similarity to HG5, they have each been denoted GluClX and are believed to be filarial orthologues of GBR-2. GluClX from *D. immitis* is 71 % identical to HG5 across a 98 amino acid overlap. Likewise, the partial sequence from *O. volvulus* has 66 % identity with HG5 covering a 352 amino acid overlap. These percentage identities have been summarised in table 14.

The next objective will be to amplify a full-length cDNA of HG5 by designing gene specific primers and using PCR. If the sequence obtained is consistent with the consensus sequence, it can then be expressed in *Xenopus* oocytes. If HG5 is an α-like subunit, it is expected to form homomeric channels that are selectively responsive to avermectin at μM concentrations and co-expression with GluClβ should result in heteromeric channels gated by glutamate and potentiated by avermectin at nM values (Cully *et al.*,1994).

To date GluClα2s and GBR-2A have been localised to the pm4 and pm5 muscle cells of the pharynx (Horrovitz, pers. comm., Dent *et al.*, 1997). The spatial expression of HG5 will need to be determined. From *C. elegans* expression studies it can be predicted that HG5 may localise to the surface of the pm4 and pm5 cells in the pharynx. However, studies of HG4 expression, accomplished for this thesis, do not match the findings found in *C. elegans*. Therefore, it will be interesting to determine whether HG5 is co-expressed with HG4 on the surface on commissures present in the nervous system of the agriculturally important parasite.

GluClα1 subunits bind avermectin when expressed as homomeric channels in *Xenopus* oocytes (Cully *et al.*, 1994). Avermectin resistance may have developed due to a mutation in GluClα's ligand binding site. A number of residues encoded by the N-terminal extracellular domain of this protein have been predicted to participate in the formation of a binding site (Wolstenholme, 1997). It is possible that an alteration of these predicted residues may prevent the binding of avermectin to the receptor. Resistance may also have developed due

to a point mutation, converting an in-frame codon into a stop codon, as is the case seen for the *C. elegans arv-15* mutant. If HG5 is an α-like subunit it may possess the ability to avermectin. Comparison of these predicted sites from avermectin susceptible and resistant HG5 genes will establish any differences, which may prevent the drug binding.

The 5' end of HG5 from an avermectin resistant isolate was successfully amplified from two individual cDNAs. Comparison of these sequences with the HG5 consensus sequence from avermectin susceptible worms was accomplished unveiling that no difference exists at the amino acid level. Therefore the N-terminal extracellular domain of HG5 from avermectin resistant nematodes does not prevent the drug binding to the receptor.

7 Discussion

The work described in this thesis provides the first report of full-length cDNA sequences/clones of the glutamate-gated chloride channel subunits from parasitic nematodes. Interesting and provocative differences have been revealed between *C. elegans* and *H. contortus*, the latter being the parasitic worm most closely related to *C. elegans* (Blaxter *et al.*, 1998). These findings call into question the validity of extrapolating data obtained from *C. elegans* to parasites. The knowledge obtained in this study is a vital first step in the understanding of the structure and function of these channels as important drug targets.

The proteins coded by HG4 and HG5 share typical features with members of the TGIC superfamily. Each subunit possesses 4 hydrophobic transmembrane domains (denoted TM1 to TM4) and 2 highly conserved extracellular cysteines, which form a disulphide-bonded cys-loop. A second pair of cysteine residues is present further downstream of the cys-loop but upstream from TM1. These features are characteristic of inhibitory glutamate-gated chloride channel and glycine receptor subunits. Both cDNAs have been amplified with the knowledge that a splice leader sequence of 22 nucleotides, known as SL1, is present upstream of the initiation codon. Two N-linked glycosylation sites are coded by each subunit as well as potential phosphorylayion sites for either protein kinase C or casein kinase II existing along the intracellular loop between TM3 and TM4.

The HG4 cDNA is composed of 1756 base pairs, of which the first 29 nucleotides make up the 5' utr region including the SL1 sequence whilst the last 431nt constitute the 3' utr. The remaining 1296 base pairs code a polypeptide of 432 amino acid residues. This translated product is 80.25 % identical to the glutamate-gated chloride channel beta subunit, GluClβ. Such a high identity suggests that HG4 is the parasitic orthologue. In contrast, the HG5 cDNA varies in size due to the different lengths of 3' utr following the stop codon. Consistent between each of the amplified clones, a 25 nt 5' utr precedes a 1308 bp coding frame which when translated yields a 436 amino acid polypeptide chain. Depending on the clone, the length of the 3' utr may be 175, 177 or 253 nucleotides. Comparison of the HG5 polypeptide with related proteins catalogued in the database reveal that it is most similar to the glutamate gated chloride channel subunits being both α- and γ-like in nature. Highest full-length amino acid identities are with GBR-2A (62 %), GBR-2B (57 %) and GluClα1 (56 %).

The degree of polymorphism between each of the amplified cDNAs has been estimated by aligning the open reading frames. A high variation of 4.49 % has been calculated for HG4 clones and up to 5.86 % has been recorded between HG5 clones. For the former value, 26 nucleotides differ along a stretch of 579 nts. Upon translation only 1 out of the 26 differences confer an amino acid alteration. Similarly, for the HG5 clone, 35 nucleotides differed over a stretch of 597 nts, but only three of these confer an alteration at the amino acid level.

Amplification of full-length HG4 cDNAs from an avermectin-resistant isolate of *H. contortus* has been achieved. Comparison of sequence from the two populations establishes that no alteration exists at the translated level, possibly interfering with avermectin binding. Likewise, amplification of the 5' terminus of HG5 from a resistant isolate exhibits no variation at the amino acid level to the consensus sequence derived from susceptible nematodes. This confirms that the N-terminal domain, including the predicted determinants of the ligand-binding site, remained unaltered in HG5 amplified from a resistant population. To summarise, avermectin resistance developed by the isolate used in this study has not resulted from amino acid variation in either the HG4 subunit or the N-terminal extracellular domain of HG5. However, HG4 and HG5 may still play a role in the development of avermectin resistance. Further work needs to be done to amplify a full-length clone of HG5 from the resistant population to determine whether a point mutation exists, preventing drug binding. Also, corresponding genomic sequences should be isolated to compare promoter and intronic regions. Resistance may be a result of the up-regulation of subunit expression; this can be determined by Northern blots comparing HG4 or HG5 mRNA levels from avermectin-susceptible and -resistant populations.

If HG4 is the parasitic orthologue of GluClβ it is be predicted that expression in Xenopus oocytes as homomeric channels will respond to glutamate at equivalent mM concentrations in a reversible manner (Cully *et al.,* 1994). The consensus sequence of HG4 is in the process of being expressed in oocytes. As HG5 is a GluClα-like subunit, it is believed that expression of homomeric channels will respond irreversibly to avermectin at μM levels (Cully *et al.*, 1994). A full-length consensus sequence of HG5 needs to be cloned in future experiments for expression work to be possible. This will also enable examination of co-expressed HG4/HG5 heteromeric channels, which are predicted to form glutamate-gated chloride channels that are potentiated by avermectin at nanomolar concentrations.

In *C. elegans,* GluClβ has been localised to the to pm4 pharyngeal muscle cells where they form receptors with related subunits (Laughton *et al.*, 1997a). As HG4 is predicted to be the parasitic orthologue, it is expected that it will also be expressed at identical sites in *H. contortus.* This theory has been tested, as detailed in Chapter 4 and 5, by synthesising antibodies to a peptide designed to a site along the N-terminal domain of HG4, which displays high heterogeneity with related proteins.

Purified antibodies are able to specifically recognise the N-terminal domain of HG4 when expressed in a prokaryotic expression system. ELISA results corroborate these findings with purified anti-HG4 antibodies binding to the peptide antigen: RSTGGTQEQEILNELLSN. In contradiction to the expected localisation of HG4, exposure of collagenase treated *H. contortus* to a 1:10 dilution of anti-HG4 antibody does not result in specific binding to the pm4 and pm5 cells. Instead immunostaining of commissures and ventral & dorsal nerve cords are observed. More specifically commissures spanning the anterior of the worm to the mid-body region, above the vulva in female nematodes are recognised by anti-HG4 antibody.

The neuronal network for *C. elegans*, defined by White *et al.* (1989), enables the prediction of the neurones in *H. contortus,* which express HG4. These include the motor neurones DA1-DA4, VA1-VA3, AS1-AS3, VD1-VD7 and DD1-DD4. The former three classes are excitatory in nature releasing acetylcholine whilst the latter two classes are inhibitory, releasing GABA. DA, VA and AS motor neurones all receive synaptic input from the AVE interneurone which spans the ventral cord originating in the nerve ring and terminating immediately anterior to the vulva. From the observations described in this report it is proposed that the AVE interneurone releases glutamate at its synapses with the above mentioned motor neurones which in turn cross-communicate utilising the same neurotransmitter. It may be questioned why this network is only seen in the nervous system above the vulva in females and equivalent regions in the male. Commissures, spanning this region, cross talk with the sublateral cords. It is therefore possible that the presence of glutamate-gated chloride channels on motor neurones innervating these cords provide an additional form of regulation. This functionality may fine-tune the resulting potential that reaches the synapses.

According to Blaxter et al., (1998) phylogenetic calculations suggest that *H. contortus* is the parasitic worm most closely related to *C. elegans.* However the expression pattern observed for HG4 questions whether *C. elegans* is an ideal model in which to study the drug targeting associated with parasitic nematodes. GluClβ is expressed in the *C. elegans* pharynx with related subunits forming the avermectin target of inhibitory glutamate-gated receptors. Based solely on *C. elegans* findings, it has previously been proposed that avermectin causes starvation of the nematode (Geary *et al.,* 1993). The localisation in *H. contortus* of HG4, reveals a set of glutamate-gated chloride channels that may regulate locomotion of the anterior portion of the body via the sublateral cords. Avermectin may therefore target these receptors inducing paralysis of the worm leading to a rapid expulsion of worms from the host. It is postulated that the difference in spatial expression between HG4 and GluCiβ is a consequence of different promoters regulating the expression of the two subunits. Isolation of the genomic sequence of HG4 therefore needs to be accomplished for comparison with the GluClβ genomic sequence. An investigation into HG4 expression in *C. elegans* using a *lac-z* reporter construct is recommended. Expression of this construct, comprising the HG4 promoter, in the presence of X-gal will determine whether the difference in expression patterns is directly related to promoter regulation.

With the spatial expression of GluClα2A confined to pm4 and pm5 cells in the pharynx (Dent *et al.*, 1997), HG5 is also expected to be expressed in an equivalent locality in *H. contortus.* However, as HG4 expression is restricted to certain commissures and ventral & dorsal cords, it is possible that HG5 is co-expressed with HG4.

Future work should include the amplification of a full-length HG5 sequence from a resistant population of *Haemonchus contortus,* as there may be a genetic mutation situated down stream of the 5' end that may confer a non-functional subunit. Expression of both HG4 and HG5 subunits, as homomeric and heteromeric receptors in *Xenopus* oocytes should be done

to corroborate that these subunits form glutamate-gated chloride channels. Co-expression using HG2 and HG3 should also be addressed, including the effect of avermectin potency on each of the receptors formed from the various subunit combinations used.

Antisera raised against HG5, HG2 and HG3 will be useful for co-localisation studies. Results from these experiments is expected to determine whether the subunits associate together as glutamate-gated chloride channels along commissures. These results may also indicate whether there is a second population of channels existing on pm4 and pm5 pharyngeal muscles.

Appendix 1, Plasmid Maps

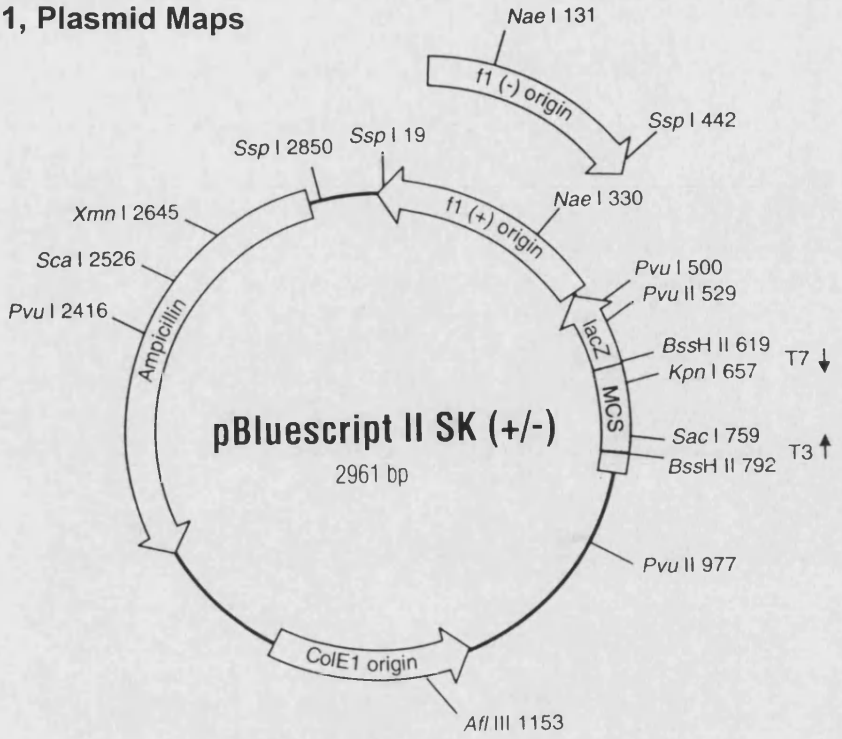

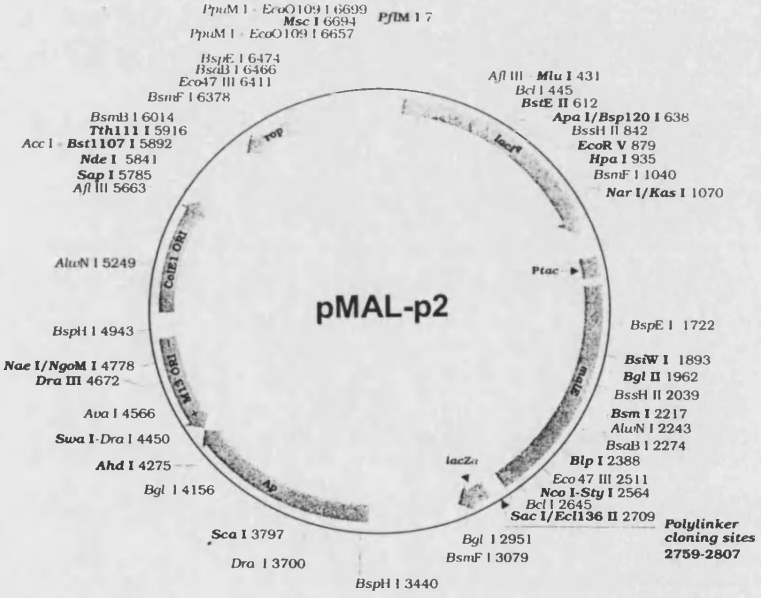

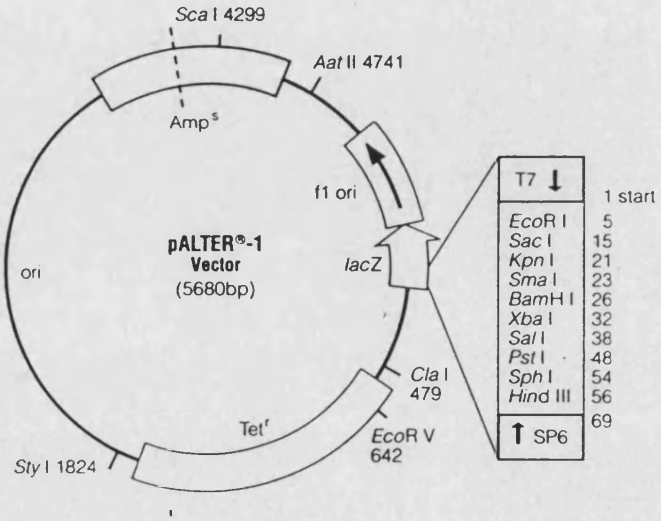

Appendix 2 Genetic Markers in *E. coli* strains

Marker	Description
Amy	Amylase
ara	Mutation destroys ability to catabolise arabinose
Cam^r	Chloramphenicol resistance due to inactivation by chloramphenicol acetyltransferase
endA1	Mutation in DNA-specific endonuclease I improves the quality of plasmid DNA isolations.
F'	Plasmid that carries a lacZ gene bearing deletions at its 5' end resulting in the synthesis of an inactive C-terminal ω-fragment of the β-galactosidase. Ideal for alpha-complementation.
gyrA46	Mutation in DNA gyrase subunit A, confers resistance to nalidixic acid.
hsdR17 (r_k^-,m_k^+)	Host specific restriction minus and modification positive; prevents cleavage of transformed DNA by the endogenous restriction endonuclease *EcoK* however modification by methylation can still occur.
lac	Unable to utilise lactose
LacI^q	Overproduces the lac repressor protein, inhibiting transcription from the lac promoter
LacZ	β-galactosidase
lacZΔM15	β-galactosidase carries a deletion of the 3' end of lacZ transcribes an inactive N-terminal fragment called an α-fragment, required for α-complementation
ProAB	Defective in proline metabolism, requires proline in minimal media in order to survive.
recA1	Recombination defective.
relA1	Allows RNA synthesis in the absence of protein synthesis.
rpsL	Bears a mutation in the S12 subunit of the 30S ribosome conferring resistance to streptomycin.
SupE44	Nonsense supression of the amber termination codon (UAG) where translation of message does not always stop when the ribosome encounters an amber codon. A mutant tRNA gene causes the substitution of a glutamine at this position allowing translation to continue.
thi	Unable to biosynthesis thiamine, requires thiamine (vitamin B1) in minimal media for growth
Tn10(tetR)	Contains the TN10 transposon, confering tetracycline resistance by active efflux of drug from the cell
traD36	Mutation of the Transfer factor prevents the tranfer of F' episome other plasmids and or chromosomal DNA to other cells.

Appendix 3, Primers

Primer	Size	Sequence
RoRi	28 mer	5′ GAC TAC GTT AGC ATC TAG AAT TCT CGA G 3′
SL1	22 mer	5′ GGT TTA ATT ACC CAA GTT TGA G 3′
HG4 GSSP1	21 mer	5′ ATG CAG CTC ACC CTA AAA AGG 3′
HG4 GSSP2	24 mer	5′ TAC TAC CTG GTC CAG TTG TAC GGT 3′
HG4 GSSP3	21 mer	5′ GAC ACC TTT TTC CCG ACC GAA 3′
HG4 GSAP1	22 mer	5′ ACC GGT GGC AGT TTA GCA TTG A 3′
HG4 GSAP2	22 mer	5′ GCA TGT GAC AGG AGC TGG TAA T 3′
HG4-CSP1	35 mer	5' GTC ATA GCG GCC GCG ATC TTG AAT GTC ACA GTA TA 3'
HG4-CAP1	32 mer	5' TGC ACT TCT AGA AAA TAC TGT TGT GTG ATG ATG GC 3'
HG4 MUTS	17 mer	5′ GGC GAT CCA CTG GTG GC 3′
HG4 pMALS	24 mer	5′ GAC GCA GTC GAC ATG TCA CAG TAT 3′
HG4 pMALA	26 mer	5′ TGC ACT CTG CAG TTA ATT GGT ATG GC 3′
HG5 GSSP1	20 mer	5′ GAT ATC GAT ACT CCG AAC AT 3′
HG5 GSSP2	28 mer	5′ TTC TGT TGC ATT TCA CGC GGT CCG AAG G 3′
HG5 GSSP3	22 mer	5′ ACC GAT CCA GAA CAA AGA TGG C 3′
HG5 GSAP1	20 mer	5′ CTG ACG TGC AAT TAC CGG TT 3′
HG5 GSAP2	21 mer	5′ CTC CGT TCC TTA TAG CGT ATT 3′
KS	17 mer	5′ TCG AGG TCG ACG GTA TC 3′
T3	20 mer	5′ AAT TAA CCC TCA CTA AAG GG 3′
T7	22 mer	5′ GTA ATA CGA CTC ACT ATA GGG C 3′

Appendix 4, Avermectin Resistant *H. contortus*

An avermectin resistant field isolate of *Haemonchus contortus* was selected for RNA extraction. This particular isolate originated from the White River in South Africa (van Wyk & Malan, 1988). Van Wyk & Malan reported the effect of infecting 5 helminth-free sheep each with a single dose of 5000 larvae. Thirty days after infection, 0.2 mg/kg body weight of Ivermectin, was administered orally. The five sheep were slaughtered 7 to 10 days after treatment and worm counts were performed. A 33% reduction in *Haemonchus contortus* numbers was calculated thus showing some degree of resistance to ivermectin. The same isolate was used to infect a Dorset lamb followed by administration of 200 μg/kg ivermectin. In accordance this treatment did not significantly affect egg counts (Coles, pers. comm).

References

Adamson, M. L. 1987. *Phylogenetic analysis of the higher classification of the Nematoda. Canadian Journal of Zoology.* 65:1478-1482.

Ajuh, P. M. & Egwang, T. G. 1994. Cloning of a cDNA encoding a putative nicotinic acetylcholine receptor subunit of the human filarial parasite *Onchocerca volvulus. Gene.* 144: 127-129.

Albertson, D. G. & Thomson, J. N. 1976. The pharynx of *Caenorhabditis elegans. Philosophical Transactions of the Royal Society of London B.* 275: 299-325.

Albiez, E. J., Walter, G., Kaiser, A., Ranque, P., Newland, H. S., White, A. T., Greene, B. M., Taylor, H. R., Büttner, D. W. 1988. Histological examination of onchocercomata after therapy with ivermectin. *Tropical Medicine & Parasitology.* 39: 93-99.

Alfonso, A., Grundahl, K., Duerr, J. S., Han, H. P. & Rand, J. B.1993. The *Caenorhabditis elegans unc-17* gene: a putative vesicular acetylcholine transporter. *Science.* 261(5121): 617-619.

Alfonso, A., Grundahl, K., McManus, J. R. & Rand, J. B. 1994. Cloning and characterisation of the choline acetyltransferase structural gene (cha-1) from *C. elegans. Journal of Neuroscience.* 14(4): 2290-2300.

Amin, J. & Weiss, D. S. 1993. $GABA_A$ receptor needs two homologous domains of the β-subunit for activation by GABA but not by pentobarbital. *Nature.* 366: 565-569.

Anderson R. C. 1992. Nematode Parasites of Vertebrates - their development and transmission. C.A.B International, Wallingford.

Arena, J. P., Liu, K. K., Paress, P. S. & Cully, D. F. 1991. Avermectin-sensitive chloride currents induced by *Caenorhabditis elegans* RNA in *Xenopus* oocytes. *Molecular Pharmacology.* 40: 368-374.

Arena, J. P., Liu, K. K., Paress, P. S., Schaeffer, J. M. & Cully, D. F. 1992. Expression of a glutamate-activated chloride current in Xenopus oocytes injected with *Caenorhabditis elegans* RNA: evidence for modulation by avermectin. *Molecular Brain Research.* 15: 339-348.

Arena, J. P. 1994. Expression of *Caenorhabditis elegans* mRNA in *Xenopus* oocytes: a model system to study the mechanism of action of avermectin. Parasitology Today. 10: 35-37.

Arena, J. P., Liu, K. K., Paress, P. S., Frazier, E. G., Cully, D. F., Mrozik, H. & Schaeffer, J. M. 1995. The mechanism of action of avermectins in *Caenorhabditis elegans*: correlation

between activation of glutamate-sensitive chloride current, membrane binding, and biological activity. *Journal of Parasitology.* 81(2) 286-294.

Avery, L. & Thomas J. H. 1997. Feeding and Defecation. In, Riddle, D. L., Blumenthal, T., Meyer, B. J., Priess, J. R., eds., *C. elegans* II, Cold Spring Harbor Press. Cold spring Harbor.

Awadzi, K., Dadzie, K. Y., Schulz-Key, H., Gilles, H. M., Fulford, A. J. & Aziz, M. A. 1986. The chemotherapy of onchocerciasis XI. A double blind comparative study of ivermectin and diethylcarbamazine and placebo in human anchocerciasis in Northern Ghana. *Annals of Tropical Medicine & Parasitology.* 80: 433-442.

Balan J. Krizkova L. Nemec P. Vollek V. 1974. Production of nematode-attracting and nematicidal substances by predacious fungi. *Folia Microbiologica.* 19(6):512-9.

Bamber B. A., Twyman, R. E., Tingey, J. J. & Jorgensen, E. M. 1997. Unc-49: one gene, multiple GABA receptors. *Society for Neuroscience Abstracts.* 23: 114.

Barnes, E. H., Dobson, R. J. & Barger, I. A. 1995. Worm control and anthelmintic resistance: adventures with a model. *Parasitology Today.* 11: 56-63.

Bascal, Z. A., Montgomery A., Holden-Dye, L., Williams, R. G., Thorndyke, M. C. & Walker, R. J. 1996. NADPH diaphorase activity in peptidergic neurones of the parasitic nematode, *Ascaris suum. Parasitology.* 112(Pt 1):125-34.

Behnke, J. M., Rose, R. & Garside, P. 1993. Sensitivity to ivermectin and pyrantel of *Ancylostoma ceylanicum* and *Necator americaus. International Journal for Parasitology.* 23: 945-952.

Bektesh, S., Van Doren, K. & Hirsh, D. 1988. Presence of the *Caenorhabditis elegans* spliced leader on different mRNAs and in different genera of nematodes. *Genes & Development.* 2: 1277-1283.

Bermudez, I., Hawkins, C. A., Taylor, A. M. & Beadle, D. J. 1991. Actions of insecticides on the insect GABA receptor complex. *Journal of Receptor Research.* 11: 221-232.

Bird, A. F. & Bird, J. 1991. *The Structure of Nematodes.* 2nd Edition. Academic Press Inc., New York.

Blair, L. S. & Campbell, W. C. 1979. Efficacy of avermectin B1a against microfilariae of *Dirofilaria immitis. American Journal of Veterinary Research.* 40(7): 1031-1032.

Blair, L. S. & Campbell, W. C. 1980. Efficacy of Ivermectin against *Dirofilaria immitis* larvae in dogs 31, 60, and 90 days after injection. *American Journal of Veterinary Research.*

41(12): 2108.

Blair, L. S. & Campbell, W. C. 1981. Immunisation of ferrets against *Dirofilaria immitis* by means of chemically abbreviated infections. *Parasite Immunology.* 3(2): 143-147.

Blanchflower, S. E., Banks, R. M., Everett, J. R., Manger, B. R. & Reading, C. 1991. New paraherquamide antibiotics with anthelmintic activity. *Journal of Antibiotics.* 44: 492-497.

Blaxter, M. L., Page, A. P., Rudin, W. & Maizels, R. M. 1992. Nematode Surface Coats:Actively Evading Immunity. Parasitology Today, 8(7): 243-247.

Blaxter, M. L. & Bird, D. 1997. Parasitic Nematodes. In, Riddle, D. L., Blumenthal, T., Meyer, B. J., Priess, J. R., eds., *C. elegans* II, Cold Spring Harbor Press. Cold spring Harbor.

Blaxter, M. L., De Ley, P., Garey, J. R., Liu, L. X., Scheldeman, P., Vierstraete, A., Vanfleteren, J. R., Mackey, L. Y., Dorris, M., Frisse, L. M., Vida, J. T. & Thomas, W. K. 1998. A molecular evolutionary framework for the phylum Nematoda. *Nature.* 392: 71-75.

Bradford M. M. 1976. A rapid and sensitive method for the quantitation of microgram quantities of protein utilizing theprinciple of protein-dye binding. *Analytical Biochemistry.* 72:248-54.

Brownlee, D. J. A., Fairweather, I., Johnston, C. F. & Shaw, C. 1994. Immunocytochemical demonstration of peptidergic and serotoninergic components in the enteric nervous system of the roundworm, *Ascaris suum* (Nematoda, Ascaroidea). *Parasitology.* 108: 89-103.

Burg, R. W., Miller, B. M., Baker, E. E.,Birnbaum, J., Currie, S. A., Hartman, R., Kong, Y. L., Monagham, R. H., olsen, G., Putter, I., Tunac, J. B., Wallick, H., Stapley E. O., Oiwa, R. & Omura, S. 1979. Avermectins, a new family of potent anthelmintic agents: producing organism and fermentation. *Antimicrobial Agents and Chemotherapy.* 15: 361-367.

Chalfie, M., Tu, Y., Euskirchen, G., Ward, W. W. & Prasher, D. C. 1994. Green fluorescent protein as a marker for gene expression. *Science.* 263: 802-805.

Chen. W., Terada, M. & Cheng, J. T. 1996, Characterisation of subtypes of gamma-aminobutyric acid receptors in an *Ascaris* muscle preparation by binding assays and binding of PF1022A, a new anthelmintic, on the receptors. *Parastology Research.* 82: 97-101.

Chomczynski, P. & Sacchi, N. 1986. Single step Method of RNA isolation by guanidinium thiocyanate-phenol-chloroform extraction. *Analytical Biochemistry.* 162: 156-159.

Claudio, T., Ballivet, M., Patrick, J. & Heinenmann, S. 1983. Nucleotide and deduced amino acid sequences of Torpedo californica acetylcholine receptor γ-subunit. *Proceedings of the National Academy of Sciences of the USA.* 80: 1111-1115.

Coen. D, M. & Scharf, S. J. 1990. The Polymerase Chain Reaction. In, John Wiley & Sons, *Current Protocols in Molecular Biology*, New York, USA.

Coles, G. C., East, J. M. & Jenkins, S. N. 1975. The mechanism of action of the anthelmintic levamisole. *Genetic Pharmacology.* 6: 309-313.

Coles, G. C., Papadopoulus, E. & Himonas, C. A. 1995. Tubulin resistance and worms. *Parasitology Today.* 11: 183-184.

Conder, G. A. & Campbell, W. C. 1995. Chemotherapy of nematode infections of veterinary importance, with special reference to drug resistance. *Advances in Parasitology.* 35: 1-84.

Conder, G. A., Zielinski, R. J., Johnson, S.S., Kuo, M. -S. T., Cox, D. L., Marshall, V. P., Haber, C. L., DiRoma, P. J., Nelson, S. J., Conklin, R. D., Lee, B. L., Geary, T. G., Rothwell, J. T. & Sangster, N. C. 1992. Anthelmintic activity of dioxapyrrolomycin. *Journal of Antibiotics.* 45: 977-983.

Crompton, D. W. & Joyner, S. M. 1980. Parasitic Worms, Wykeham Publications, Oxford, UK.

Cookson, E. Tang. L. & Selkirk, M. E. 1993, Conservation of primary sequence of gp29, the major soluble cuticular glyciprotein, in three species of lymphatic filariae. *Molecular and Biochemical Parasitology.* No 58, p155-160.

Cross, H. F., Bronsvoort. B. M., Wahl, G., Renz, A., Achukwi, D. & Trees, A. J. 1997. The entry of ivermectin and suramin into *Onchocerca ochengi* nodules. *Annals of Tropical Medicine & Parasitology.* 91(4): 393-401.

Cull-Candy, S. G. & Usherwood, P. N. R. 1973. Two populations of L-glutamate receptors on locust muscle fibres. *Nature New Biology.* 246: 62-64.

Cully, D. F., Vassilatis, D. K., Lui, K. K., Paress, P. S., Van der Ploeg, L. L., Schaeffer, J. M. & Arena, J. P. 1994. Cloning of an avermectin-sensitive glutamate-gated chloride channel from *Caenorhabditis elegans. Nature.* 371: 707-711.

Cully, D. F., Wilkinson, H., Vassilatis, D. K., Etter, A. & Arena J. P. 1996a. Molecular biology and electrophysiology of glutamate-gated chloride channels of vertebrates. *Parasitology.* 113: S191-S200.

Cully, D. F., Paress, P. S., Lui, K. K., Schaeffer, J. M. & Arena, J. P. 1996b. Identification of a *Drosophila melanogaster* glutamate-gated chloride channel sensitive to the antiparasitic agent avermectin. *The Journal of Biological Chemistry.* 271(33): 20187-20191.

Davis, R. E. 1996. Spliced leader RNA trans-splicing in metazoa. Parasitology Today. 12(1): 33-40.

Del Castillo, J. , De Mello, W. C. & Morales, T. 1964. Mechanism of the paralyzing action of piperazine on *Ascaris* muscle. *British Journal of Pharmacology.* 22: 463-477.

Dent, J. A., Davis, M. W. & Avery, L. 1997. *arv-15* encodes a chloride channel subunit that mediates inhibitory glutamatergic neurotransmission and ivermectin sensitivity in *C. elegans. EMBO Journal.* 6(19): 5867-5879.

Driscoll, M., Dean, E., Reilly, e, Bergholz, E. & Chalfie, M. 1989. Genetic and molecular analysis of a *Caenorhabditis elegans* β-tubulin that conveys benzimidazole sensitivity. *Journal of Cell Biology.* 109: 2993-3003.

Duke, B. O. L., Zea-Flores, G., Castro, J., Cupp, E. W. & Muñoz, B. 1990. Effects of multiple monthly doses of ivermectin on adult Onchocerca volvulus. *American Journal of Tropical Medicine and Hygiene.* 43(6): 657-664.

Duke, B. O. L., Zea-Flores, G., Castro, J., Cupp, E. W. & Muñoz, B. 1991a. Comparison of the effects of a single dose and of four six-monthly doses of ivermectin on adult Onchocerca volvulus. *American Journal of Tropical Medicine and Hygiene.* 45(1): 132-137.

Duke, B. O. L., Pacqué, M. C., Muñoz, B., Greene, B. M. & Taylor, H. R. 1991b. Viability of adult *Onchocerca volvulus* after six 2-weekly doses of ivermectin. *Bulletin of the World Health Organisation.* 69(2): 163-168.

Emmons, S. W., Klass, M. R., Hirsh, D. 1979. Analysis of the constancy of DNA sequences during development and evolution of the nematode *Caenorhabditis elegans. Proceedings of the National Academy of Sciences of the United States of America.* 76(3):1333-7.

Etter, A., Cully, D. F., Schaeffer, J. M., Lui, K. K. & Arena, J. P. 1996. An amino acid substitution in the pore region of a glutamate-gated chloride channel enables the coupling of ligand binding to channel gating. *The Journal of Biological Chemistry.* 271(27): 16035-16039.

Fleming, J. T., Squire, M. D., Barnes, T. M., Tornoe, C., Matsuda, K., Ahnn, J., Fire, A., Sulston, J. E., Barnard, E. A., Sattelle, D. B. & Lewis, J. A. 1997. Caenorhabditis elegans levamisole resistance genes lev-1, unc-29, and unc-38 encode functional nicotinic acetylcholine receptor subunits. *The Journal of Neuroscience.* 17(15): 5843-5857.

Fire, A., White Harrison, S. & Dixon, D. 1990. A modular set of *lacZ* fusion vectors for studying gene expression in *Caenorhabditis elegans. Gene.* 93: 189-198.

Frohman, M. A., Dush, M. K. & Martin, G. R. 1988. Rapid production of full-length cDNAs from rare transcripts: Amplification using a single gene-specific oligonucleotide primer. *Proceedings of the National Academy of Sciences of the USA.* 85: 8998-9002.

Frohman, M. A. & Martin, G. R. 1989. Rapid amplification of cDNA ends using nested PCR. *Technique.* 1(3): 165-170.

Geary, T. G., Sims, S. M., Thomas, E. M., Vanover, L., Davis, J. P., Winterrowd, C. A., Klein, R. D., Ho, N. F. H. & Thompson, D. P. 1993. *Haemonchus contortus*: Ivermectin-induced paralysis of the pharynx. *Experimental Parasitology.* 77: 88-96.

Geerts, S. Coles, G. C. & Gryseels, B. 1997. Anthelmintic resistance in human helminths: Learning from the problems with worm control in livestock. *Parasitology Today.* 13(4): 149-151.

Grabley, S., Hammann, P., Thiericke, R., Wink, J., Philipps, S. & Zeeck, A. 1993. Secondary metabolites by chemical screening. 21. Clonostachydiol, a novel anthelminic macrodiolide from the fungus Clonostachys cylindrospora (strain FH-A 6607). *Journal of Antibiotics.* 46: 343-345.

Grønvold, J. Wolstrup, J. Nansen, P. Henriksen, S. A. 1993. Nematode-trapping fungi against parasitic cattle nematodes. *Parasitology Today.* 9(4): 137-140

Gutteridge, W. E. 1993. Chemotherapy. In Cox, F. E. G *eds., Modern Parasitology, A text book of parasitology.* 2nd Edition, Blackwell Scientific Pubilcations, Oxford, UK.

Harvey, R. J., Vreugdenhil, E., Zaman, S. H., Bhandal, N. S., Usherwood, P. N. R., Barnard, E. A. & Darlison, M. G. 1991. Sequence of a functional invertebrate $GABA_A$ receptor subunit which can form a chimeric receptor with a vertebrate α subunit. *The EMBO Journal.* 10(11): 3239-3245.

Hoekstra, R., Visser, A., Wiley, L. J. Weiss, A. S., Sangster, N. C. & Roos, M. H. 1997. Characterisation of an acetylcholine receptor gene of *Haemonchus contortus* in relation to levamisole resistance. *Molecular and Biochemical Parasitology.* 84: 179-187.

Hodgkin, J. Plasterk, R. H. A. & Waterston, R. H. 1995. The nematode *Caenorhabditis elegans* and its genome. *Science.* 270: 410-414

Holding, C. & Monk, M. 1990. Detection of a single copy gene sequence in a single cell by PCR amplification. *Genetical Research.* 55: 120.

Holden-Dye, L., Hewitt, G. M., Wann, K. T., Krogsgaard-Larsen, P. & Walker, R. J. 1988. Studies involving avermectin and the 4-aminobutyric acid (GABA) receptor of *Ascaris suum* muscle. *Pesticide Science.* 24: 231-245.

Holden-Dye, L. & Walker, R. J. 1990. Avermectin and avermectin derivatives are antagonists at the 4-aminobutyric acid (GABA) receptor on the somatic muscle cells of *Ascaris*; is this the site of anthelmintic action? *Parasitology.* 101: 265-271.

Hong, C., Hunt, K. R. & Coles, G. C. 1996. Occurrence of anthelmintic resistant nematodes on sheep farms in England and Goat farms in England and Wales. *Veterinary Record.* 139: 83-86.

Huganir, R. L. & Greengard, P. 1987. Regulation of receptor function by protein phosphorylation. *TIPS.* 8: 472-477.

Hutchinson, C. A., Phillips, S., Edgell, M. H., Gillam, S., Jahnke, P. & Smith, M. 1978. Mutagenesis at a specific position in a DNA sequence. *Journal of Biological Chemistry.* 253(18): 6551-6560.

Jeffrey, H. C. & Leech. R. M. 1972, *Atlas of medical helminthology and protozoology.* 2nd Edition, Churchill Livingstone, Oxford, UK.

Johnson, D. C. & Stretton, A. O. W. 1985. Localisation of choline acetyltransferase within identified motor neurones of the nematode *Ascaris. The Journal of Neuroscience.* 5(8): 1984-1992.

Johnson, D. C. & Stretton, A. O. W. 1987. GABA-immunoreactivity in inhibitory motor neurones of the nematode Ascaris. *The Journal of Neuroscience.* 7(1): 223-235.

Kass, I. S., Wang, C. C., Walrond, J. P. & Stretton, A. O. W. 1980. Avermectin B_{1a}, a paralysing anthelmintic that affects interneurones and inhibitory motor neurones in *Ascaris. Proceedings in the National Academy of Sciences USA.* 77(10): 6211-6215.

Kass, I. S., Stretton, A. O. W & Wang, C. C. 1984. The effects of avermectin and drugs related to acetylcholine and 4-aminobutyric acid on neurotransmission in *Ascaris suum. Molecular & Biochemical Parasitology.* 13(2): 213-215.

Keating, C. D., Holden-Dye, L., Thorndyke, M. C., Williams, R. G., Mallett, A. & Walker, R. J. 1995. The FMRFamide-like neuropeptide AF2 is present in the parasitic nematode *Haemonchus contortus. Parasitology.* 111: 515-521.

Krause, M. & Hirsh, D. 1987. A trans-spliced leader sequence on actin mRNA in *C. elegans.*

Cell. 49: 753-761.

Kreienkamp, H-J., Maeda, R. K., Sine, S. M. & Taylor, P. 1995. Intersubunit contacts governing assembly of the mammalian nicotinic acetylcholine receptor. *Neuron.* 14: 635-644.

Kwa, M. S. G., Veenstra, J. G. van Dijk, M. & Roos, M. H. 1995. β-Tubulin genes from the parasitic nematode Haemonchus contortus modulate drug resistance *in Caenorhabditis elegans. Journal of Molecular Biology.* 246: 500-510.

Lacey, E. & Gill, G. H. 1994. Biochemistry of benzimidazole resistance. *Acta Tropica.* 56: 245-262.

Laughton, D. L. 1993. A Characterisation of nematode neuroreceptors. *PhD Thesis University if Bath.*

Laughton, D. L., Amar, M., Thomas, P., Towner, P., Harris, P., Lunt, G. G. & Wolstenholme A. J. 1994. Cloning of a putative inhibitory amino acid receptor subunit from the parasitic nematode *Haenomchus contortus. Receptors and Channels.* 2: 155-163.

Laughton, D. L., Wheeler, S. V., Lunt, G. G. & Wolstenholme, A. J. 1995. The β-subunit of *Caenorhabditis elegans* avermectin receptor responds to glycine and is encoded by chromosome 1. *Journal of Neurochemistry.* 64(5): 2354-2357.

Laughton, D. L., Lunt, G. G. & Wolstenholme, A. J. 1997a. Reporter gene constructs suggest that the *Caenorhabditis elegans* avermectin receptor β-subunit is expressed solely in the pharynx. *The Journal of Experimental Biology.* 200: 1509-1514.

Laughton, D. L., Lunt, G. G. & Wolstenholme, A. J. 1997b. Alternative splicing of a *Caenorhabditis elegans* gene produces two novel inhibitory amino acid receptor subunits with identical ligand binding domains but different ion channels. *Gene.* 201: 119-1125.

Lewis. J. A., Wu. C. -H., Levine, J. H. & Berg, H. 1980. Levamisole-resistant mutants of the nematode *Caenorhabditis elegans* appear to lack pharmacological acetylcholine receptors . *Neuroscience.* 5: 967-989.

Lewis, J. A., Elmer, J. S., Skimming, J., McLafferty, S., Fleming, J. & McGee, T. 1987. Cholinergic receptor mutants of the nematode *Caenorhabditis elegans. The Journal of Neuroscience.* 7: 3059-3071.

Lewis. J. A. & Fleming, J. T. 1995. Chapter 1 Basic Culture Methods. *Ceanorhabditis elegans, Modern Biological analysis of an organism* edited by Epstein, H. F. & Shakes, D. C. Academic Press, Inc.

Li, H., Avery, L., Denk, W. & Hess, G. P. 1997. Identification of chemical synapses in the pharynx of Caenorhabditis elegans. *Proceedings of the National Academy of Sciences of the USA.* 94: 5912-5916.

Lichtenfels, J. R., Pilitt, P. A. & Hoberg, E. P. 1994. New morphological characters for identifying individual specimens of *Haemonchus* spp. (Nematoda: Trichostrongyloidae) and a key to species in ruminants of North America. Journal of Parasitology. 80(1): 107-119.

Martin, R. J. 1993. Neuromuscular transmission in nematode parasites and antinematodal drug action. *Pharmacology & Therapeutics.* 58(1):13-50.

Martin, R. J. & Pennington, A. 1989. A patch clamp study of effects of dihydroavermectin on *Ascaris* muscle. *British Journal of Pharmacology.* 98: 747-756.

Martin, R. J., Valkanov, M. A., Dale V. M. E., Robertson A. P. & Murray, I. 1996. Electrophysiology of *Ascaris* muscle and anti-nematodal drug action. Parasitology. 113: S137-S156.

McIntire, S. L., Jorgensen, E., Kaplan. J. & Horvitz., H. R. 1993a. Genes required for GABA function in *Caenorhabditis elegans. Nature.* 364: 334-337.

McIntire, S. L., Jorgensen, E., Kaplan. J. & Horvitz., H. R. 1993b. The GABAergic nervous system of *Caenorhabditis elegans. Nature.* 364: 337-341.

McKellar, Q. A. & Benchaoui, H. A. 1996. Avermectins and milbemycins. *Journal of Veterinary Therapeutics.* 19: 331-351.

McLaren, D. J. 1976. Nematode sense organs. *Advances in Parasitology.* 14: 195-265

Miller, D. M. & Shakes, D. C. 1995. Immunofluorescence microscopy. In, Epstein, H. F. & Shakes, D. C. eds., *Caenorhabditis elegans*: Modern Biological Analysis of an organism. Academic Press.

Moore, D. D. 1987. Construction of recombinant DNA libraries. In, John Wiley & Sons, *Current Protocols in Molecular Biology*, New York, USA.

Munn, E. A., Greenwood, C. A. & Coadwell, W. J. 1987. Vaccination of young lambs by means of a protein fraction extracted from *H. contortus. Parasitology.* 94: 385-397.

Nansen P. Grønvold J. Henriksen SA. Wolstrup J. 1988. Interactions between the predacious fungus *Arthrobotrys oligospora* and third-stage larvae of a series of animal-parasitic nematodes. *Veterinary Parasitology.* 26(3-4):329-337.

Noda, M., Takahashi, H., Tanabe, T., Toyosato, M., Furutani, Y., Hirose, T., Asai, M., Inayama, S., Miyata, T. & Numa, S. 1982. Primary structure of α-subunit precursor of *Torpedo californica* acetylcholine receptor deduced from cDNA sequences. *Nature* 299: 793-797.

Noda, M., Takahashi, H., Tanabe, T., Toyosato, M., Kikyotani, S., Hirose, T., Asai, M., Takashima, H., Inayama, S., Miyata, T. & Numa, S. 1983a. Primary structure of β and δ subunit precursors of *Torpedo californica* acetylcholine receptor deduced from cDNA sequences. *Nature.* 301: 251-255.

Noda, M., Takahashi, H., Tanabe, T., Toyosato, M., Kikyotani, S., Furutani, Y., Hirose, T., Takashima, H., Inayama, S., Miyata, T. & Numa, S. 1983b. Structural homology of *Torpedo californica* acetylcholine receptor subunits. *Nature.* 302: 528-532.

Nomoto, H., Takahashi, N., Nagaki, Y., Endo, S., Arata, Y. & Hayashi, K. 1986. Carbohydrate structures of acetylcholine receptor from *Torpedo californica* and distribution of oligosaccharides among the subunits. *European Journal of Biochemistry.* 157: 233-242.

Novak, J. & Vanek, Z. 1992. Screening for a new generation of anthelmintic compounds. *In vitro* selection of the nematode *Caenorhabditis elegans* for ivermectin resistance. *Folia Microbiologica.* 37(3): 237-238

Ortells, M. O. & Lunt, G. G. 1994. The transmembrane region of the nicotinic acetylcholine receptor: is it an all-helix bundle? *Receptors and Channels.* 2: 53-59.

Ou, X., Thomas, R., Chacón, M. R., Tang, L. & Selkirk, M. E. 1995. *Brugia malayi*: differential Susceptibility to and metabolism of hydrogen peroxide in adults and microfilariae. *Experimental Parasitology.* 80: 530-540.

Overend, D. J., Phillips, M. L., Poulton, A. L. & Foster, C. E. D. 1994. Anthelmintic resistance in Australian sheep nematode populations. *Australian Veterinary Journal.* 71: 117-121.

Perkins, L. A., Hedgecock, E. M., Thomson, J. N. & Culotti, J. G. 1986. Mutant sensory cilia in the nematode *Caenorhabditis elegans. Developmental Biology.* 117:456-487.

Platt, H. M. 1994. Foreward. In, S. Lorenzen, ed, The phylogenetic systematics of free living nematodes, pp. i-ii. The Royal Society of London.

Plaisier, A. P., Alley, E. S., Boatin, B. A., Van Oortmarssen, G. J., Remme, H., De Vlas, S. J., Bonneux, L. & Habbema, J. D. F. 1995. Irreversible effects of ivermectin on adult

parasites in Onchocercerciasis patients in the Onchocerciasis Control Programme in West Africa. *Journal of Infectious Diseases.* 172: 204-210.

Raizen, D. M. & Avery, L., 1994. Electrical Activity and behaviour in the Pharynx of *Caenorhabditis elegans. Neuron.* 12: 483-495.

Raizen, D. M., Lee, R. Y. N. & Avery, L. 1995. Interacting genes required for pharyngeal excitation by motor neurone MC in *Caenorhabditis elegans. Genetics.* 141(4): 1365-1382.

Rajasekeriah, G. R., Deb, K. R., Dhage. K. R. & Bose, S. 1989. Response to adult Necator americanus to some known anthelmintics in hamsters. *Annals of Tropical Medicine and Parasitology.* 83: 279-285.

Rand, J. B. & Nonet, M. L. 1997. Synaptic Transmission. In, Riddle, D. L., Blumenthal, T., Meyer, B. J., Priess, J. R., eds., *C. elegans* II, Cold Spring Harbor Press. Cold spring Harbor.

Reinemeyer, C. R., Rohrbach, B. W., Grant, V. M. & Radde, G. L.1992. A survey of the ovine parasite control practice in Tennesse. *Veterinary Parasitology.* 42: 111-122.

Revah, F., Galzi, J.-L., Giraudat, J., Haumont, P.-Y., Lederer, F. & Changeux, J.-P. 1990. The non-competitive blocker [^{3}H]chlorpromazine labels three amino acids of the acteylcholine receptor γ subunit: Implications for the α–helical organisation of regions MII and for the structure of the ion channel. *Proceedings of the National Academy of Sciences of the USA.* 87: 4675-4679.

Richards, J. C., Behnke, J. M. & Duce, I. R. 1995. *In vitro* studies on the relative sensitivity to ivermectin of *Necator americanus* and *Ancylostoma ceylanicum. International Journal for Parasitology.* 25(10): 1185-1191.

Rogers, W. P. 1968. Neurosecretory granules in the infective stage *of Haemonchus contortus. Parasitology.* 58: 657-662.

Rohrer, S. P., Birzin, E. T., Eary, C. H., Schaeffer, J. M. & Shoop, W. L. 1994. Ivermectin binding sites in sensitive and resistant *Haemonchus contortus. Journal of Parasitology.* 80(3): 493-497.

Rohrer, S. P., Birzin, E. T., Costa, S. D., Arena J. P., Hayes, E. C. & Schaeffer, J. M. 1995. Identification of neurone-specific ivermectin binding sites in *Drosophila melanogaster* and *Schistocerca americana.* Insect Biochemistry & Molecular Biology. 25(1): 11-17.

Sanger, F., Nicklen, S. & Coulson, A. R. 1977. DNA sequencing with chain-terminating

inhibitors. . *Proceedings of the National Academy of Sciences of the USA.* 74 (12): 5463-5467.

Sangster, N. C., Davis, C. W. & Collins, G. H. 1991. Effects of cholinergic drugs on longitudinal contraction in levamisole-susceptible and –resistant *Haemonchus contortus*. *International Journal for Parasitology.* 21(6): 689-695.

Sasaki, T., Takagi, M., Yaguchi, T., Miyadoh, S., Okada, T. & Koyama, M. 1992. A new anthelmintic cyclodepsipeptide, PF1022A. *Journal of Antibiotics.* 45: 692-697.

Schallig, H. D. F. H. & Van Leeuwen, M. A. W. 1997. Protective immunity to the blood-feeding nematode *Haemonchus contortus* induced by vaccination with parasitic low molecular weight antigens. *Parasitology.* 114: 293-299.

Schallig, H. D. F. H., Van Leeuwen, M. A. W., Hendrikx, W. M. L. 1994. Immune responses of Texel sheep to excretory/secretory products of adult *Haemonchus contortus*. *Parasitology.* 108: 351-357.

Schmieden, V., Kuhse, J. & Betz, H. 1993. Mutation of glycine receptor subunit creates beta-alanine receptor responsive to GABA. *Science.* 262: 256-258.

Schots, A., Van der Leede, B. J., De Jongh, E. & Egberts, E. 1988. A method for the determination of antibody affinity using a direct ELISA. *Journal of Immunological Methods.* 109: 225-233.

Shoop, W. L., Egerton, J. R., Eary, C. H. & Suhayda, D. 1990. Anthelmintic activity of paraherquamide in sheep. *Journal of Parasitology.* 76: 349-351.

Sine, S. M. 1993. Molecular dissection of subunit interfaces in the acetylcholine receptor: identification of residues that determine curare selectivity. . *Proceedings of the National Academy of Sciences of the USA.* 90: 9436-9440.

Skinner, T. M. 1997. Cloning and localisation of nematode inhibitory amino acid receptors. *PhD Thesis University of Bath.*

Smith, H. & Campbell, W. C. 1996. Effect of ivermectin on *Caenorhabditis elegans* larvae previously exposed to alcoholic immobilisation. *Journal of Parasitology.* 82(1): 187-188.

Smith, G. B. & Olsen, R. W. 1995. Functional domains of $GABA_A$ receptors. *TiPS.* 16: 162-168.

Smyth, J. D. 1994. *Introduction to animal parasitology.* 3rd Edition Cambridge University Press, Cambridge.

Starich, T. A., Herman, R. K., Kari, C. K., Yeh, W. H., Schackwitz, W. S., Schuyler, M. W., Collet, J., Thomas, J. H., Riddle, D. L. 1995. Mutations affecting the chemosensory

neurones of Caenorhabditis elegans. *Genetics.* 139(1): 171-188.

Strong, L. & Wall, R. 1990. The Chemical control of livestock parasites: problems and alternatives. *Parasitology Today.* 6(9): 291-296.

Stringfellow, F. 1986. Cultivation of *Haemonchus contortus* (nematoda: Trichostrongylidae) from infective larvae to the adult male and the egg-laying female. Journal of Parasitology. 72(2): 339-345.

Sulston, J. E. & Brenner, S. 1974. The DNA of *Caenorhabditis elegans. Genetics.* 77(1):95-104.

Sulston, J. E., Schierenberg, E., White, J. G. &Thomson, J. N. 1983, The embryonic cell lineage of the nematode *Caenorhabditis elegans. Developmental Biology.* 100: 64-119.

Sutherland, I. H. & Campbell, W. C. 1990. Development, pharmacokinetics and mode of action of ivermectin. *Acta Leidensia.* 59(1-2): 161-168.

Tang, L., Ou, X., Henkle-Dührsen, K. & Selkirk, M. E. 1994. Extracellular and cytoplasmic CuZn superoxide dismutases from *Brugia* lymphatic filarial nematode parasites. *Infection and Immunity.* 62(3): 961-967.

Tarleton, R. L., Zhang, L. & Downs, M. O. 1997. "Autoimmune rejection" of neonatal heart transplants in experimental Chagas disease is a parasitic-specific response to infected host tissue. . *Proceedings of the National Academy of Sciences of the USA.* 94: 3932-3937.

Terada, M. 1992. Neuropharmacological mechanism of action of PF1022A, an antinematode anthelmintic with a new structure of cyclodepsipeptide, on Angiostrongylus cantonensis and isolated frog rectus. *Japanese Journal of Parasitology.* 41: 108-117.

Unwin, N. 1993. Nicotinic acetylcholine receptor at 9 Å resolution. *Journal of Molecular Biology.* 229: 1101-1124.

Unwin, N. 1995. Acetylcholine receptor channel imaged in the open state. *Nature.* 373: 37-78.

van Wyk JA. Malan FS. 1988. Resistance of field strains of Haemonchus contortus to ivermectin, closantel, rafoxanide and the benzimidazoles in South Africa. *Veterinary Record.* 123(9):226-8.

Vassilatis, D. K., Elliston, K. O., Paress, P. S., Hamelin, M., Arena, J. P. Schaeffer, J. M., Van der Ploeg, L. H. & Cully, D. F. 1997. Evolutionary relationship of the ligand-gated ion

channels and the avermectin-sensitive glutamate-gated chloride channels. *Journal of Molecular Evolution.* 44(5) 501-508.

Veglia, F. 1915. The anatomy and life-history of *H. contortus*. *Third and fourth reports of the Director of Veterinary Research, Department of Agriculture, Union of South Africa. Pretoria.*

Verrall S. & Hall ZW. 1992. The N-terminal domains of acetylcholine receptor subunits contain recognition signals for the initial steps of receptor assembly. *Cell.* 68(1):23-31,

Waller, P. J. 1992. Prospects for Biological control of Nematode parasites of ruminants. *New Zealand Veterinary Journal.* 40: 1-3.

Waller, P. J. 1993. Nematophagous Fungi: Prospective Biological Control Agents of Animal Parasitic Nematodes? *Parasitology Today.* 9(11): 429-431.

Waller, P. J., Dobson, R. J., Obendorf, D. L. & Gillham, R. J. 1995. Anthelmintic resistance in nematode parasites of sheep: learning from the Australian experience. *The Veterinary Record.* 136: 411-413.

Wharton, D. A. 1986. *A Functional Biology of Nematodes.* Crom Helm Ltd., London.

Wheeler, J. E., Kendall, S. J., Butters, J., Holloman, D. W. & Hall, L. 1995. Using allele-specific oligonucleotide probes to characterise benzimidazole resistance in *Rhynchosporium secalis*. *Pesticide Science.* 43: 201-209.

White, J. G., Southgate, E. Thomson, J. N. & Brenner, S. 1986. The structure of the nervous system of the nematode *Caenorhabditis elegans. Philosophical . Transactions of the Royal Society of London B.* 314: 1-340.

Whitfield, P.J. 1993 Parasitic Helminths. *Modern Parasitology, A text book of parasitology*, edited by Cox, F. E. G. 2nd Edition, Blackwell Scientific Pubilcations, Oxford.

Wolstenholme, A. J. 1997. Glutamate-gated Cl^- channels in *Caenorhabditis elegans* and parasitic nematodes. *Biochemical Society Transactions.* 25: 830-834.

Wood, W. B. 1988. Introduction to *C. elegans*. In Wood, W. B. and the Community *of C. elegans* Researchers, eds., The Nematode *Caenorhabditis elegans*. Cold Spring Harbor Press, Cold Spring Harbour.

World Health Organisation report. 1995, Fact sheet No. 98 http//www.who.org/programmes/inf/facts/fact98.htm

World Health Organisation report. 1996, Fact sheet No. 102

http//www.who.org/programmes/inf/facts/fact102.htm

World Health Organisation.1997. Press Release http//www.who.org/press/1997/pr97-07.html